Stony Brook University

OFFICIAL COPY

The official electronic file of this thesis or dissertation is maintained by the University Libraries on behalf of The Graduate School at Stony Brook University.

© All Rights Reserved by Author.

I. Synthesis of Aryl C-Nucleosides and Retinoid Analogs

II. Investigation into Docking Studies of Bisabosqual Analogs

A Dissertation Presented

by

Erik Stolarzewicz

to

The Graduate School

in Partial Fulfillment of the Requirements

for the Degree of

Doctor of Philosophy

in

Chemistry

Stony Brook University

December 2010

STONY BROOK UNIVERSITY

THE GRADUATE SCHOOL

ERIK STOLARZEWICZ

We, the dissertation committee for the above candidate

for the Doctor of Philosophy degree, hereby recommend

acceptance of this dissertation.

Professor Kathlyn A. Parker
Department of Chemistry

Professor Iwao Ojima
Department of Chemistry

Professor Benjamin Hsiao
Department of Chemistry

Professor Marcia Simon
Department of Oral Biology and Pathology

This dissertation is accepted by the Graduate School

Lawrence Martin
Dean of the Graduate School

Abstract of the Dissertation

I. Synthesis of Aryl C-Nucleosides and Retinoid Analogs

II. Investigation into Docking Studies of Bisabosqual Analogs

by

Erik Stolarzewicz

Doctor of Philosophy

in

Chemistry

Stony Brook Univeristy

2010

Currently, there are three major approaches used for the synthesis of aryl C-2-deoxyriboses. The first approach uses a common sugar derivative developed by Kool, 1,2-dideoxy-3,5-*O*-*p*-toluoyl-α-1-chloro-D-ribofuranose. The second approach uses Woski's 2-deoxyribonolactone glycal. The third approach uses a functionalize sugar involving tin reagents developed by Daves. All three methods have certain drawbacks. In efforts to finding a more efficient and alternative approach to making aryl *C*-

deoxynucleosides, we developed a nine step synthetic route from commercially available inexpensive starting materials.

In humans, epidermal keratinocytes are unique in their ability to convert Vitamin A1 (retinol) into Vitamin A2 (3,4-didehydroretinol). Each of these alcohols can be further metabolized to generate retinoid acids which serve as transcription factor ligands which can alter epidermal homeostasis. Currently unknown are the panel of genes which each of these ligands modulates. As a prerequisite for assessing the impact of each acid, their metabolism must be compared. For these purposes 3,4-didehydroretinoic acid and ^{3}H-3,4-didehydroretinoic acid were synthesized.

One important step in the biosynthesis involving the formation of cholesterol is the NADPH-requiring enzyme squalene synthase. Recently, four new squalene synthase inhibitors were found, they are Bisbosqual A, B, C and D. Using Discovery Studio from Accelrys, protein ligand docking studies were carried out on Bisabosqual A,B,C and D to understand the IC_{50} data reported by Minagawa. Insights into these studies were used to design Bisabosqual analogs for future synthesis.

This body of work is dedicated to my parents,
my wife and my family.

Table of Contents

List of Abbreviations……………………………………………………...viii

List of Figures……………………………………………………………..xiii

List of Schemes…………………………………………………………xvii

List of Tables……………………………………………………………xix

Acknowledgements……………………………………………………...xx

Chapter I

Synthesis of Aryl-C Nucleosides for Use in Sequencing by Hybridization……………………………………………………………..2

1.1 Introduction……………………………………………………………4

1.2 Synthesis of Peptide Nucleic Acids………………………..…………...6

1.3 Synthetic Approaches towards Aryl C-Nucleosides………………………10

1.4 Synthesis of Aryl C-Nucleosides……………………………………..12

1.4.1 Synthesis of Pyrene Nucleoside…………………………………………17

1.4.2 Synthesis of Aryl C-Nucleosides…………………………………………20

1.5 Synthesis of Pyrene Riboside……………………………………………22

1.6 Conclusion…………………………………………………………….23

1.7 Experimental Section……………………………………………………56

1.8 References…………………………………………………………….59

Chapter II

Synthesis of Labelled 3,4-Didehydro Retinoic Acid. Introduction of Tritium at C-4 in the Final One-pot Procedure……………………………..……………93

2.1 Introduction…………………………………………………………….93

2.2 Synthetic Approaches…………………………………………………….96

2.3 Results and Discussion……………………………………………………...100

2.3.1 Preparation of 4-Oxygenated Retinoic Acid Methyl Esters…………………100

2.3.2 Preparation of 3,4-ddRA, Purification, and HPLC Characterization…….….101

2.3.3 Preparation of 4-T 3,4-ddRA……………………………………………..101

2.3.4 Gene Expression of treated T-labeled ATRA and T-labeled 3,4-ddRA……..102
2.4 Experimental Section……………………………………………………………..105
2.4.1. HPLC-Mass Spectroscopy…………………………………………………..114
2.4.2. Purification of Unlabelled 3,4-ddRA………………………………………..114
2.4.3. Purification of ^{3}H-3,4-ddRA……………………………………………..123
2.5 References……………………………………………………………………127
2.6 Appendix……………………………………………………………………..131

Chapter III

Binding Site of the Bisabsoqual Natural Products in Human Squalene Synthase..137
3.1 Introduction……………………………………………………………………137
3.2 Background………………………………………………………………..……..138
3.2.1 Identification of the active site of squalene synthases…………..………………..139
3.2.2 Pfizer crystal structure………………………………………………...……….141
3.3 Structural Results and Discussion of Bisabosqual A-D and CP-320-473...………..144
3.3.1 Validation Data CP-320473……………………………………..………..145
3.3.2 Bisabosqual A Data……………………………………………….…………146
3.3.3 Bisabosqual B Data……………………………………………….…………148
3.3.4 Bisabosqual C Data………………………………………………...…..150
3.3.5 Bisabosqual D Data……………………………………………..….….....152
3.4 Correlation of Binding Energies with IC$_{50}$ values for Squalene Synthases………...154
3.4.1 Binding Energy Correlations for MM-GBSW and MM-PBSA with IC$_{50}$ Data……………………………………………………………………………..155
3.5 Analogs designed to be improved Squalene Synthase Inhibitors………..………...156
3.5.1 Compound 3.6 Data……………………………………………….....…...157
3.5.2 Compound 3.7 Data…………………………………………...…...…..158
3.5.3 Compounds 3.8-3.15 Data………………………………………..……158
3.5.4 Proposed Binding of Presqualene by overlaying to Bisabosqual A…….……….162
3.6 Conclusion…………………………………………………………………….163
3.7 Experimental Section………………………………………………………......164
3.8 References…………………………………………………………………….194
List of Full References…………………………………………………….…….198

List of Abbreviations

α	alpha
β	beta
δ	delta, or chemical shift
μ	micro, or 10^{-6} unit
π	pi bond, or orbital
Δ	heat
ΔG	free energy
hv	light
Å	angstrom, or 10^{-10} unit
Ac	acetyl
AcOH	acetic acid
Aq.	aqueous
Ar	aryl
ATRA	*all-trans* retinoic acid
b	broad
BAI1	brain-specific angiogenesis inhibitor 1
BCL2A1	B-cell CLL/Lymphoma 2, Bcl-2-related protein A1
BRCA2	breast cancer 2 susceptibility protein
bd	broad dublet
Bn	benzyl
bp	boiling point
bs	broad singlet
Bz	benzoyl
t-Bu	*tert*-Butyl
n-BuLi	*n*-butyllithium

^{o}C	Celsius
CDK4	cyclin-dependent kinase 4
cm^{-1}	reciporcal centimeter
cpm	counts per minute
d	doublet
dd	doublet of doublet
dpm	disintegrations per minute, a measure of radioactivity
DIPEA	diisopropylethylamine
DMAP	dimethylaminopyridine
DME	dimethoxyethane
DMF	*N*,*N*,-Dimethylformamide
DMSO	dimethylsulfoxide
Dowex 50X-800	acidic resin
DNA	deoxyribonucleic acid
EDC	1-ethyl-3-(3-dimethylaminopropyl) carbodiimide
eq.	equivalent (s)
ESF1	E2F transcription factor 1
ESF3	E2F transcription factor 3
ESR1	estrogen receptor 1
Et	ethyl
Et_2O	diethyl ether
EtOAc	ethyl acetate
FADD	Fas (TNFRSF6)-associated via death domain
FASL,FASLG	TNF superfamily, member 6
FasR	Fas receptor
g	gram

h	hour (s)
HPLC	high performance liquid chromatography
HRMS	high resolution mass spectrometry
Hz	hertz
IC_{50}	concentration for 50% inhibition
IFNB1	interferon, beta 1, fibroblast
IL6	interleukin 6 (interferon, beta 2)
Imd	imidazole
IR	infrared spectroscopy
in vacuo	under vacuum
J	first order coupling constant (NMR)
K	Kelvin
kcal	kilocalorie
L	liter
LDA	lithium diisopropylamide
LDL	low-density lipoprotein
m	multiplet
Me	methyl
mg	milligram
MHz	megahertz
min	minute (s)
mL	milliliter
mmol	millimole
MnO_2	manganese dioxide
mol	mole
MOM	methoxymethyl ether

mp	melting point
MD	molecular dynamics
MM-GBSW	Molecular Mechnanics Generalized Born with Simple Switching
MM-PBSA	Molecular Mechanics Poisson Boltzmann Surface Area
MS	mass spectrometry
$NaBT_4$	tritiated (Hot) sodium borohydride
NADPH	nicotinamide adenine dinucleotide phosphate
nm	wavelength
NBS	*N*-bromosuccinimide
NCS	*N*-chlorosuccinimde
NHEK-F	normal human foreskin keratinocytes
NMR	Nuclear Magnetic Resonance
Novapak C18	reverse phase column for HPLC
p-TsOH, PTSA	para-toluenesulfonyl (tosyl)
PDB	Protein Data Bank
pH	measure of the acidity or basicity of a solution
Ph	phenyl
PNA	Peptide Nucleic Acid
ppm	parts per million (NMR)
Pyr	pyrene
Py	pyridine
q	quartet
3,4ddRA	3,4-Didehydroretinoic acid
RA	retinoic acid
R_f	retention factor
RMSD	root mean square deviation
rt	room temperature
RT-PCR	real time polymerase chain reaction

s	singlet
SBH	sequence by hybridization
Sunfire C18	reverse phase column for HPLC
t	time, or triplet (NMR)
TBAF	tetra-*N*-butylammonium fluoride
TFA	trifluoroacetic acid
THF	tetrahydrofuran
TLC	Thin Layer Chromatography
T_m	melting temperatures
TMS	trimethylsilyl
TP73	tumor protein 73
Ts	para-toluenesulfonyl (tosyl)
UV	ultraviolet
Vitamin A1 acid	*all-trans* retinoic acid, ATRA
Vitamin A2 acid	3,4-didehydroretinoic acid, 3,4-ddRA

List of Figures

Figure 1.1 Alignment of base sequence probes for SBH……………………………...3

Figure 1.2 Structure of a Peptide Nucleic Acid and DNA strand……………………..…4

Figure 2.1. Structures of Retinol, 3,4-ddRA, RA, and 3,4-didehydroretinol……………93

Figure 2.2. Gene expression in NHEK-F. Real time RT-PCR conformation of changes in gene expression due to treatment with Vitamin A1 (ATRA) or A2 acids (3,4ddRA) of several genes…………………………………………………………………………103

Figure 2.3. Gene expression in NHEK-F. Real time RT-PCR conformation of changes in gene expression due to treatment with Vitamin A1 (ATRA) or A2 acids (3,4ddRA) of FASGL gene………………………………………………………………………104

Figure 2.4. Reverse- phase gradient Preparative HPLC Trace. Partial Purification of all trans 3,4-ddRA resolution of ddRA……………………………………….…………115

Figure 2.5. Reverse-phase gradient HPLC analysis of partially purified ddRA (2.4) (peak 3) from the previous separation on NovaPackC18 column…………………..….116

Figure 2.6. Retinoic acid (A) and 3,4-didehydroretinoic acid (B) were characterized by retention times on reverse phase HPLC on a Nova-Pak HR C18 column (upper panel) and by UV spectroscopy (lower panel)……………………………………………..…118

Figure 2.7. HPLC traces of One pot crude, crystallized, Bligh/Dyer, Multi-step Clean and pure RA on the new solvent gradient with retention times……………………..….120

Figure 2.8. Reverse- phase gradient Preparative HPLC Trace. Partial Purification of all trans 3,4-ddRA resolution of ddRA………………………………………………….121

Figure 2.9. Reverse- phase gradient Preparative HPLC Trace. Partial Purification of al trans 3,4-ddRA resolution of ddRA……………………………………………….....122

Figure 2.10. Reverse- phase gradient Preparative HPLC Trace. Purification and retention times of all trans 3,4-ddRA resolution and ATRA…………………………………..…123

Figure 2.11. Reverse- phase gradient Preparative HPLC Trace. Purification of tritiated 3,4-ddRA using Novapak column system……………………………………...……125

Figure 2.12. Reverse- phase gradient Preparative HPLC Trace. Purification of tritiated 3,4-ddRA using Novapak column system the second time……………………..……126

Figure 3.1. The Bisabosqual Natural Products……………………………………...138

Figure 3.2. Biosynthetic conversion of two FPP molecules to squalene and two GGPP molecules to phytoene……………………………………………………………….139

Figure 3.3- Sequences of Squalene Synthases……………………………………....140

Figure 3.4, The binding site region of human squalene synthase with the “flap” (residues 50-54)…………………………………………………………………………...141

Figure 3.5. CP-420472 bound by Squalene Synthase……………………………….142

Figure 3.6. Active site channel from two different perspectives……………………...143

Figure 3.7. Numbering systems for bisabosquals and for CP-320473………………..144

Figure 3.8. Images of the docked ligand CP-320473 in the active site with neighboring residues……………………………………………………………………………145

Figure 3.9. Superimposed on the image of CP-320473 is the structure of the docked ligand.Validation picture…………………………………………………..…....146

Figure 3.10. Bisabosqual A docked in human SQS…………………………………...147

Figure 3.11. Bisabosqual A docked in human SQS. The image on the left shows the protein surface without the flap. The image on the right shows bisabosqual with the nearest neighbor residues……………………………………………………………147

Figure 3.12. Bisabosqual A in the binding pocket site with the conserved residues shown as stick figures with the rest of the protein rendered as an electrostatic potential surface…………………………………………………………………………..148

Figure 3.13 Bisabosqual B with its neighboring residues in the active site…………....149

Figure 3.14. Image of docked Bisabosqual B shown in the active site with neighboring residues. The protein surface area is rendered showing the electrostatic potential…..…149

Figure 3.15. Image of docked Bisabosqual B shown in the active site with neighboring residues. The protein surface area is rendered showing the electrostatic potential…..…150

Figure 3.16. Bisabosqual C with its neighboring residues in the active site…………..150

Figure 3.17. Image of docked Bisabosqual C shown in the binding site with neighboring residues. The protein surface area is rendered showing the electrostatic potential…….151

Figure 3.18. Bisabosqual D with its neighboring residues in the active site…………..152

Figure 3.19. Image of docked Bisabosqual D shown in the active site with neighboring residues. The protein surface area is rendered showing the electrostatic potential……153

Figure 3.20. Correlation between MM-PBSA calculated binding energy and experimental IC_{50} data……………………………………………………………155

Figure 3.21. Correlation between MM-GBSW calculated binding energy and experimental IC_{50} data…………………………………………………..…………..156

Figure 3.22. Structures of Bisabosqual Analogs **3.6** and **3.7**…………………………157

Figure 3.23. Compound 3.6 with its neighboring residues in the active site…………157

Figure 3.24. Compound 3.7 with its neighboring residues in the active site…………158

Figure 3.25. Rationally designed bisabosqual analogs 3.8-3.15………………………159

Figure 3.26. Compounds **3.8-3.15** superimposed with each compound color coded as follows as stick representation…………………………………………………………160

Figure 3.27. Compounds **3.8-3.15** superimposed with surface area generated without the flap and with the flap………………………………………………………………...160

Figure 3.28. Correlation between MM-GBSW calculated binding energy and experimental IC_{50} data for Squalene Synthase with the extrapolated data for compounds **3.6-3.15**…………………………………………………………………………....161

Figure 3.29. Presqualene overlayed with surface area rendered with the flap (left image) and structure of presqualene…………………………………………………………162

Figure 3.30. Presqualene overlayed with bisabosqual A (shown in yellow) with its neighboring residues in the active site…………………………………………………162

Figure 3.31. CDOCKER Parameter Values……………………………………………166

Figure 3.32. Score Ligand Poses Parameter Values…………………………...……167

Figure 3.33. Ligand Minimization with Solvent Models Parameter Values…………..168

Figure 3.34. Calculate Binding Energy Parameter Values………………………….....170

Figure 3.35. Image of docked compound **3.6** shown in the active site with neighboring residues. The protein surface area is rendered showing the electrostatic potential…….177

Figure 3.36. Image of docked compound **3.7** shown in the active site with neighboring residues. The protein surface area is rendered showing the electrostatic potential…....178

Figure 3.37. Compound 3.8 with its neighboring residues in the active site…………..180

Figure 3.38. Image of docked compound **3.8** shown in the active site with neighboring residues. The protein surface area is rendered showing the electrostatic potential…….180

Figure 3.39. Compound 3.9 with its neighboring residues in the active site…………..182

Figure 3.40. Image of docked compound **3.9** shown in the active site with neighboring residues. The protein surface area is rendered showing the electrostatic potential…….182

Figure 3.41. Compound 3.11 with its neighboring residues in the active site…………184

Figure 3.42. Image of docked compound **3.11** shown in the active site with neighboring residues. The protein surface area is rendered showing the electrostatic potential…….184

Figure 3.43. Compound 3.12 with its neighboring residues in the active site……..…..186

Figure 3.44. Image of docked compound **3.12** shown in the active site with neighboring residues. The protein surface area is rendered showing the electrostatic potential…….186

Figure 3.45. Compound 3.13 with its neighboring residues in the active site…………188

Figure 3.46. Image of docked compound **3.13** shown in the active site with neighboring residues. The protein surface area is rendered showing the electrostatic potential…….188

Figure 3.47. Compound 3.14 with its neighboring residues in the active site…………190

Figure 3.48. Image of docked compound **3.14** shown in the active site with neighboring residues. The protein surface area is rendered showing the electrostatic potential…….190

Figure 3.49. Compound 3.15 with its neighboring residues in the active site…………192

Figure 3.50. Image of docked compound **3.15** shown in the active site with neighboring residues. The protein surface area is rendered showing the electrostatic potential…….192

List of Schemes

Scheme 1.1 Synthesis of Peptide Nucleic Acid……………………………..………5
Scheme 1.2. Kool's Method for Synthesis of Aryl C-Nucleosides……………….……...7
Scheme 1.3. Formation of Ribonolactone in Woski's Method for Aryl C-Nucleosides...8
Scheme 1.4. Woski's Method for Synthesis of Aryl C-Nucleosides continued…..……..9
Scheme 1.5. Daves Method for Synthesis of Aryl C-Nucleosides. ……………………...9
Scheme 1.6. Kozikowski Cycloaddtion Approach…………………………...…….10
Scheme 1.7. Initial attempts to form a pyrene cycloadduct with dimethoxy protected olefin. ……………………………………………………………………………11
Scheme 1.8. Synthesis of pyrene cycloadduct **1.25a** using cyclohexyl protected chiral olefin……………………………………………………………………….…12
Scheme 1.9. Potential diastereoisomer formation from unprotected diol **1.26a**……..….13
Scheme 1.10. Protection/Deprotection for ring cleavage……………………………….14
Scheme 1.11. Formation of hemiacetal from reductive cleavage………………………14
Scheme 1.12. Byproducts from elimination and dehydration of hemiacetal intermediate……………………………………………………………………...15
Scheme 1.13. Formation of Nucleoside followed by Phosphoramide Activation………16
Scheme 1.14. Dimethoxyltrityl protected isoxazoline **1.32** undergoing hydrogenation...17
Scheme 1.15. Synthesis of Aryl C-Nucleosides…………………………………...……18
Scheme 1.16. Synthesis of Aryl C-Nucleosides continued……………………………..19
Scheme 1.17. Formation of Chiral Alkyne **1.34**………………………………………..20
Scheme 1.18. Formation of Boronic Ester **1.35** followed by cycloaddition…………….21
Scheme 1.19. Generation of Aryl C-Riboside **1.38…**………………………………..22
Scheme 2.1. Two Industrial Synthetic Approaches…………………………….…....95
Scheme 2.2. Potier Protocol………………………………………………………….95
Scheme 2.3. First Approach at 3,4-Didehydroretinoic Acid **(2.4)**………………………96
Scheme 2.4 Second Approach at 3,4-Didehydroretinoic Acid **(2.4)**…………………....97
Scheme 2.5. Third Approach at 3,4-Didehydroretinoic Acid **(2.4)**……………………..98

Scheme 2.6. Third Approach at 3,4-Didehydroretinoic Acid **(2.4)** and **(2.10)**………….98

Scheme 2.7. Synthesis of T-labeled 3,4-ddRA………………………………………....99

Scheme 2.8. 4-oxo RA ester under methanolic conditions. …………………………...100

Scheme 2.9. Formation of 4-oxo ester under MnO_2...101

Scheme 2.10. Generation of 3,4-Didehydroretioc Acid………………………………..101

List of Tables

Table 1.1 Free Energies (-ΔG^0_{25}(kcal/mol) and Melting Temperatures……………..……..6

Table 1.2. 1,3-Dipolar Cycloaddition Reactions from **1.24**……………………….……...18

Table 1.3. Nucleoside Formation from TBS-Isoxazolines **1.27a-f**……………….………19

Table 2.1 Retention times for ^{3}H 3,4-ddRA and cold 3,4-ddRA. Red indicates crude preparation of the material…………………………………………………………..….126

Table 3.1. Inhibitory activities of bisabosquals A, B, C and D against squalene synthases……………………………………………………………………………..154

Table 3.2. IC_{50} values for Bisabosqual A-D in the Hep G2 assay[9], the three scoring functions, and calculated binding energies…………………………………………..…155

Table 3.3. Compounds **3.6-3.15** were designed, not synthesized or tested. The data was extrapolated from the known tested inhibitory activity. Compound **3.10** failed to be docked in the active site…………………………………………………………..161

Acknowledgements

My journey at Stony Brook has been one of struggle, endurance and perseverance. I've shared it with many friends and colleagues since starting here. There are a lot of people who are responsible for my development as a chemist and deserve credit. Let me start by saying that I would like to apologize in advance for anyone that I do miss in this acknowledgement.

First and foremost, my sincerest respect and appreciation goes to my research advisor Professor Kathlyn Parker. Her ability to make light of any situation amazes me. She is very knowledgeable in the field of organic chemistry that you can approach her on any issue. She is very approachable, easygoing, and understanding both in and out of the laboratory. It's been a pleasure working with her throughout the years.

Secondly, I am deeply grateful to my chairman, Distinguished Professor Iwao Ojima for being part of my journey here at Stony Brook. His direct firm constructive criticism is highly valued and inspires me to work harder. I would like to thank Professor Benjamin Hsiao for being a very active third member of my committee and his input while I progressed through earning this degree. I would also like to thank Professor Marcia Simon for serving as the fourth member of my committee and taking time away from her busy schedule.

I would like to thank our collaborators who we had the pleasure of working with during my time here. In the Department of Oral Biology and Pathology, Dr. Juliana Tafrova for doing all the HPLC traces of the compounds that we synthesized. I would like to thank Jodi Shalusky and Tina Yeh from Accelrys for all their support on molecular modeling. The countless hours of questions and help I have received from them. I could have not done any of it without them.

In the Chemistry Department, there are many people who make the place the work. I want to thank our NMR specialist, Dr. James Marecek, for his priceless expertise in the field of NMR spectroscopy. He is always there when you need him. I would like to also thank Francis Picart for all his help with the molecular modeling projects and NMR. When to comes to paperwork and making sure I am where I need to be with deadlines in the department and university, I need to thank Katherine Hughes, Diane Godden, Donna Barrington, and Heidi Ciofi. I would be lost without them. I would like to thank Dr. Mohammad Akhtar for all his help in my undergraduate teaching. A real professional when it comes to dealing with students. I need to thank also Marjorie Kandel. She was my organic chemistry lab instructor as an undergraduate here at Stony Brook. She was one of the reasons why I decided to purse the field of organic chemistry. I would like to also thank Professor Nancy Goroff for all her moral support and help. Thank you for being there.

I want to thank all the past and present Parker group members I was able to work with over the years. They have all had some type of impact on my life: In particular Dr. Ioannis Katsoulis, who was a big inspiration for me during my initial days in the laboratory, Dr. Yeon-Hee Lim, for being such a lively positive person, Dr. Fei You, Dr. Peng Wang, Dr. Zhou Zhou, Paul Schuber, Joe Carvalho and Bill Berger.

I wish to thank all my friends and colleagues in the department, especially the people who joined the department with me. I also want to thank in particular Dr. Debbie Stoner-Ma and Dr. Asim Okur for being there when it counted. To all my colleagues that knew when to step out of the laboratory and take a break to clear our heads: Dr. Sean Curtis, Dr. Jeff Webb and Dr. Chris Olivieri.

Finally, I would like to deeply thank my parents, Mr. Mieczyslaw Stolarzewicz and Mrs. Marcjanna Stolarzewicz. They were always there to help, support, encourage, and nourish me through this degree. I would not have been able to accomplish this without their unconditional love and support. Lastly, I would like to thank my wife, Katarzyna, for her support, encouragement and patience during this entire degree. I would like to also thank all my family from here in America and in Poland including those who have passed away. Thank you.

Sincerely,
Erik Stolarzewicz

Chapter I

Synthesis of Aryl-C Nucleosides for Use in Sequencing by Hybridization

1.1 Introduction………………………………………………………………....2

1.2 Synthesis of Peptide Nucleic Acids……………………………………..….4

1.3 Synthetic Approaches towards Aryl C-Nucleosides…………………..….6

1.4 Synthesis of Aryl C-Nucleosides…………………………………….….10

1.4.1 Synthesis of Pyrene Nucleoside…………………………………….…12

1.4.2 Synthesis of Aryl C-Nucleosides…………………………………….…..17

1.5 Synthesis of Pyrene Riboside…………………………………………...20

1.6 Conclusion……………………………………………………………..22

1.7 Experimental Section……………………………………………………23

1.8 References……………………………………………………………..56

1.9 Appendix…………………………………………………………….59

Chapter 1 - Synthesis of Aryl-C Nucleosides for Use in Sequencing by Hybridization

1.1 Introduction

Sequencing by Hybridization (SBH) is a DNA sequencing technique in which a (SBH chip) short sequences of probes (nucleotides) is introduced to a target DNA sequence. A probe will hybridize (bind) to a complementary Watson-Crick sequence of the target DNA. Standard DNA sequencing is done by gel electrophoresis which takes a decent amount of time. Our interest is to look for a more robust and faster way of sequencing DNA by SBH efficiently. There are two considerations when trying to do SBH. You must obtain sequences and do sequence reconstruction. The standard scheme is use of *k-mers* of some given length as probes for DNA sequencing like 5'-ATCGCA-3', 5'-ATCTCAATAGGAT-3', and 5'-ATCCTG-3.' Oligomer probes of natural bases are used and placed on the SBH. An unknown DNA sequence is placed on the chip and will hybridize to give you the complementary base pair to the oligomer probe. The amount of small k-mer oligmer probes is limited on how many you can place on an SBH chip. The goal is to have many small lengths of oligomer probes and this can be achieved potentially by use of a gapped-probe method. The idea is to have gapped probes which are the use of natural bases as well as "universal base" candidates (peptide nucleic acids or deoxynucleosides) for shorter library of probes in DNA sequencing. The term universal base refers to the ability of having one nucleic base hybridize equally among all the four naturally occurring DNA bases.

A gapped probe sequence would look like the following: NNN***N*N**NN. Positions containing the symbol N are called "*designated sites*"(natural bases) and positions containing the symbol * are for "*universal base candidates.*" Peptide nucleic acids (PNAs) were initially synthesized in the search for universal base candidate in optimizing DNA sequencing. The gapped probes would be very small in length and sequence reconstruction of the DNA sequences would be done as follows.

Putative sequence = . . . b1b2b3b4b5b6b7b8

Probe-1 = b1b2b3* * b6* * b9

Probe-2 = b4b5b6* * b9* * b12

Probe-3 = b7b8b9* * b12* * b15

Probe-4 = b1b2b3* * b6* * c9

Probe-5 = b4b5b6* * c9* * c12

Probe-6 = b7b8c9* * c12* * c15

b= natural base *=universal base

Figure 1.1 Alignment of base sequence probes for SBH.

Directly above is a putative DNA sequence, the gapped probes would in essence align and overlap to give the entire fifteen base sequence from small gapped probes without having to have a long k-mer oligomer probe. This would allow for more gapped probes to fit on an SBH chip.

In efforts to find a potential universal base candidate, we began by synthesizing a peptide nucleic acid for nucleoside analogs in oligonucleotide probes as a test case study.

Peptide nucleic acids (PNA) duplex with DNA and universal base-containing PNA probes would exhibit T_m profiles parallel to those of duplexes consisting of DNA and corresponding DNA probes. The advantages are that they are simpler to prepare than nucleoside base analogs and would allow for testing of several base candidates quickly by T_m experiments for hybridization behavior for universality with other natural bases. If a potential base candidate is found, the nucleoside base analog is synthesized and incorporated into an oligonucleotide base probe.

1.2 Synthesis of Peptide Nucleic Acids

Peptide Nucleic Acids (PNAs)[1,2] are analogues of DNA in which the backbone is a pseudopeptide rather than that of a sugar. As mentioned before PNA mimics the behavior of DNA and binds complementary nucleic acid strands. The neutral backbone of PNAs result in very high affinity for complementary DNA and RNA sequences, generating considerable interest in therapeutics.

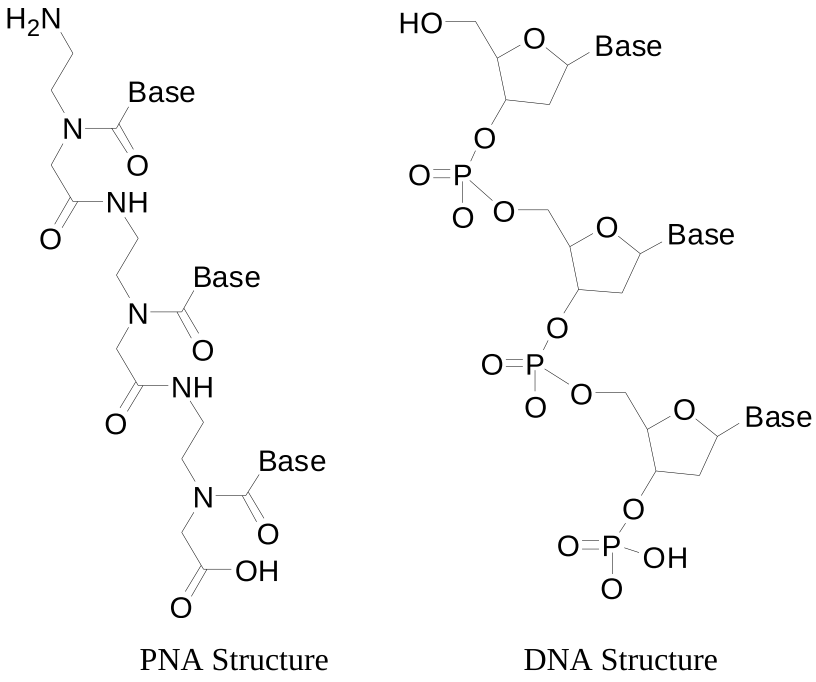

Figure 1.2 Structure of a Peptide Nucleic Acid and DNA strand.

As can be seen above, the DNA backbone consists of a deoxyribose phosphate backbone. In the PNA backbone, a repeating N-2-amino ethyl unit is linked by peptide bonds. No pentose sugar moieties or phosphate groups are present. The natural bases of purines and pyrimidines (attached through methlylene carbonyl linkages) can be used in PNA's or can be altered to introduce non-natural bases in order to find universal bases that will mimic the behavior of DNA. In the search for these candidates, we begin synthesis of PNAs with aromatic substituents. In this document, we start by synthesizing several PNAs and then several deoxyribosides that will be probed for optimal hybridization behavior. Finally, to show the practicality of the synthetic method, an aryl riboside is synthesized.

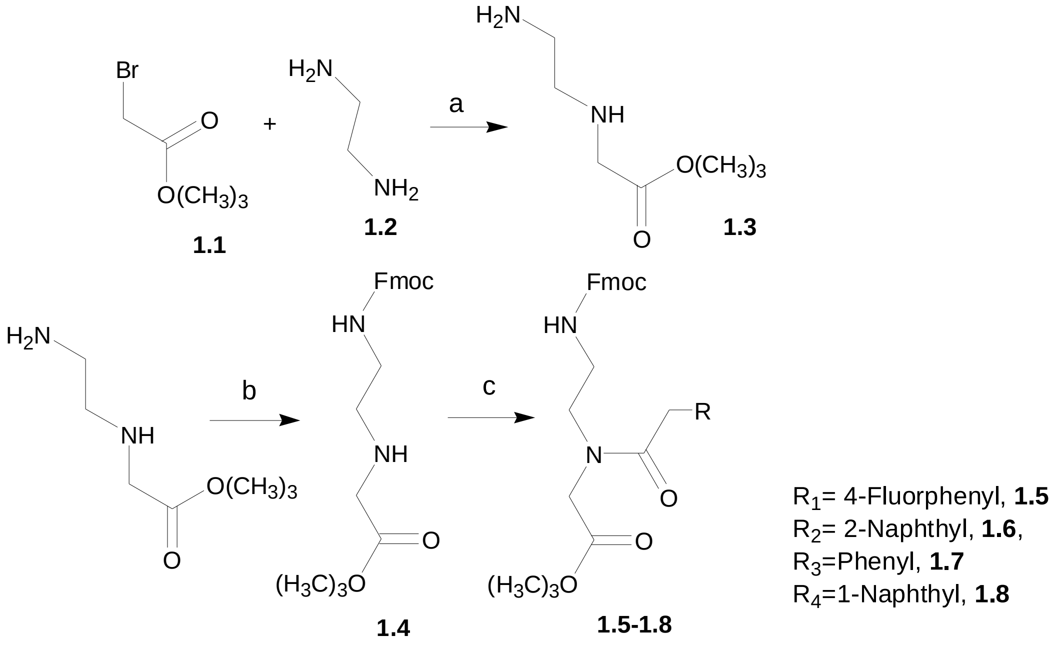
Br
O
O(CH3)3
1.1
+
H2N
NH2
1.2
a
H2N
NH
O(CH3)3
O
1.3
H2N
NH
O(CH3)3
O
b
Fmoc
HN
NH
O
(H3C)3O
1.4
c
Fmoc
HN
N
R
O
O
(H3C)3O
1.5-1.8
R1= 4-Fluorphenyl, 1.5
R2= 2-Naphthyl, 1.6,
R3=Phenyl, 1.7
R4=1-Naphthyl, 1.8

a) CH_2Cl_2, 0°C, 76% b) Fmoc, DIPEA, r.t., 61% c) DMF, EDC, carboxylic acid.

Scheme 1.1 Synthesis of Peptide Nucleic Acid.

Following the Thomson[3] Protocol for making a peptide nucleic acid, we first synthesized the peptide backbone. The first step involved protection of ethylenediamine (**1.2**) with *tert*-butyl bromoacetate (**1.1**). This was accomplished in 76% yield. The second step was protection of the other amine group with Fmoc-succinimide. This proved much more difficult than initially expected as this was supposed to crystallize out of solution at -20^{o}C in 24 hours. Scratching on the side of the flask was necessary and was allowed 36 hours to crystallize and then filtered with a 61% yield. The final step involved a coupling reaction with EDC to obtain the desired PNA **1.5**. Previous Parker group members have synthesized other PNAs **1.6-1.8** as models for SBH.

After synthesis of compound **1.5** for model experiments, focus began towards the synthesis of aryl C-deoxyribosides more specifically to a pyrene nucleoside. Preliminary Results from one of Kool's[4] papers shows good indication of pyrene as a universal base candidate. In Table 1.1, T_m profiles show equal consistency among all four natural DNA bases in duplex pairing. A universal base candidate would contain such properties.

Tm (^{o}C) for DNA Duplexes Containing P-X Pairs (P=Pyrene)

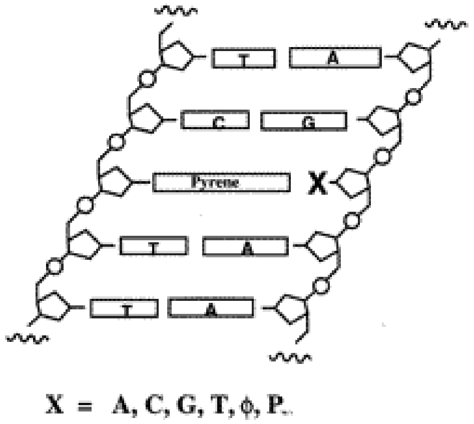

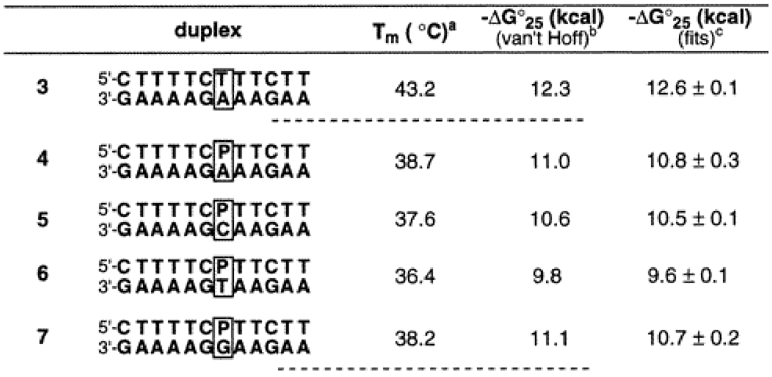

	duplex	T_m (°C)^a	$-\Delta G^\circ_{25}$ (kcal) (van't Hoff)^b	$-\Delta G^\circ_{25}$ (kcal) (fits)^c
3	5'-C T T T T C T T T C T T 3'-G A A A A G A A A G A A	43.2	12.3	12.6 ± 0.1
4	5'-C T T T T C P T T C T T 3'-G A A A A G A A A G A A	38.7	11.0	10.8 ± 0.3
5	5'-C T T T T C P T T C T T 3'-G A A A A G C A A G A A	37.6	10.6	10.5 ± 0.1
6	5'-C T T T T C P T T C T T 3'-G A A A A G T A A G A A	36.4	9.8	9.6 ± 0.1
7	5'-C T T T T C P T T C T T 3'-G A A A A G G A A G A A	38.2	11.1	10.7 ± 0.2

(Conditions: 100 mM NaCl, 10 mM $MgCl_2$, 10 mM Na·PIPES pH 7.0, 5.0 M DNA.)

Table 1.1 Free Energies ($-\Delta G^0_{25}$(kcal/mol) and Melting Temperatures.

1.3 Synthetic Approaches towards Aryl C-Nucleosides

Currently, there are three major approaches used for the synthesis of aryl C-2-deoxyriboses. The first and most direct approach used by Kool, in which the metalated form of the aglycon is reacted with a suitable sugar derivative, has not typically been successful in making bulky aromatic nucleosides in our hands. The common sugar derivative developed by Kool, 1,2-dideoxy-3,5-*O*-*p*-toluoyl-α-1-chloro-D-ribofuranose, often used in the synthesis is acid sensitive and slightly unstable allowing for a two week lifespan of use before full decomposition occurs. Efforts to synthesize desired large polycyclic aromatic nucleosides using this approach with organocadminum reagents were unsuccessful in our hands. Pyrene was our desired aromatic because of its potential universal base properties shown by Kool as mentioned before.

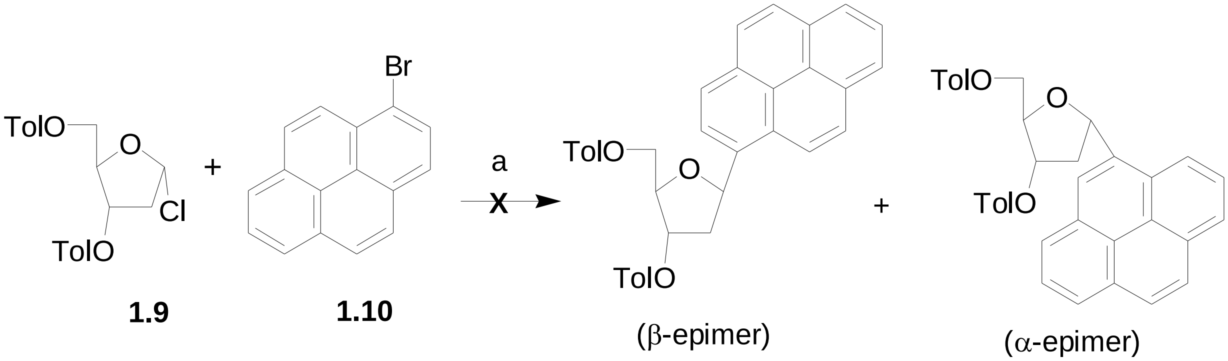

1.9

1.10

a) Mg, THF, $CdCl_2$

Scheme 1.2. Kool's Method for Synthesis of Aryl C-Nucleosides.

Recently, organo-cuprates[5] were discovered to increase the C-glycosylation yield for this reaction in place of the cadmium reagent. The drawback here is that this still involves the use of the 1,2-dideoxy-3,5-*O*-*p*-toluoyl-α-1-chloro-D-ribofuranose and that the reaction favors predominantly the alpha anomer instead of the desired beta anomer form of the natural four bases.

The second approach, an alternative protected glycal, 2-deoxyribonolactone, has been developed by Woski[6] et al in efforts to synthesize nucleosides. Aryllithium reagents were added to the ribonolactone followed by stereoselective reduction of the resulting hemiacetal.

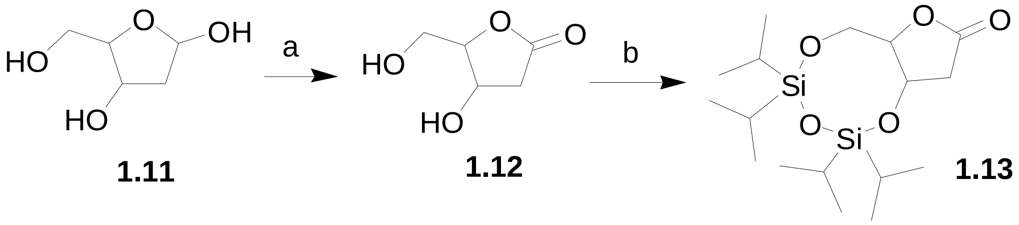

a)Br$_2$, H$_2$O b) Cl(iPr)$_2$Si-O-Si(iPr)$_2$Cl, DMF

Scheme 1.3. Formation of Ribonolactone in Woski's Method for Aryl C-Nucleosides.

Woski's use of 2-deoxyribose (**1.11**) with the disiloxane protecting group gives an 86% yield. Using this quite stable and efficient precursor **1.13**, Chen[7] showed (Scheme 1.4) that a brominated aryl compound **1.14** in the presence of *t*-butyl lithium and THF yields a disiloxane protected nucleoside product **1.15**. The yield is modest with that of 42%, but the reaction is highly stereoselective with. a 10:1 ratio of β:α anomers. However, the yield for the initial approach by Kool[8] for a pyrene-nucleoside was modest with 48% as well. Using this idea, we attempted to synthesize our pyrene nucleoside with 1-bromopyrene (**1.16**).The first drawback of this approach was synthesizing **1.12**. This first step involves stirring **1.11** in water for 5 days which was nonpractical for us. After synthesizing **1.12,** protection of the 5' hydroxyl and 3' hydroxyl group were protected in 45% yield compared to Woski's 86% reported. The reaction is moisture sensitive and proved to be difficult. Attempts at the stereoselectively addition of the pyrene Grignard reagent with ribonolactone **1.13** were unsuccessful in my hands. Yields were trace amounts and various conditions with smaller aromatic substiuents like phenyl were attempted. The result always ended up with several UV active spots on thin layer chromatography.

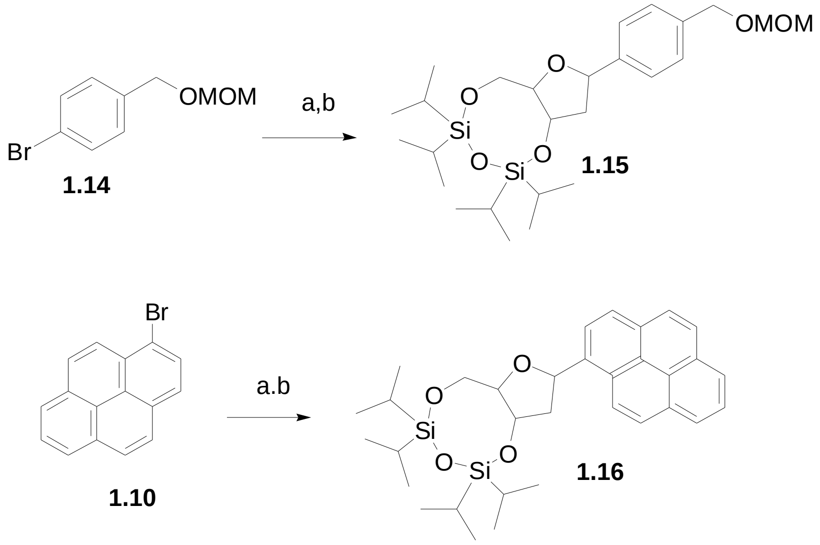
Br
OMOM
1.14
a,b
O
OMOM
O
Si
O
Si
O
1.15
Br
1.10
a.b
O
O
Si
O
Si
O
1.16

a) t-BuLi, -78°C, **1.13**, b) BF_3-Et_2O, Et_3SiH

Scheme 1.4. Woski's Method for Synthesis of Aryl C-Nucleosides continued.

However, even with this protocol, Woski found poor yields with the larger Grignard reagents. Once again in our hands, yields for our desired nucleosides were poor and the use of an expensive disiloxane reagent made this synthetic approach nonpractical.

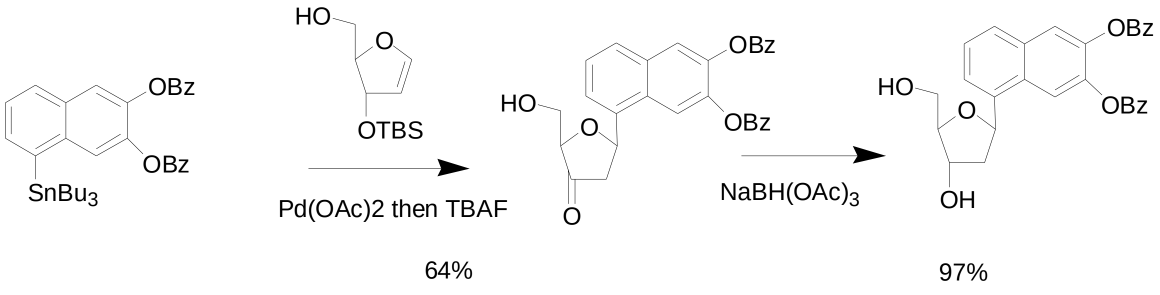
OBz
OBz
SnBu3
HO
O
OTBS
Pd(OAc)2 then TBAF
64%
HO
O
O
OBz
OBz
NaBH(OAc)3
HO
O
OH
OBz
OBz
97%

Scheme 1.5. Daves' Method for Synthesis of Aryl C-Nucleosides.

The third approach available involves introduction of an appropriately functionalized sugar. Daves'[9] protected glycal is somewhat inopportune to synthesize in which a Heck-type coupling is employed with expensive tin reagents to form the C-C bond. Daves' Heck reaction-based approach is efficient, but the preparation and handling of the sensitive furanoglycal intermediate along with the cost drawbacks of the expensive reagents made optimization of this scheme appear not to have the potential for reward. Therefore, we never attempted this approach.

Consideration of the requirements for a practical synthesis caused us to examine schemes that would not require the use of the disiloxane reagent or, in fact, the use of 2-deoxyribose or the 2-deoxyribonolactone. In efforts to finding a more efficient and alternative approach to making aryl *C*-deoxynucleosides, we developed a nine step synthetic route from commercially available inexpensive starting materials.

1.4 Synthesis of Aryl C-Nucleosides

In the search for an alternative approach, we recognized the potential of the stereoselective cycloaddition of nitrile oxides to a chiral olefin (available in two steps from cheap D-mannitol) introduced by Kozikowski[10] which we focused on as part of our approach to synthesizing aryl

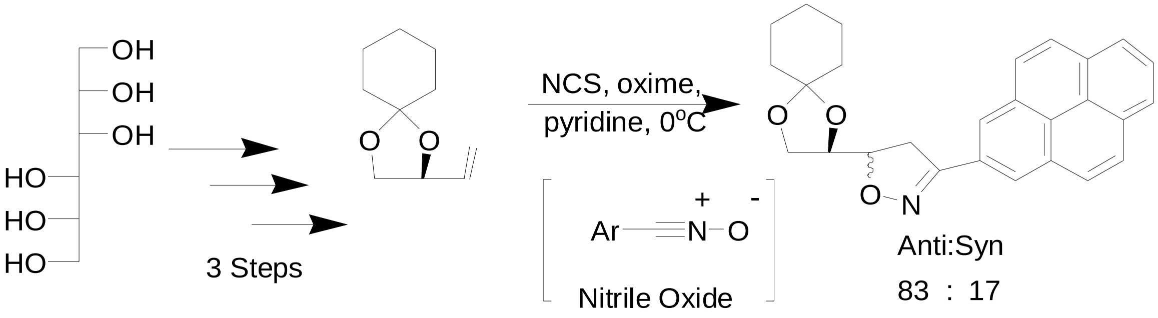

Scheme 1.6. Kozikowski Cycloaddtion Approach.

nucleosides. Kozikowski showed that the stereoselectivity in the cycloaddition reaction (Scheme 1.6) of nitrile oxides to olefins gives an approximately 6:1 ratio of diastereomers with the desired erythro isoxazoline adduct predominating and isomers separable by chromatography.

Progress towards synthesizing a pyrene isoxalozine cycloadduct was hindered initially by

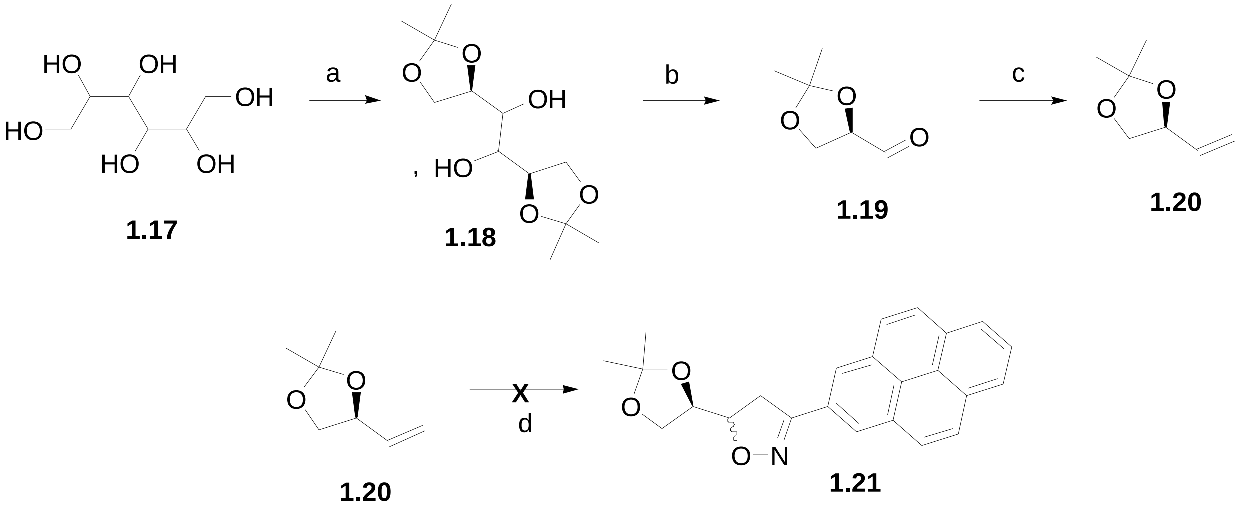

a) Dimethoxypropane, pTsOH, Acetone, 32% b) $NaIO_4$, CH_2Cl_2, 86% c) Ph_3PCH_3Br, nBuLi, THF, d) NCS, oxime, pyridine 0^oC.

Scheme 1.7. Initial attempts to form a pyrene cycloadduct with dimethoxy protected olefin.

the modest conversion to the chiral olefin **1.20**. Starting from commercially available D-mannitol, protection with 2,2 dimethoxypropane gave modest yields (32%) of **1.18** with half the starting material being recovered. The starting material was reused several times. Compound **1.18** would undergo oxidative cleavage with sodium periodate followed by a Wittig reaction to give compound **1.20**. Due to its volatility, trace yields were obtained and difficult to isolate from the Wittig salt from the reaction. Attempts to take the crude product directly and form the pyrene isoxazoline were unsuccessful in our hands. These problems were confirmed and a solution was found by adapting to cyclohexyl protected glyceraldehydes which had been used by Bergmeier[11].

Protection of D-mannitol with cyclohexanone gave an improved yield for the first step from 32% to 59% with this different route and the Wittig reaction of aldehyde **1.23** to **1.24** had proved to be more stable. The 1,3 dipolar cycloaddition with a pyrene oxime that was synthesized from the aldehyde with the chiral olefin **1.24** gave the desired pyrene isoxazoline in a 83:17 anti/syn ratio. The diastereoisomers were separable by column chromatography on silica gel.

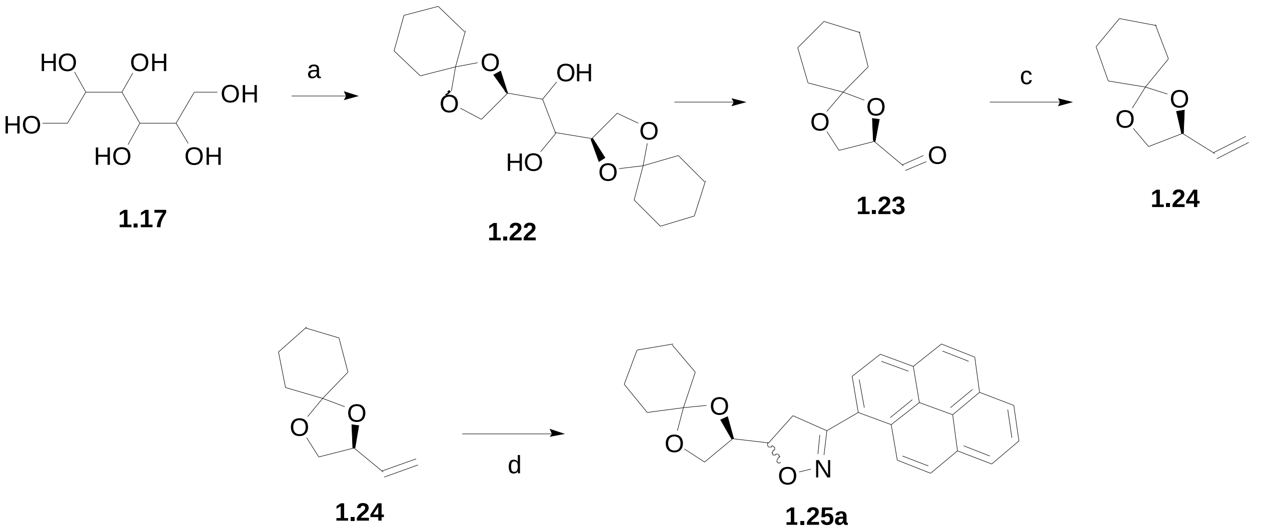

a) $(OCH_3)_3CH$, Cyclohexanone, BF_3-Et_2O, DMSO, 59% b) $NaIO_4$, MeCN/$H_2$0, 89% c) Ph_3PCH_3Br, nBuLi, THF, 77% d) NCS, oxime, pyridine 0^oC, 73%.

Scheme 1.8. Synthesis of pyrene cycloadduct **1.25a** using cyclohexyl protected chiral olefin.

1.4.1 Synthesis of Pyrene Nucleoside

A series of experiments were run in efforts to find what was achievable from the isoxazoline. A Dowex 50X-800 was used to deprotect the cyclohexyl group which

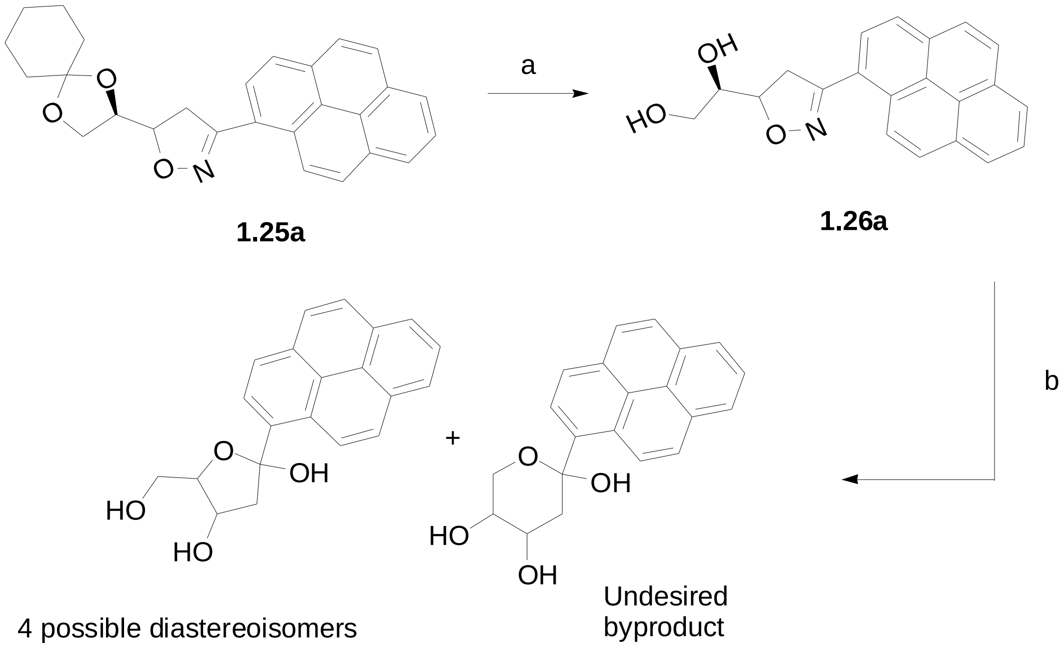

a) Dowex 50X-800, MeOH, 24 hr, r.t. or TFA, 0^oC, H_2O, CH_2Cl_2 b) Ozone, CH_2Cl_2, Me_2S or Raney Nickel, $B(OH)_3$, H_2, MeOH/THF/ H_2O 4/1/1

Scheme 1.9. Potential diastereoisomer formation from unprotected diol **1.26a.**

gave yields of 50% after 24 hours at room temperature. Trifluoroacetic acid conditions were used to increase the yield of product **1.26a** with minimal success. Compound **1.26a** would be subjected to reductive cleavage by Raney nickel conditions, ozonolysis or Samarium (II) iodide. This would potentially give 4 diastereoisomer compounds. It would open the ring and form a beta hydroxy ketone and cyclize into the six and five member nucleoside rings. Since the C-1 hydroxyl is still present, the rings are constantly opening and closing in equilibrium. NMR resulted in many mixtures of products.

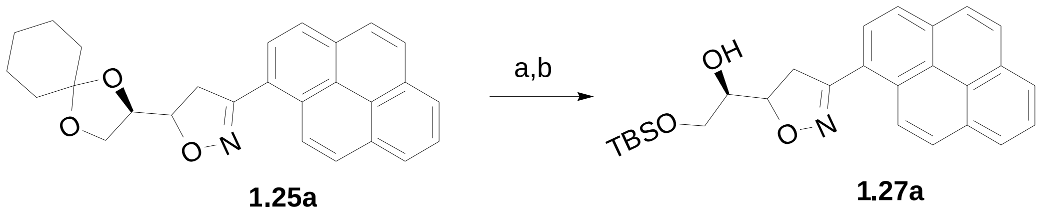

1.25a **1.27a**

a) 1,4-Dioxane,AcOH,reflux b) TBSCl, Imidazole, DMF

Scheme 1.10. Protection/Deprotection for ring cleavage.

The first improvement in the scheme was to change conditions for deprotection to the diol. The use of acetic acid at reflux for several hours gave yields of 85% and higher and the completion time was reduced. Secondly, to prevent the formation of the undesired six membered ring, the primary hydroxyl was protected with *tert*-butyl silane and then compound **1.27a** underwent hydrogenation. The hydrogenation was very clean with 90% or higher yields.

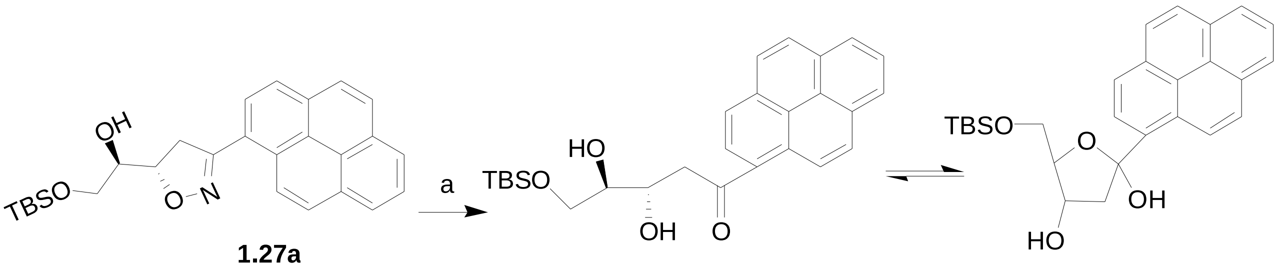

1.27a

a) Raney Ni, H_2, $B(OH)_3$,H_2O,

Scheme 1.11. Formation of hemiacetal from reductive cleavage.

The next step involved removal of the C-1 hydroxyl. Silane reduction should proceed by previously developed approaches[12] providing predominantly the beta C-aryl glycoside. This proved to be quite difficult since the lactol is very Lewis acid sensitive. Standard reduction conditions involved use of borane trifluoride etherate as the Lewis acid. This proved to result in poor yields (5-20%) of the formation of the desired nucleoside. It resulted mostly in undesired elimination and dehydration products that have been investigated and confirmed by

Litvinovskaya[13] et al in other similar dihydroxy keto derivative systems. The search for weaker Lewis acids for reduction has been explored. It has been also shown that under harsher

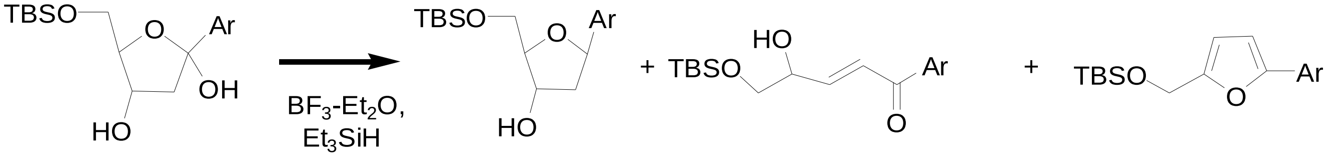

Scheme 1.12. Byproducts from elimination and dehydration of hemiacetal intermediate.

conditions during hydrogenation where more boric acid is involved, we can eliminate one step in our synthesis by directly getting our desired glycoside. However, this led to low resulting (10 - 20%) yields of the nucleoside with a 2:1 β/α ratio as well. Shi[14] et al. showed that reduction of lactols can be achieved in high levels of stereoselectivity with sodium cyanoborohydride in the presence of dichloroacetic acid in trifluoroethanol. Applying this to our scheme, we found that our starting material is slightly soluble in trifluoroethanol. The solvent was changed to tetrahydrofuran and difluoroacetic acid was used instead as well. The reaction was hard to monitor since the starting material and product sit very close to each other. The yields obtained increased to about 30-40%. Further optimization will have to be done. Various conditions involving different acids were done using all the same substrate. The sodium cyanoborohydride/difluoro acetic acid conditions were found to be the best.

The beta and alpha anomers could be separated by flash column chromatography. The

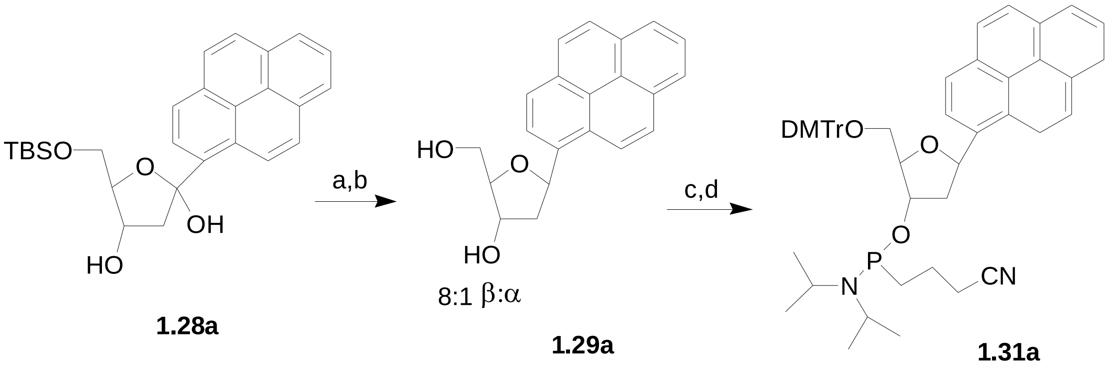

a) CF_3CH_2OH,CCl_3COOH, $NaBH_3CN$ b) TBAF,THF c) DMTrCl, DMAP, Pyridine d)CH_2Cl_2, DIPEA, $(iPr)_2NP(Cl)OCH_2CH_2CN$

Scheme 1.13. Formation of Nucleoside followed by Phosphoramide Activation.

remaining three steps of the synthesis involved TBS deprotection with tetrabutyl ammonium fluoride, reprotection with 4,4-dimethoxytrityl chloride at the 5 hydroxyl group and phosphoramidite protection at the 3-hydroxyl group. Silane deprotection gave 95%+ yields. The use of 4,4-dimethoxytrityl chloride with dimethlyaminopyridine in pyridine involved careful work up. The dimethoxytrityl group is acid labile. Silica gel is acidic and must be pre-equilibrated with triethylamine before the crude product was loaded onto the column. The same applied for compound **1.29a.** This compound will undergo automated DNA synthesis and be used in making oligomer probes for sequencing by hybridization.

In order to cut two steps out of the synthesis, diol **1.26a** had been protected with 4,4-dimethoxytrityl group and then underwent Raney nickel hydrogenation followed by

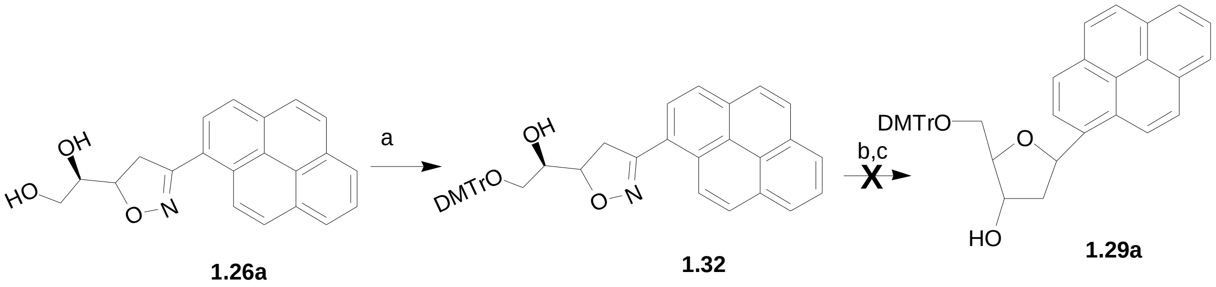

a) DMTrCl, DMAP, Pyridine b)Ra-Ni, $B(OH)_3$, H_2O c)BF_3-Et_2O, Et_3SiH

Scheme 1.14. Dimethoxyltrityl protected isoxazoline **1.32** undergoing hydrogenation.

silane reduction. The dimethoxytrityl group didn’t survive the acid conditions and resulted in unidentifiable products. Therefore, we used the TBS-based synthetic route to synthesize several other aromatic compounds.

1.4.2 Synthesis of Aryl C-Nucleosides

There are currently six aromatic substrates that have undergone this synthetic approach. They are phenyl, 1-napthyl, 2-napthyl, 5-anthracenyl, 5-acenapthyl, and 1-pyrenyl. All isoxazolines were synthesized using the Kozikowski protocol and shown in Figure 1.3. The complete details of the synthesis of each of these nucleosides will be now discussed.

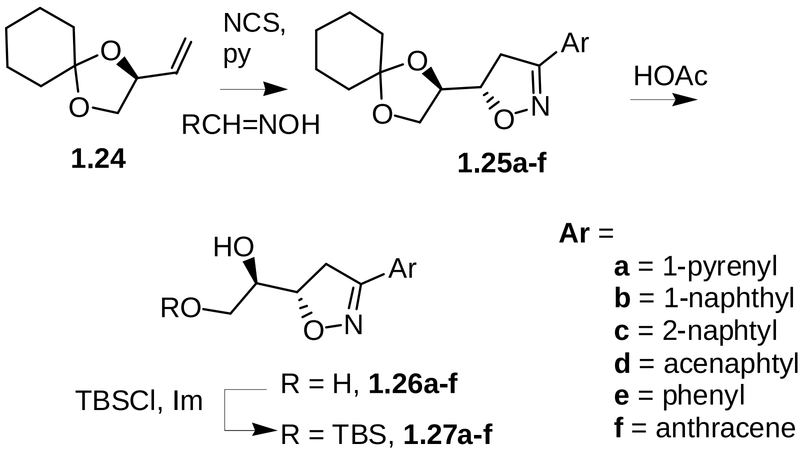
NCS,
py
RCH=NOH
HOAc
1.24
1.25a-f
Ar
HO
RO
O–N
TBSCl, Im
R = H, 1.26a-f
R = TBS, 1.27a-f
Ar =
a = 1-pyrenyl
b = 1-naphthyl
c = 2-naphtyl
d = acenaphtyl
e = phenyl
f = anthracene

Scheme 1.15. Synthesis of Aryl C-Nucleosides.

Compound Ar =	Percent Yields for Cyclohexyl Isoxazolines	Anti/Syn Isomer Ratio of Isoxalozines	Deprotection/ Protection Percent Yields for TBS isoxazolines (2 steps)
R = pyrene	**1.25a**, 73%	83:17	**1.27a,** 90%
R = 1-naphthyl	**1.25b**, 63%	74:26	**1.27b,** 73%
R = 2-naphthyl	**1.25c**, 52%	71:29	**1.27c**, 68%
R = acenaphthyl	**1.25d**, 48%	6:1	**1.27d**, 63%
R = phenyl	**1.25e**, 74%	6:1	**1.27e**, 67%
R = anthracene	**1.25f**, 68%	68:32	**1.27f**, 87%

Table 1.2. 1,3-Dipolar Cycloaddition Reactions of **1.24**. Anti/Syn ratios determined by NMR data.

Starting from chiral olefin **1.24**, the Kozikowski cycloaddtion was performed to yield cycloadducts **1.25a-f** in 48-74% total yields with anti:syn ratios shown in Table 1.2. The diastereoisomers were separated by column chromatography. After deprotection and reprotection of the primary alcohol, we were able to obtain compounds **1.27a-f** in 63-90% yields.

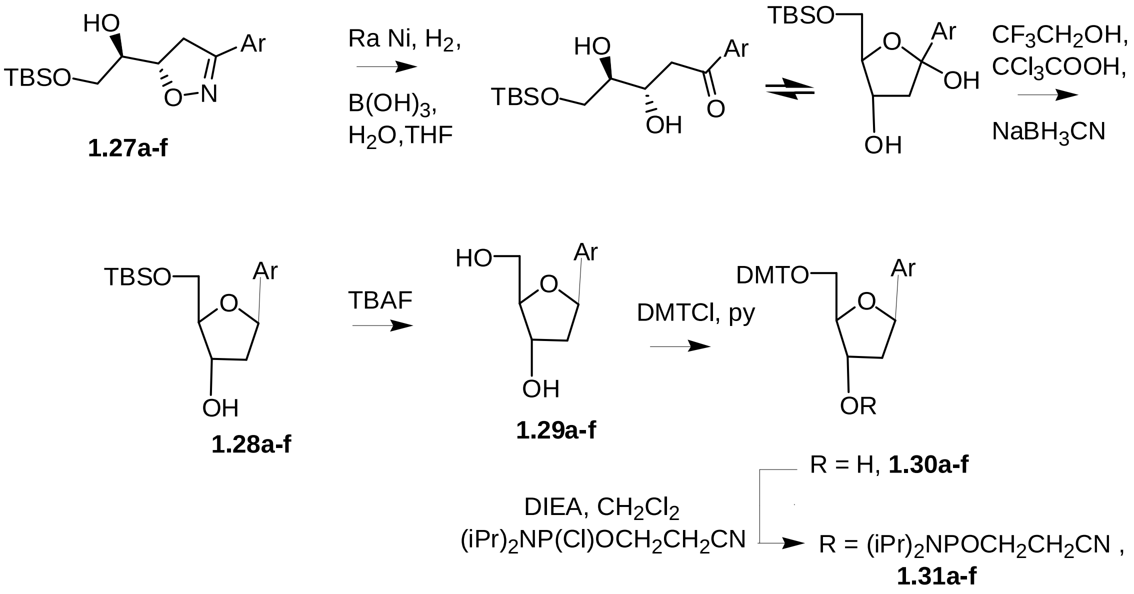
1.27a-f
Ra Ni, H2,
B(OH)3,
H2O,THF
CF3CH2OH,
CCl3COOH,
NaBH3CN
1.28a-f
TBAF
1.29a-f
DMTCl, py
R = H, 1.30a-f
DIEA, CH2Cl2
(iPr)2NP(Cl)OCH2CH2CN
R = (iPr)2NPOCH2CH2CN ,
1.31a-f

Scheme 1.16. Synthesis of Aryl C-Nucleosides continued.

Compound Ar =	Percent Yields for Nucleoside (2 steps)	β/α Isomer Ratio	DMT/ Phosphoramide Percent Yields for Nucleoside (3 steps)
R = 1-pyrenyl	**1.28a**, 37%	3:1	**1.31a,** 41 %
R = 1-naphthyl	**1.28b**, 41%	5:1	**1.31b,** 51%
R = 2-naphthyl	**1.28c**, 36%	3.5:1	**1.31c**, 47%
R = acenaphthyl	**1.28d**, 39%	4.5:1	**1.31d**, 64%
R = phenyl	**1.28e**, 46%	4:1	**1.31e**, 70%
R = anthracene	**1.28f**, 48%	3:1	**1.31f**, 55%

Table 1.3. Nucleoside Formation from TBS-Isoxazolines **1.27a-f**. β/α Isomer ratio were determined by NMR data

This was subjected to opening of the isoxazoline ring and hemiacetal reduction to give nucleosides **1.28a-f** in 36-48% yields in 2 steps. Formation of the phosphoramide **1.31a-f** completed the synthesis of nucleoside to be used in oligomer synthesis in additional 3 steps having yields ranging from 41-70%. Further demonstrating the practicality of this synthetic route, we synthesized aryl-C ribonucleosides.

1.5 Synthesis of Pyrene Riboside

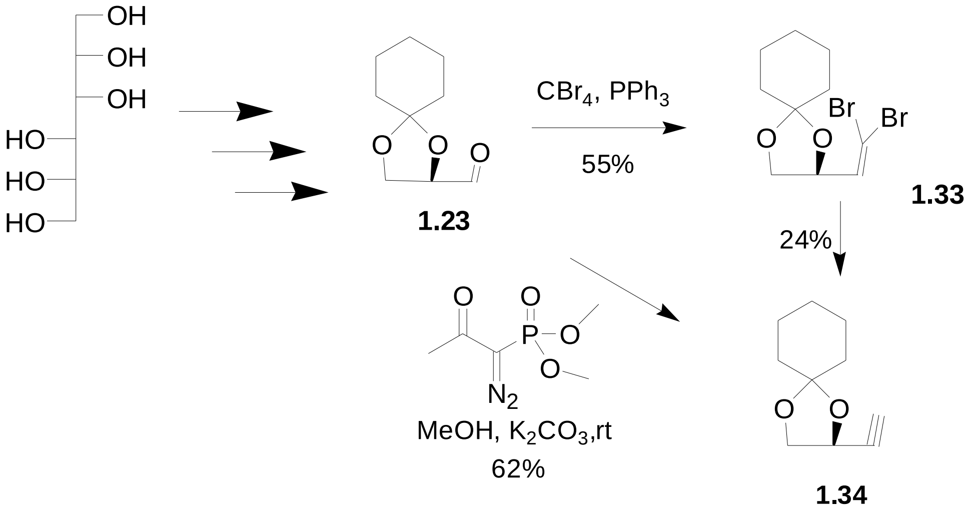

Scheme 1.17. Formation of Chiral Alkyne **1.34**.

Slight modification of our current route allows us to make the riboside as shown in Scheme 1.17. Starting from cyclohexylidene aldehyde **1.23** we first followed a modified[15] Corey-Fuchs sequence by the dibromoalkene **1.33** to alkyne **1.34.** The yields in our hands were poor. Furthermore, it has been claimed that partial racemization can occur. Using the Bestmann-Ohira[16] reagent, the aldehyde was converted to compound **1.34** in a single step with 62% yield. The vinyl boronic ester **1.35** was first prepared by a protocol developed by Jiang[17] et al. This involved a three step one pot reaction that led to trace material only. The vinyl boronic ester **1.35** was obtained in quantitively yield by a Zirconium-catalyzed regioselective hydroboration reported by Kobayashki.[18]

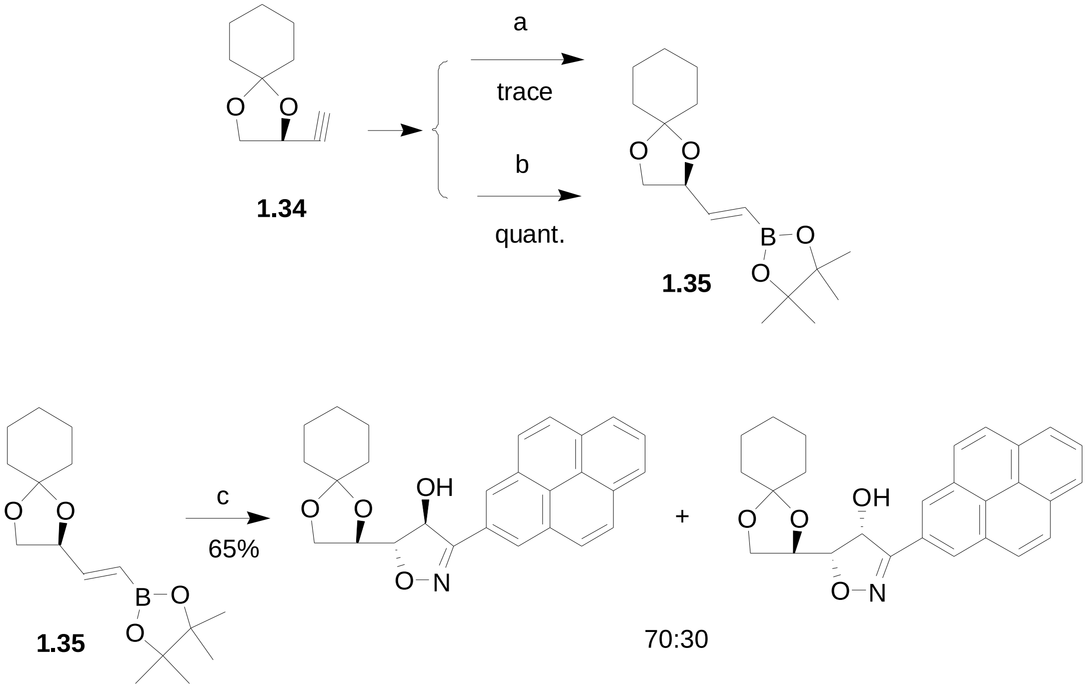

1.34

1.35

1.35

1.36

a) BH_3-SMe_2, DME, Cyclohexene, Me_3NO, Pinacol b) Pinacolborane, Cp_2ZrHCl, Et_3N c) $Na_2CO_3\text{-}_{1.5}H_2O_2$, THF

Scheme 1.18. Formation of Boronic Ester **1.35** followed by cycloaddition.

The vinyl boronic ester **1.35** was reacted with sodium percarbonate to yield cycloadduct **1.36** in 65% total yield with an anti:syn ratio of 70:30. Isomers were separated by column chromatography.

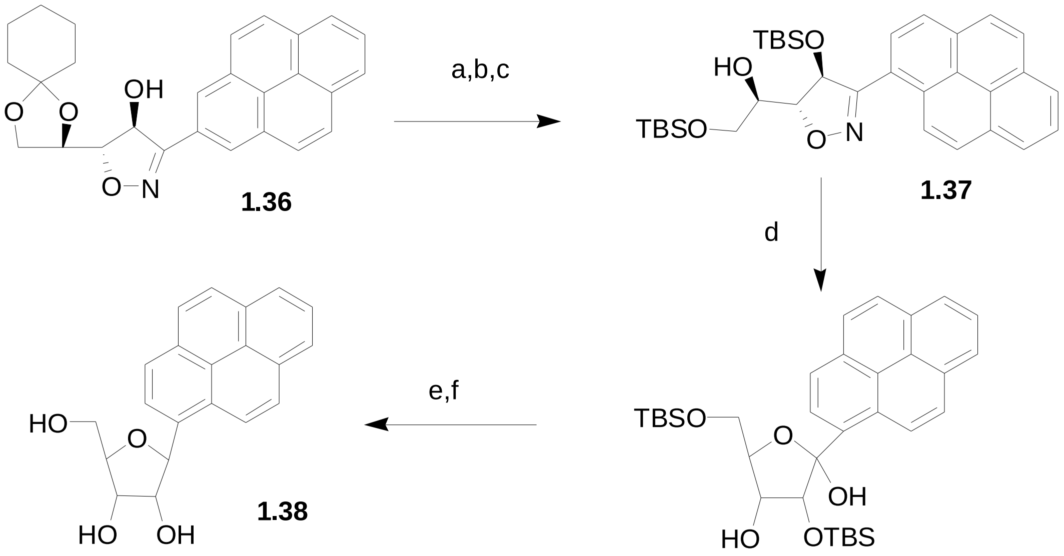

a) TBSCl, DMF, Imidazole; b)AcOH, MeOH or PTSA; c) TBSCl, DMF, Imidazole; d) Raney Ni, H_2, $B(OH)_3$, H_2O,THF; e) CF_3CH_2OH,CCl_3COOH, $NaBH_3CN$; f) TBAF,THF

Scheme 1.19. Generation of Aryl C-Riboside **1.38.**

After a series of protection and deprotection steps, we were able to obtain compound **1.37**. Using the key step from the deoxyriboside synthesis, we were able to reduce the C1 hydroxyl group to afford compound **1.38**. Having the methodology developed, the synthetic portion of the project is completed and the future work will be the synthesis of the oligomer probes.

1.6 Conclusion

In summary, the synthetic approach allows for the synthesis of aryl C-deoxyribosides as well as ribosides from cheap starting materials. The synthetic route is reliable with modest yields in comparison to known current methods in the community. We synthesized a series of six aryl c-nucleosides and one pyrenyl riboside. Future work would involve synthesis of other ribosides, as well as, the synthesis of locked nucleic acids.

1.7 Experimental Section

General Methods

Unless noted otherwise, all oxygen and moisture-sensitive reactions were executed in oven-dried glassware sealed under a positive pressure of dry argon. Moisture-sensitive solutions and anhydrous solvents were transferred via standard syringe and cannula techniques. Unless stated otherwise, all commercial reagents, were used as received. All solvents were dried under argon atmosphere: THF and diethyl ether were distilled over Na-benzophenone; CH_2Cl_2 was distilled from CaH_2. Extracts from work-up procedures were dried over Na_2SO_4 unless otherwise noted. Flash chromatography was performed with silica gel (32-63 mM); analytical TLC was performed with 0.25 mm EM silica gel 60 F254 plates that were visualized by UV irradiation (254 nm) or by staining with 10% PMA. IR spectra were recorded on a Galaxy Series FTIR 3000 infrared and Perkin-Elmer 1600 Series FT-IR spectrophotometers. NMR spectra were obtained with Gemini-300 MHz (Varian), Inova-400 MHz (Varian), Inova-500 MHz (Varian), and Inova-600 MHz (Varian) instruments. Chemical shifts for proton NMR are reported in parts per million (ppm) with chloroform-*d* set at 7.26 ppm as a reference. Chemical shifts for carbon NMR are reported in ppm with the center line of the triplet for chloroform-d set at 78.00 ppm. The following abbreviations are used in the experimental section for the description of ^1H-NMR spectra: singlet (s), doublet (d), triplet (t), quartet (q), multiplet (m), and doublet of doublets (dd). Coupling constants, *J*, are reported in Hertz (Hz).

Synthetic Procedure for *tert*-Butyl *N*-(2-aminoethyl)glycinate (1.3)[3]

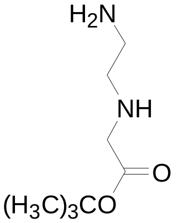

At a reaction temperature of 0~2°C, a 7.42 mL ethylenediamine (**1.2**) solution was mechanically stirred in 50.4 mL of dichloromethane. It had a 2 mL solution of tert-butyl bromoacetate (**1.1**) in 10.8 mL of dichloromethane added to it over one hour dropwise so that an increase in temperature was not observed. Afterwards, the mixture was stirred and allowed to warm to room temperature overnight. Following this, the reaction mixture was washed with water three times (3 x 10 mL) and the combined aqueous solution was washed once with 9.4 mL of dichloromethane. The organic layer was dried over sodium sulfate, filtered, and concentrated to give a yellow oil (376 mg, 76%). Spectroscopic data is comparable to the literature. ^{1}H NMR: ($CDCl_3$, ppm) 3.31 ppm (s, 2H), 2.83 ppm (t, 2H, J = 6.9Hz, J = 8.2 Hz), 2.71 ppm (m, 3H), 1.45 ppm (s, 9H).

Synthetic Procedure for Compound for *t*-Butyl *N*-[2-(*N*-fluorenylmethoxycarbonyl)-aminoethyl]glycinate Hydrochloride (1.4)[3]

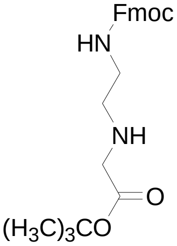

Compound **1.3** (624 mg, 3.81 mmole) was placed in a 250-mL round bottomed flask with 53.4 mL of dichloromethane. To this solution 0.4 mL of diisopropylethylamine was added with mechanical stirring. A solution of 730 mg of Fmoc chloride in 10.1 mL of dichloromethane was added dropwise at room temperature over 40 minutes. The solution mixture was stirred overnight and washed with 6N HCl five times (5 x 15 mL) and once with brine (15 mL). The organic layer was dried over anhydrous magnesium sulfate, filtered, and concentrated. A few drops of dichloromethane were added to prevent impurities from crystallizing in the product. The solution mixture was stored in a refrigerator at –20°C overnight to crystallize. The crystals were collected by vacuum filtration. The crystals had a yellowish tint color. They were washed with a few drops of dichloromethane to yield white crystals. The filtrate was recollected and placed once again in the refrigerator at -20°C for further crystal formation. Compound **1.4** (903 mg, 2.35 mmol) was retrieved giving a percent yield of 61%. Spectroscopic data is comparable to the literature[3]. ^{1}H NMR: ($CDCl_3$, ppm) 7.76 ppm (d, 2H, J= 7.2Hz), 7.73 ppm (d, 2H, J = 10.3Hz), 7.56 ppm (t, 1H, J=8.4Hz, J=7.7Hz), 6.09ppm (s, 1H), 5.39ppm (bs,1H), 4.41 ppm (d, 2H, J = 8.2Hz), 4.23 ppm (d, 1H, J= 6.4 Hz), 3.42 (s, 2H), 2.78 ppm (t, 2H, J=8.3Hz, J=11.2Hz), 1.45 ppm (s,9H).

Synthetic Procedure for 4-fluorophenylacetic PNA, {[2-(9H-Fluoren-9-ylmethoxycarbonylamino)-ethyl]-[2-(4-fluoro-phenyl)-acetyl]-amino}-acetic acid methyl ester (1.5)

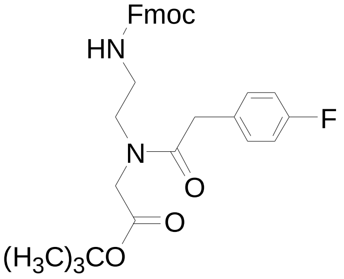

A small scale of compound **1.4** (100 mg, .26 mmole) was placed into 1.4 mL of anhydrous DMF. 98 mg of 4-fluorophenylacetic acid was further introduced to the solution mixture and dissolved with mechanical stirring. Following this addition, 98 mg of EDC was added in two equal amounts over 20 minutes at room temperature. This resulting mixture was stirred overnight and concentrated. The addition of water (5 mL) with vigorously shaking resulted in a precipitate to form. After several minutes, the solution became a sticky viscous oil. Dichloromethane (10 mL) had been used to wash, dissolve, and extract the oil into solution. Flash chromatography on silica gel eluting with 10% MeOH/ CH_2Cl_2 solvent was performed to separate and obtain the desired PNA backbone product **1.5**. The resulting clear oil weighed 160 mg to give a yield of 80%. ^{1}H NMR: ($CDCl_{3,}$ ppm) 7.8-7.7 ppm (m,1H), 7.65-7.6 ppm (m, 2H), 7.4 ppm (m, 2H), 7.3-7.15 ppm (m, 4H), 6.95 (m,3H) 6.41 ppm (m, 1H,), 4.13 ppm (q, 1H, J=6.6Hz, J=11.2Hz), 3.56 ppm (m, 2H), 3.4-3.2 ppm (m, 2H), 2.71(m, 2h), 1.45 ppm (s,9H).

3,5-*O*-((1,1,3,3-tetraisopropyl)disiloxanediyl)-2-deoxy-D-ribono-1,4,-lactone (1.13)[6]

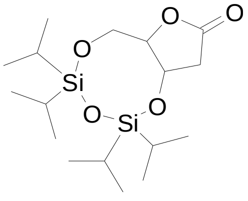

To a solution of 2-deoxy-D-ribose **1.11** (1.00 g, 7.45 mmol) in water (6 mL) was added Br_2 (2 mL). After addition, the flask turned all red and was sealed. The reaction mixture was stirred at rt for 4 days. After the fourth day, the reaction was neutralized with Ag_2CO_3 until the pH of solution was 6.5-7.0. The mixture was then filtered and the filtrate was concentrated at 40°C to yield 2-deoxyribonolactone. The crude product was directly dissolved in anhydrous DMF and imidazole (1.30 g, 18.8 mmol) and 1,3 dichloro-1,1,3,3-tetraisopropyldisiloxane (5.95 mL, 11.3 mmol) were added. The solution stirred for rt for 24hr, and extracted with ether. The organic layer was washed with water, sat. aqueous $NaHCO_3$, and brine. Dried with magnesium sulfate and placed on the column. Product yield (1.45g, 5.04 mmole) was 52% as an oil. Spectroscopic data is comparable to the literature.[6]

^{1}H NMR (250 MHz) $CDCl_3$- δ4.61(m, 1H), 4.15-4.20 (m,2H), 3.90(m,1H), 2.80(dd,1H), 2,71(dd,1H, J= 7.1 Hz, J=10.3 Hz),1.07-1.00(m, 28H)., IR- 2800-2940cm^{-1},1798cm^{-1}

2,3,-*O*-Isopropylidiene-D-glyceraldehyde (1.19) [3]

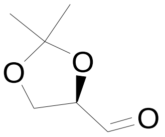

20.00g (.076 mol) of compound **1.18** was disolved in 200 mL of dichloromethane. Sodium periodate (32.4 g) was place in the reaction mixture with vigorous stirring. 5mL of distilled water was added and the reaction was stirred for one hour. 30 grams of anhydrous magnesium sulfate was added to the reaction mixture and allowed to stir for an additional 15 minutes. The reaction was filtered and washed with dichloromethane. The crude solution was distilled at 63°C at to remove the dichloromethane and to obtain compound **1.19** in 86% yield (16.91g, .130 mole). Spectroscopic data is comparable to the literature.

^{1}H NMR ($CDCl_3$) δ 9.58 (d,1H, J=9.2 Hz), 4.28(m,1H), 4.01–3.99(m,2H), 1.45(s,3H),1.39 (s,3H)

1,2:5,6,-di-*O*-cylcohexylidiene-D-mannitol (1.22) [10]

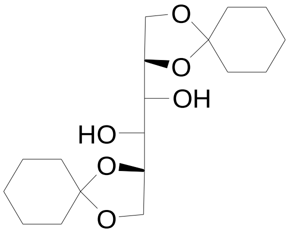

A solution of D-mannitol (400 g, 2.196 mol), cyclohexanone (670 mL, 6.42 mol), trimethyl orthoformate, boron trifluoride etherate (25 mL) and dimethyl sulfoxide was stirred at room temperature. The solution was cloudy at first and became clear after several hours. It was allowed to stir for 24 hours. The reaction mixture was poured into saturated aqueous $NaHCO_3$ (3 x 800 mL) and extracted with diethyl ether (3 x 1 L). The extract was washed with water (500 mL), dried with magnesium sulfate, and concentrated under reduced pressure. The amorphous precipitate was recrystallized from n-hexanes to yield white crystals (443 g, 59% yield) M.P. 105.5° C. Spectroscopic data is comparable to the literature.

Synthesis of 2,3-*O*-Cyclohexylidiene-D-glyceraldehyde (1.23) [10]

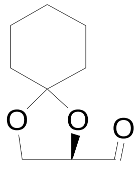

To a solution of 1,2:5,6,-di-O-cylcohexylidiene-D-mannitol diol (40.0 g, 116.8 mmol) in 60% aqueous acetonitrile (200 mL) cooled to 0 °C. Sodium periodate (47.5 g, 220 mmol) was added in portions over 15 minutes. Then the solution was allowed to warm to room temperature, stirred for 2 hours and filtered. The filtrate was portioned between with water and chloroform. The combined organic solution was washed with water and brine, dried (Mg_2SO4), and concentrated. The resulting oil was distilled under reduced pressure (85°C, 15 mmHg) to give colorless oil. (19.0g, 110.4 mmol) The resulting crude oil can also be used directly for the next step. Spectroscopic data is comparable to the literature.

^{1}H 400 Mhz NMR ($CDCl_3$) δ 9.72 (s, 1H), 4.37 (q. 1H) 4.15-4.03(m, 2H), 1.43-1.67 (m, 10H)

Synthesis of (2*S*)-1,2-*O*-Cyclohexylidenebut-3-ene-1,2-diol (1.24) [10]

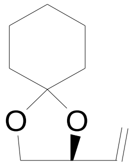

To a mixture of methyltriphenylphosphonium bromide (47.1 g, .132 mol) in 300 mL dry THF at room temperature was slowly added dropwise a 2.5M solution of n-BuLi (55 mL) under an argon atmosphere. The solution was stirred for one hour and then cooled to –78°C and a solution of freshly distilled aldehyde (19.0 g, 110.4 mmol) was added slowly to the mixture and stirred for one hour at this temperature where afterwards it was allowed to warm to room temperature for 20 hours. The reaction mixture was quenched with a saturated aqueous solution of NH_4Cl, extracted with ethyl acetate, washed with brine, dried (Mg_2SO_4) filtered, concentrated and flash column chromatographed with hexanes. The product obtained was a yellow oil (10.95 g, 59%, 65.17 mmole). Spectroscopic data is comparable to the literature.

R_f = .75 (Hex/EA 3:1), IR(neat) 3104,1652, 1142 cm^{-1} ^{1}H 400Mhz NMR ($CDCl_3$) δ 5.78 (m, 1H), 5.30 (d. 1H) 5.17 (d, 1H), 4.48 (q, 1H) 4.08 (dd,1H) 3.59 (t, 1H), 1.37-1.72 (m, 10H)

Synthesis of TBS Olefin, 1-(*tert*-Butyl-dimethyl-silanyloxy)-but-3-en-2-ol

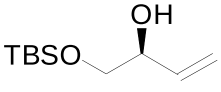

A solution of aldehyde **1.24** in dry dichloromethane had Dowex 50X-800 added to it and stirred at room temperature. The reaction was monitored to completion by TLC and then filtered through celite. To this solution is added tert-butyl dimethysilylchloride and imidazole. The reaction is stirred at room temperature until completion as monitored by TLC .The reaction is quenched with water and diethyl ether is added to extract the solution. The solution is extracted three times and the combined organics are washed by aqueous saturated $NaHCO_3$, water, and brine successively. It was dried, filtered and concentrated. The crude material was purified by flash chromatography (silica gel, 3:1 Hexanes/Ethyl Acetate). The major product obtained was as colorless oil.

R_f = .65 (Hex/EA 3:1), IR(neat) 3404, 3198, 1662, 1132 cm^{-1} ^{1}H 400Mhz NMR ($CDCl_3$) δ 5.72 (m, 1H), 5.32 (d. 1H) 5.18 (d, 1H), 4.48 (q, 1H) 4.09 (dd, 1H) 3.61(t, 1H), 0.976 (bs, 9H), 0.152 (6H).

General Procedure for 1,3 Dipolar Cycloaddition of Isoxazolines

5-(1,4-Dioxa-spiro[4.5]dec-2-yl)-3-pyren-1-yl-4,5-dihydro-isoxazole (1.25a)

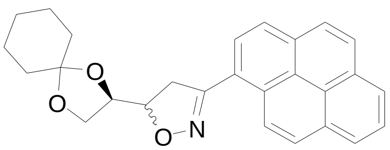

To a magnetically stirred solution of cyclohexylidiene olefin (850 mg, 5.06 mmol), *N*-chlorosuccinimide (743 mg, 5.56 mmol) and dry pyridine (7.59 mmol, 0.65 mL) in 200 mL THF at 0°C under argon, was added dropwise the desired aromatic oxime (1.24g, 5.059 mmol) dissolved in THF. The mixture was allowed to warm up to room temperature and stirred for 24 hours. The mixture was washed with 1N HCl, aqueous saturated $NaHCO_3$, water, and brine successively. It was dried, filtered and concentrated. The crude material was purified by flash chromatography using dichloromethane as the elutant. The product obtained was a yellow-brown solid (1.698 g, 73%). The ratio of anti : syn isomers is was found to be 83:17 from the proton NMR peak shifts. *Major Diastereoisomer* 3,4, anti-^{1}H 600MHz NMR ($CDCl_3$) δ 9.21 (d, 1H), 7.93 (m, 2H), 7.97-8.22 (m, 8H), 4.77 (ddd, 1H), 4.28 (m, 2H), 4.08 (dd, 1H), 3.77(m, 2H), 1.40-1.70 (10H). ^{13}C NMR ($CDCl_3$) δ 157.5,134.2, 131.2, 130.8, 128.8, 128.2, 127.8, 127.3, 126.6, 125.0, 110.6, 80.5, 67.2, 40.9, 36.8, 34.8, 25.3, 24.3, 24.0. HRMS (ESI) Calcd. for $C_{27}H_{26}NO_3$ $[(M + H)]^+$ 412.913, found 412.913.

Minor Diastereoisomer 3,4, syn-^{1}H 300 MHz NMR ($CDCl_3$) δ 8.98 (d, 1H), 7.93 (m, 2H), 7.47-7.62 (m, 5H), 4.86 (ddd, 1H), 4.39 (dd, 1H) 4.15 (m, 2H), 4.02 (dd, 1H), 3.68-3.49 (m, 2H), 1.40-1.70 (10H).

5-(1,4-Dioxa-spiro[4.5]dec-2-yl)-3-naphthalen-1-yl-4,5-dihydro-isoxazole (1.25b)

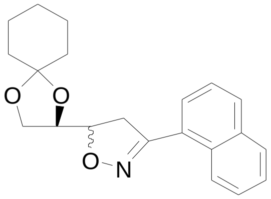

To a magnetically stirred solution of cyclohexylidiene olefin (3.0 g, 17.85 mmol), N-chlorosuccinimide (3.00 g, 22.32 mmol, 1.25 eq) and dry pyridine (32.13 mmol, 2.55 mL, 1.8 eq) in 180 mL dry THF at 0°C under argon, was added dropwise the desired aromatic oxime (3.36 g, 19.64 mmol, 1.1 eq) dissolved in THF. The mixture was allowed to warm up to room temperature and stirred for 24 hours. The mixture was washed with 1N HCl, aqueous saturated $NaHCO_3$, water, and brine successively. It was dried, filtered and concentrated. The crude material was purified by flash chromatography using dichloromethane as the elutant. The products were obtained as a white solid. Total yield for both isomers (4.11 g, 63%).

Major Diastereoisomer 3,4, anti-^{1}H 300 MHz NMR ($CDCl_3$) δ 9.05 (d, 1H), 7.93 (m, 2H), 7.42-7.60 (m, 5H), 4.69 (ddd, 1H), 4.22 (m, 2H), 4.07 (dd, 1H), 3.64-3.73(m, 2H), 1.40-1.70 (10H). ^{13}C NMR ($CDCl_3$) δ 157.5, 134.2, 131.2, 130.8, 128.8, 128.2, 127.8, 127.3, 126.6, 125.0, 110.6, 80.5, 67.2, 40.9, 36.8, 34.8, 25.3, 24.3, 24.0. (3.18 g, 49%). HRMS (ESI) Calcd. for $C_{21}H_{24}NO_3$ $[(M + H)]^+$ 338.1756, found 338.1757.

Minor Diastereoisomer 3,4, syn-^{1}H 300 MHz NMR ($CDCl_3$) δ 8.98 (d, 1H), 7.93 (m, 2H), 7.47-7.62 (m, 5H), 4.86 (ddd, 1H), 4.39 (dd, 1H) 4.15 (m, 2H), 4.02 (dd, 1H), 3.68-3.49(m, 2H), 1.40-1.70 (10H). ^{13}C NMR ($CDCl_3$) δ 157.5,134.2, 131.2, 130.8, 128.8, 128.2, 127.8, 127.3, 126.6, 125.0, 110.6, 80.5, 67.2, 40.9, 36.8, 34.8, 25.3, 24.3, 24.0.(924 mg, 14%).

5-(1,4-Dioxa-spiro[4.5]dec-2-yl)-3-naphthalen-2-yl-4,5-dihydro-isoxazole (1.25c)

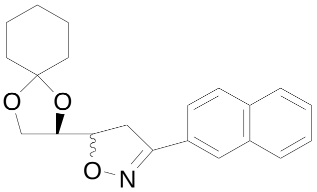

To a magnetically stirred solution of cyclohexylidiene olefin (2.40 g, 14.23 mmol), N-chlorosuccinimide (2.38 g, 17.78 mmol, 1.25 eq) and dry pyridine (28.46 mmol, 2.50 mL, 2.0 eq) in 180 mL dry THF at 0^oC under argon, was added dropwise the desired aromatic oxime (2.70 g, 15.65 mmol, 1.1 eq) dissolved in THF. The mixture was allowed to warm up to room temperature and stirred for 24 hours. The mixture was washed with 1N HCl, aqueous saturated $NaHCO_3$, water, and brine successively. It was dried, filtered and concentrated. The crude material was purified by flash chromatography using dichloromethane as the elutant. The products were obtained as a white solid. .

Major Diastereoisomer 3,4, anti-^{1}H 300MHz NMR ($CDCl_3$) δ 7.83-8.01 (m, 5H), 7.55 (m, 3H), 4.74 (ddd, 1H), 4.17 (m, 2H), 4.02 (dd, 1H), 3.57(m, 2H), 1.40-1.70 (10H). ^{13}C NMR ($CDCl_3$) δ 156.7,133.9, 132.9, 128.4, 128.2, 127.8, 127.7,127.0, 126.8,126.6, 123.4, 110.2, 82.5, 66.8, 53.3, 37.6, 36.5, 34.5, 25.0, 23.9, 23.6. (2.02 g, 52%).

HRMS (ESI) Calcd. for $C_{21}H_{24}NO_3$ $[(M + H)]^+$ 338.1747, found 338.1756.

3-Acenaphthen-4-yl-5-(1,4-dioxa-spiro[4.5]dec-2-yl)-4,5-dihydro-isoxazole (1.25d)

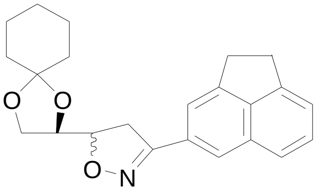

To a magnetically stirred solution of cyclohexylidiene olefin (1.00 g, 6.00 mmol), N-chlorosuccinimide (900 mg, 6.60 mmol) and dry pyridine (9.00 mmol, 0.72 mL) in 25mL chloroform at -10^oC to 0^oC under argon, was added dropwise the desired aromatic oxime (1.15g, 6.06 mmol) dissolved in THF. The mixture was allowed to warm up to room temperature and stirred for 24 hours. The mixture was washed with 1N HCl, aqueous saturated $NaHCO_3$, water, and brine successively. It was dried, filtered and concentrated. The crude material was purified by flash chromatography using dichloromethane as the elutant. The product obtained was a yellow-brown solid (0.595 g, 48%). The ratio of anti : syn isomers is was found to be 78:22 from the proton NMR peak shifts.

Major Diastereoisomer 3,4, anti-^{1}H 600MHz NMR ($CDCl_3$) δ 8.75 (d, 1H), 7.58 (m, 3H), 7.25-7.51 (m, 2H), 4.66 (ddd, 1H), 4.18 (m, 2H), 4.05 (dd, 1H), 3.82(m, 2H), 3.43 (m,4H), 1.42-1.76 (10H). HRMS (ESI) Calcd. for $C_{25}H_{26}NO_3$ $[(M + H)]^+$ 364.1913, found 364.1916.

5-(1,4-Dioxa-spiro[4.5]dec-2-yl)-3-phenyl-4,5-dihydro-isoxazole (1.25e)[10]

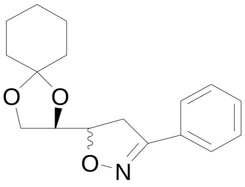

To a magnetically stirred solution of cyclohexylidiene olefin (3.00 g, 17.85 mmol), N-chlorosuccinimide (3.00 g, 22.32 mmol, 1.25 eq) and dry pyridine (32.13 mmol, 2.55 mL, 1.8 eq) in 180 mL dry THF at 0°C under argon, was added dropwise the desired aromatic oxime (2.375 g, 19.64 mmol, 1.1 eq) dissolved in THF. The mixture was allowed to warm up to room temperature and stirred for 24 hours. The mixture was washed with 1N HCl, aqueous saturated $NaHCO_3$, water, and brine successively. It was dried, filtered and concentrated. The crude material was purified by flash chromatography using dichloromethane as the elutant. The products were obtained as a white solid. Total yield for both isomers (4.810 g, 74%). Anti-Syn ratio is 6 to 1.
Major Diastereoisomer 3,4, anti-^{1}H 300 MHz NMR ($CDCl_3$) δ 7.68 (m, 2H), 7.42 (m, 3H), 4.65 (ddd, 1H), 4.03-4.17 (m, 2H), 3.98 (dd, 1H), 3.51(m, 2H), 1.35-1.69 (10H). ^{13}C NMR ($CDCl_3$) δ 157.4,130.9, 130.1, 129.5, 127.5, 111.1, 83.4, 74.8, 67.7, 38.6,37.3, 35.3, 25.8, 24.8, 24.5. (4.18 g, 63%). HRMS (ESI) Calcd. for $C_{25}H_{26}NO_3$ $[(M + H)]^+$ 288.1600, found 288.1591.

Minor Diastereoisomer 3,4, syn-^{1}H 300 MHz NMR ($CDCl_3$) δ 7.68 (m, 2H), 7.42 (m, 3H), 4.65 (ddd, 1H), 4.03-4.17 (m, 2H), 3.98 (dd, 1H), 3.51(m, 2H), 1.35-1.69 (10H). ^{13}C NMR ($CDCl_3$) δ 157.4, 130.9, 130.1, 129.5, 127.5, 111.1, 83.4, 74.8, 67.7, 38.6, 37.3, 35.3, 25.8, 24.8, 24.5. (628 mg, 11%).

3-Anthracen-9-yl-5-(1,4-dioxa-spiro[4.5]dec-2-yl)-4,5-dihydro-isoxazole (1.25f)

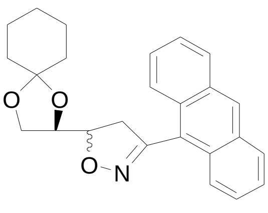

To a magnetically stirred solution of cyclohexylidiene olefin (1.055 g, 6.27 mmol), *N*-chlorosuccinimide (1.00 g, 7.54 mmol) and dry pyridine (9.42 mmol, 0.76 mL) in 1:1 / CH_2Cl_2 : THF at 0°C under argon, was added dropwise the desired aromatic oxime (1.39g, 6.279 mmol) dissolved

in THF. The mixture was allowed to warm up to room temperature and stirred for 18 hours. The mixture was washed with 1N HCl, aqueous saturated NaHCO$_3$, water, and brine successively. It was dried, filtered and concentrated. The crude material was purified by flash chromatography using dichloromethane as the elutant. The product obtained was a yellow-brown solid (1.6435 g, 67.6%). The ratio of anti : syn isomers is unassignable due to overlapping of NMR peaks.
Major Diastereoisomer 3,4, anti-^{1}H 300MHz NMR (CDCl3) δ 8.53 (s, 1H), 8.03 (d, 4H), 7.53(m, 4H), 4.99 (ddd, 1H), 4.57 (dd, 1H), 4.32 (dd, 1H), 3.97(dd, 1H), 3.59 (d, 2H), 1.47-1.73 (10H). ^{13}C 300Mhz NMR (CDCl3) δ 156.7, 131.4, 132.9, 128.4, 128.2, 127.8, 127.7, 127.0, 126.8,126.6, 123.5, 110.9, 81.7, 67.1, 42.8, 36.7, 34.8, 25.4, 24.3, 24.0, R_f =.56
HRMS (ESI) Calcd. for $C_{25}H_{26}NO_3$ $[(M + H)]^+$ 388.1913, found 388.1913.

Minor Diastereoisomer 3,4, syn-^{1}H 600 MHz NMR (CDCl3) δ 8.51 (s, 1H), 8.15 (d, 2H), 8.02 (d,2H) 7.53(m, 4H), 4.99 (ddd, 1H), 4.39 (dd, 1H), 4.18(dd, 2H), 3.55 (d, 2H), 1.46-1.74 (10H). R_f =.47

Deprotection of Isoxazoline followed by Reprotection of Primary Hydroxyl Group

1-(3-Pyren-2-yl-4,5-dihydro-isoxazol-5-yl)-ethane-1,2-diol (1.26a)

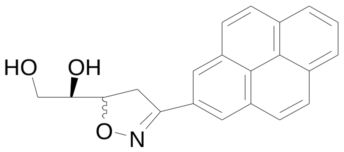

To a solution of 1:1 mixture of 1,4 dioxane/water (40 mL) and the isoxazoline (1.69 g, 4.131 mmol) is added glacial acetic acid (20 mL). The reaction is heated to 90^{o}C and stirred for 3 hours. The reaction is then lowered to room temperature and quenched with 2% NaHCO$_3$. The mixture is extracted with dichloromethane, washed with sat. NaHCO$_3$, water, and brine successively. It was dried (Mg$_2$SO$_4$, filtered and concentrated. The crude material was purified by flash chromatography (silica gel, 2:1 to 1:1 Hexanes/Ethyl Acetate).The product was obtained as a yellow-white solid (1.211g, 89%).
Major Diastereoisomer 3,4, anti-^{1}H 500MHz NMR (Acetone, ppm) δ 9.21 (d, 1H), 7.93 (m, 2H), 7.97-8.22 (m, 8H), 4.82 (ddd, 1H), 3.70-3.95(m, 3H). HRMS (ESI) Calcd. for $C_{21}H_{18}NO_3$ $[(M + H)]^+$ 398.2154, found 398.2151.

1-(3-Naphthalen-1-yl-4,5-dihydro-isoxazol-5-yl)-ethane-1,2-diol (1.26b)[3]

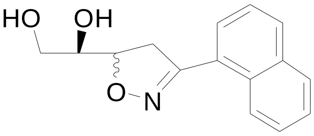

The isoxazoline (1.97 g, 5.39 mmol) was dissolved in a solution of 1:1:1 mixture of 1,4 Dioxane/H_2O/ AcOH (45 mL). The reaction mixture is refluxed for 7 hours at 100^{o}C then cooled to r.t. The solution mixture was reduced under pressure and then extracted with chloroform (3 x 20 mL) and then the combined extracts were washed with 25% aqeous $NaHCO_3$. The crude material was purified on a column starting with 1:1 Hexanes/Ethyl acetate and ending with 100% Ethyl Acetate. The product was a white solid. (993 mg, 74% yield)

Major Diastereoisomer 3,4, anti-^{13}C 300Mhz NMR (CD_3OD) δ 8.85 (d, 1H), 7.87 (m, 2H), 7.49-7.57 (m, 1H) 7.64(m, 3H) 4.78 (ddd, 1H), 3.55-3.72 (m, 2H), 3.85 (dd, 1H), 3.51(m, 2H). ^{13}C NMR (CD_3OD) δ 157.8, 134.2, 130.7, 130.5, 128.5, 128.5, 127.8, 127.3, 126.8, 126.1, 124.9, 80.7, 72.2, 63.2, 38.6.

1-(3-Naphthalen-2-yl-4,5-dihydro-isoxazol-5-yl)-ethane-1,2-diol (1.26c)

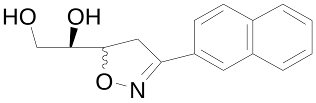

The isoxazoline (2.018 g, 5.43 mmol) was dissolved in a solution of 1:1:1 mixture of 1,4 Dioxane/H_2O/ AcOH (45 mL). The reaction mixture is refluxed for 11 hours at 110^{o}C then cooled to r.t. The solution mixture was reduced under pressure and then extracted with chloroform (3 x 20 mL) and then the combined extracts were washed with 25% aqeous $NaHCO_3$. The crude material was purified on a column starting with 1:1 Hexanes/Ethyl acetate and ending with 100% Ethyl Acetate. The product was a white solid. (933 mg, 73% yield). ^{1}H 300 MHz NMR (CD_3OD) δ 8.05 (m, 3H), 7.42-7.60 (m, 5H), 4.89 (ddd, 1H), 3.82-377 (m, 3H), 3.64-3.73(m, 2H). ^{13}C NMR (CD_3OD) δ 157.8,134.2, 131.5, 128.8, 128.1, 127.8, 127.4,127.2, 126.7,126.6, 125.0, 79.4, 63.8, 40.1.

1-(3-Acenaphthen-4-yl-4,5-dihydro-isoxazol-5-yl)-ethane-1,2-diol (1.26d)

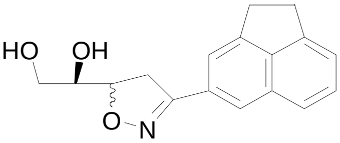

The isoxazoline (595 mg, 1.64 mmol) was dissolved in 20 mL of dichloromethane at 0^{o}C. To the solution mixture is added 80% aqueous trifluoroacetic acid (15 mL) and stirred for 3.5 hours at 0^{o}C.

Afterwards, the mixture is diluted with water and the aqueous layer is extracted with chloroform. The combined organic layers are washed successively with 2% aqeous $NaHCO_3$ and brine. The crude material was purified on a column (3:2 Hex/EA) and obtained as a white solid. (310 mg, 67%). ^1H 300 MHz NMR (C_3D_6O) δ 8.62 (m, 1H), 7.55-7.02 (m, 4H) , 4.71 (m, 1H), 3.49-3.76 (m, 2H), 4.08-4.32 (m, 3H), 3.36 (m, 4H).

1-(3-Phenyl-4,5-dihydro-isoxazol-5-yl)-ethane-1,2-diol (1.26e)

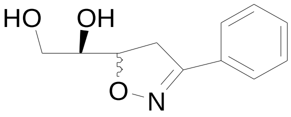

The isoxazoline (3.49 g, 12.2 mmol) was dissolved in a solution of 1:1:1 mixture of 1,4 Dioxane/H_2O/ AcOH (45 mL). The reaction mixture is refluxed for 6 hours at 120^{o}C then cooled to r.t. The solution mixture was reduced under pressure and then extracted with chloroform (6 x 20 mL) and then the combined extracts were washed with 25% aqeous $NaHCO_3$. The crude material was purified on a column starting with 1:1 Hexanes/Ethyl acetate and ending with 100% Ethyl Acetate. The product was a white solid. (1.39 g, 80% yield with 1.06 g of starting material recovered.)

Major Diastereoisomer 3,4, anti-^1H NMR 300Mhz (CD_3OD, ppm) δ 7.71 (m, 2H), 7.47 (m, 3H), 4.75 (ddd, 1H), 3.65-3.70 (m, 2H), 3.78 (dd, 1H), 3.51(m, 2H). ^{13}C NMR (CD_3OD) δ 157.4, 130.1, 129.7, 128.6, 126.6, 81.6, 72.8, 63.1, 35.5.

HRMS (ESI) Calcd. for $C_{11}H_{14}NO_3$ $[(M + H)]^+$ 208.0974, found 208.0974.

1-(3-Anthracen-9-yl-4,5-dihydro-isoxazol-5-yl)-ethane-1,2-diol (1.26f)

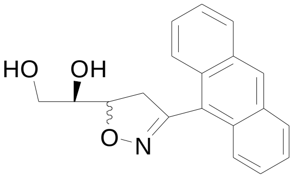

The isoxazoline (5.14 g, 13.3 mmol) was dissolved in a solution of 1:1:1 mixture of 1,4 Dioxane/H_2O/ AcOH (45 mL). The reaction mixture is refluxed for 6 hours at 120 ^{o}C then cooled to r.t. The solution mixture was reduced under pressure and then extracted with chloroform (6 x 20 mL) and then the combined extracts were washed with 25% aqeous $NaHCO_3$. The crude material was purified on a column starting with 1:1 Hexanes/Ethyl acetate and ending with 100% Ethyl Acetate. The product was a white solid. (3.77 g, 92% yield)

^1H NMR 300Mhz (CD_6O, ppm) δ 8.77 (m, 1H), 8.19 (m, 4H), 7.63 (m, 4H), 5.21 (m,1H), 4.64 (m, 1H), 4.11 (dd, 1H), 3.65-3.70 (m, 1H), 2.91 (m,2H). HRMS (ESI) Calcd. for $C_{19}H_{18}NO_3Si$ $[(M + H)]^+$ 308.1287, found 308.1288.

Synthesis of 2-(*tert*-Butyl-dimethyl-silanyloxy)-1-(3-pyren-2-yl-4,5-dihydro-isoxazol-5-yl)-ethanol (1.27a)

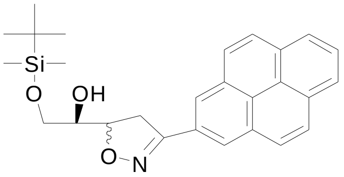

In a solution of dry DMF with the pyrene isoxazoline diol (1.211 g, 3.65 mmol) is added tert-butyl dimethysilylchloride (660 mg, 4.38 mmol) and imidazole (600 mg, 8.76 mmol). The reaction is stirred at room temperature for 15 to 20 minutes. The reaction is quenched with water and diethyl ether is added to extract the solution. The solution is extracted three times and the combined organics are washed by aqueous saturated $NaHCO_3$, water, and brine successively. It was dried, filtered and concentrated. The crude material was purified by flash chromatography (silica gel, 3:1 Hexanes/Ethyl Acetate). The major product obtained was a clear oil. (1.498 g, 92.2%). The minor product was protection of both hydroxyl groups. (62 mg, 3.0%). R_f =.47

Major Diastereoisomer 3,4, anti-^{1}H 500MHz NMR (CDCl3) δ 9.21 (d, 1H), 7.93 (m, 2H), 7.97-8.22 (m, 8H), 4.82 (ddd, 1H), 3.80-3.95(m, 3H), 3.77(m, 2H), .956(bs, 9H), .156 (6H). ^{13}C NMR 300 Mhz(CD_3OD) δ 158.1, 132.2, 131.3, 130.7, 128.9, 128.4, 127.8, 127.3, 126.6, 124.7, 123.5, 80.8, 72.1, 64.5, 40.9, 38.8, 25.3, 18.1, -6.38.). HRMS (ESI) Calcd. for $C_{27}H_{32}NO_3Si$ $[(M + H)]^+$ 446.2151, found 446.2152.

Synthesis 2-(*tert*-Butyl-dimethyl-silanyloxy)-1-(3-naphthalen-1-yl-4,5-dihydro-isoxazol-5-yl)-ethanol (1.27b)

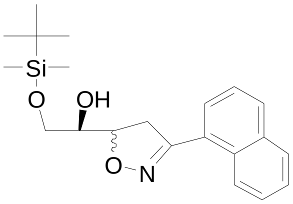

In a solution of dry DMF (11 mL) with the diol (1.35 g, 5.25 mmole) is added tert-butyl dimethysilylchloride (1.12 g, 7.82 mmol, 1.2 eq.) and imidazole (1.06 g, 15.65 mmol, 2.4 eq.). The reaction is stirred at room temperature for 15 minutes.The reaction is quenched with water and diethyl ether is added to extract the solution. The solution is extracted three times and the combined organics are washed by aqueous saturated $NaHCO_3$, water, and brine successively. It was dried, filtered and concentrated. The crude material was purified by flash chromatography (silica gel, 3:1 Hexanes/Ethyl Acetate). The major product obtained was a clear oil. (1.86 g, 4.93 mmole, 94%).

Major Diastereoisomer 3,4, anti-^{13}C 300Mhz NMR (CD_3OD) δ 8.85 (d, 1H), 7.87 (m, 2H), 7. 49-7.57 (m, 1H) 7.64(m, 3H) 4.78 (ddd, 1H), 3.55-3.72 (m, 2H), 3.85 (dd, 1H), 3.51(m, 2H). ^{13}C NMR (CD_3OD) δ 157.8, 134.2, 130.7, 130.5, 128.5, 128.5, 127.8, 127.3, 126.8, 126.1, 124.9, 80.7, 72.2, 63.2, 38.6.

Synthesis of 2-(*tert*-Butyl-dimethyl-silanyloxy)-1-(3-naphthalen-2-yl-4,5-dihydro-isoxazol-5-yl)-ethanol (1.27c)

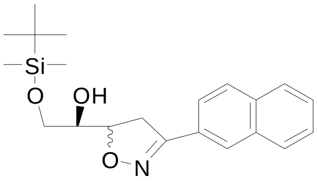

In a solution of dry DMF (20 mL) with the diol (733 mg, 2.85 mmole) is added tert-butyl dimethysilylchloride (5.16g, 3.42 mmol, 1.2 eq.) and imidazole (465 mg, 6.84 mmol, 2.4 eq.). The reaction is stirred at room temperature for 10 minutes. The reaction is quenched with water and diethyl ether is added to extract the solution. The solution is extracted three times and the combined organics are washed by aqueous saturated $NaHCO_3$, water, and brine successively. It was dried, filtered and concentrated. The crude material was purified by flash chromatography (silica gel, 4:1 Hexanes/Ethyl Acetate). The major product obtained was a clear oil. (1.03 g, 98%).

Major Diastereoisomer 3,4, anti-^{1}H 300MHz NMR (CD_3OD) δ 7.83-7.99 (m, 5H), 7.58 (m, 2H), 4.96 (ddd, 1H), 4.07 (dd, 1H), 3.67(m, 3H), 3.49 (dd, 1H), 1.40-1.70 (10H). ^{13}C NMR ($CDCl_3$) δ 157.8,134.2, 131.5, 128.8, 128.1, 127.8, 127.4,127.2, 126.7,126.6, 125.0, 110.2, 79.4, 63.8, 40.1, 26.1, 18.5, -5.1. IR 3446, 2895, 1114, 910 cm^{-1}

HRMS (ESI) Calcd. for $C_{25}H_{26}NO_3$ $[(M + H)]^+$ 372.1995, found 372.1996.

Synthesis of 1-(3-Acenaphthen-4-yl-4,5-dihydro-isoxazol-5-yl)-2-(*tert*-butyl-dimethyl-silanyloxy)-ethanol (1.27d)

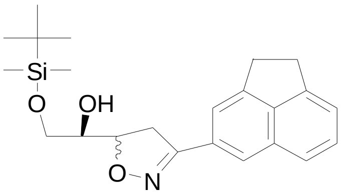

In a solution of dry DMF with the isoxazoline diol (310 mg, 1.09 mmol) is added tert-butyl dimethysilylchloride (166 mg, 1.28 mmol) and imidazole (162 mg, 2.41 mmol). The reaction is stirred at room temperature for 45 minutes.The reaction is quenched with water and diethyl ether is added to extract the solution. The solution is extracted three times and the combined organics are washed by aqueous saturated NaHCO3, water, and brine successively. It was dried, filtered and concentrated. The crude material was purified by flash chromatography (silica gel, 3:1 Hexanes/Ethyl Acetate). The major product obtained was a clear oil. (407 mg, 93.6%)

Major Diastereoisomer 3,4, anti-^{1}H 300MHz NMR (CDCl3) δ 8.77 (d, 1H), 7.58 (m, 2H), 7.41 (d, 1H), 7.28 (d, 1H), 4.71 (ddd, 1H), 3.92(d, 2H), 3.63-3.81 (m,3H), 3.42 (m,4H), .961 (d, 9H), .186 (d, 6H) ^{13}C 300Mhz NMR (CDCl3) δ 158.3, 149.8, 146.4, 139.8, 130.3, 123.6, 122.1,120.5, 118.8, 79.3, 64.2, 39.4, 30.6, 26.1,18.5,–5.1. IR (neat) 3363, 3238, 2959, 1195, 904 cm^{-1} HRMS (ESI) Calcd. for $C_{23}H_{32}NO_3Si$ [(M + H)]$^+$ 398.2151, found 398.2155.

2-(*tert*-Butyl-dimethyl-silanyloxy)-1-(3-phenyl-4,5-dihydro-isoxazol-5-yl)-ethanol (1.27e)

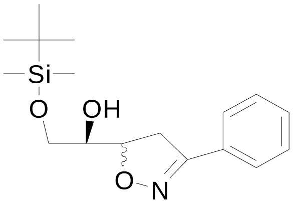

In a solution of dry DMF (15 mL) with the diol (1.35g, 6.52 mmole) is added tert-butyl dimethysilylchloride (1.12 g, 7.82 mmol, 1.2 eq.) and imidazole (1.06 g, 15.65 mmol, 2.4 eq.). The reaction is stirred at room temperature for 10 minutes. The reaction is quenched with water and diethyl ether is added to extract the solution. The solution is extracted three times and the combined organics are washed by aqueous saturated $NaHCO_3$, water, and brine successively. It was dried, filtered and concentrated. The crude material was purified by flash chromatography (silica gel, 4:1 Hexanes/Ethyl Acetate). The major product obtained was a clear oil. (1.76 g, 86%).

Major Diastereoisomer 3,4, anti-^{1}H 300 MHz NMR (CD_3OD) δ 7.71 (m, 2H), 7.47 (m, 3H), 4.75 (ddd, 1H), 3.65-3.70 (m, 2H), 3.78 (dd, 1H), 3.51(m, 2H). ^{13}C NMR (CD_3OD) δ 157.4, 130.1, 129.7, 128.6, 126.6, 81.6, 72.8, 63.1, 35.5.

Synthesis of 1-(3-Anthracen-9-yl-4,5-dihydro-isoxazol-5-yl)-2-*(tert*-butyl-dimethyl-silanyloxy)-ethanol (1.27f)

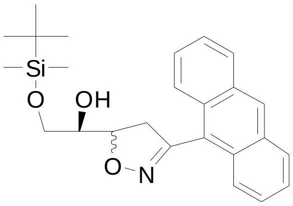

In a solution of dry DMF with the isoxazoline diol (310 mg, 1.09 mmol) is added tert-butyl dimethysilylchloride (166 mg, 1.28 mmol) and imidazole (162 mg, 2.41 mmol). The reaction was stirred at room temperature for 45 minutes. The reaction is quenched with water and diethyl ether is added to extract the solution. The solution is extracted three times and the combined organics are washed by aqueous saturated $NaHCO_3$, water, and brine successively. It was dried, filtered and concentrated. The crude material was purified by flash chromatography (silica gel, 3:1 Hexanes/Ethyl Acetate). The major product obtained was a clear oil. (407 mg, 93.6%)

Major Diastereoisomer 3,4, anti-^{1}H 500MHz NMR (CDCl3) δ 8.53 (s, 1H), 8.03 (t, 4H), 7.53 (quintet, 4H), 5.03 (ddd, 1H), 4.11 (dd, 1H), 3.91 (dd, 2H), 3.64(dd, 1H), 3.54 (dd, 1H), .965 (s, 9H), .167(d,6H) ^{13}C 300Mhz NMR (CDCl3) δ 157.2,131.4, 130.2, 128.9, 126.9, 125.7, 125.2,80.8, 63.8, 42.3, 26.1, 18.6, -5.1 IR 3368, 2929, 2885, 1256, 1055 cm^{-1}.
HRMS (ESI) Calcd. for $C_{25}H_{32}O_3Si$ $[(M + H)]^+$ 422.2151, found 422.2152.

Preparation (1.28a) of 2-(*tert*-Butyl-dimethyl-silanyloxymethyl)-5-pyren-1-yl-tetrahydro-furan-3-ol with BF_3-Et_2O and Et_3SiH Approach

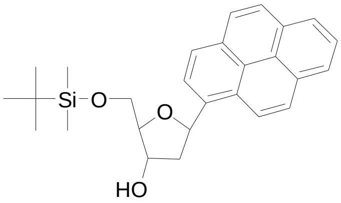

To a round bottom flask was added a catalytic amount of Raney Nickel 2800 in 190 proof ethanol. The flask is charged and flushed three times with hydrogen and stirred for 1 ½ hours. Afterwards, the protected tert-butyl silyl pyrene isoxazoline (1.49g, 3.36 mole) is added with boric acid (8.33g, 134.4 mmole). The solution was stirred for 4 to 6 hours. The reaction mixture is filtered through cellite and concentrated. The solution is diluted with methanol and water. The solution is extracted with dichloromethane three times. The combined organics are washed with 2 % $NaHCO_3$, water, and brine successively. It was dried twice by Mg_2SO_4, filtered and concentrated. The crude material was used directly for the next step.

To a solution of dry dichloromethane and the crude material, is added triethylsilane(16.8 mmole, 2.68 mL) at -78 ^{o}C under argon and then boron trifluoride dietherate (10.1 mmole, 1.29 mL). The solution turns from a yellow to red color after additions. The solution is stirred at this temperature for six hours. Afterwards, the reaction is quenched with aqueous saturated $NaHCO_3$. The solution is diluted with dichloromethane followed by usual aqueous workup of saturated $NaHCO_3$, water, and brine successively. It was dried, filtered and concentrated. The crude material was purified by flash chromatography (silica gel, 3:1 Hexanes/Ethyl Acetate) to give a 8:1 β:α epimer ratio (381 mg, 26% yield).

^{1}H 400MHz NMR ($CDCl_3$) (β-epimer) δ 8.33-8.01 (m, 8H), 6.26 (ddd, 1H), 4.60(m, 1H), 4.23(dd, 1H), 4.06 (d, 1H), 3.93 (m, 1H), 2.64(m, 1H), 2.24 (m,1H), .98((9H,s), R_f=.38,

IR (neat) 3380, 3208, 2857, 1095, 907 cm^{-1}

HRMS (ESI) Calcd. for $C_{27}H_{32}O_3Si$ Na [(M + Na)]$^+$ 455.2018, found 455.2019.

^{1}H 400MHz NMR ($CDCl_3$) (α-epimer) δ 8.33-8.01 (m, 8H), 6.17 (ddd, 1H), 4.64(m, 1H), 4.33(dd, 1H), 4.03 (d, 1H), 3.87 (m, 1H), 3.08(m, 1H), 2.23 (m, 1H). R_f=.41

Byproduct (198mg, 44%) δ 8.75 (d, 1H), 8.33-8.01 (m, 8H), 6.82 (d, 1H), 6.51(d,1H), 4.83(s,2H), .98(m, 9H), .183(m,6H) R_f=.89

Preparation (1.28a) of 2-(*tert*-Butyl-dimethyl-silanyloxymethyl)-5-pyren-1-yl-tetrahydro-furan-3-ol with Na BH_3CN and Cl_2CHOOH Method

To a round bottom flask with the isoxazoline **1.28a** (400 mg, 8.96 mmol) and boric acid (2.78 g, 44.8 mmol) was added a catalytic of Raney Nickel 2800 in 5:1 ratio of THF/water (30 mL). The solution is charged 5 times with hydrogen on a balloon attachment. The solution is stirred for 14 hours. The reaction mixture is filtered through cellite and concentrated. The solution is diluted with dichloromethane and water. The organic layer is separated and the aqeous layer extracted with dichloromethane twice more and combined with the organic layers. The organic layers are washed with sat. aq. $NaHCO_3$ and brine. The crude material was purified by flash chromatography (silica gel, 3:1 Hexanes/Ethyl Acetate) to give (270 mg, 67% yield with 96 mg (24%) recovered starting material). Material was split for multiple reactions.

To a solution of the pyrene hemiacetal (76 mg, 0.167 mmole) and $NaBH_3CN$ (0.835 mmole, 0.85 mL, 5.0 eq.) in anhydrous THF (15 mL) at -25°C, the solution was stirred for 15 minutes and then dichloroacetic acid (66 mg, 0.51 mmole, 3.0 eq.) at -25°C was added to the reaction mixture. The solution was allowed to warm to 0° C for over a span of 1.5 hours. The reaction quenched with saturated aqueous $NaHCO_3$ and extracted with diethyl ether. The organic layers were combined, dried, concentrated and purified by chromatography on silica gel (4:1 Hexanes/Ethyl Acetate).

NMR spectrum the same as above from boron trifluoride etherate procedure.

(β-epimer) 28 mg 35% R_f=.38 , α epimer 8 mg (11%, R_f=.41) ,14.2 mg Starting material (19.0%) R_f=.29. Total overall yield 37% with recovered starting material.

2-(*tert*-Butyl-dimethyl-silanyloxymethyl)-5-naphthalen-1-yl-tetrahydro-furan-3-ol (1.28b)[1]

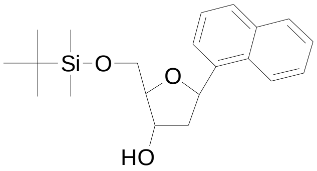

To a round bottom flask was added a catalytic amount of Raney Nickel 2800 in tetrahydrofuran (60 mL) and water (13.5 mL). The flask is charged and flushed five times with hydrogen and stirred for 4 hours with the protected tert-butyl silyl isoxazoline (550 mg, 1.48 mmole) was added with boric acid (551 mg, 8.89 mmole). The reaction mixture is filtered through cellite and concentrated. The solution is extracted with dichloromethane three times. The combined organics are washed with 2 % $NaHCO_3$, water, and brine successively. It was dried twice by Mg_2SO_4, filtered and concentrated. The crude material was used directly for the next step.

To a solution of dry trifluoroethanol (20 mL) and the crude material, is added sodium cyanoborohydride at -25 °C under argon and stirred for 15 minutes, then dichloroacetic acid is added (2.0 eq, 0.26 mL). The solution is stirred at this temperature for one hour. Afterwards, the reaction is quenched with aqueous saturated $NaHCO_3$. The solution is diluted with dichloromethane followed by usual aqueous workup of saturated $NaHCO_3$, water, and brine successively. It was dried, filtered and concentrated. The crude material was purified by flash chromatography (silica gel, 3:1 Hexanes/Ethyl Acetate) to give (211 mg, 41% yield)

^{1}H 400MHz NMR (CDCl3) 8.03(1H,d) 7.96(1H,d), 7.80(2H,t) 7.57(3H,m), 5.99(1H,m), 4.58(m,1H), 4.19(1H,m), 4.02(1H,dd) 3.81(1H,m), 2.60(m,1H), 2.19(1H,m), .980(9H,s),.17(6H,s).^{13}C 300Mhz NMR (CDCl3) δ 138.26,133.87,130.69,129.06,127.98,

126.24,125.86,125.77,123.50,122.38, 86.93,74.96,64.39, 43.04, 25.10,16.62,−5.95.
HRMS (ESI) Calcd. for $C_{21}H_{30}NO_3Si$ Na $[(M + Na)]^+$ 381.1864, found 381.1862.

2-(*tert*-Butyl-dimethyl-silanyloxymethyl)-5-naphthalen-2-yl-tetrahydro-furan-3-ol (1.28c) [1]

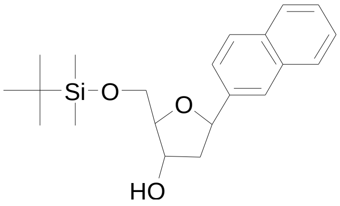

To a round bottom flask was added a catalytic amount of Raney Nickel 2800 in tetrahydrofuran (60 mL) and water (13.5 mL). The flask is charged and flushed five times with hydrogen and stirred for 4 hours with the protected tert-butyl silyl isoxazoline (600 mg, 1.68 mmole) is added with boric acid (621 mg, 10.02 mmole). The reaction mixture is filtered through cellite and concentrated. The solution is extracted with dichloromethane three times. The combined organics are washed with 2 % $NaHCO_3$, water, and brine successively. It was dried twice by Mg_2SO_4, filtered and concentrated. The crude material was used directly for the next step.To a solution of dry trifluoroethanol (20 mL) and the crude material, is added sodium cyanoborohydride at -35 ^oC under argon and stirred for 15 minutes, then dichloroacetic acid is added (2.5 eq, 0.35 mL). The solution is stirred at this temperature for one hour. Afterwards, the reaction is quenched with aqueous saturated $NaHCO_3$. The solution is diluted with dichloromethane followed by usual aqueous workup of saturated $NaHCO_3$, water, and brine successively. It was dried, filtered and concentrated. The crude material was purified by flash chromatography (silica gel, 3:1 Hexanes/Ethyl Acetate). (166 mg, 36% yield) ^1H 500 MHz NMR (CDCl3) 7.85 (4H,m) 7.46 (3H, m), 5.37 (1H, dd), 4.49 (m, 1H), 4.02 (1H,m), 3.90 (1H,dd), 3.78 (1H,m), 2.80 (bs,2H), 2.11(2H,m), .972 (9H,s),.15(6H,s). ^{13}C 300 Mhz NMR (CDCl3) δ 138.56, 133.97, 130.59, 129.06, 127.98, 126.24,125.86,124.77,123.50,122.38, 86.93,76.96,64.39, 43.14, 26.25,17.09,−5.11.

5-Acenaphthen-5-yl-2-(*tert*-butyl-dimethyl-silanyloxymethyl)-tetrahydro-furan-3-ol (1.28d)[1]

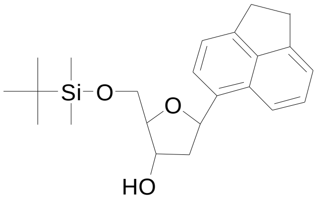

To a round bottom flask was added Raney Nickel 2800 (200 mg) in 95% ethanol (20 mL). The flask was charged and flushed three times with hydrogen and stirred for 1 ½ hours. Then the protected isoxazoline (400 mg, 1.02 mmol) is added with boric acid (6.35 g, 102.5 mmol). The solution is stirred for 18 hours under hydrogen. The reaction mixture is filtered through cellite and concentrated. The solution is diluted with methanol and water. The solution is extracted with dichloromethane three times. The combined organics are washed with 2 % $NaHCO_3$, water, and brine successively. It was dried twice by Mg_2SO_4, filtered and concentrated. The crude material was used directly for the next step. To a solution of dry dichloromethane and the crude material, is added triethylsilane (3.76 mmol, 0.60 mL) at -78 ^{o}C under argon and then boron trifluoride dietherate (4.69 mmol, 0.60 mL). The solution turns from a yellow to red color after additions. The solution is stirred at this temperature for 8 hours. Afterwards, the reaction is quenched with aqueous saturated $NaHCO_3$. The solution is diluted with dichloromethane followed by usual aqueous workup of saturated $NaHCO_3$, water, and brine successively. It was dried, filtered and concentrated. The crude material was purified by flash chromatography (silica gel, 3:1 Hexanes/Ethyl Acetate) to give a (171 mg) 39% yield.

^{1}H 400MHz NMR ($CDCl_3$) δ 7.73 (d, 1H), 7.63 (d, 1H), 7.43 (t, 1H), 7.23(m, 3H), 5.78 (ddd, 1H), 4.50(m, 1H), 4.13(dd, 1H), 3.94(m,1H), 3.76 (m, 2H), 3.37(m, 4H), 2.43(m, 1H), 2.18 (m,1H), .926(s, 9H), .112(6H).^{13}C 400Mhz NMR ($CDCl_3$) δ 146.6,145.7, 139.5, 133.7, 129.1,128.0, 124.7, 119.1,87.0, 74.8, 64.9, 43.0, 30.7, 30.1, 26.1, -5.1. HRMS (ESI) Calcd. for $C_{23}H_{33}NO_3Si$ $[(M + H)]^+$ 385.2199, found 385.2193.

2-(*tert*-Butyl-dimethyl-silanyloxymethyl)-5-phenyl-tetrahydro-furan-3-ol (1.28e)[1]

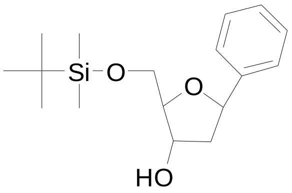

To a round bottom flask is added a catalytic amount of Raney Nickel 2800 in tetrahydrofuran (60 mL) and water (13.5 mL). The flask is charged and flushed five times with hydrogen and stirred for 4 hours with the protected tert-butyl silyl isoxazoline (850 mg, 2.64 mmole) is added with boric acid (985 mg, 15.88 mmole). The reaction mixture is filtered through cellite and concentrated. The solution is extracted with dichloromethane three times. The combined organics are washed with 2 % $NaHCO_3$, water, and brine successively. It was dried twice by Mg_2SO_4, filtered and concentrated. The crude material was used directly for the next step. To a solution of dry trifluoroethanol (35 mL) and the crude material, is added sodium

cyanoborohydride at -25 ^{o}C under argon and stirred for 10 minutes, then dichloroacetic acid is added (3.0 eq, 0.54 mL). The solution is stirred at this temperature for one hour. Afterwards, the reaction is quenched with aqueous saturated $NaHCO_3$. The solution is diluted with dichloromethane followed by usual aqueous workup of saturated $NaHCO_3$, water, and brine successively. It was dried, filtered and concentrated. The crude material was purified by flash chromatography (silica gel, 3:1 Hexanes/Ethyl Acetate). (324 mg, 46% yield)
^{1}H 300MHz NMR (Acetone) 7.48(2H,d) 7.36(3H,m), 5.19(1H,m), 4.51(m,1H), 4.24(1H,d), 4.02(1H,m) 3.81(1H,m), 2.25(m,1H), 1.96(1H,m), .99 (9H,s),.18(6H,s).^{13}C 300 Mhz NMR (CDCl3) δ 128.29,127.36, 126.23, 88.21, 80.15, 73.62, 64.46, 44.76, 25.7, −5.78.

5-Anthracen-9-yl-2-(*tert*-butyl-dimethyl-silanyloxymethyl)-tetrahydro-furan-3-ol (1.28f)

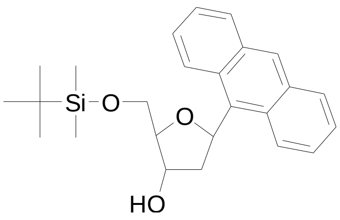

To a round bottom flask is added a catalytic amount of Raney Nickel 2800 in tetrahydrofuran (50 mL) and water (11 mL). The flask is charged and flushed five times with hydrogen and stirred for 4 hours with the protected tert-butyl silyl isoxazoline (395mg, 1.16mole) is added with boric acid (130 mg, 2.70 mmole). The reaction mixture is filtered through cellite and concentrated. The solution is extracted with dichloromethane three times. The combined organics are washed with 2 % $NaHCO_3$, water, and brine successively. It was dried twice by Mg_2SO_4, filtered and concentrated. The crude material was used directly for the next step.

To a solution of dry trifluoroethanol (16 mL) and the crude material, is added sodium cyanoborohydride at -25 ^{o}C under argon and stirred for 10 minutes, then dichloroacetic acid is added (3.0 eq, .21 mL). The solution is stirred at this temperature for one hour. Afterwards, the reaction is quenched with aqueous saturated $NaHCO_3$. The solution is diluted with dichloromethane followed by usual aqueous workup of saturated $NaHCO_3$, water, and brine successively. It was dried, filtered and concentrated. The crude material was purified by flash chromatography (silica gel, 3:1 Hexanes/Ethyl Acetate) to give 174 mg in 48% yield.
^{1}H 300MHz NMR ($CDCl_3$) 8.61 (m,1H), 8.06 (1H,m), 7.62 (1H,m) 7.38(2H,m), 5.86(1H,m), 4.31(m,1H), 4.24(1H,d), 4.02(1H,m) 3.81(1H,m), 2.08(m,1H), 1.96(1H,m), .91 (9H,s),.18(6H,s).

2-Hydroxymethyl-5-pyren-1-yl-tetrahydro-furan-3-ol (1.29a)[1]

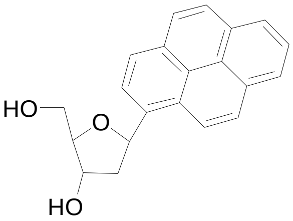

In dry THF at room temperature, the protected pyrene nucleoside (221 mg, .508 mmol) has added dropwise a 1M solution of tetrabutylammonium fluoride in THF (0.81 mL, 0.81 mmol) under an argon atmosphere for 3 hours. The solution mixture is concentrated and diluted by a 1:1 ratio of Hexanes/Ethyl Acetate. The solution mixture is loaded directly for flash column chromatography (silica gel, 1:1 Hexanes/Ethyl Acetate). The product obtained is a yellow-white solid. (151 mg, 92.0%) Spectroscopic data is comparable to the literature. MP 148-150°C. R_f = .093

^{1}H 400MHz NMR (CDCl3) δ 8.29 (d, 1H), 8.19-8.11 (m, 4H), 8.052-7.98 (m, 3H), 6.24 (ddd, 1H), 4.60 (m, 1H), 4.23 (dd, 1H), 3.94 (m, 2H), 2.64 (m, 1H), 2.29 (m,1H). IR (thin film) 3367, 3268, 2877, 1085, 1045, 841, 756 cm^{-1}

HRMS (ESI) Calcd. for $C_{21}H_{19}O_3$ [(M + H)]$^+$ 319.1334, found 319.1330.

2-Hydroxymethyl-5-naphthalen-1-yl-tetrahydro-furan-3-ol (1.29b)[1]

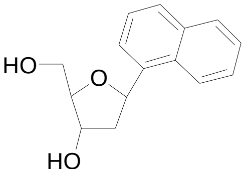

In dry THF at room temperature, the protected nucleoside (105 mg, .430 mmol) has added dropwise a 1M solution of tetrabutyl ammonium fluoride in THF (1.30 mL, 1.32 mmol) under an argon atmosphere for 3 hours. The solution mixture is concentrated and diluted by a 1:1 ratio of Hexanes/Ethyl Acetate. The solution mixture is loaded directly for flash column chromatography (silica gel, 1:1 Hexanes/Ethyl Acetate) (66 mg, 93% yield) Spectroscopic data is comparable to the literature. ^{1}H 400MHz NMR (CDCl3) 8.05 (1H,d) 7.92 (1H,d), 7.83 (2H,t) 7.55(3H,m), 5.95(1H,m), 4.55(m,1H), 4.17(1H,m), 4.05(1H,dd) 3.81(1H,m), 2.60(m,1H), 2.19(1H,m). ^{13}C 300 Mhz NMR (CDCl3) δ 138.56,133.77,130.79,129.06,127.95,126.26,125.86,125.75,123.54,122.35, 86.93,74.96, 64.43, 43.07, 16.67. HRMS (ESI) Calcd. for $C_{15}H_{16}O_3Na$ [(M + Na)]$^+$ 267.0997, found 267.0996.

2-Hydroxymethyl-5-naphthalen-2-yl-tetrahydro-furan-3-ol (1.29c)[1]

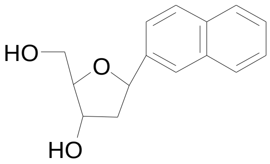

In dry THF at room temperature, the protected nucleoside (126 mg, 0.516 mmol) has added dropwise a 1M solution of tetrabutyl ammonium fluoride in THF (1.51 mL, 1.53 mmol) under an argon atmosphere for 3 hours. The solution mixture is concentrated and diluted by a 1:1 ratio of Hexanes/Ethyl Acetate. The solution mixture is loaded directly for flash column chromatography (silica gel, 1:1 Hexanes/Ethyl Acetate) (80 mg, 94% yield) Spectroscopic data is comparable to the literature.

^{1}H 500MHz NMR (CDCl3) 7.85(4H,m) 7.46(3H,m), 5.37(1H,dd), 4.49(m,1H), 4.02(1H,m), 3.90(1H,dd), 3.78(1H,m), 2.30(m,1H), 2.11(1H,m). ^{13}C 300 Mhz NMR (CDCl3) δ 138.56,133.97,130.59,129.26,127.88, 126.27,125.89,124.77,123.40,122.48, 86.93,76.96,64.59, 43.14,18.72.

5-Acenaphthen-5-yl-2-hydroxymethyl-tetrahydro-furan-3-ol (1.29d)[1]

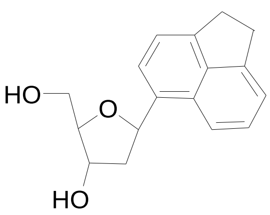

In dry THF at room temperature, the protected nucleoside (170 mg, 0.443 mmol) has added dropwise a 1M solution of tetrabutyl ammonium fluoride in THF (1.3 mL, 1.32 mmol) under an argon atmosphere for 3 hours. The solution mixture is concentrated and diluted by a 1:1 ratio of Hexanes/Ethyl Acetate. The solution mixture is loaded directly for flash column chromatography (silica gel, 1:1 Hexanes/Ethyl Acetate) to give 101.2 mg in 85% yield. Spectroscopic data is comparable to the literature. ^{1}H 400MHz NMR (CDCl3) δ 7.68 (d, 1H), 7.57 (d, 1H), 7.41 (t, 1H), 7.24(m, 3H), 5.74 (ddd, 1H), 4.38(m, 1H), 4.04(dd, 1H), 3.76 (m, 3H), 3.34(m, 4H), 2.38(m, 1H), 2.08.^{13}C 400Mhz NMR (CDCl3) δ 146.6,146.1, 139.6, 132.9, 129.3,128.1, 124.1, 119.2, 87.2, 73.8, 63.6, 42.9, 30.7, 30.1.

2-Hydroxymethyl-5-phenyl-tetrahydro-furan-3-ol (1.29e)[1]

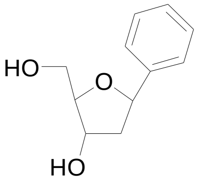

In dry THF at room temperature, the protected nucleoside (225 mg, .704 mmol) has added dropwise a 1M solution of tetrabutyl ammonium fluoride in THF (1.4 mL, 1.40 mmol) under an argon atmosphere for 3 hours. The solution mixture is concentrated and diluted by a 1:1 ratio of Hexanes/Ethyl Acetate. The solution mixture is loaded directly for flash column chromatography (silica gel, 1:1 Hexanes/Ethyl Acetate) (134mg, 98%) Spectroscopic data is comparable to the literature. ^{1}H 400MHz NMR (CDCl3) δ 7.38 (5H,m), 5.20 (1H,m), 4.40 (1H,m), 4.01(1H,m), 3.78 (2H,d), 2.24(1H,m), 1.99(1H,m).

5-Anthracen-9-yl-2-hydroxymethyl-tetrahydro-furan-3-ol (1.29f)

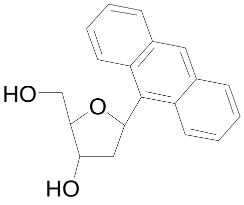

In dry THF at room temperature, the protected nucleoside (150 mg, .310 mmol) has added dropwise a 1M solution of tetrabutyl ammonium fluoride in THF (.60 mL, .600 mmol) under an argon atmosphere for 3 hours. The solution mixture is concentrated and diluted by a 1:1 ratio of Hexanes/Ethyl Acetate. The solution mixture is loaded directly for flash column chromatography (silica gel, 1:1 Hexanes/Ethyl Acetate) (98mg, 86%) ^{1}H 400MHz NMR (CD_6O) δ 8.60 (m,1H), 8.05 (1H,m), 7.62 (1H,m) 7.38(2H,m), 5.82(1H,m), 4.27(1H,m), 4.01(1H,m), 3.78(2H,d), 2.06(1H,m), 2.10(1H,m)

2-[Bis-(4-methoxy-phenyl)-phenyl-methoxymethyl]-5-pyren-1-yl-tetrahydro-furan-3-ol (1.30a)[1]

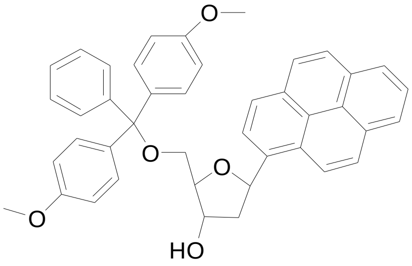

The nucleoside (115 mg, 0.361 mmole) is coevaporated with dry pyridine twice 5 mL and redissolved in dry pyridine (5 mL). 4,4-Dimethoxytrityl chloride (185 mg, 0.542 mmol) is added with a catalytic amount of DMAP at room temperature under an argon atmosphere. The reaction mixture is stirred for 6 hours at room temperature. Afterwards, a 2:1 ratio of ethyl acetate/ brine is added and extracted. The combined extracts are dried (Na_2SO4), filtered and concentrated. The crude material was purified by flash column chromatography. The column is preloaded with 3:1 Hexane/Ethyl Acetate with 5% Triethylamine, The product is eluted with 2:1 Hexane/Ethyl Acetate to yield an oil (125 mg). 56% yield. Spectroscopic data is comparable to the literature.

^{1}H 600MHz NMR (CD_6O) δ 8.48 (d, 1H), 8.42 (d,1H), 8.28 (d, 3H), 8.19(d, 1H), 8.17 (q, 2H), 8.06(t, 1H), 7.58 (d, 2H), 7.47(dd, 4H) 7.31 (t, 2H), 7.21 (t, 1H) 6.90(dd, 4H) 6.21 (ddd, 1H), 4.50(m, 1H), 4.23(dd, 1H), 4.03(m, 1H), 3.75(s, 6H) 3.40 (m, 2H) 2.64(m, 1H), 2.29 (m,1H). HRMS (ESI) Calcd. for $C_{44}H_{35}O_5$ $[(M + H)]^+$ 643.2484, found 643.2482.

2-[Bis-(4-methoxy-phenyl)-phenyl-methoxymethyl]-5-naphthalen-1-yl-tetrahydro-furan-3-ol (1.30b)[1]

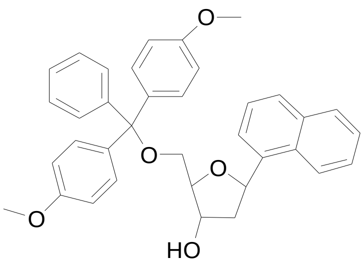

The nucleoside (66 mg, .271 mmole) is coevaporated with dry pyridine twice 5 mL and redissolved in dry pyridine (5 mL). 4,4-Dimethoxytrityl chloride (140 mg, .410 mmol) is added with a catalytic amount of DMAP at room temperature under an argon atmosphere. The reaction mixture is stirred for 6 hours at room temperature. Afterwards, a 2:1 ratio of ethyl acetate/ brine is added and extracted. The combined extracts are dried (Na_2SO4), filtered and concentrated. The crude material was purified by flash column chromatography. The column is preloaded with 3:1 Hexane/Ethyl Acetate with 5% Triethylamine, The product is eluted with 2:1 Hexane/Ethyl Acetate to yield an oil. Product Yield 73% 114 mg. Spectroscopic data is comparable to the literature.

^{1}H 400MHz NMR (CD_6O) 8.05(1H,d) 7.92(1H,d), 7.83(2H,t),7.61(1H.d), 7.55(3H,m), 7.28-7.22(5H,m), 6.88(4H,dd) 5.95(1H,m), 4.55(m,1H), 4.17(1H,m), 4.05(1H,dd) 3.81(1H,m), 3.77(6H,s) 2.60(m,1H), 2.19(1H,m).

^{13}C 300 Mhz NMR (C_3D_6O) 159.0, 138.56,135.1,133.77,130.79, 129.06, 127.95, 127.8, 126.70, 126.26,125.86,125.75,123.54, 122.35, 86.93,78.11, 74.96,64.43, 54.07,44.13,43.0, 20.42,18.67.

2-[Bis-(4-methoxy-phenyl)-phenyl-methoxymethyl]-5-naphthalen-2-yl-tetrahydro-furan-3-ol (1.30c)[1]

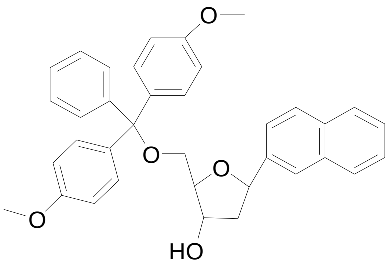

The nucleoside (80 mg, 0.327 mmole) is coevaporated with dry pyridine twice 5 mL and redissolved in dry pyridine (5 mL). 4,4-Dimethoxytrityl chloride (165 mg, 0.490 mmol) is added with a catalytic amount of DMAP at room temperature under an argon atmosphere. The reaction mixture is stirred for 6 hours at room temperature. Afterwards, a 2:1 ratio of ethyl acetate/ brine is added and extracted. The combined extracts are dried (Na_2SO4), filtered and concentrated. The crude material was purified by flash column chromatography. The column is preloaded with 3:1 Hexane/Ethyl Acetate with 5% Triethylamine, The product is eluted with 2:1 Hexane/Ethyl Acetate to yield an oil. Product yield 64%, 114 mg. Spectroscopic data is comparable to the literature.

^{1}H 500MHz NMR (C_3D_6O) 7.85 (4H,m) 7.46(3H,m)7.51(1H.m),7.33-7.28 (5H,m) 6.88 (4H,dd), 5.37(1H,dd), 4.46(m,1H), 4.04(1H,m), 3.91(1H,dd),3.79(7H,m), 2.28(m,1H), 2.13(1H,m). ^{13}C 300 Mhz NMR (C_3D_6O) δ 159.33, 139.24, 138.56,133.97,130.59,129.26,127.68,126.77,126.27, 125.89,124.77,123.40,121.48, 86.53,78.44, 76.65,64.53, 54.77, 43.14, 20.45,19.03.

5-Acenaphthen-5-yl-2-[bis-(4-methoxy-phenyl)-phenyl-methoxymethyl]-tetrahydro-furan-3-ol (1.30d)[1]

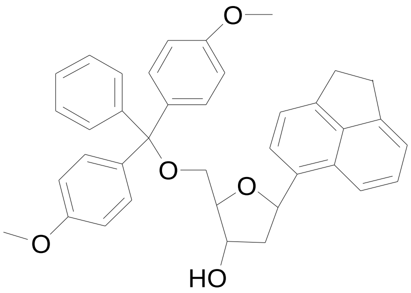

The nucleoside (101.2 mg, 0.375 mmol) was coevaporated with dry pyridine twice 5 mL and redissolved in dry pyridine (5 mL). 4,4-dimethoxytrityl chloride (0.600 mmol, 202 mg) is added with a catalytic amount of DMAP at room temperature under an argon atmosphere. The reaction mixture is stirred for 6 hours at room temperature. Afterwards, a 2:1 ratio of ethyl acetate/ brine is added and extracted. The combined extracts were dried (Na_2SO_4), filtered and concentrated. The crude material was purified by flash column chromatography. The column is preloaded with 3:1 Hexane/Ethyl Acetate with 5% Triethylamine, The product is eluted with 2:1 hexane/ethyl acetate to yield an oil (131 mg, 61%). R_f = .236 (Hex/EA 3:1)

^{1}H 300MHz NMR (C_3D_6O) δ 7.89 (d, 1H), 7.75 (d,1H), 7.60 (d, 2H), 7.40 (m, 6H) 7.38-7.23 (m, 7H), 6.90(dd, 4H) 5.77 (ddd, 1H), 4.50(m, 1H), 4.20(dd, 1H), 4.09(m, 2H), 3.78(s, 6H) 3.37 (m, 4H) 2.91(m, 1H), 2.51(m, 1H), 2.14 (m,1H). ^{13}C 300Mhz NMR (Acetone) δ 158.9, 146.6,146.1, 136.4, 134.4, 132.9, 130.4, 129.3,128.1, 127.9, 126.8,124.1, 119.2, 86.5, 77.7, 73.8, 63.6, 59.9, 54.8, 43.6, 30.7, 30.1, 20.2, 13.8.

2-[Bis-(4-methoxy-phenyl)-phenyl-methoxymethyl]-5-phenyl-tetrahydro-furan-3-ol (1.30e)[1]

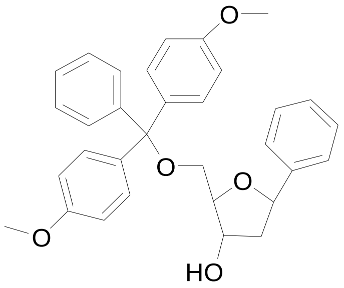

The nucleoside (124 mg, 0.639 mmole) was coevaporated with dry pyridine twice 5 mL and redissolved in dry pyridine (5 mL). 4,4-Dimethoxytrityl chloride (325 mg, 0.958 mmol) is added with a catalytic amount of DMAP at room temperature under an argon atmosphere. The reaction mixture is stirred for 6 hours at room temperature. Afterwards, a 2:1 ratio of ethyl acetate/ brine is added and extracted. The combined extracts are dried (Na_2SO4), filtered and concentrated. The crude material was purified by flash column chromatography. The column is preloaded with 3:1 Hexane/Ethyl Acetate with 5% Triethylamine, The product is eluted with 2:1 Hexane/Ethyl Acetate to yield an oil. Recovered 261mg. 83% yield. Spectroscopic data is comparable to the literature.

^{1}H 300MHz NMR (C_3D_6O) δ 7.5 (2H,m), 7.4-7.11 (m, 13H), 6.8 (m, 4H), 5.16 (1H,m), 4.38 (1H,m), 4.21(1H,m), 4.11 (2H,m), 3.81 (s, 6H) , 2.21 (1H,m) , 1.95 (1H,m)

5-Anthracen-9-yl-2-[bis-(4-methoxy-phenyl)-phenyl-methoxymethyl]-tetrahydro-furan-3-ol (1.30f)

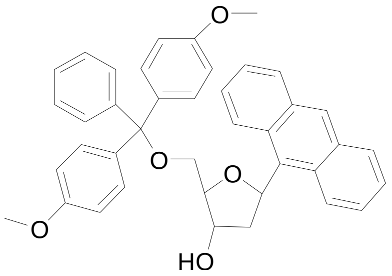

The nucleoside (90 mg, .29 mmole) was coevaporated with dry pyridine twice (5 mL) and redissolved in dry pyridine (5 mL). 4,4-Dimethoxytrityl chloride (165 mg, .44 mmol) is added with a catalytic amount of DMAP at room temperature under an argon atmosphere. The reaction mixture is stirred for 6 hours at room temperature. Afterwards, a 2:1 ratio of ethyl acetate/ brine is added and extracted. The combined extracts are dried (Na_2SO4), filtered and concentrated. The crude material was purified by flash column chromatography. The column is preloaded with 3:1 Hexane/Ethyl Acetate with 5% Triethylamine, The product was eluted with 2:1 Hexane/Ethyl Acetate to yield an oil (141mg, 66%).

^{1}H 300MHz NMR (C_3D_6O) δ 8.60 (m,1H), 8.05 (1H,m), 7.62 (1H,m) 7.42(2H,m), 7.4-7.113(m, 9H), 6.81 (m, 4H), 5.48 (1H,m), 4.38 (1H,m), 4.27(1H,m), 4.03(1H,m), 3.82 (s, 6H) 3.78(2H,d), 2.07(2H,m).

General Procedure for Preparation of 3'-*O*'-Phosphoramidites

Diisopropyl-phosphoramidous acid 2-[bis-(4-methoxy-phenyl)-phenyl-methoxymethyl]-5-pyren-1-yl-tetrahydro-furan-3-yl ester 2-cyano-ethyl ester (1.31a) [1]

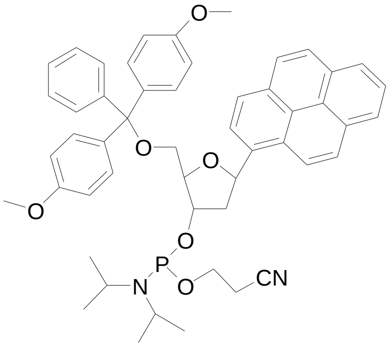

The DMT ether (120 mg, 0.194 mmol) was dissolved in 1mL dry dichloromethane and to this were added diisopropylethylamine (0.18 mL, 0.77 mmol) and 2-cyanoethyl *N*,*N*-diisopropylchlorophosphoramidite (.290 mmol, .07 mL). The reaction mixture was stirred for 1 hour or until completion monitored by TLC. The reaction mixture was concentrated and loaded directly to the flash silica gel column (pre-equilibrated with 6.25% triethylamine in hexanes) and eluted. R_f = .30 (Hex/EA 3:1). Product Yield 127 mg, 80%. Spectroscopic data is comparable to the literature.

^{1}H 600MHz NMR (C_3D_6O) δ 8.71 (1H,d), 8.4(1H,t), 8.05(d,1H), 7.99-7.95(m,3H) 7.90-7.80(m, 4H),7.60 (d,4H), 7.23(2H) 7.09(m,2H), 6.80(d,4H), 6.35(1H,m), 4.90(m,1H), 4.68(1H,m), 3.8-3.4 (m,6H), 3.25(m,6H), 2-75-2.90(1H,m),2.40(1H,m), 1.80(2H,m), 1.1(12H,m). HRMS (ESI) Calcd. for $C_{51}H_{53}N_2O_6SiNaP$ $[(M + Na)]^+$ 843.3559, found 843.3530.

Diisopropyl-phosphoramidous acid 2-[bis-(4-methoxy-phenyl)-phenyl-methoxymethyl]-5-naphthalen-1-yl-tetrahydro-furan-3-yl ester 2-cyano-ethyl ester (1.31b)[1]

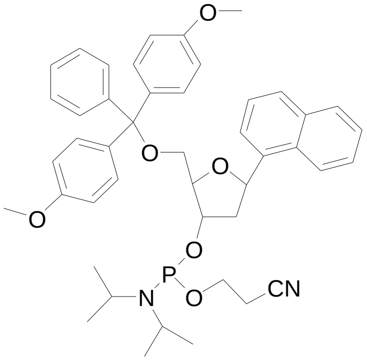

The DMT ether (114 mg, 0.197 mmol) was dissolved in 1.0 mL dry dichloromethane and to this were added diisopropylethylamine (0.19 mL, 0.78 mmol) and 2-cyanoethyl *N,N*-diisopropylchlorophosphoramidite (0.290 mmol, 0.07 mL). The reaction mixture was stirred for 1 hour or until completion monitored by TLC. The reaction mixture was concentrated and loaded directly to the flash silica gel column (pre-equilibrated with 6.25% triethylamine in hexanes) and eluted. R_f = .34 (Hex/EA 3:1). Product Yield 129 mg, 85%. Spectroscopic data is comparable to the literature.

^{1}H 400MHz NMR (C_3D_6O) 8.05(1H,d) 7.92(1H,d), 7.83(2H,t),7.61(1H.d), 7.55(3H,m), 7.28-7.22(5H,m), 6.88(4H,dd) 5.68(1H,m), 4.55(m,1H), 4.17(1H,m), 4.05(1H,dd) 3.81(1H,m), 3.77(6H,s) 3.44(4H,m), 2.60(m,1H), 2.19(1H,m),1.84(2H,m), 1.22-1.29(12H,m).

Diisopropyl-phosphoramidous acid 2-[bis-(4-methoxy-phenyl)-phenyl-methoxymethyl]-5-naphthalen-2-yl-tetrahydro-furan-3-yl ester 2-cyano-ethyl ester (1.31c)[1]

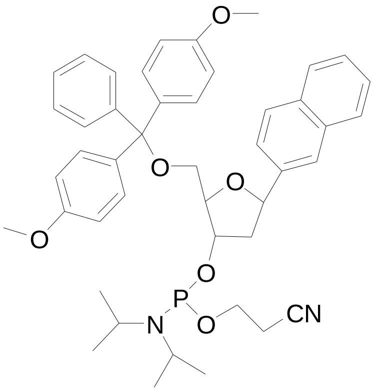

The DMT ether (114 mg, 0.197 mmol) was dissolved in 1mL dry dichloromethane and to this were added diisopropylethylamine (0.18 mL, 0.77 mmol) and 2-cyanoethyl *N,N*-diisopropylchlorophosphoramidite (0.290 mmol, 0.07mL). The reaction mixture was stirred for 1 hour or until completion monitored by TLC. The reaction mixture was concentrated and loaded directly to the flash silica gel column (pre-equilibrated with 6.25% triethylamine in hexanes) and eluted. R_f = .33 (Hex/EA 3:1). Product Yield 124 mg, 82%. Spectroscopic data is comparable to the literature.

^{1}H 500MHz NMR (C_3D_6O) 7.85(4H,m) 7.46(3H,m)7.51(1H.m),7.33-7.28(5H,m) 6.90 (4H,dd),5.39(1H,dd), 4.44(m,1H), 4.03(1H,m), 3.92(1H,dd),3.79-3.71(7H,m), 3.51(4H,m), 2.28(m,1H), 2.13(1H,m), 1.82(2H,m), 1.22-1.27(12H,m).

Diisopropyl-phosphoramidous acid 5-acenaphthen-5-yl-2-[bis-(4-methoxy-phenyl)-phenyl-methoxymethyl]-tetrahydro-furan-3-yl ester 2-cyano-ethyl ester (1.31d)[1]

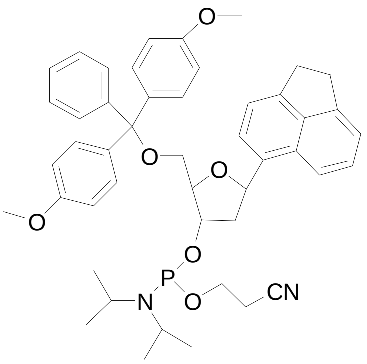

The DMT ether (130 mg, .227 mmol) was dissolved in 10mL dry dichloromethane and to this were added diisopropylethylamine (0.908 mmol, 117 mg, 0.16 mL) and 2-cyanoethyl *N,N*-diisopropylchlorophosphoramidite (0.340 mmol, 0.16 mL). The reaction mixture was stirred for 1 hour or until completion monitored by TLC. The reaction mixture was concentrated and loaded directly to the flash silica gel column (pre-equilibrated with 6.25% triethylamine in hexanes) and eluted.(162mg, 92%) R_f = .552 (Hex/EA 3:1). Spectroscopic data is comparable to the literature.

^{1}H 600MHz NMR (C_3D_6O) δ 7.92 (d, 1H), 7.75 (d,1H), 7.60 (d, 2H), 7.40 (m, 6H) 7.38-7.23 (m, 7H), 6.92(dd, 4H) 5.81 (m, 1H), 4.80(m, 1H), 4.55(m, 1H), 4.09(m, 2H), 3.74(s, 6H) 3.39 (m, 6H) 2.91(m, 1H), 2.71(m, 1H), 2.24 (m,1H), 1.90(2H,m), 1.19(12H,m).

Diisopropyl-phosphoramidous acid 2-[bis-(4-methoxy-phenyl)-phenyl-methoxymethyl]-5-phenyl-tetrahydro-furan-3-yl ester 2-cyano-ethyl ester (1.31e)1

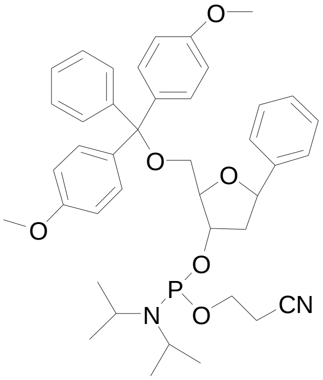

The DMT ether (230 mg, 0.194 mmol) was dissolved in 1mL dry dichloromethane and to this were added diisopropylethylamine (0.43 mL, 1.85 mmol) and 2-cyanoethyl *N,N*-diisopropylchlorophosphoramidite (0.696 mmol, 0.16 mL). The reaction mixture was stirred for 1 hour or until completion monitored by TLC. The reaction mixture was concentrated and loaded directly to the flash silica gel column (pre-equilibrated with 6.25% triethylamine in hexanes) and eluted. (Hex/EA 3:1). Spectroscopic data is comparable to the literature. Product Yield 286 mg, 89%.

^{1}H 600MHz NMR (C_3D_6O) δ 7.81 (2H,d), 7.61 (6H,m), 7.30 (6H,m), 7.10 (2H,m), 6.91(4H,m), 5.45 (1H,m), 4.80 (1H,m), 4.60 (1H,m), 3.61(4H,m), 3.40(6H,m) 3.38 (2H,m),2.40-2.60 (1H,dddd), 2.20(1H,m) 1.80(1H,m), 1.21(12H,m).

Diisopropyl-phosphoramidous acid 5-anthracen-9-yl-2-[bis-(4-methoxy-phenyl)-phenyl-methoxymethyl]-tetrahydro-furan-3-yl ester 2-cyano-ethyl ester (1.31f)

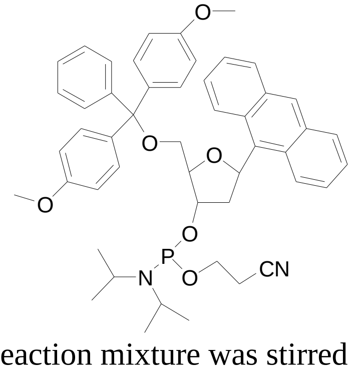

The DMT ether (130 mg, .27 mmol) was dissolved in 1mL dry dichloromethane and to this were added diisopropylethylamine (.18 mL, .77 mmol) and 2-cyanoethyl *N,N*-diisopropylchlorophosphoramidite (.32 mmol, .08 mL). The reaction mixture was stirred for 1 hour or until completion monitored by TLC. The reaction mixture was concentrated and loaded directly to the flash silica gel column (pre-equilibrated with 5% triethylamine in hexanes) and eluted. R_f = .27 (Hex/EA 3:1). Product Yield 131 mg, 70%. Spectroscopic data is comparable to the literature.

^{1}H 500MHz NMR (C_3D_6O) 8.55(m,1H), 7.98 (1H,m), 7.85(4H,m) 7.46(3H,m)7.51(1H.m),7.33-7.28(5H,m) 6.90 (4H,dd),5.82(1H,m), 4.44(m,1H), 4.03(1H,m), 3.92 (1H,dd), 3.79-3.71(7H,m), 3.51(4H,m), 2.08(m,1H), 2.13(1H,m), 1.82(2H,m), 1.22-1.27(12H,m).

Synthesis of 1,2-cyclohexylidenedioxybut-3-yne (1.34) [17]

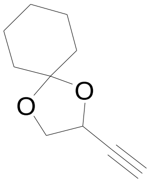

A solution of aldehdye **1.23** (491 mg, 2.85 mmol) and the Bestmann reagent (620 mg, 3.425 mmol) in 40mL of methanol was cooled to $0^{o}C$. Potassium carbonate (788 mg, 5.71 mmol) was gradually added for 30 minutes. The mixture was allowed to warm to rt and was stirred for overnight (12 hours). The solution went from cloudy to clear overnight. To the reaction mixture was added saturated aqueous ammonium chloride and extracted with pentane (2 x 100 mL). The organic layer was separated and purified by flash chromatography in pentane-diethyl ether 8:1 ratio. 297mg of product was recovered in 53% yield. Spectroscopic data is comparable to the literature.

^{1}H 400MHz NMR ($CDCl_3$) δ 4.71(1H, ddd), 4.15(1H,dd) 3.93(1H,dd), 2.47(s,1H), 1.3-1.60(10H), IR(neat) 3104,1652,1142 cm^{-1} HRMS (ESI) Calcd. for $C_{10}H_{15}O_2$ $[(M + H)]^+$ 167.1077, found 167.1072.

2-[2-(4,4,5,5-Tetramethyl-[1,3,2]dioxaborolan-2-yl)-vinyl]-1,4-dioxa-spiro[4.5]decane (1.35)[18]

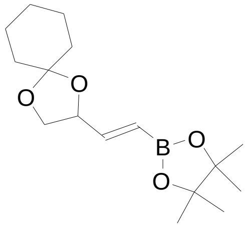

Method 1: Under dry argon, BH3-SMe2 complex (100 uL of a 10M solution in dimethyl sulfide, 1.00 mmol) in (1 mL; DME) was stirred at room temperature. After addition of cyclohexene, a colorless precipitate formed within 2 hour and then alkyne was added. Stirring continued until a clear solution formed. Trimethylamine *N*-oxide was added and after 1 hour pinacol was added. The reaction was stirred until no further consumption of diol was indicated. The solvent was

removed and loaded directly onto a column for purification in 10:1hexanes/ether. Trace amounts detected. Resulted in starting material recovery.

Method 2: To a mixture of alkyne (1.0 g, 7.14 mmol) and 4,4,5,5-tetramethyl-[1,3,2] dioxaborolane (958 mg, 7.49 mmol) was added bis(cyclopentadienyl)zirconium chloride hydride (183 mg, 0.714 mmol) and triethylamine (0.72 mg, 0.714 mmol). The resulting mixture was heated at 60°C for 16 h and diluted with hexanes. The precipitate was removed by filtering over a short pad of silica gel and washed with hexanes. The filtrate was concentrated and dried in vacuum to give 1.76g (93% yield) of desired product.

^{1}H 400MHz NMR ($CDCl_3$) δ 6.51 (1H, dd), 5.71(1H, dd), 4.41(1H, ddd), 4.10(1H,dd) 3.73(1H,dd), 1.45-1.70 (10H,m). HRMS (ESI) Calcd. for $C_{16}H_{27}O_4BNa$ $[(M + Na)]^+$ 317.1900, found 317.1899.

5-(1,4-Dioxa-spiro[4.5]dec-2-yl)-3-pyren-1-yl-4,5-dihydro-isoxazol-4-ol (1.36)

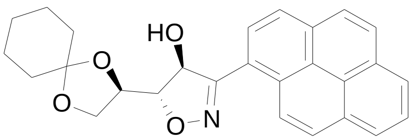

To a magnetically stirred solution of the boronic ester (384 mg, 1.30 mmole), in dry THF at room temperature under argon with pyrene oxime chloride (514mg, 1.82mmol) was added in one pot sodium percarbonate(612 mg, 3.91 mole) at 0°C and stirred overnight. The mixture was allowed to stir at room temperature for 18 hours or until judged to be completed by TLC. The mixture was washed with 1N HCl, aqueous saturated $NaHCO_3$, water, and brine successively. It was dried, filtered and concentrated. The crude material was purified by flash chromatography using a 4:1 ration of Hexanes/Ethyl acetate (541g, 74%).

^{1}H 300MHz NMR (CDCl3) δ 9.11 (d, 1H), 8.73 (m, 1H), 8.02-8.37 (m, 10H), 5.67 (m,1H), 4.63 (m, 1H), 4.29 (dd, 1H), 4.19 (m,1H), 4.01 (m, 1H), 1.40-1.70 (10H). ^{1}H 400MHz NMR (CDCl3) δ158.9, 132.2, 131.1, 130.0, 129.9, 129.4, 127.8, 127.3, 126.6, 124.7, 122.1, 110.9, 88.0, 81.8, 73.5, 67.1, 37.0, 34.8, 25.3, 24.3, 24.0.

2-(tert-Butyl-dimethyl-silanyloxy)-1-[4-(tert-butyl-dimethyl-silanyloxy)-3-pyren-1-yl-4,5-dihydro-isoxazol-5-yl]-ethanol (1.37)

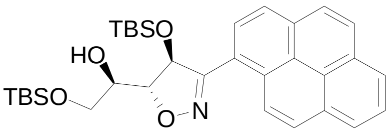

In a solution of dry DMF with the isoxazoline diol (410 mg, 1.29 mmol) is added tert-butyl dimethysilylchloride (176 mg, 1.48 mmol) and imidazole (172 mg, 2.61 mmol). The reaction is stirred at room temperature for 30 min or until completion by TLC.The reaction is quenched with water and diethyl ether is added to extract the solution. The solution is extracted three times and the combined organics are washed by aqueous saturated NaHCO3, water, and brine successively. It was dried, filtered and concentrated. The crude material was purified by flash chromatography (silica gel, 3:1 Hexanes/Ethyl Acetate). The major product obtained was a clear oil. (386 mg, 86%).

^{1}H 300MHz NMR (CDCl3) δ 9.11 (d, 1H), 8.62 (m, 1H), 8.02-8.34 (m, 9H), 5.66 (m, 1H), 4.50 (m, 1H), 4.23 (dd, 1H), 4.17 (m,1H), 4.03 (m, 1H), 0. 93-.97(m, 18H), 0.12-.14 (m, 12H). ^{13}C NMR 400 Mhz(CD$_3$OD) δ 158.1, 132.2, 131.3, 130.1, 129.2, 128.4, 127.8, 127.3, 126.6, 124.7, 122.5, 80.9, 72.1, 64.5, 40.9, 38.8, 25.6, 25.3, 18.2, 18.1, -5.59, -4.6.

2-Hydroxymethyl-5-pyren-1-yl-tetrahydro-furan-3,4-diol (1.38)

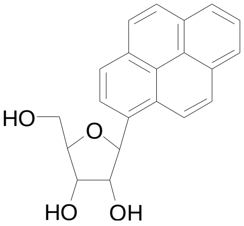

To a round bottom flask with the isoxazoline **1.37** (300 mg, .90 mmole) and boric acid (268 mg, 4.42 mmol) is added a catalytic of Raney Nickel 2800 in 5:1 ratio of THF/water (20 mL). The solution is charged 5 times with hydrogen on a balloon attachment. The solution is stirred for 14 hours. The reaction mixture is filtered through cellite and concentrated. The solution is diluted with dichloromethane and water. The organic layer is separated and the aqeous layer extracted with dichloromethane twice more and combined with the organic layers. The organic layers are washed with sat. aq. NaHCO$_3$ and brine. The crude material was used directly for the next step. To a solution of the hemiacetal was added NaBH$_3$CN (4.435 mmole, 4.5 mL, 5.0 eq.) in anhydrous THF (15 mL) at -25°C, the solution was stirred for 15 minutes and then dichloroacetic acid (660 mg, 2.70 mmole, 3.0 eq.) at -25°C was added to the reaction mixture. The solution was allowed to warm to 0° C for over a span of 1.5 hours. The reaction quenched with saturated aqueous NaHCO$_3$ and extracted with diethyl ether. The organic layers were combined, dried, concentrated and used directly for the last step without further purification. The crude was dissolved in dry THF (5 mL) and TBAF (3.01 mL, 3.00 mmol) was added and stirred for 3 hours or until complete by TLC monitoring. Solution was concentrated and purified by chromatography on silica gel (10:1 CH_2Cl_2/MeOH).

^{1}H 300MHz NMR (C_3D_6O)) δ 8.29 (d, 1H), 8.2-8.1 (m, 4H), 8.06-7.98 (m, 3H), 6.19 (ddd, 1H), 4.60 (m, 1H), 4.23 (dd, 1H), 3.86-3.90 (m, 2H), 3.61 (m,1H) ^{13}C 400 Mhz NMR (C_3D_6O) 138.56,135.1,133.77,130.79, 129.06, 127.95, 127.8, 126.70,126.26,125.86,125.75,123.54, 122.35, 86.93, 83.2,78.11, 74.96,62.43, 54.07,44.13,43.0, 20.42,18.67.

1.8 References

---

[1] Kool, E.T.; Rumney, S.; Paris, P.L.; Ren, R.X.; Chaudhuri, N.C. Napthalene, Phenanthrene, and Pyrene as DNA Base Analogues: Synthesis, Structure, and Fluorescene in DNA, *J.Am.Chem.Soc*., **1996**; 118; 7671-7678.

[2] Woski, S.A.; Challa, H. Solution Phase Synthesis of Potential DNA Binding Molecules Based on the PNA Backbone. *Tetra. Lett*., **1999**; 40; 419-422.

[3] Thomson, S.A.; Josey, J.A.; Cadilla, R.; Gaul, M.D.; Hassman, F.;Luzzio, M.J.; Pipe, A.J.; Reed, K.L.; Ricca, D.J.; Wiethe, R.W.; Noble, S.A. Fmoc Mediated Synthesis of Peptide Nucleic Acids. *Tetrahedron*,**1995**, *51*, 6179-6194.

[4] Kool, E.T.; Matray, T.J. Selective and Stable DNA Base Pairing without Hydrogen Bonds. *J. Am. Chem.Soc.* **1998**,*120*, 6191-6192.

[5] (a) Beuck, C.; Singh, I.; Bhattacharya, W.H.; Parmar, V.S.; Seitz, O.; Weinhold, W. Polycyclic Aromatic DNA-Base Surrogates: High-Affinity Binding to an Adenine-Specific Base-Flipping DNA Methyltransferase. *Angew. Chem. Int. Ed*. **2003**, *42*, 3958-3960.

(b) Singh, I.; Parmar, V.S.; Seitz, O.; Prasad, A.K.; Hecker, W._Local disruption of DNA-base stacking by bulky base surrogates. *Chem.Comm*, **2002**, 500-501.

[6] (a) Wichai,U. Woski, S.A. Disiloxane-Protected 2-Deoxyribonolactone as an Efficient Precursor to 1,2-Dideoxy-1-β-aryl-d-ribofuranoses. *Org. Lett.*,**1999**, *8*, 1173-1175.

(b) Wichai, U., Woski, S. A. An improved route to 1,2-dideoxy-β-1-phenyl-D -ribofuranose. *Bioorg. Med. Chem. Lett*., **1998**, *8*, 3465-3468.

[7] Chen, D.W.; Janda, K. D.; Beuscher, A.E.; Stevens, R.C. Wirsching P. Lerner, R.A.

Preparation of Stilbene-Tethered Nonnatural Nucleosides for Use with Blue-Fluorescent Antibodies, *J. Org.Chem*, **2001**; 1725-1732.

[8] Kool, E. T.; Chaudhuri, N.C. An Efficient Method for the Synthesis of Aromatic C-nucleosides. *Tet.Lett.,* **1995;** 36; 1795-1798

[9] (a) Zhang, H.C.; Daves, G. D. Jr. Syntheses of Two Pyridine C-Nucleosides as "Deletion-Modified" Analogs of dT and dC. *J. Org. Chem.* **1992**, *57*,4690-4696.

(b) Farr, R.. N; Kwok,D.-I.;Cheng, J.C.-Y.;Daves, G.D.,Jr. Synthetic C-glycosides related to the gilvocarcin, ravidomycin, and chrysomycin antibiotics. *J. Org. Chem.* **1992**, *57*, 2093-2100.

(c) Farr,R.. N; Kwok,D.-I.; Daves, G.D.,Jr. C-Glycoside synthesis by palladium-catalyzed iodoaglycon-glycal coupling.*Organometallics.* **1990**,*97*,3151-3156.

(d) Farr,R.. N; Daves, G.D., Efficient Synthesis of 2′-Deoxy-β-D-furanosyl C-Glycosides. Palladium-Mediated Glycal-Aglycone Coupling and Stereocontrolled β- and α-Face Reductions of 3-Keto-furanosyl Moieties Jr. *J. Carbohydrate Chem.* **1990**, *9*,653-660.

(e) Daves, G.D.,Jr. Syntheses of 2'-deoxypseudouridine, 2'-deoxyformycin B, and 2',3'-dideoxyformycin B by palladium-mediated glycal-aglycon coupling *Acc. Chem. Res.* **1990**, *23*, 201-206. For recent applications of the Daves approach to aryl C-glycosides, see (a) Hsieh, H. –P.; McLaughlin, L.W. *J. Org. Chem.* **1995**,*60*,5356-5459 and (b) Wang, Z.-W.;Wiebe,L.I.; Balzarini, J.; De Clercq, E.; Knaus,E. E. *J. Org. Chem.* **2000**,*65*, 9214-9219.

[10] (a) Kozikowski, A. P.; Ghosh, A.K. Diastereoselection in intermolecular nitrile oxide cycloaddition (NOC) reactions: confirmation of the "anti-periplanar effect" through a simple synthesis of 2-deoxy-D-ribose. *J. Am. Chem.Soc.* **1982**, *104*, 5788. and Diastereofacial Selection in Nitrile Oxide Cycloaddition Reactions. *J. Org. Chem.* **1984**,*49* ,2762-2772.

(b) Kozikowski, A. P. Asymmetric induction in nitrone cycloadditions: a total synthesis of acivicin by double asymmetric induction. Acc. *Chem.Res.* **1984**, *17*, 410-416.

(c) see also Gravestock, M.B.; Patron, R. M.; Todd, C. J. Stereoselective Cycloaddition of Nitrile Oxides to a Dispiroketal- Protected But-3-ene-1,2-diol.*Tetrahedron Assymetry*, **1995**,*6*, 2723-2730.

(d) Jager, V.; Schohe, R., Synthesis of amino sugars via isoxazolines DL- and D-lividosamine (2-amino-2, 3-dideoxy-*ribo*-hexose) derivatives from 4-vinyl-1,3-dioxolanes and nitroacetaldehyde acetals. *Tetrahedron*, **1984**, 2199.

---

[11] Bergeimer, S.R; Stanchina, D.M. Acylnitrene Route to Vicinal Amino Alcohols. Application to the Synthesis of (−)-Bestatin and Analogues*J. Org. Chem.* **1999**, *64*, 2852- 2859.

[12] (a) Chen, D.W.; Janda, K.; Preparation of Stilbene-Tethered Nonnatural Nucleosides for Use with Blue-Fluorescent Antibodies, *J. Org.Chem*, **2001**; 1725-1732.
b) Kool, E.T.; Rumney, S.; Paris, P.L.; Ren, R.X.; Chaudhuri, N.C. Napthalene, Phenanthrene, and Pyrene as DNA Base Analogues: Synthesis, Structure, and Fluorescene in DNA, *J.Am.Chem.Soc*., **1996**; 118; 7671-7678.

[13] Litvinovskaya, R.P.; Drach, S.V., Khripach, V.A. Synthesis of polyhydroxylated steroid side chains through 22-isoxazol-5'-ylsteroid.s *Rus, J. Org, Chem*. **1998**, *34*, 647-654.

[14] Shi, H.; Liu, H.; Bloch, R.; Mandville, G.. A Novel Efficient and Stereoselective Synthesis of cis- or trans-2,5-Disubstituted Tetrahydrofurans.*Tetrahedron*, **2001**, *57*, 9335-9341.

[15] Jiang, B.; Ma, P. An Improved Synthesis of 3,4-*O*-Isopropylidene Butyne. *Synth.Communication*,**1995**, 25,3641.

[16] (a) Bestmann, H.J.; Roth, G.J.; Muller, S.; An Improved One-pot Procedure for the Synthesis of Alkynes from Aldehydes. *Synlett*, **1996**, 521

(b) Brown, D.G.; Velthuisen, E.J.; Commerford, R.G.; Hoye, T.R. A Convenient Synthesis of Dimethyl (Diazomethyl) phosphonate. *J .Org.Chem*., **1996**, 61, 2540-2541.

(c) Baum, J.S.; Shook, D.A. Diazo transfer reactions with p-acetamidobenzenesulfonylazide. *Synth. Commun*., **1987**,17, 1709-1716.

(d) Kitamura, M.; Tokunaga, M.; Noyori,R. Asymmetric Hydrogenation of .beta.-Keto Phosphonates: A Practical Way to Fosfomycin *J.Am.Chem.Soc*. **1995**, 117, 2931-2932.

[17] Zhang, A.; Kan, Y.; Zhao, G-L.; Jiang, B.1,3-Dipolar Cycloaddition of Chirally Modified Vinylboronic Ester with Nitrile Oxides. *Tetrahedron*, **2000**, *56*, 965-970.

[18] Kobayashki, M.; Kotoku, N.; Sumii, Y.; Hayashi, T. Synthesis of CD-ring structure of cortistatin A, an anti-angiogenicsteroidal alkaloid from marine sponge. *Tet. Lett.* **2008**, *49*, 7078–7081.

Appendix for Chapter I

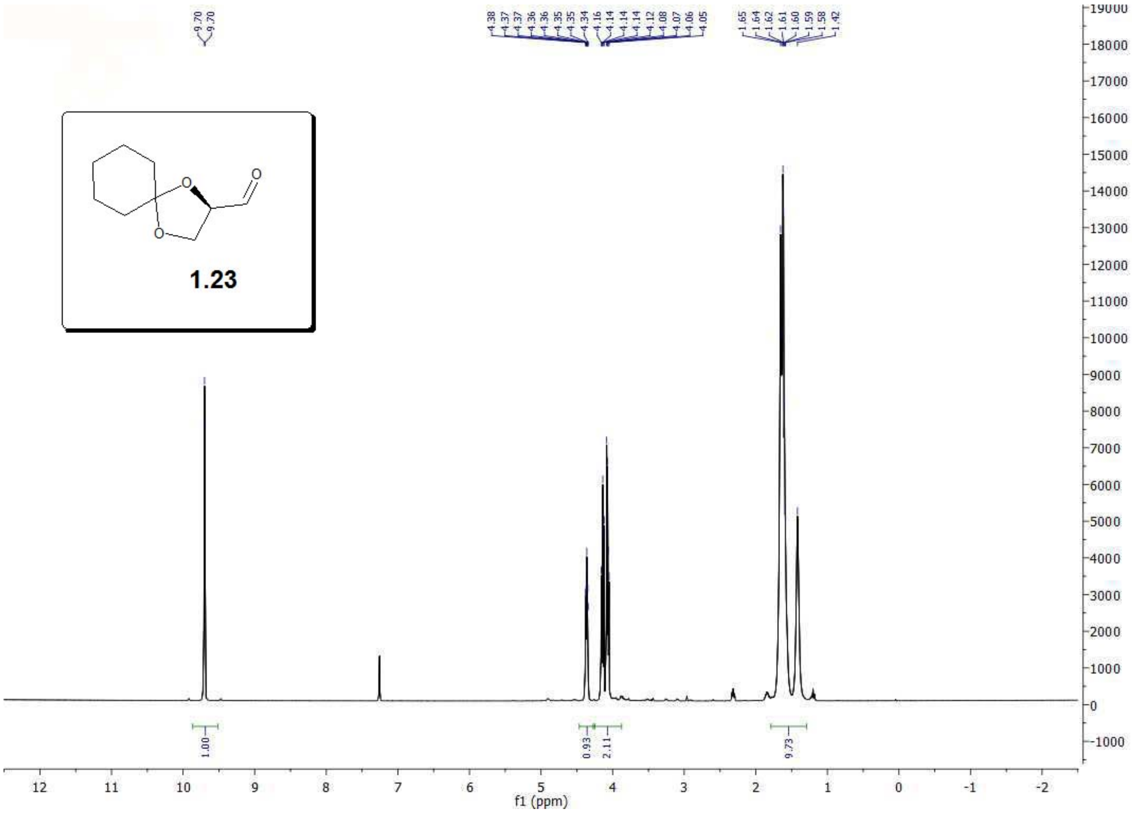

1.23

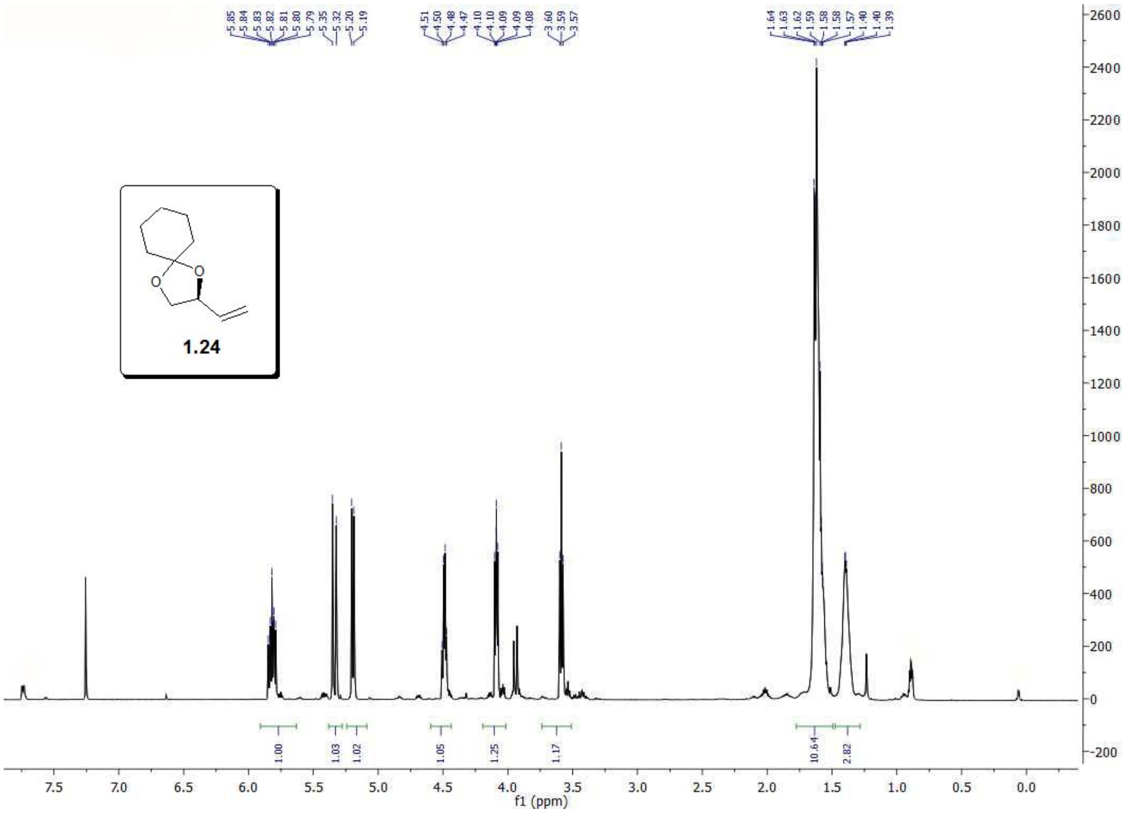

1.24

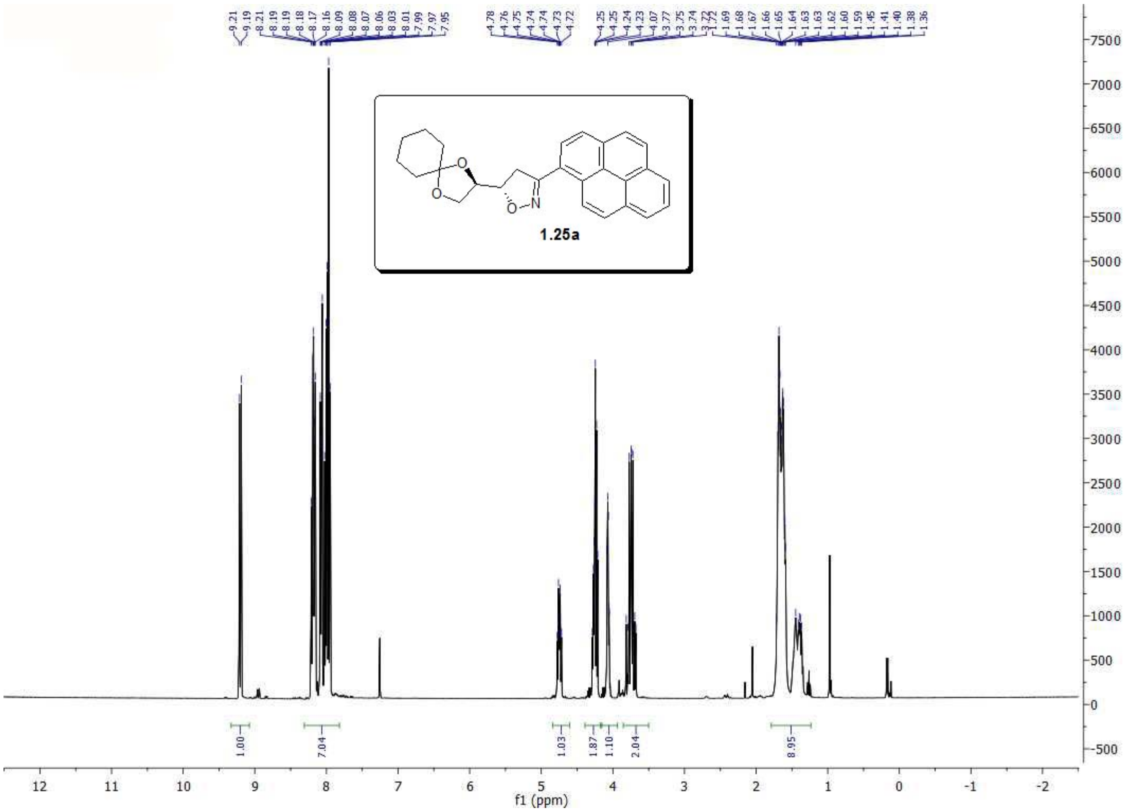
9.21
9.19
8.21
8.19
8.19
8.18
8.17
8.16
8.09
8.08
8.07
8.06
8.03
8.01
7.99
7.97
7.95
4.78
4.76
4.75
4.74
4.74
4.73
4.72
4.25
4.25
4.24
4.23
4.07
3.77
3.75
3.74
3.72
1.72
1.69
1.68
1.67
1.66
1.65
1.64
1.63
1.62
1.60
1.59
1.45
1.41
1.40
1.38
1.36
O
O
O–N
1.25a
1.00
7.04
1.03
1.87
1.10
2.04
8.95
12
11
10
9
8
7
6
5
4
3
2
1
0
-1
-2
f1 (ppm)
7500
7000
6500
6000
5500
5000
4500
4000
3500
3000
2500
2000
1500
1000
500
0
-500

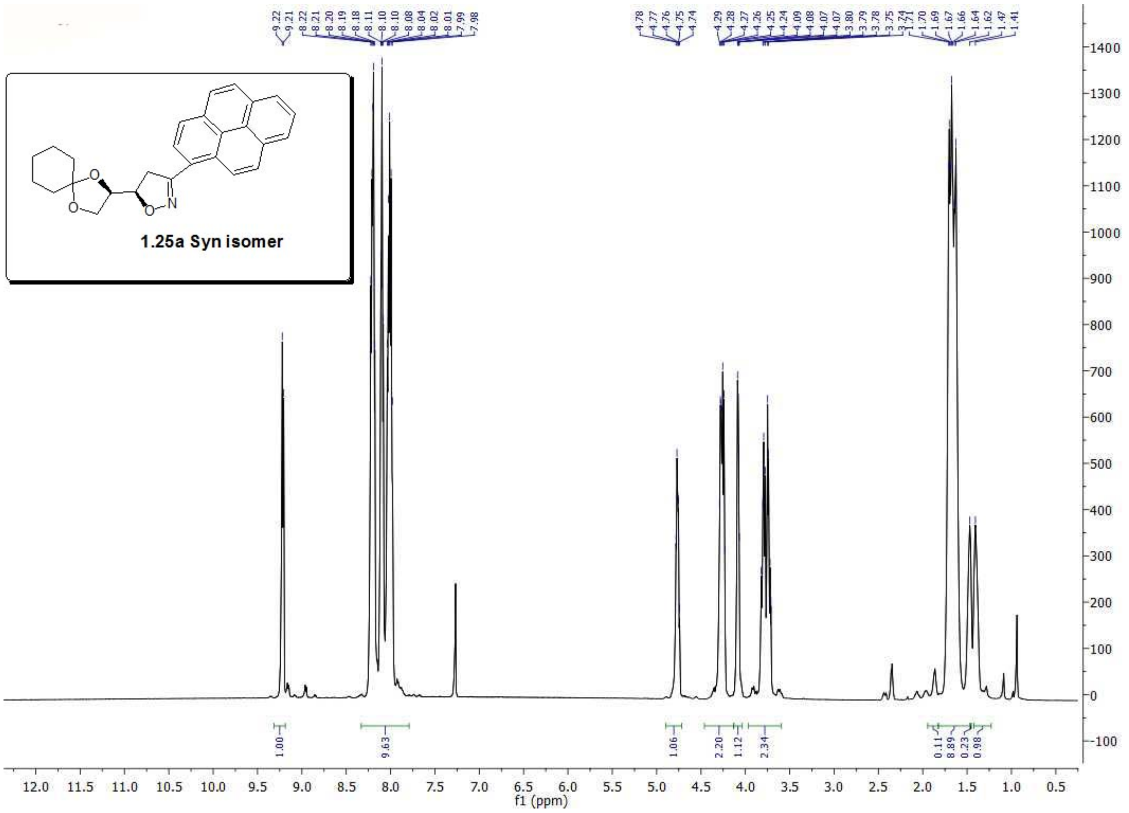
9.22
9.21
8.22
8.21
8.20
8.19
8.18
8.11
8.10
8.10
8.08
8.04
8.02
8.01
7.99
7.98
4.78
4.77
4.76
4.75
4.74
4.29
4.28
4.27
4.26
4.25
4.24
4.09
4.08
4.07
4.07
3.80
3.79
3.78
3.75
3.74
3.71
1.70
1.69
1.67
1.66
1.64
1.62
1.47
1.41
O
O
O–N
1.25a Syn isomer
1.00
9.63
1.06
2.20
1.12
2.34
0.11
8.89
0.23
0.98
12.0
11.5
11.0
10.5
10.0
9.5
9.0
8.5
8.0
7.5
7.0
6.5
6.0
5.5
5.0
4.5
4.0
3.5
3.0
2.5
2.0
1.5
1.0
0.5
f1 (ppm)
1400
1300
1200
1100
1000
900
800
700
600
500
400
300
200
100
0
-100

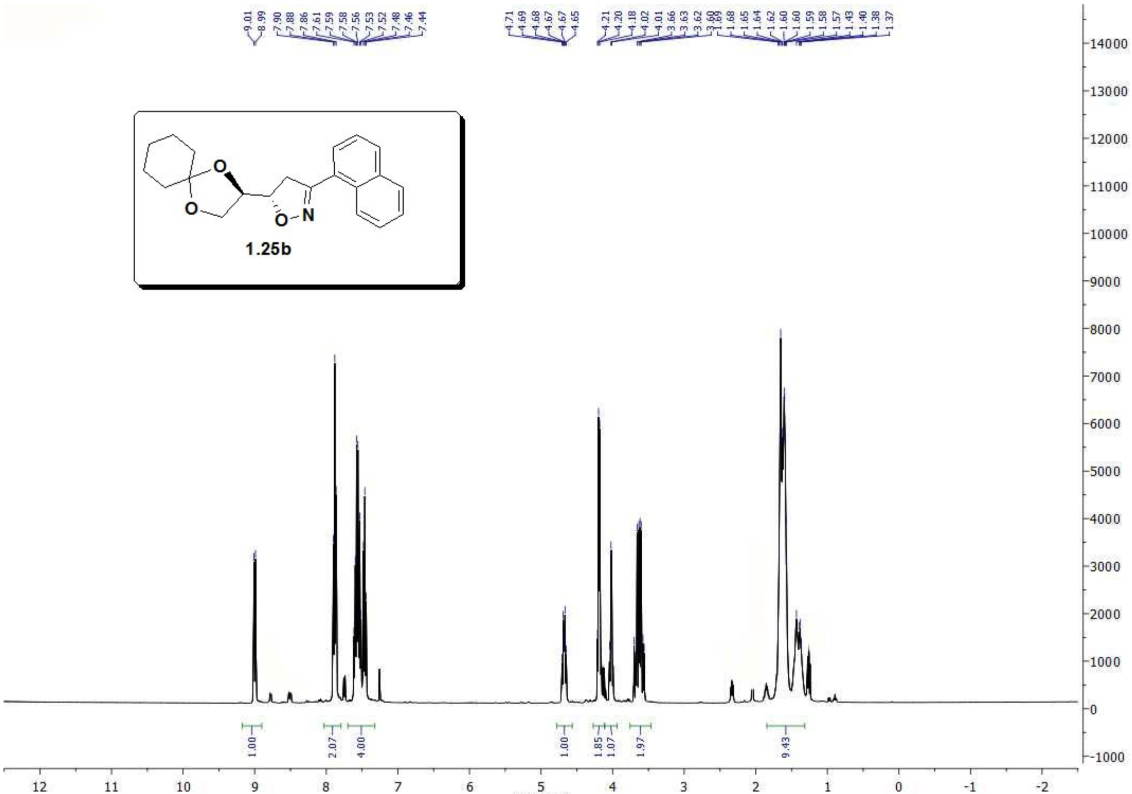
9.01
8.99
7.90
7.88
7.86
7.61
7.59
7.58
7.56
7.53
7.52
7.48
7.46
7.44
4.71
4.69
4.68
4.67
4.67
4.65
4.21
4.20
4.18
4.02
4.01
3.66
3.63
3.62
3.60
1.69
1.68
1.65
1.64
1.62
1.60
1.60
1.59
1.58
1.57
1.43
1.40
1.38
1.37
O
O
O
N
1.25b
1.00
2.07
4.00
1.00
1.85
1.07
1.97
9.43
12
11
10
9
8
7
6
5
4
3
2
1
0
-1
-2
f1 (ppm)
14000
13000
12000
11000
10000
9000
8000
7000
6000
5000
4000
3000
2000
1000
0
-1000

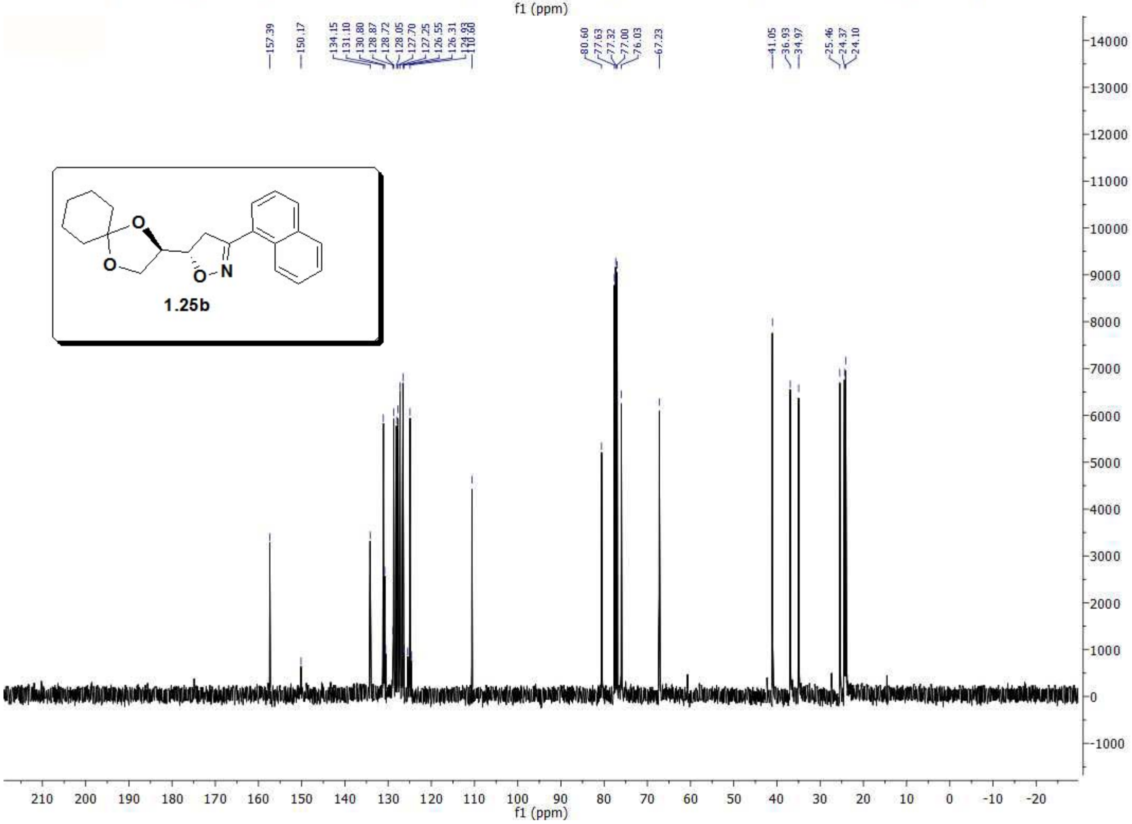
157.39
150.17
134.15
131.10
130.80
128.87
128.72
128.05
127.70
127.25
126.55
126.31
124.93
110.60
80.60
77.63
77.32
77.00
76.03
67.23
41.05
36.93
34.97
25.46
24.37
24.10
O
O
O
N
1.25b
210
200
190
180
170
160
150
140
130
120
110
100
90
80
70
60
50
40
30
20
10
0
-10
-20
f1 (ppm)
14000
13000
12000
11000
10000
9000
8000
7000
6000
5000
4000
3000
2000
1000
0
-1000

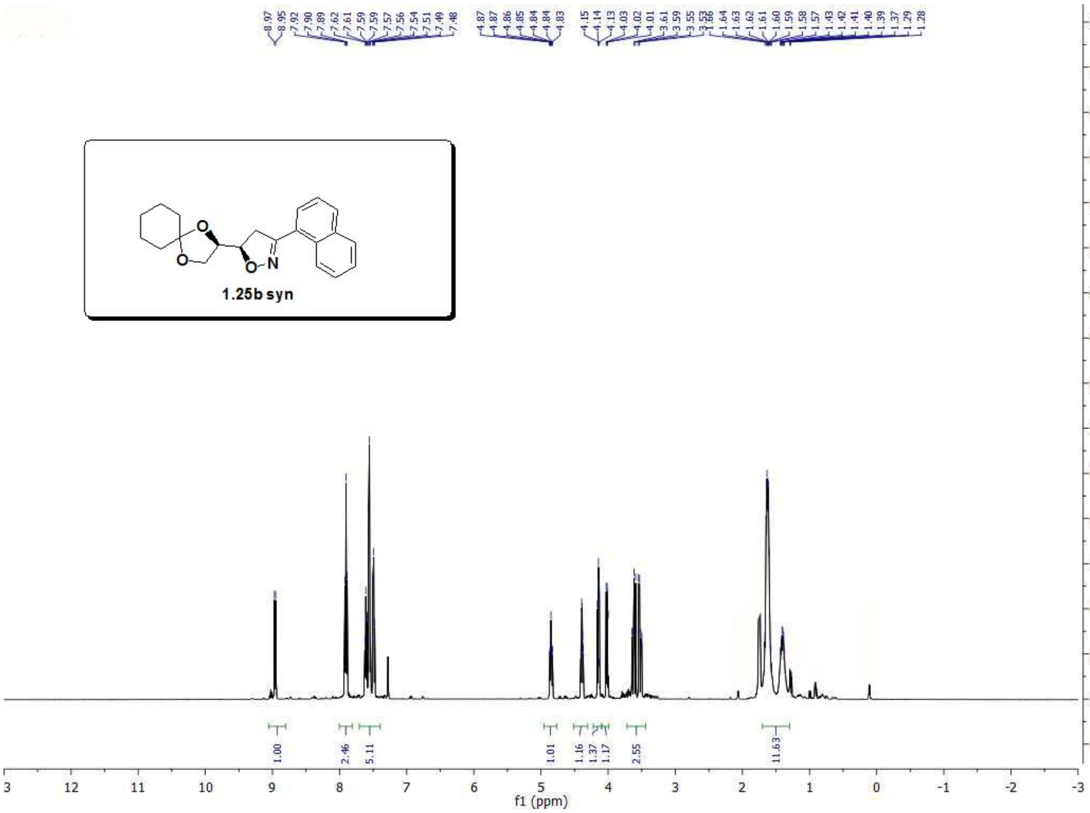
1.25b syn

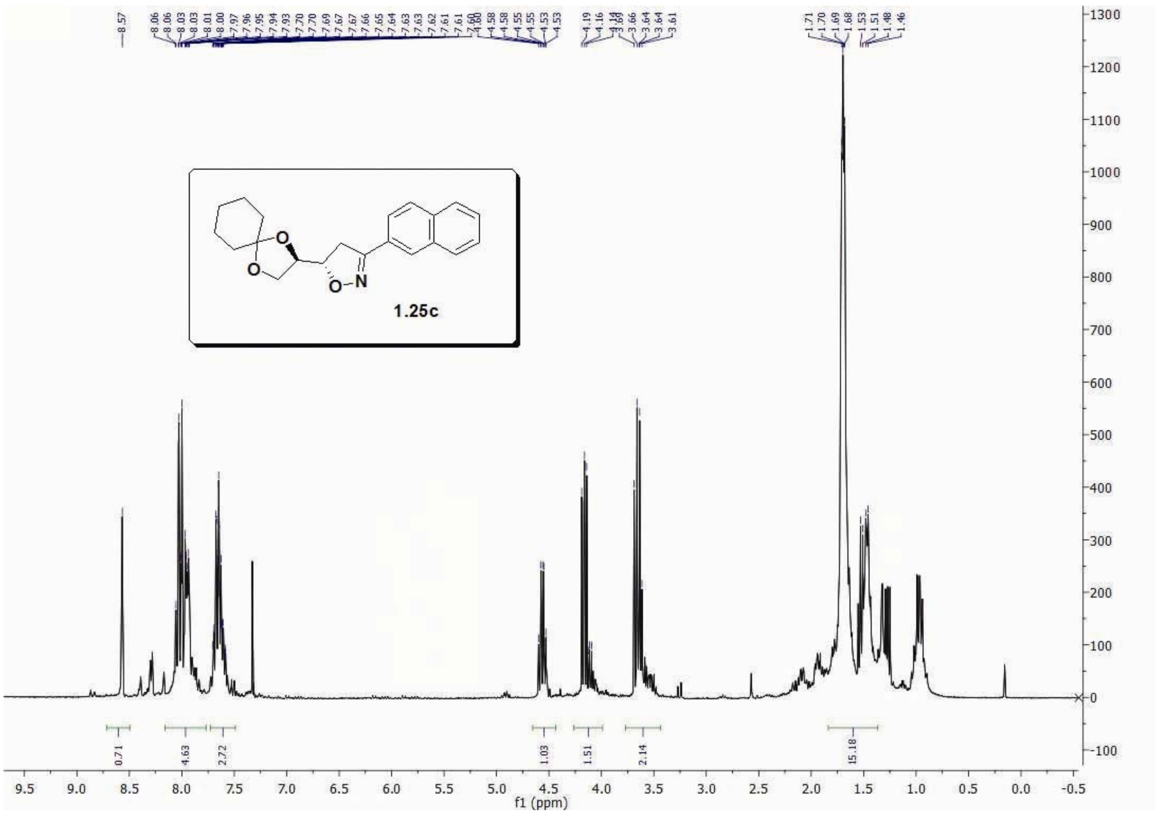
1.25c

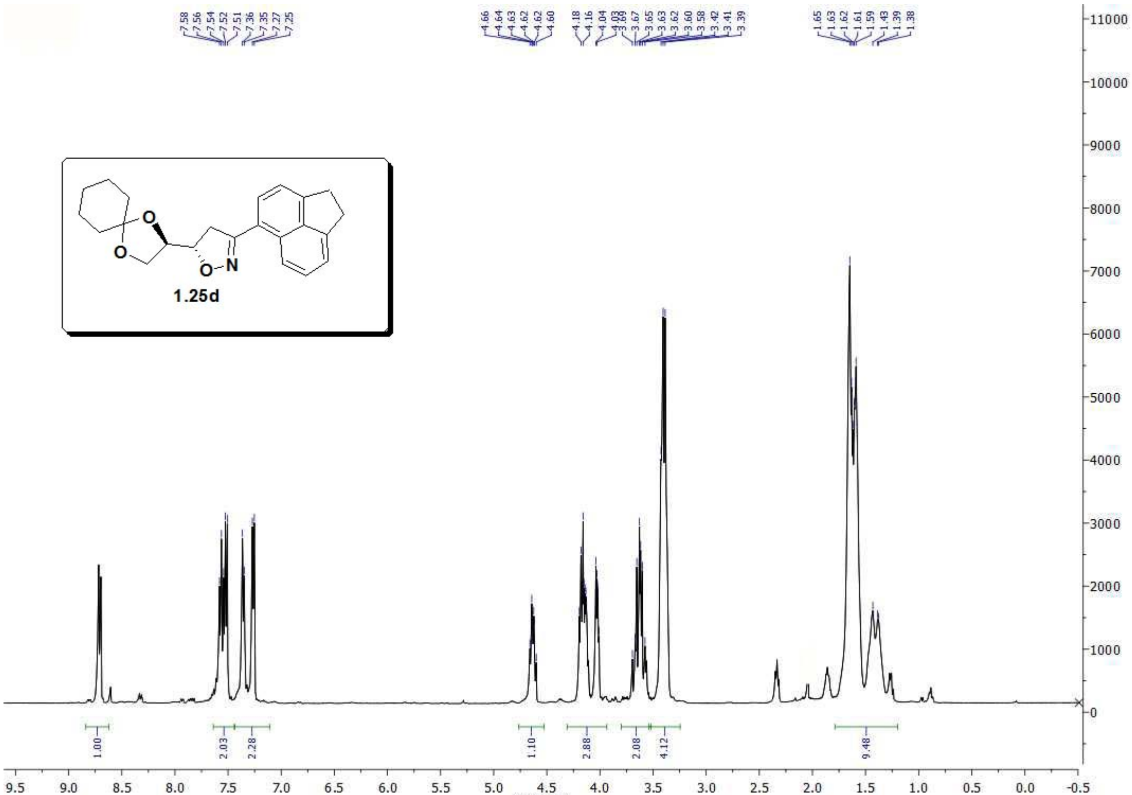
7.58
7.56
7.54
7.52
7.51
7.36
7.35
7.27
7.25
4.66
4.64
4.63
4.62
4.62
4.60
4.18
4.16
4.04
4.03
3.69
3.67
3.65
3.63
3.62
3.60
3.58
3.42
3.41
3.39
1.65
1.63
1.62
1.61
1.59
1.43
1.39
1.38
O
O
O-N
1.25d
1.00
2.03
2.28
1.10
2.88
2.08
4.12
9.48
11000
10000
9000
8000
7000
6000
5000
4000
3000
2000
1000
0
9.5
9.0
8.5
8.0
7.5
7.0
6.5
6.0
5.5
5.0
4.5
4.0
3.5
3.0
2.5
2.0
1.5
1.0
0.5
0.0
-0.5
f1 (ppm)

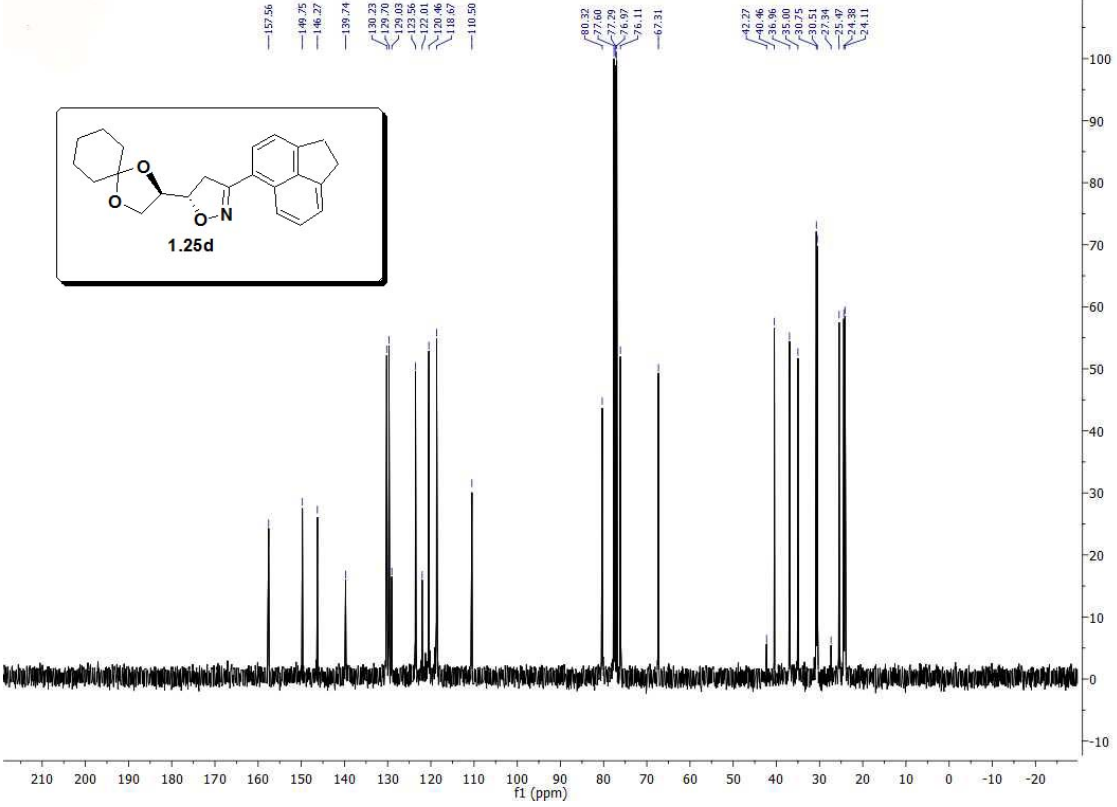
157.56
149.75
146.27
139.74
130.23
129.70
129.03
123.56
122.01
120.46
118.67
110.50
80.32
77.60
77.29
76.97
76.11
67.31
42.27
40.46
36.96
35.00
30.75
30.51
27.34
25.47
24.38
24.11
O
O
O-N
1.25d
100
90
80
70
60
50
40
30
20
10
0
-10
210
200
190
180
170
160
150
140
130
120
110
100
90
80
70
60
50
40
30
20
10
0
-10
-20
f1 (ppm)

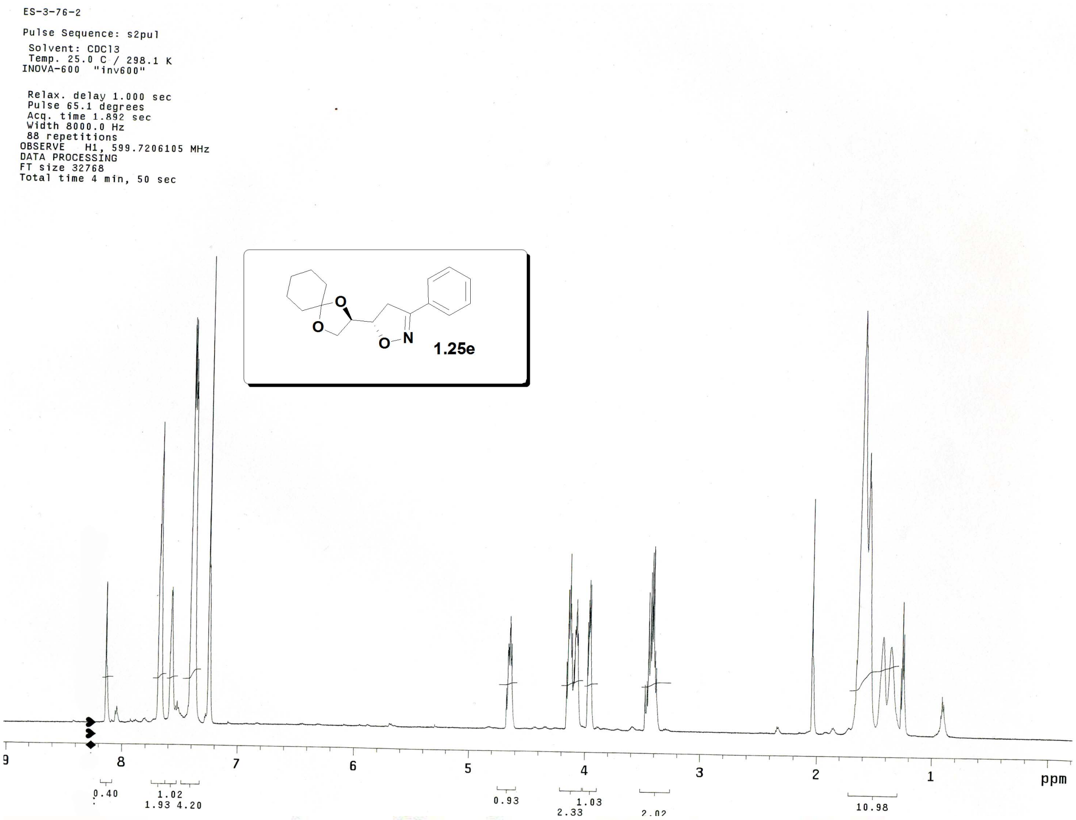

```
ES-3-76-2

Pulse Sequence: s2pul
 Solvent: CDCl3
 Temp. 25.0 C / 298.1 K
INOVA-600  "inv600"

 Relax. delay 1.000 sec
 Pulse 65.1 degrees
 Acq. time 1.892 sec
 Width 8000.0 Hz
 88 repetitions
OBSERVE   H1, 599.7206105 MHz
DATA PROCESSING
FT size 32768
Total time 4 min, 50 sec
```

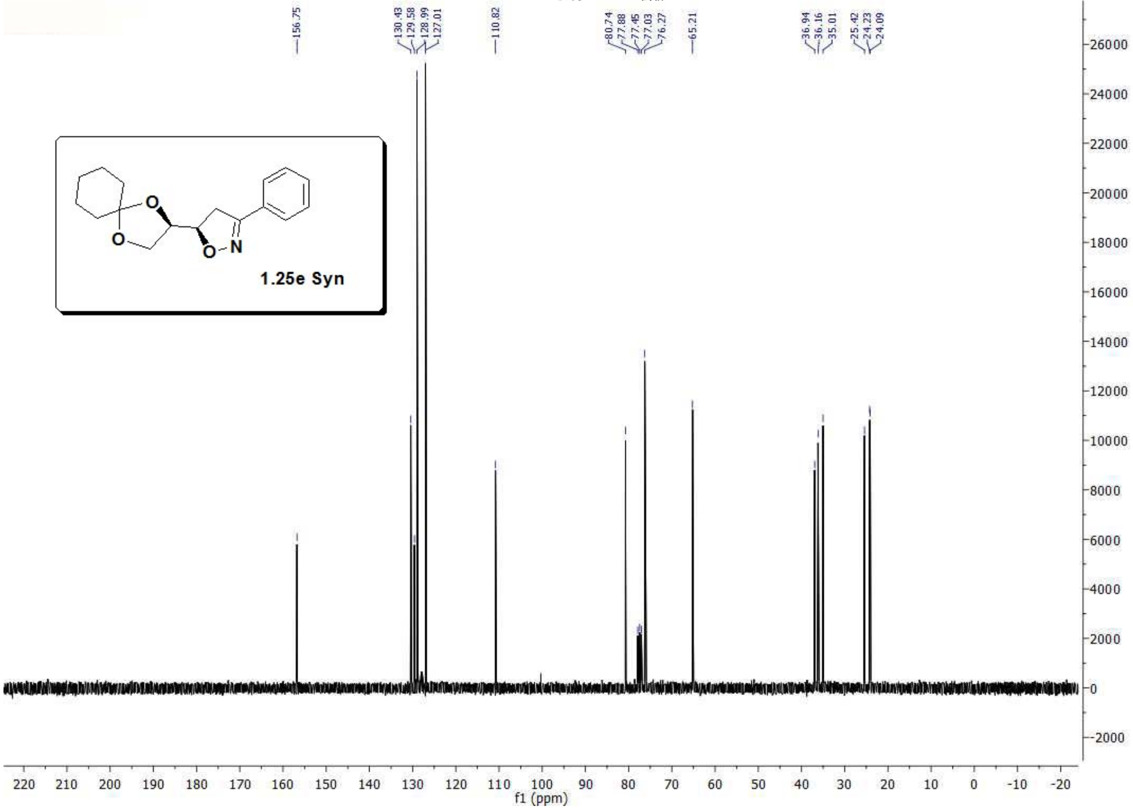

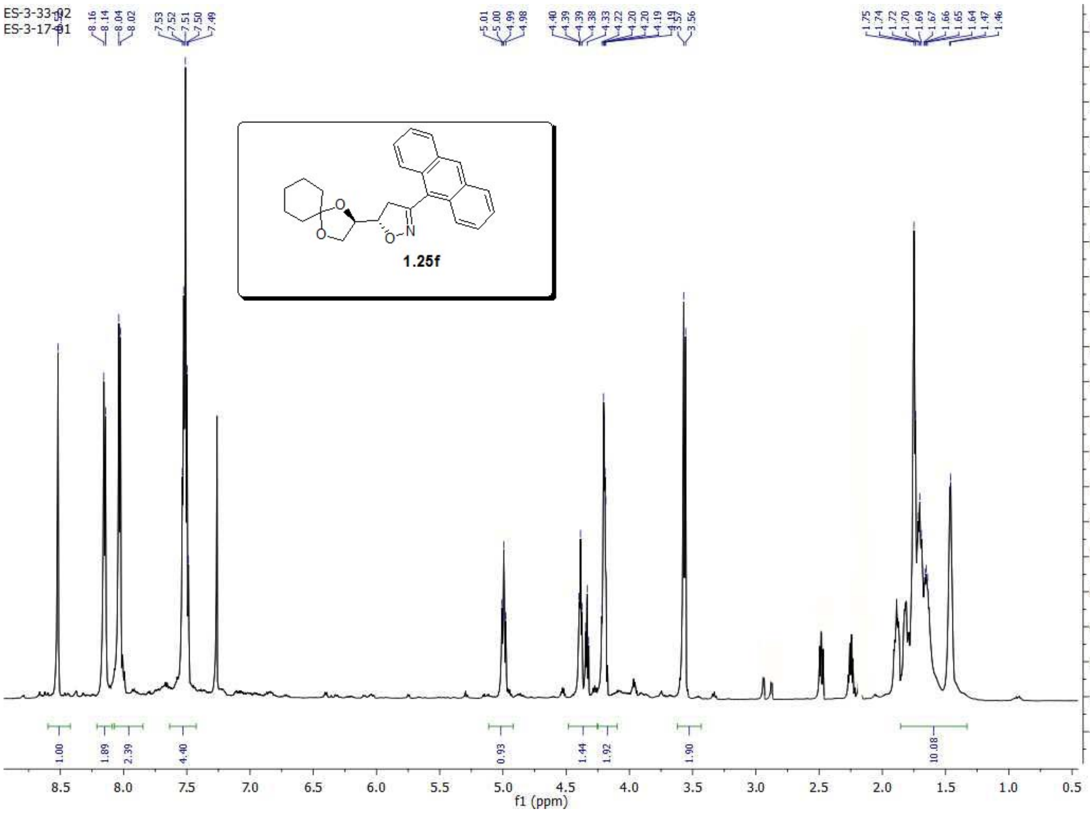
ES-3-33-02
ES-3-17-01
8.16 8.14 8.04 8.02 7.53 7.52 7.51 7.50 7.49
5.01 5.00 4.99 4.98 4.40 4.39 4.39 4.38 4.33 4.22 4.20 4.20 4.19 4.19 3.57 3.56
1.75 1.74 1.72 1.70 1.69 1.67 1.66 1.65 1.64 1.47 1.46
O
O
O
N
1.25f
1.00 1.89 2.39 4.40 0.93 1.44 1.92 1.90 10.08
f1 (ppm)

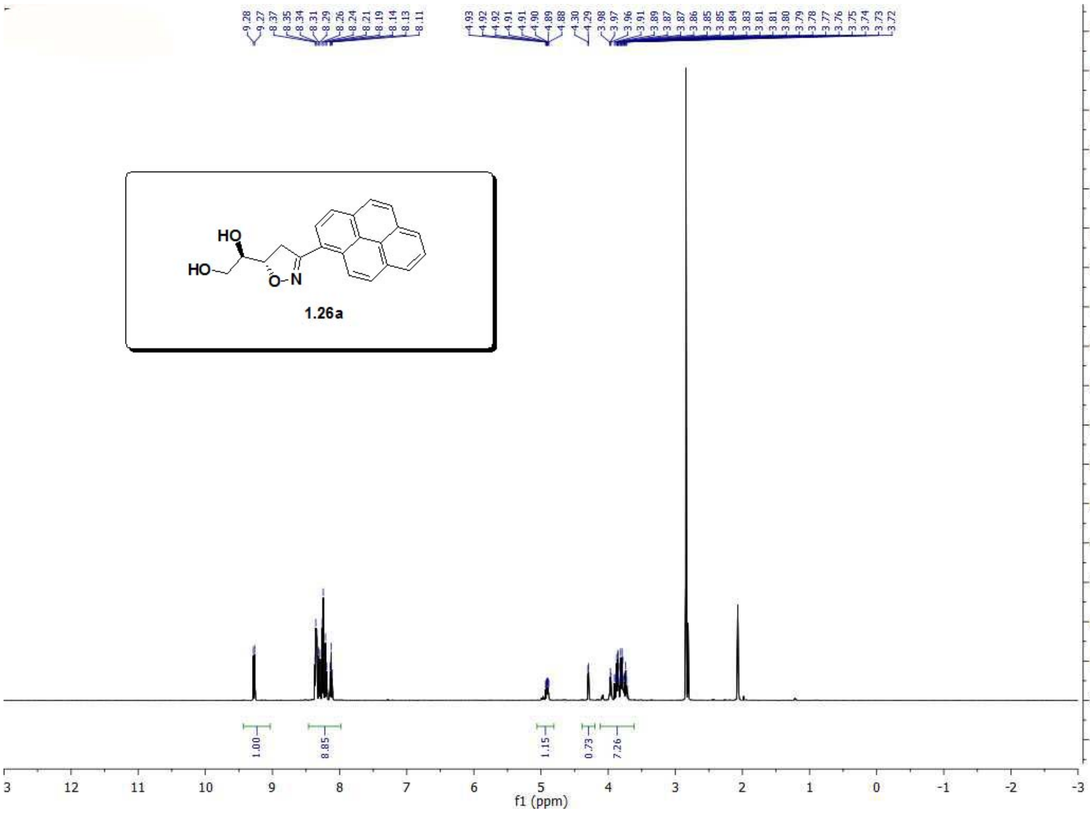
9.28 9.27 8.37 8.35 8.34 8.31 8.29 8.26 8.24 8.21 8.19 8.14 8.13 8.11
4.93 4.92 4.92 4.91 4.90 4.89 4.88 4.30 4.29 3.98 3.97 3.96 3.91 3.89 3.87 3.86 3.85 3.84 3.83 3.81 3.81 3.80 3.79 3.78 3.77 3.76 3.75 3.74 3.73 3.72
HO
HO
O-N
1.26a
1.00 8.85 1.15 0.73 7.26
f1 (ppm)

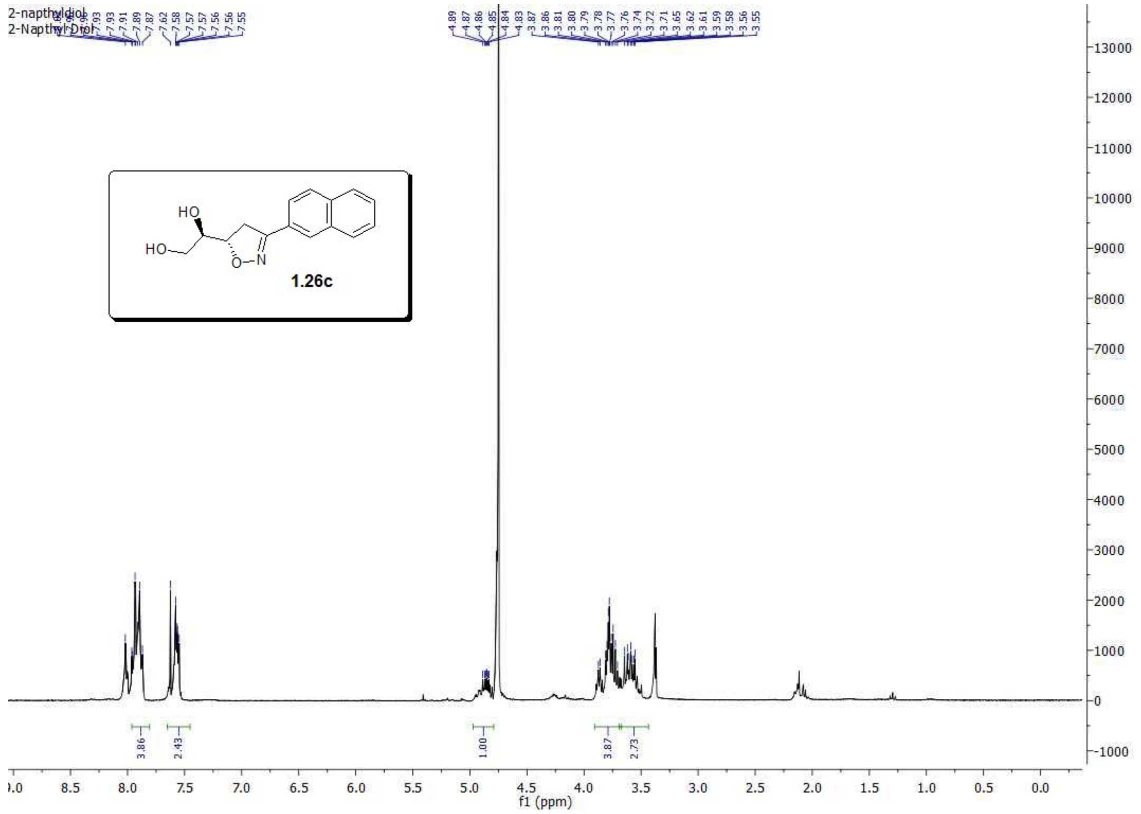

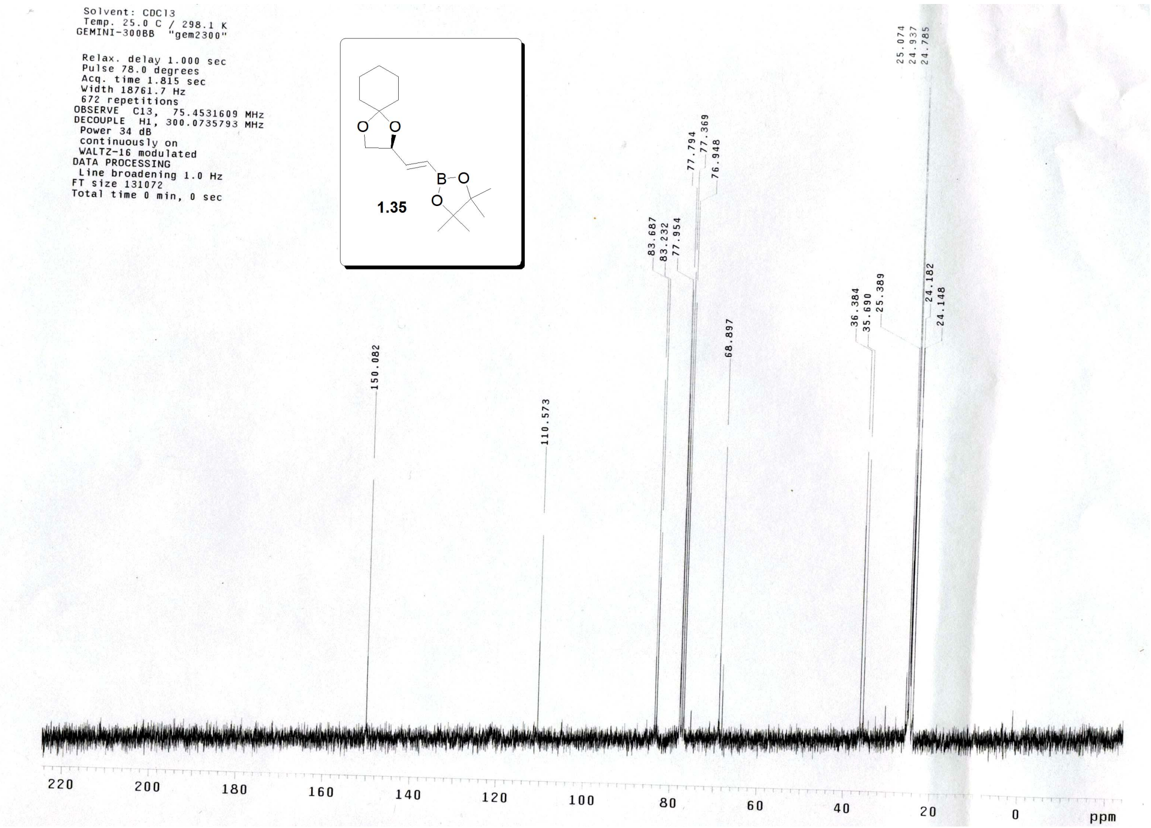

```
  Solvent: CDCl3
  Temp. 25.0 C / 298.1 K
 GEMINI-300BB  "gem2300"

  Relax. delay 1.000 sec
  Pulse 78.0 degrees
  Acq. time 1.815 sec
  Width 18761.7 Hz
  672 repetitions
 OBSERVE  C13,  75.4531609 MHz
 DECOUPLE  H1, 300.0735793 MHz
  Power 34 dB
  continuously on
  WALTZ-16 modulated
 DATA PROCESSING
  Line broadening 1.0 Hz
 FT size 131072
 Total time 0 min, 0 sec
```

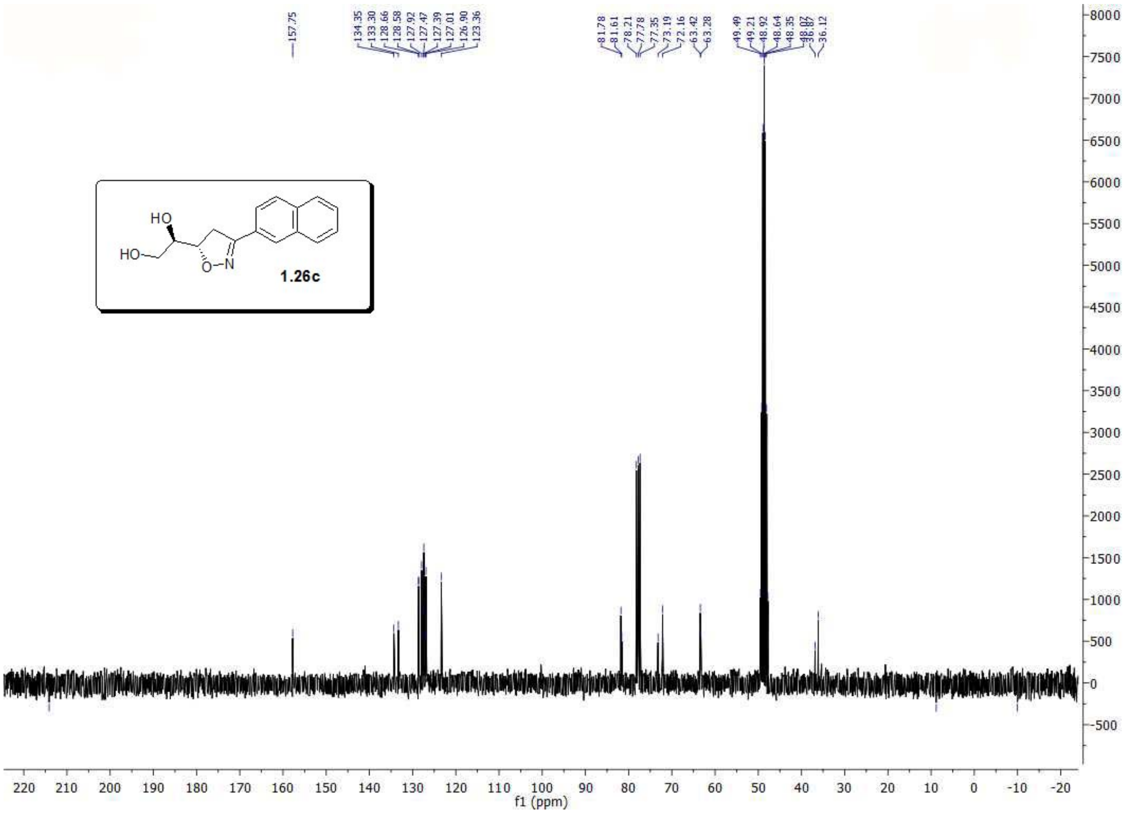

157.75
134.35
133.30
128.66
128.58
127.92
127.47
127.39
127.01
126.90
123.36
81.78
81.61
78.21
77.78
77.35
73.19
72.16
63.42
63.28
49.49
49.21
48.92
48.64
48.35
48.07
36.87
36.12
HO
HO
O–N
1.26c
220 210 200 190 180 170 160 150 140 130 120 110 100 90 80 70 60 50 40 30 20 10 0 -10 -20
f1 (ppm)
8000 7500 7000 6500 6000 5500 5000 4500 4000 3500 3000 2500 2000 1500 1000 500 0 -500

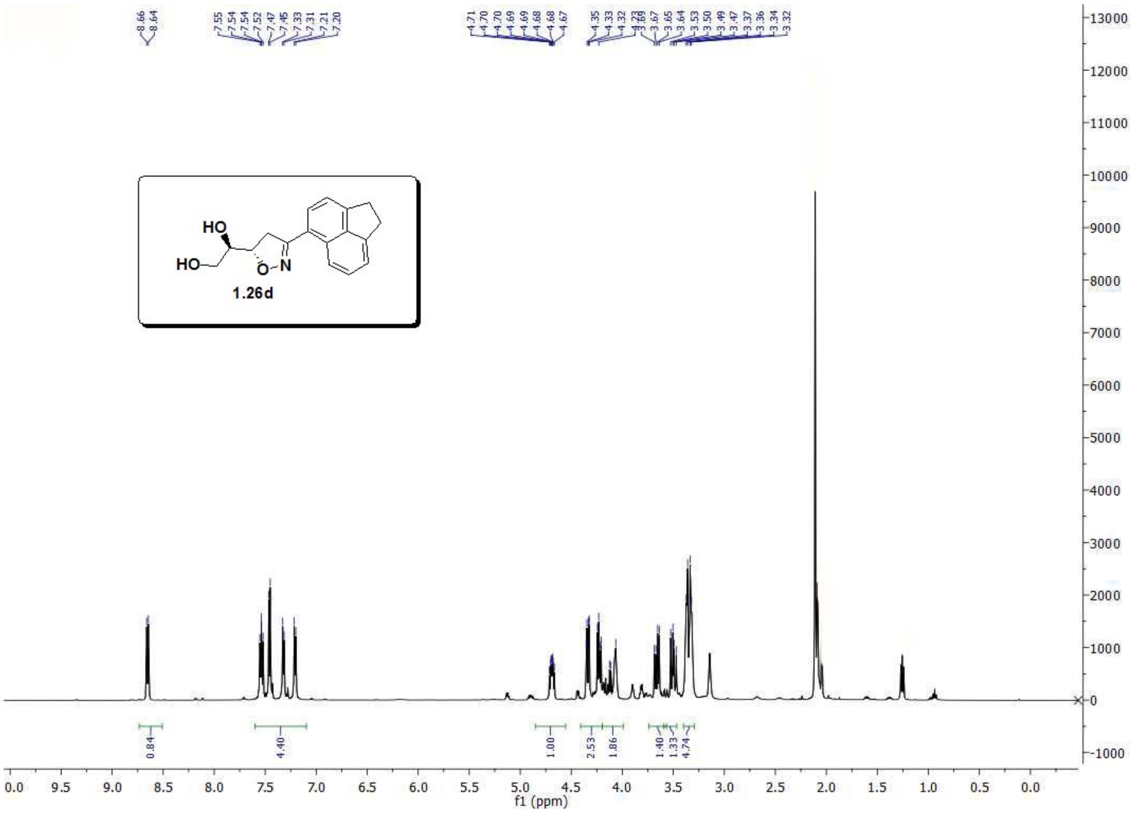

8.66
8.64
7.55
7.54
7.54
7.52
7.47
7.45
7.33
7.31
7.21
7.20
4.71
4.70
4.69
4.69
4.68
4.68
4.67
4.35
4.33
4.32
3.67
3.65
3.64
3.53
3.50
3.49
3.47
3.37
3.36
3.34
3.32
HO
HO
O–N
1.26d
0.84
4.40
1.00
2.53
1.86
1.40
1.33
4.74
0.0 9.5 9.0 8.5 8.0 7.5 7.0 6.5 6.0 5.5 5.0 4.5 4.0 3.5 3.0 2.5 2.0 1.5 1.0 0.5 0.0
f1 (ppm)
13000 12000 11000 10000 9000 8000 7000 6000 5000 4000 3000 2000 1000 0 -1000

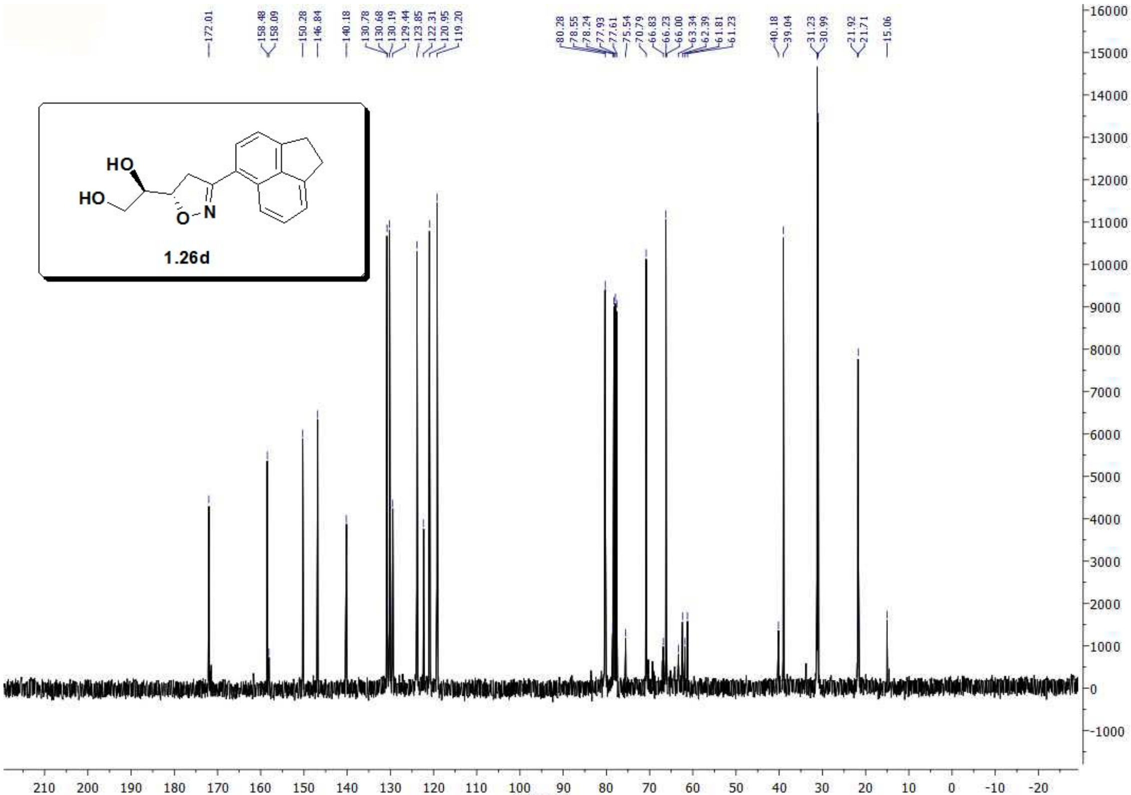
172.01
158.48
158.09
150.28
146.84
140.18
130.78
130.68
130.19
129.44
123.85
122.31
120.95
119.20
80.28
78.55
78.24
77.93
77.61
75.54
70.79
66.83
66.23
66.00
63.34
62.39
61.81
61.23
40.18
39.04
31.23
30.99
21.92
21.71
15.06
HO
HO
O
N
1.26d
16000
15000
14000
13000
12000
11000
10000
9000
8000
7000
6000
5000
4000
3000
2000
1000
0
-1000
210
200
190
180
170
160
150
140
130
120
110
100
90
80
70
60
50
40
30
20
10
0
-10
-20
f1 (ppm)

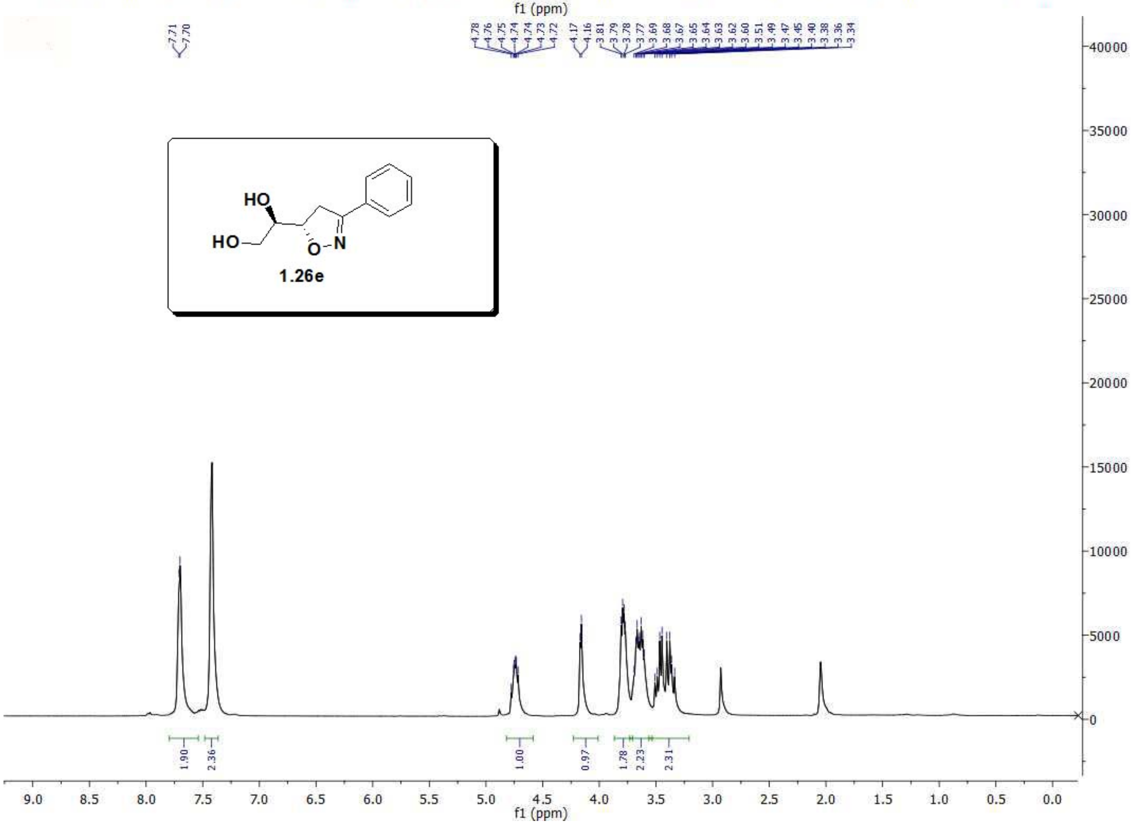
7.71
7.70
4.78
4.76
4.75
4.74
4.74
4.73
4.72
4.17
4.16
3.81
3.79
3.78
3.77
3.69
3.68
3.67
3.65
3.64
3.63
3.62
3.60
3.51
3.49
3.47
3.45
3.40
3.38
3.36
3.34
HO
HO
O
N
1.26e
40000
35000
30000
25000
20000
15000
10000
5000
0
1.90
2.36
1.00
0.97
1.78
2.23
2.31
9.0
8.5
8.0
7.5
7.0
6.5
6.0
5.5
5.0
4.5
4.0
3.5
3.0
2.5
2.0
1.5
1.0
0.5
0.0
f1 (ppm)

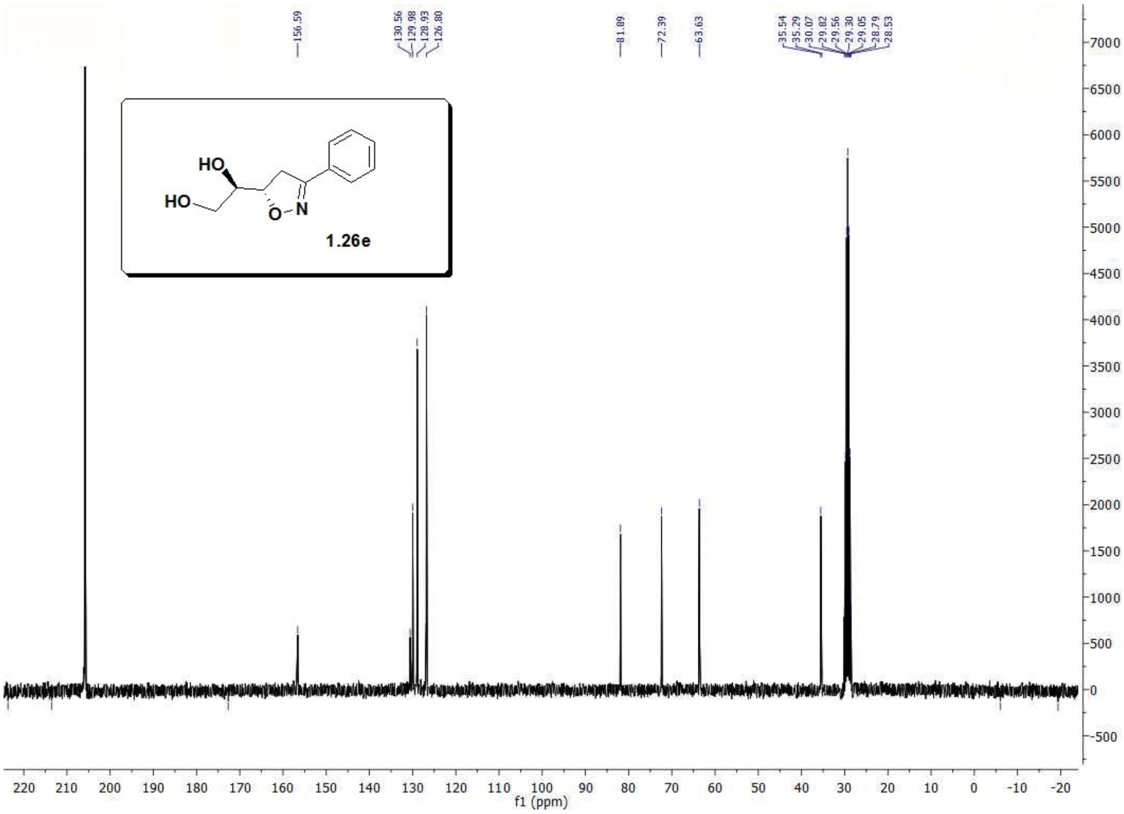
156.59
130.56
129.98
128.93
126.80
81.89
72.39
63.63
35.54
35.29
30.07
29.82
29.56
29.30
29.05
28.79
28.53
HO
HO
O
N
1.26e
7000
6500
6000
5500
5000
4500
4000
3500
3000
2500
2000
1500
1000
500
0
-500
220 210 200 190 180 170 160 150 140 130 120 110 100 90 80 70 60 50 40 30 20 10 0 -10 -20
f1 (ppm)

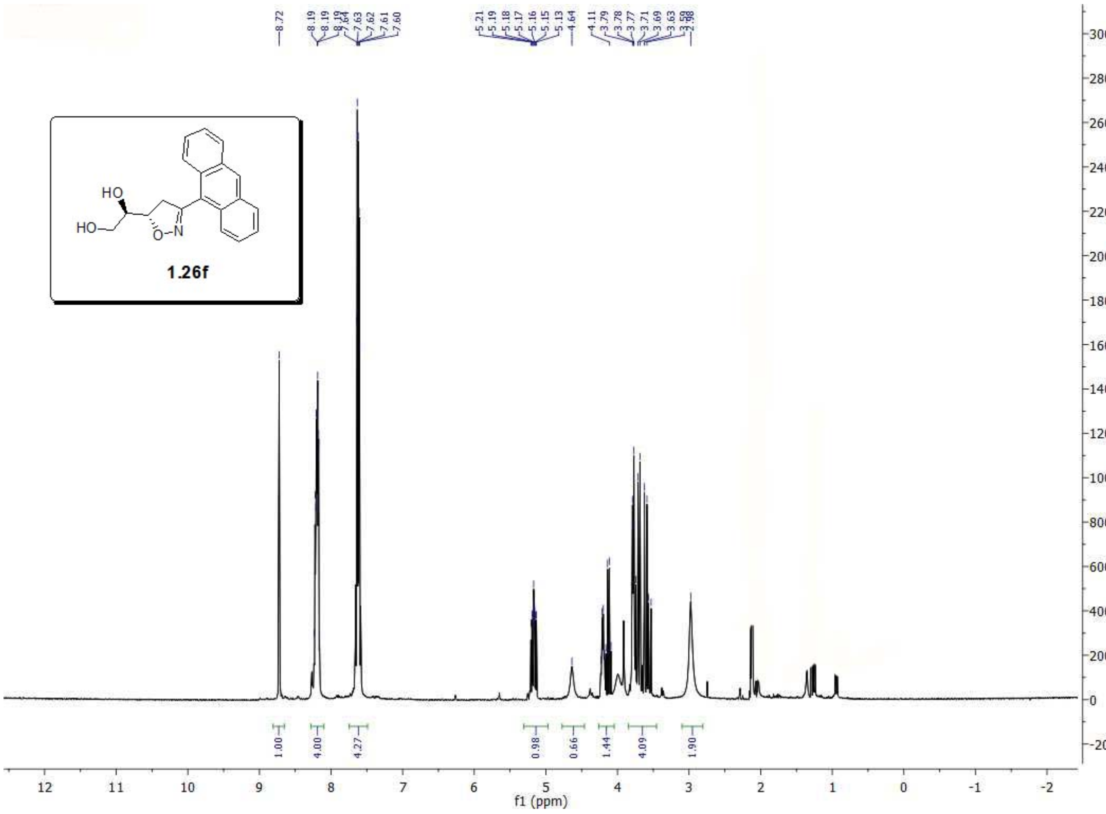
8.72
8.19
8.19
8.19
7.64
7.63
7.62
7.61
7.60
5.21
5.19
5.18
5.17
5.16
5.15
5.13
4.64
4.11
3.79
3.78
3.77
3.71
3.69
3.63
3.59
2.98
HO
HO
O
N
1.26f
3000
2800
2600
2400
2200
2000
1800
1600
1400
1200
1000
800
600
400
200
0
-200
1.00
4.00
4.27
0.98
0.66
1.44
4.09
1.90
12 11 10 9 8 7 6 5 4 3 2 1 0 -1 -2
f1 (ppm)

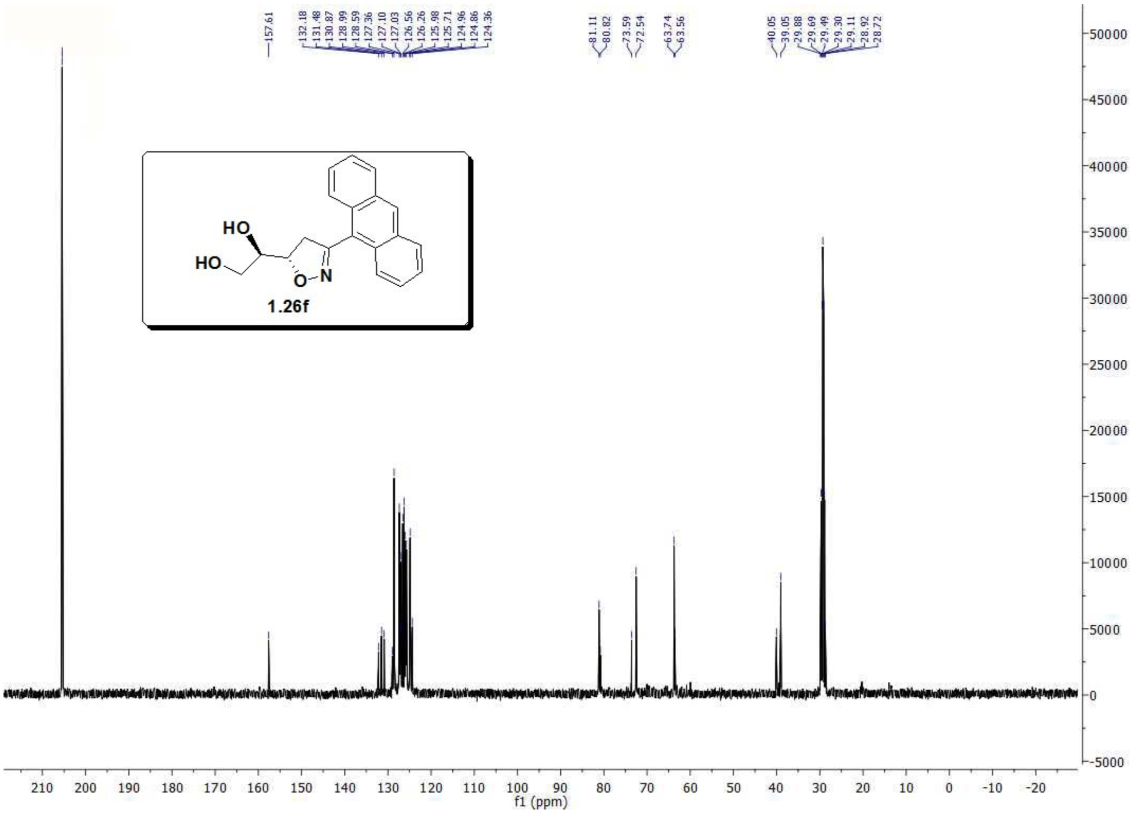
157.61
132.18
131.48
130.87
128.99
128.59
127.36
127.10
127.03
126.56
126.26
125.98
125.71
124.96
124.86
124.36
81.11
80.82
73.59
72.54
63.74
63.56
40.05
39.05
29.88
29.69
29.49
29.30
29.11
28.92
28.72
HO
HO
O–N
1.26f
f1 (ppm)

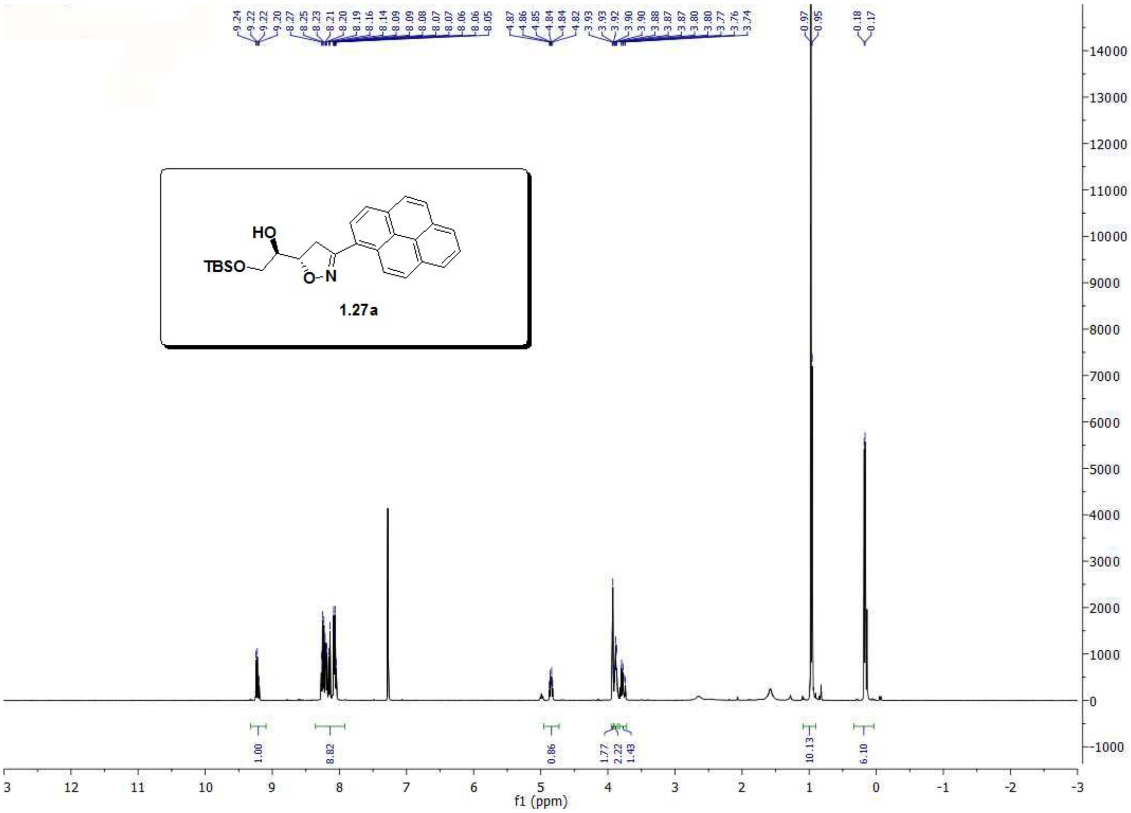
9.24
9.22
9.20
8.27
8.25
8.23
8.21
8.20
8.19
8.16
8.14
8.09
8.08
8.07
8.07
8.06
8.05
4.87
4.86
4.85
4.84
4.84
4.82
3.93
3.93
3.92
3.90
3.88
3.87
3.80
3.77
3.76
3.74
0.97
0.95
0.18
0.17
HO
TBSO
O–N
1.27a
1.00
8.82
0.86
1.77
2.22
1.43
10.13
6.10
f1 (ppm)

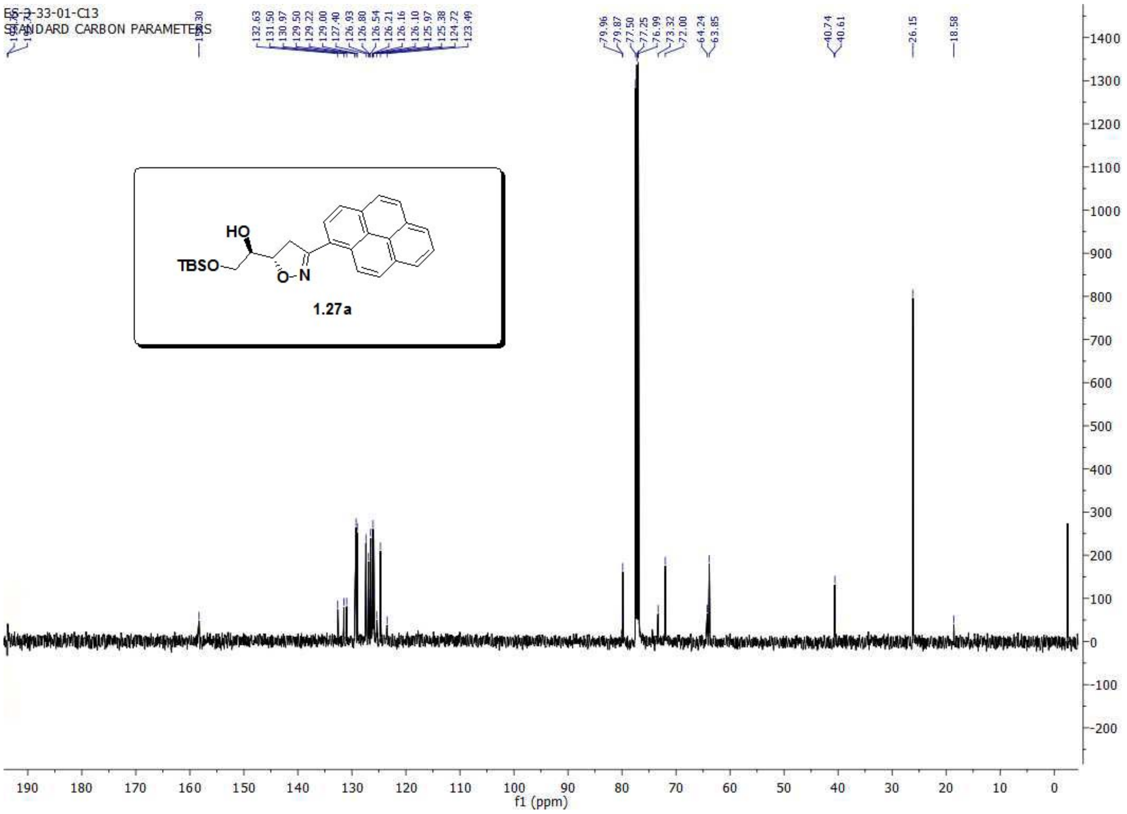
ES-3-33-01-C13
STANDARD CARBON PARAMETERS
158.30
132.63
131.50
130.97
129.50
129.22
129.00
127.40
126.93
126.80
126.54
126.21
126.16
126.10
125.97
125.38
124.72
123.49
79.96
79.87
77.50
77.25
76.99
73.32
72.00
64.24
63.85
40.74
40.61
26.15
18.58
HO
TBSO
O–N
1.27a
190
180
170
160
150
140
130
120
110
100
90
80
70
60
50
40
30
20
10
0
f1 (ppm)
1400
1300
1200
1100
1000
900
800
700
600
500
400
300
200
100
0
-100
-200

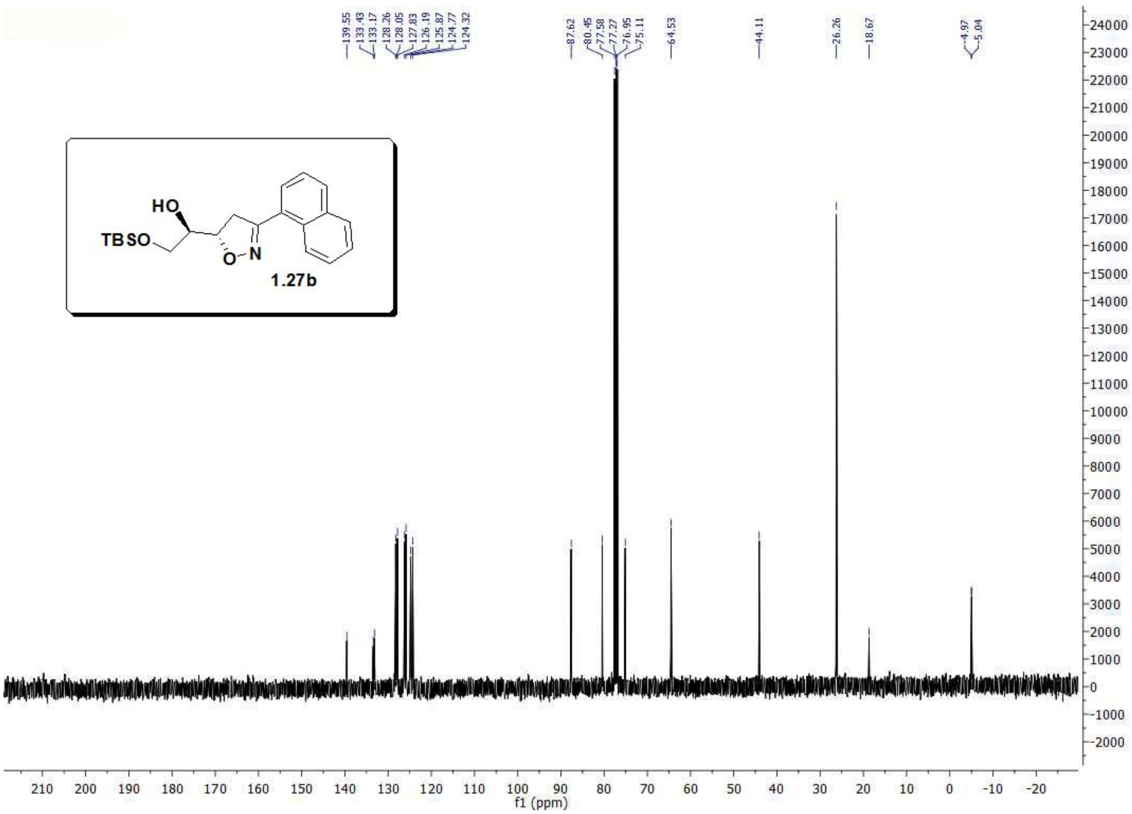
139.55
133.43
133.17
128.26
128.05
127.83
126.19
125.87
124.77
124.32
87.62
80.45
77.58
77.27
76.95
75.11
64.53
44.11
26.26
18.67
-4.97
-5.04
HO
TBSO
O–N
1.27b
210
200
190
180
170
160
150
140
130
120
110
100
90
80
70
60
50
40
30
20
10
0
-10
-20
f1 (ppm)
24000
23000
22000
21000
20000
19000
18000
17000
16000
15000
14000
13000
12000
11000
10000
9000
8000
7000
6000
5000
4000
3000
2000
1000
0
-1000
-2000

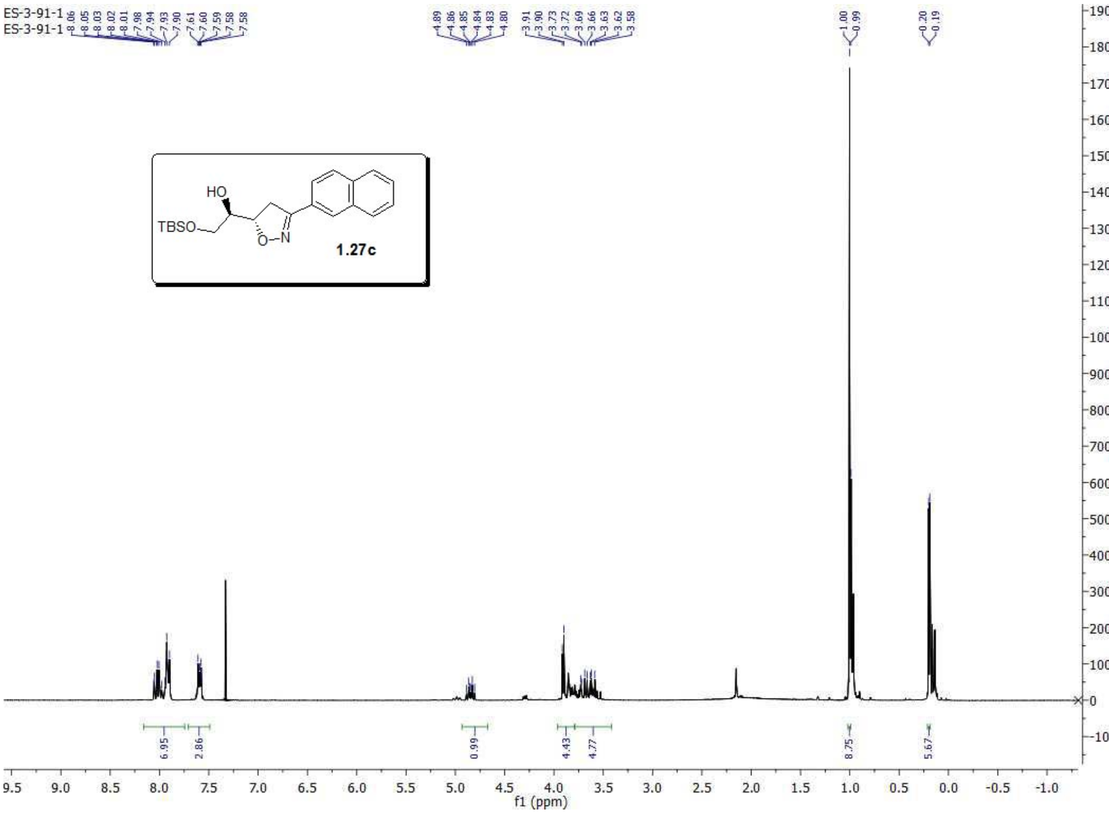
ES-3-91-1
ES-3-91-1
8.06 8.05 8.03 8.02 8.01 7.98 7.94 7.93 7.90 7.61 7.60 7.59 7.58 7.58
4.89 4.86 4.85 4.84 4.83 4.80
3.91 3.90 3.73 3.72 3.69 3.66 3.63 3.62 3.58
1.00 0.99
0.20 0.19
HO
TBSO
O–N
1.27c
6.95
2.86
0.99
4.43
4.77
8.75
5.67
19000
18000
17000
16000
15000
14000
13000
12000
11000
10000
9000
8000
7000
6000
5000
4000
3000
2000
1000
0
-1000
9.5 9.0 8.5 8.0 7.5 7.0 6.5 6.0 5.5 5.0 4.5 4.0 3.5 3.0 2.5 2.0 1.5 1.0 0.5 0.0 -0.5 -1.0
f1 (ppm)

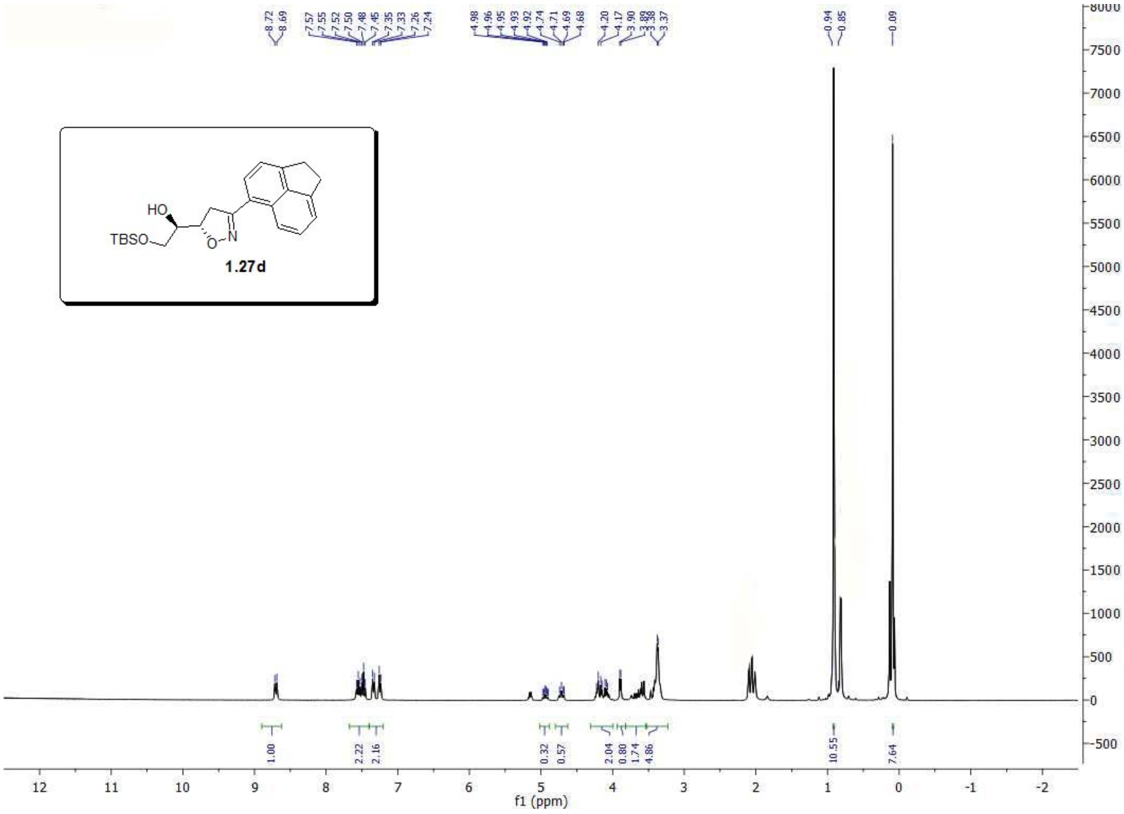
8.72 8.69
7.57 7.55 7.52 7.50 7.48 7.45 7.35 7.33 7.26 7.24
4.98 4.96 4.95 4.93 4.92 4.74 4.71 4.69 4.68
4.20 4.17 3.90 3.88 3.38 3.37
0.94 0.85
0.09
HO
TBSO
O–N
1.27d
1.00
2.22
2.16
0.32
0.57
2.04
0.80
1.74
4.86
10.55
7.64
8000
7500
7000
6500
6000
5500
5000
4500
4000
3500
3000
2500
2000
1500
1000
500
0
-500
12 11 10 9 8 7 6 5 4 3 2 1 0 -1 -2
f1 (ppm)

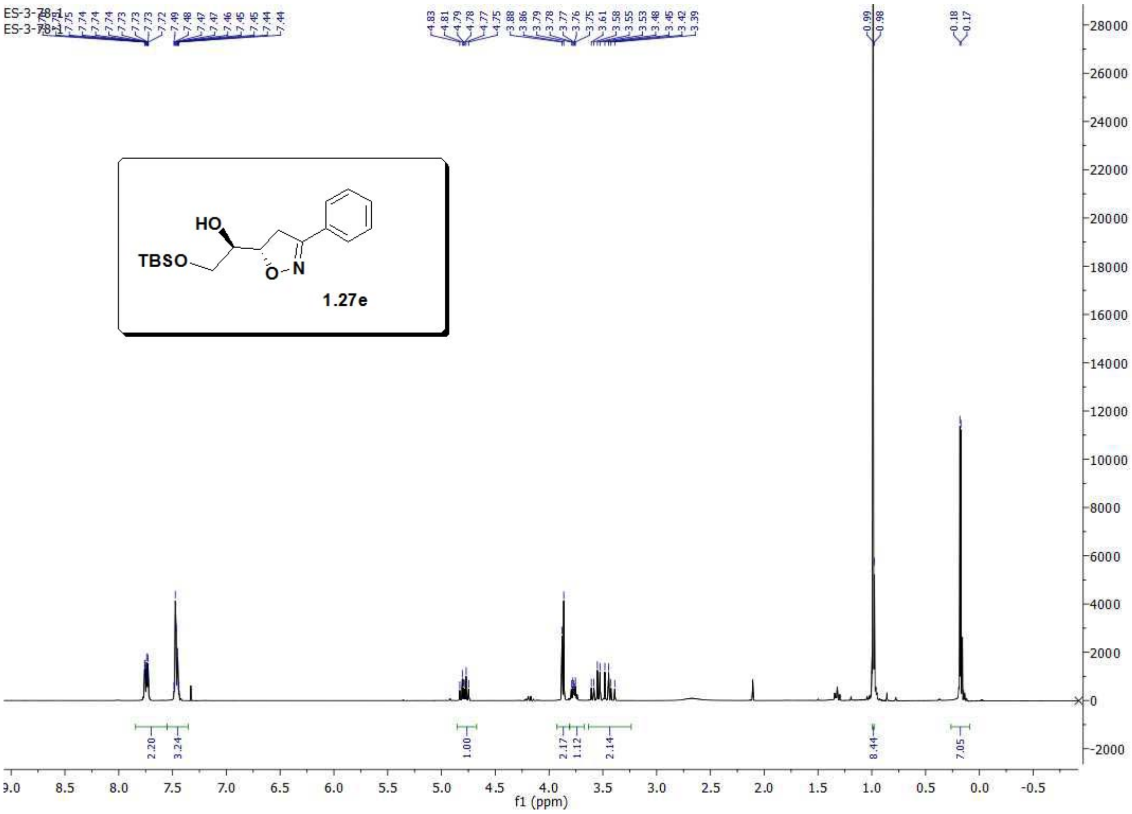
ES-3-78-1
ES-3-78-1
7.75
7.74
7.74
7.74
7.73
7.73
7.73
7.72
7.49
7.48
7.47
7.47
7.46
7.45
7.45
7.44
7.44
4.83
4.81
4.79
4.78
4.77
4.75
3.88
3.86
3.79
3.78
3.77
3.76
3.75
3.61
3.58
3.55
3.53
3.48
3.45
3.42
3.39
0.99
0.98
0.18
0.17
HO
TBSO
O
N
1.27e
2.20
3.24
1.00
2.17
1.12
2.14
8.44
7.05
28000
26000
24000
22000
20000
18000
16000
14000
12000
10000
8000
6000
4000
2000
0
-2000
9.0
8.5
8.0
7.5
7.0
6.5
6.0
5.5
5.0
4.5
4.0
3.5
3.0
2.5
2.0
1.5
1.0
0.5
0.0
-0.5
f1 (ppm)

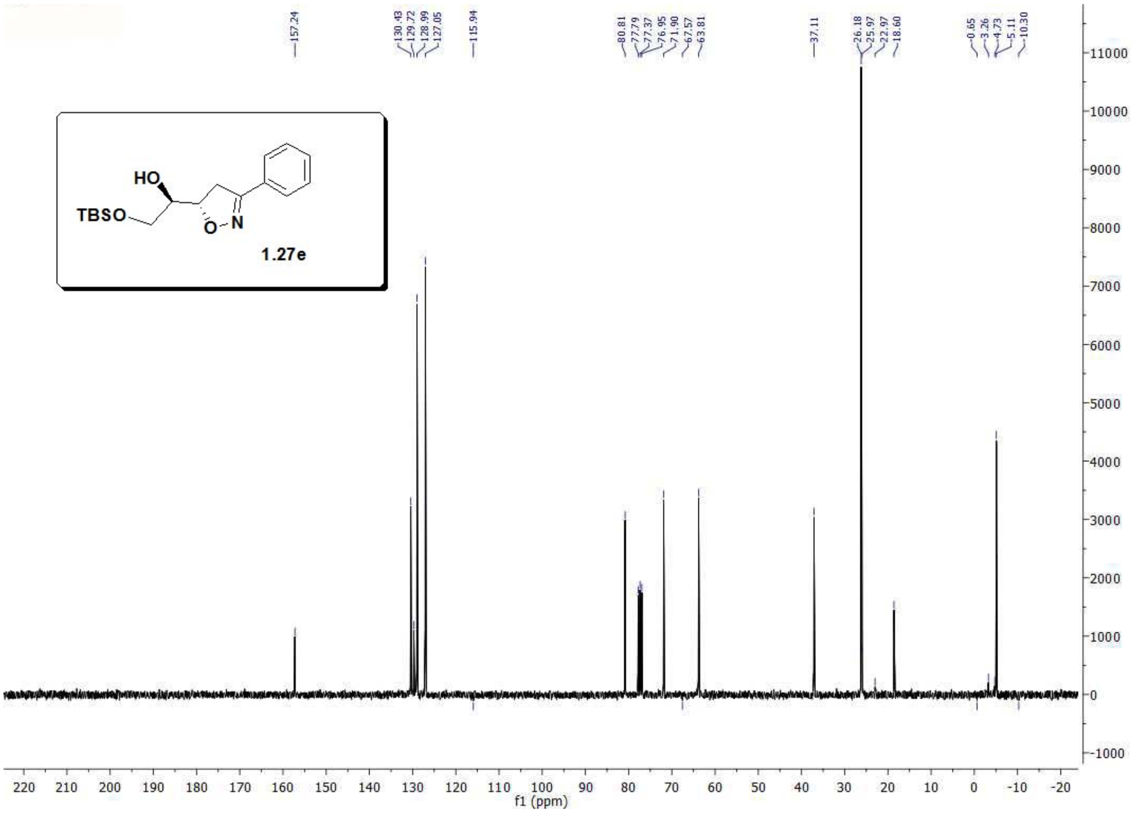
157.24
130.43
129.72
128.99
127.05
115.94
80.81
77.79
77.37
76.95
71.90
67.57
63.81
37.11
26.18
25.97
22.97
18.60
-0.65
-3.26
-4.73
-5.11
-10.30
HO
TBSO
O
N
1.27e
11000
10000
9000
8000
7000
6000
5000
4000
3000
2000
1000
0
-1000
220
210
200
190
180
170
160
150
140
130
120
110
100
90
80
70
60
50
40
30
20
10
0
-10
-20
f1 (ppm)

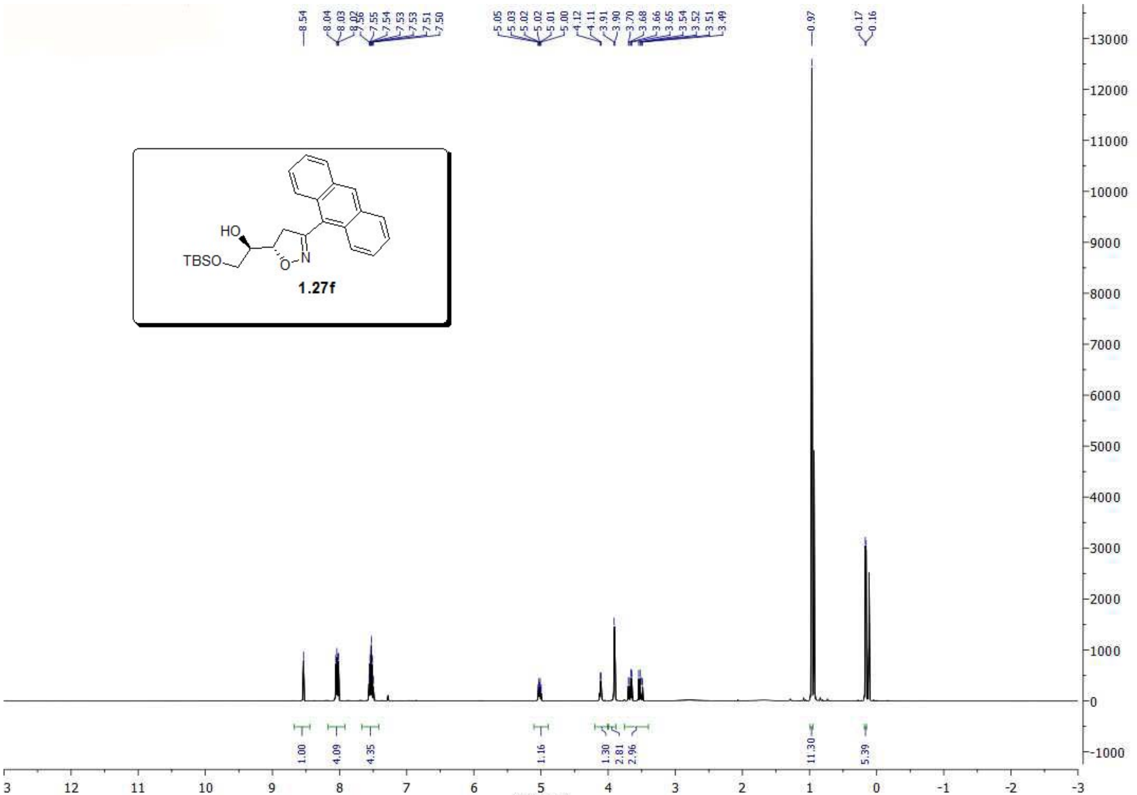
8.54
8.04
8.03
8.02
7.56
7.55
7.54
7.53
7.53
7.51
7.50
5.05
5.03
5.02
5.02
5.01
5.00
4.12
4.11
3.91
3.90
3.70
3.68
3.66
3.65
3.54
3.52
3.51
3.49
0.97
0.17
0.16
HO
TBSO
O-N
1.27f
1.00
4.09
4.35
1.16
1.30
2.81
2.96
11.30
5.39
f1 (ppm)

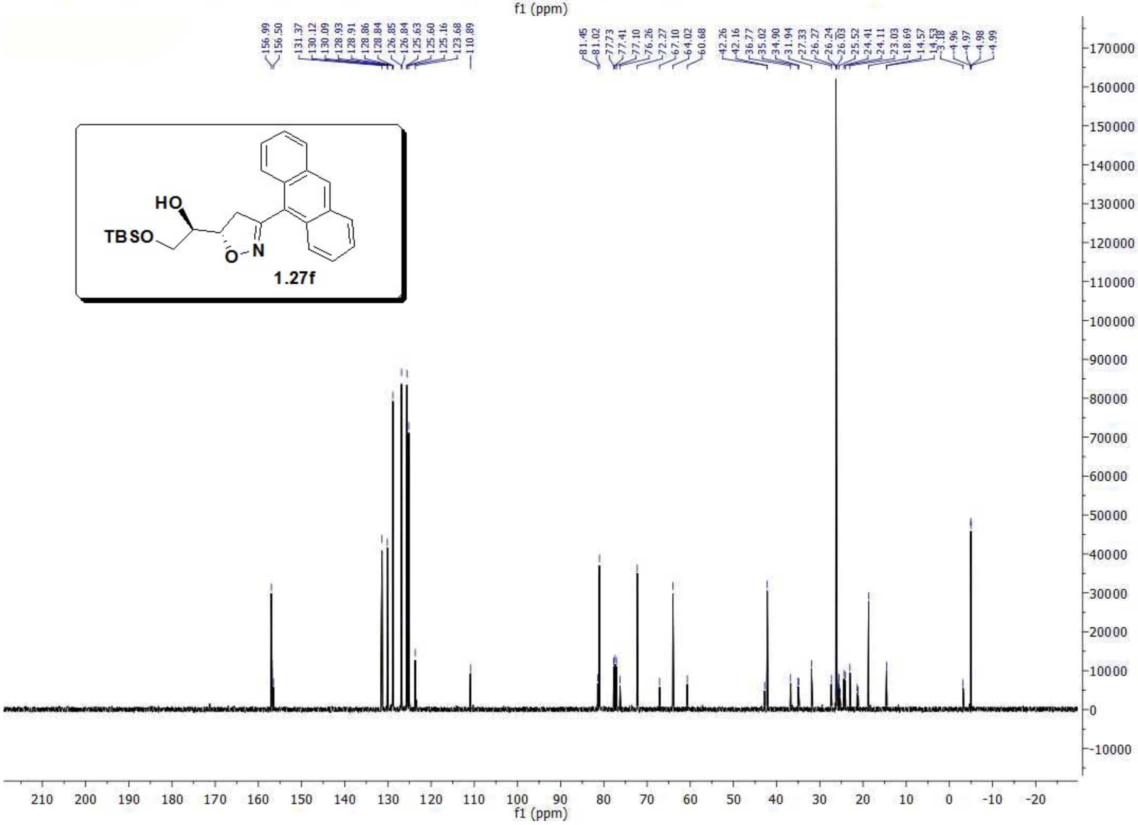
156.99
156.50
131.37
130.12
130.09
128.93
128.91
128.86
128.84
126.85
126.84
125.63
125.60
125.16
123.68
110.89
81.45
81.02
77.73
77.41
77.10
76.26
72.27
67.10
64.02
60.68
42.26
42.16
36.77
35.02
34.90
31.94
27.33
26.27
26.24
26.03
25.52
24.41
24.11
23.03
18.69
14.57
14.53
3.18
4.96
4.97
4.98
4.99
HO
TBSO
O-N
1.27f
f1 (ppm)

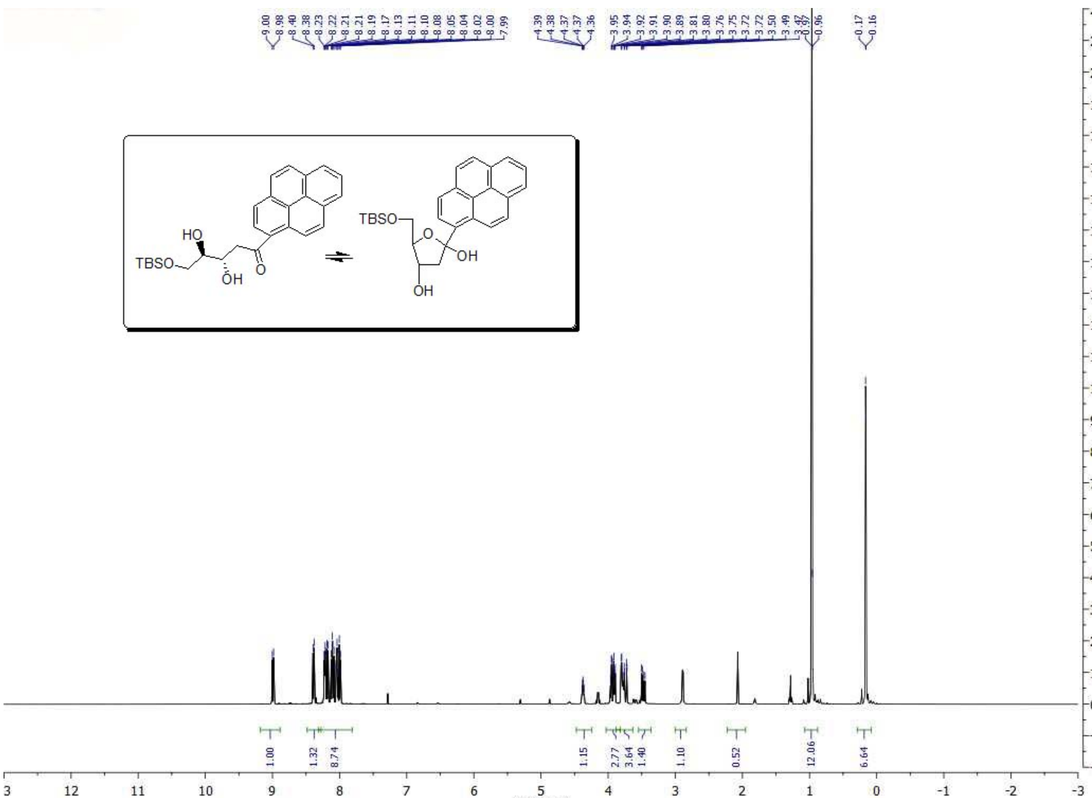

9.00
8.98
8.40
8.38
8.23
8.22
8.21
8.19
8.17
8.13
8.11
8.10
8.08
8.05
8.04
8.02
8.00
7.99
4.39
4.38
4.37
4.37
4.36
3.95
3.94
3.92
3.91
3.90
3.89
3.81
3.80
3.76
3.75
3.72
3.72
3.50
3.49
3.47
0.97
0.96
0.17
0.16
TBSO
HO
OH
O
TBSO
O
OH
OH
1.00
1.32
8.74
1.15
2.77
3.64
1.40
1.10
0.52
12.06
6.64
f1 (ppm)

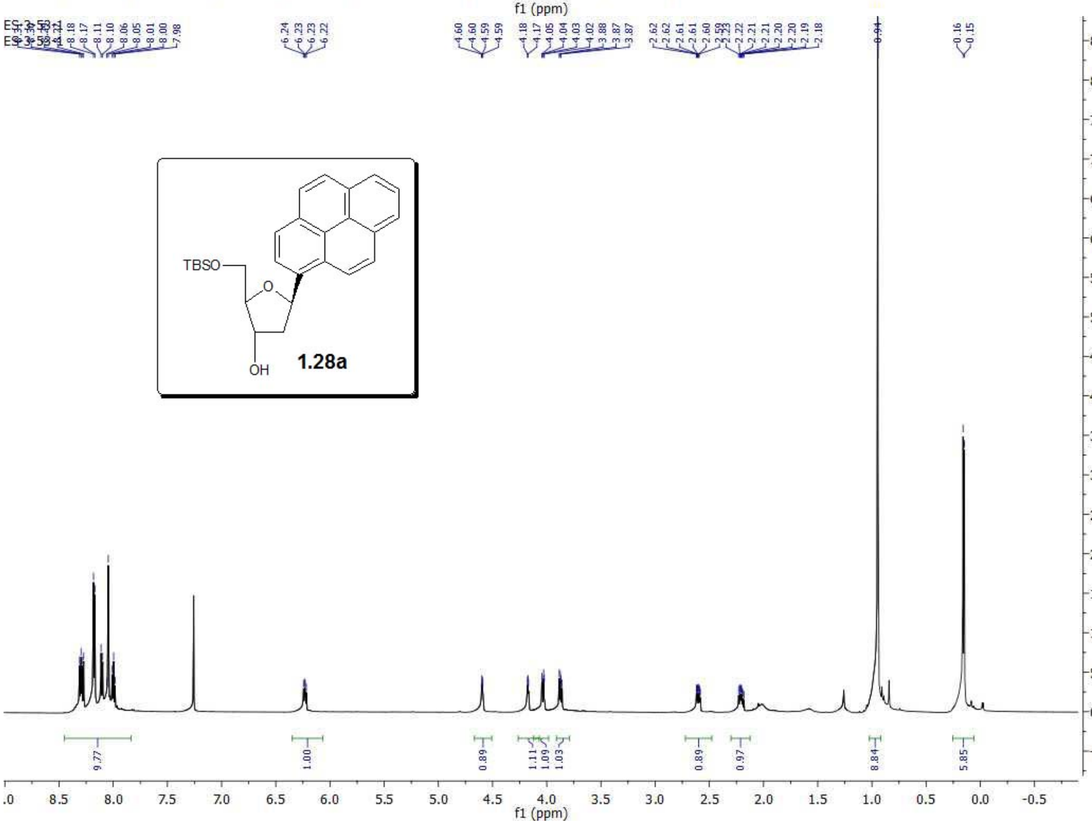

6.24
6.23
6.23
6.22
4.60
4.60
4.59
4.59
4.18
4.17
4.05
4.04
4.03
4.02
3.88
3.87
3.87
2.62
2.62
2.61
2.60
2.59
2.23
2.22
2.21
2.21
2.20
2.19
2.18
0.94
0.16
0.15
8.18
8.17
8.11
8.10
8.06
8.05
8.01
8.00
7.98
TBSO
O
OH
1.28a
9.77
1.00
0.89
1.11
1.09
1.03
0.89
0.97
8.84
5.85
f1 (ppm)

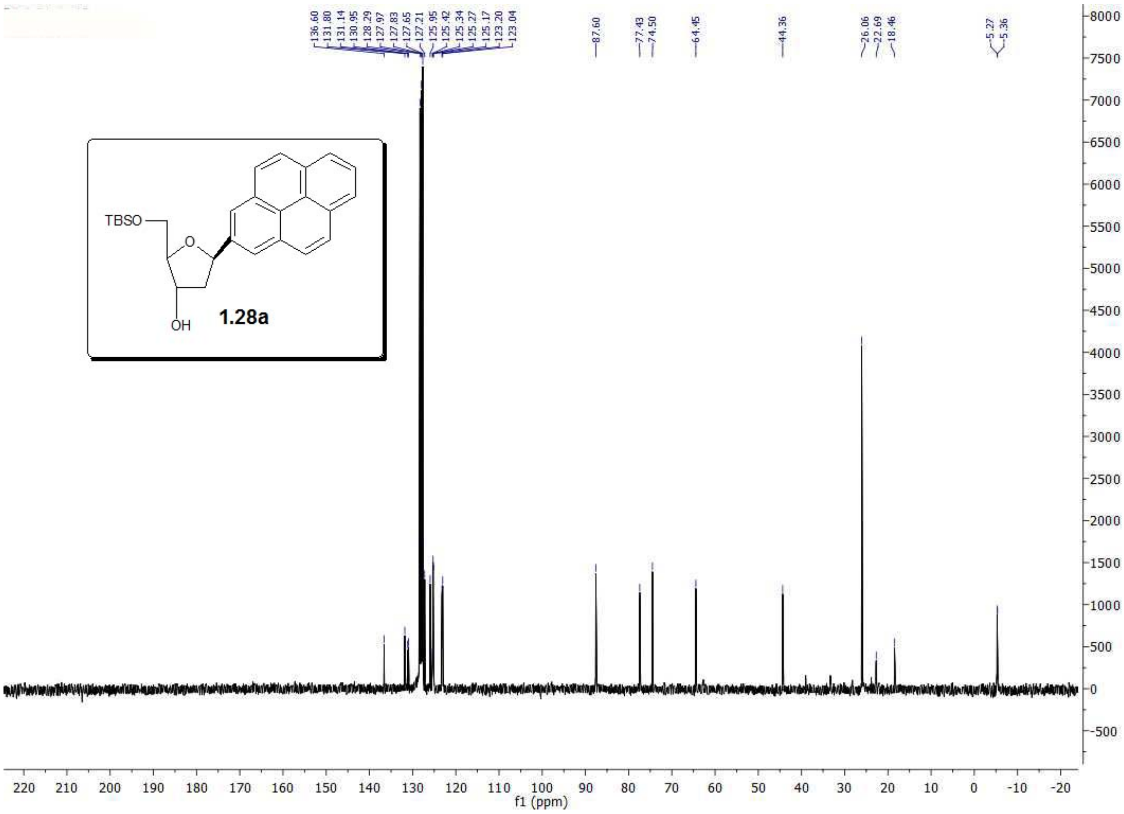
136.60
131.80
131.14
130.95
128.29
127.97
127.83
127.65
127.21
125.95
125.42
125.34
125.27
125.17
123.20
123.04
87.60
77.43
74.50
64.45
44.36
26.06
22.69
18.46
-5.27
-5.36
TBSO
O
OH
1.28a
f1 (ppm)
220 210 200 190 180 170 160 150 140 130 120 110 100 90 80 70 60 50 40 30 20 10 0 -10 -20
8000 7500 7000 6500 6000 5500 5000 4500 4000 3500 3000 2500 2000 1500 1000 500 0 -500

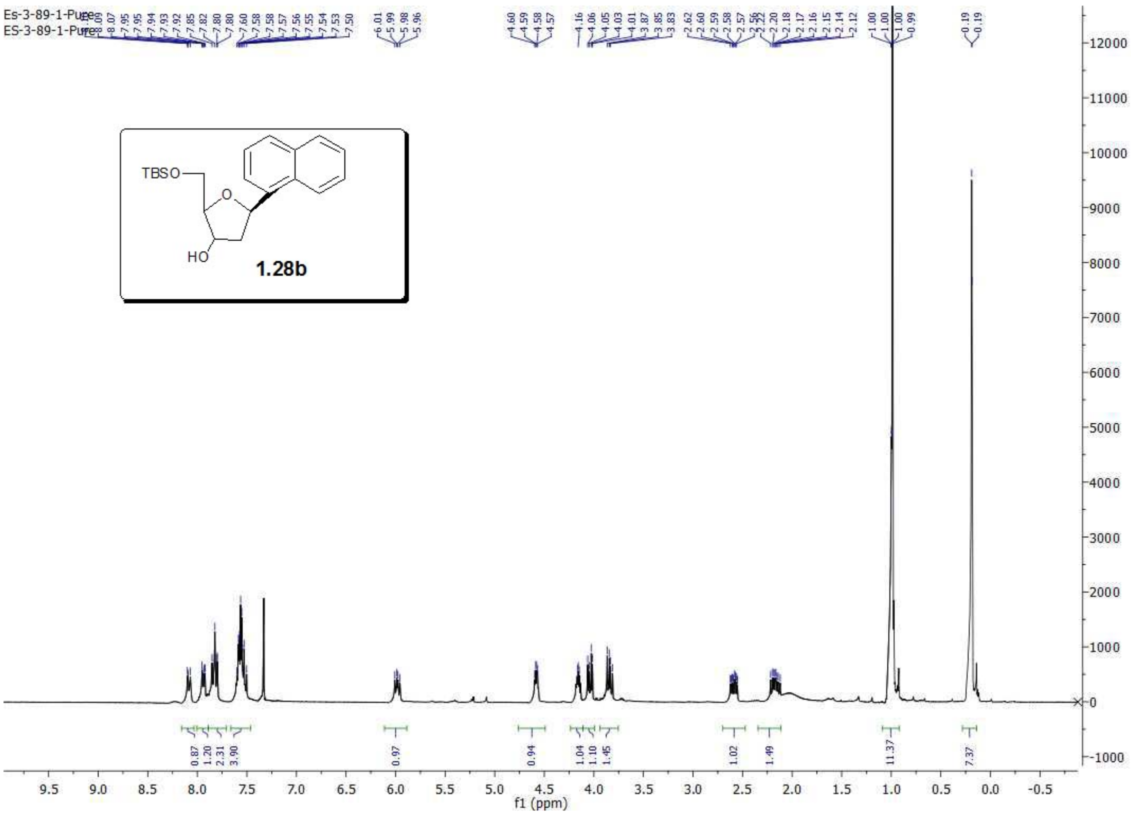
Es-3-89-1-Pure
ES-3-89-1-Pure
8.09
8.07
7.95
7.95
7.94
7.93
7.92
7.85
7.82
7.80
7.80
7.60
7.58
7.58
7.57
7.56
7.55
7.54
7.53
7.50
6.01
5.99
5.98
5.96
4.60
4.59
4.58
4.57
4.16
4.06
4.05
4.03
4.01
3.87
3.85
3.83
2.62
2.60
2.59
2.58
2.57
2.56
2.22
2.20
2.18
2.17
2.16
2.15
2.14
2.12
1.00
1.00
1.00
0.99
0.19
0.19
TBSO
O
HO
1.28b
0.87
1.20
2.31
3.90
0.97
0.94
1.04
1.10
1.45
1.02
1.49
11.37
7.37
f1 (ppm)
9.5 9.0 8.5 8.0 7.5 7.0 6.5 6.0 5.5 5.0 4.5 4.0 3.5 3.0 2.5 2.0 1.5 1.0 0.5 0.0 -0.5
12000 11000 10000 9000 8000 7000 6000 5000 4000 3000 2000 1000 0 -1000

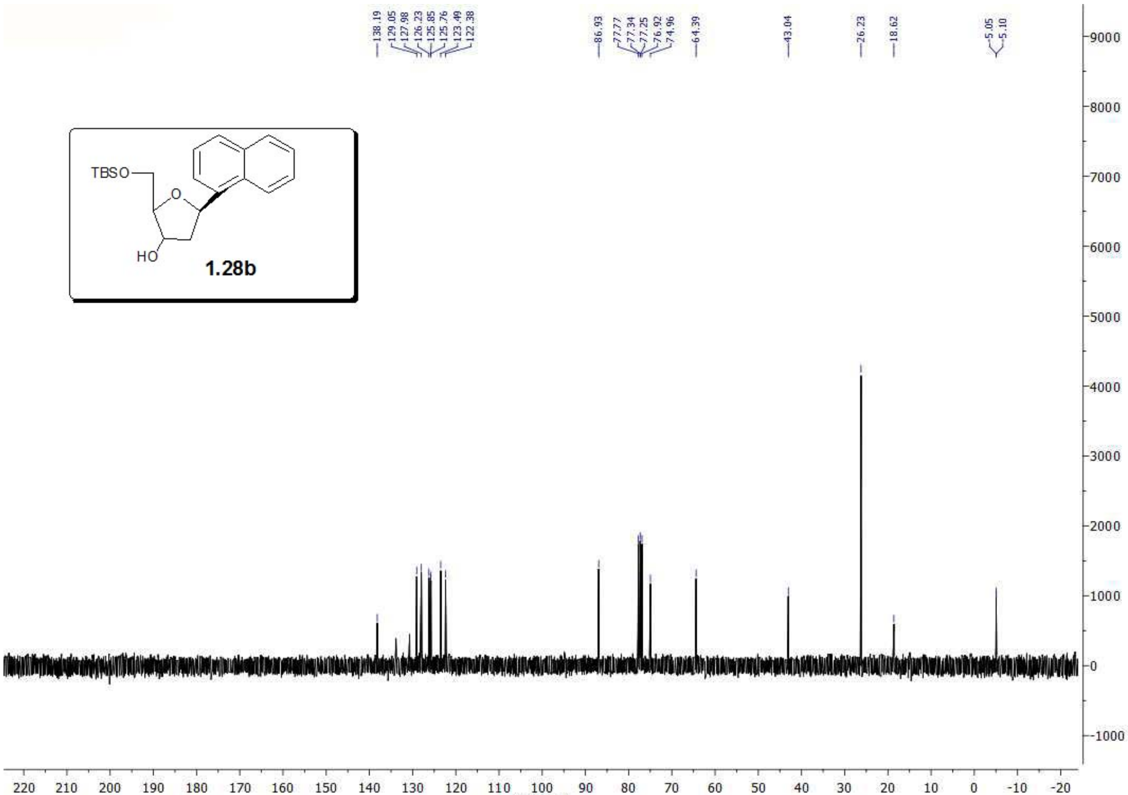
138.19
129.05
127.98
126.23
125.85
125.76
123.49
122.38
86.93
77.77
77.34
77.25
76.92
74.96
64.39
43.04
26.23
18.62
-5.05
-5.10
TBSO
O
HO
1.28b
9000
8000
7000
6000
5000
4000
3000
2000
1000
0
-1000
220 210 200 190 180 170 160 150 140 130 120 110 100 90 80 70 60 50 40 30 20 10 0 -10 -20
f1 (ppm)

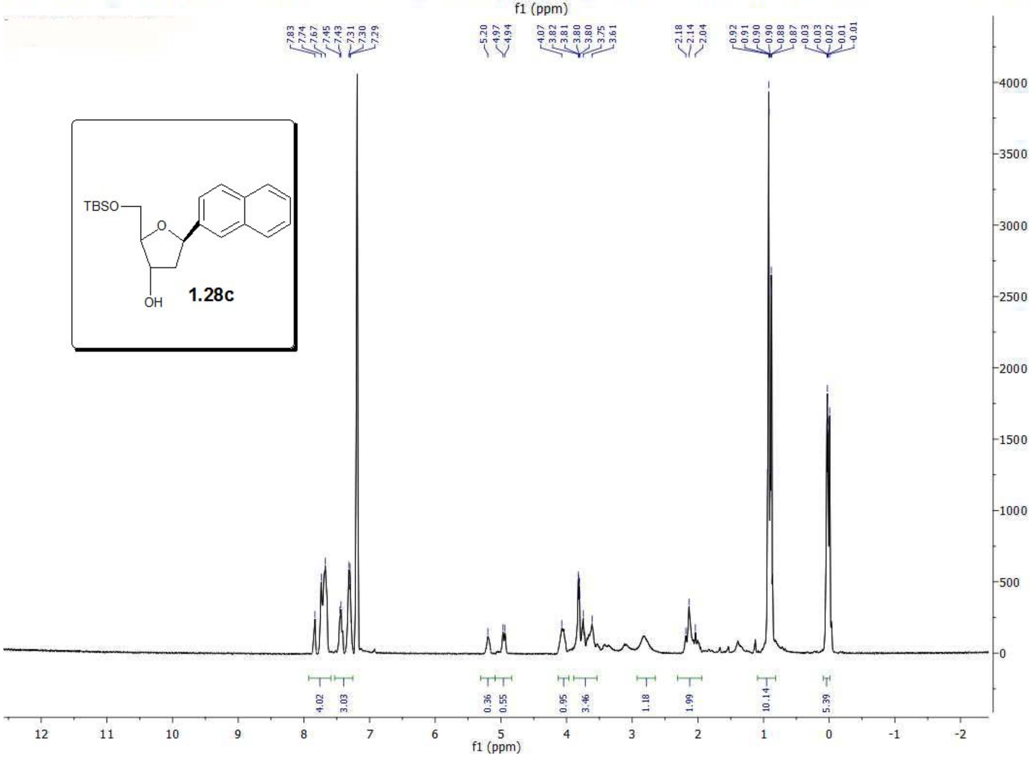
7.83
7.74
7.67
7.45
7.43
7.31
7.30
7.29
5.20
4.97
4.94
4.07
3.82
3.81
3.80
3.80
3.75
3.61
2.18
2.14
2.04
0.92
0.91
0.90
0.90
0.88
0.87
0.03
0.02
0.01
-0.01
TBSO
O
OH
1.28c
4000
3500
3000
2500
2000
1500
1000
500
0
4.02
3.03
0.36
0.55
0.95
3.46
1.18
1.99
10.14
5.39
12 11 10 9 8 7 6 5 4 3 2 1 0 -1 -2
f1 (ppm)

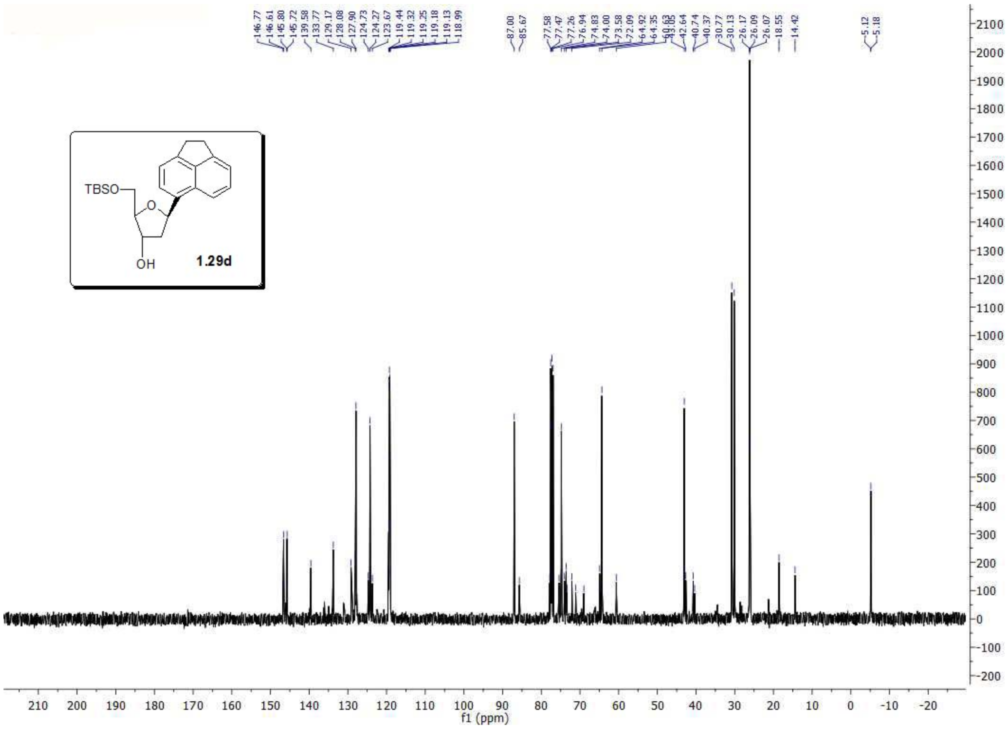
146.77
146.61
145.80
145.72
139.58
133.77
129.17
128.08
127.90
124.73
124.27
123.67
119.44
119.32
119.25
119.18
119.13
118.99
87.00
85.67
77.58
77.47
77.26
76.94
74.83
74.00
73.58
72.09
64.92
64.35
60.63
43.05
42.64
40.74
40.37
30.77
30.13
26.17
26.09
26.07
18.55
14.42
-5.12
-5.18
TBSO
O
OH
1.29d
2100
2000
1900
1800
1700
1600
1500
1400
1300
1200
1100
1000
900
800
700
600
500
400
300
200
100
0
-100
-200
210
200
190
180
170
160
150
140
130
120
110
100
90
80
70
60
50
40
30
20
10
0
-10
-20
f1 (ppm)

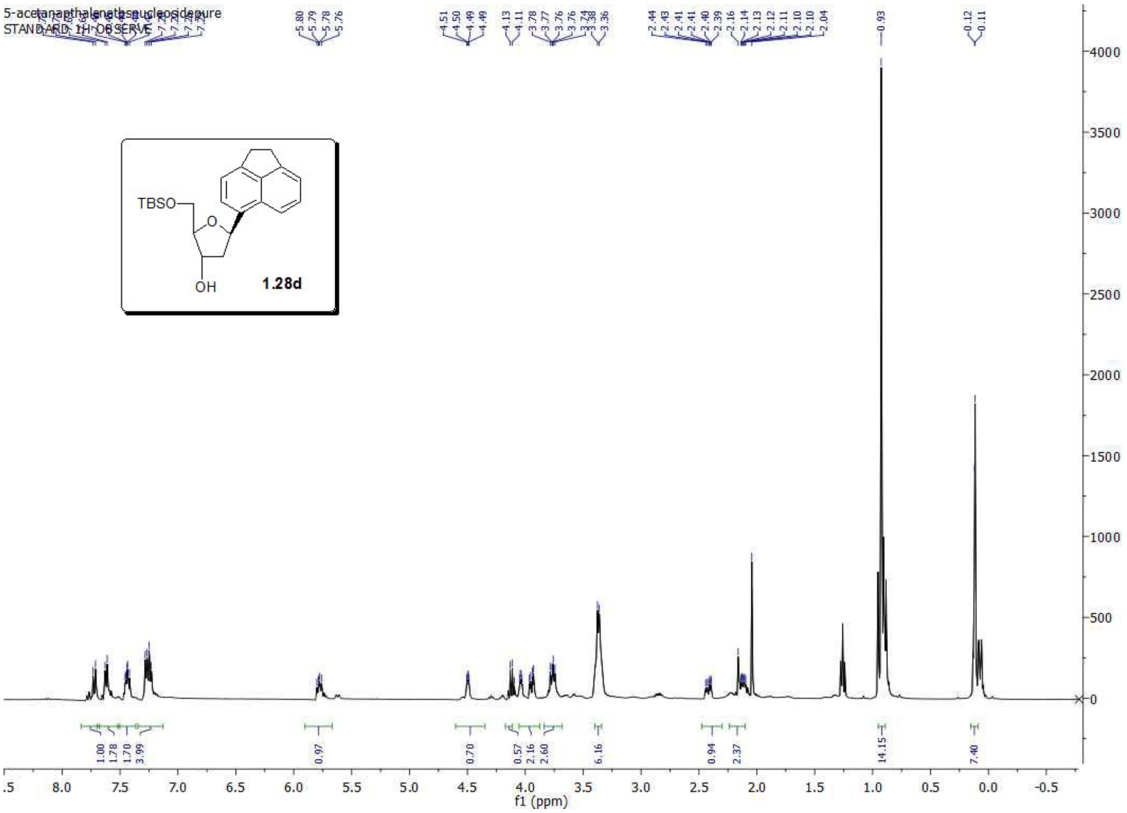
5-acetanapthalenetbsnucleosidepure
STANDARD 1H OBSERVE
5.80
5.79
5.78
5.76
4.51
4.50
4.49
4.49
4.13
4.11
3.78
3.77
3.76
3.76
3.74
3.38
3.36
2.44
2.43
2.41
2.41
2.40
2.39
2.16
2.14
2.13
2.12
2.11
2.10
2.10
2.04
0.93
0.12
0.11
TBSO
O
OH
1.28d
4000
3500
3000
2500
2000
1500
1000
500
0
1.00
1.78
1.70
3.99
0.97
0.70
0.57
2.16
2.60
6.16
0.94
2.37
14.15
7.40
.5
8.0
7.5
7.0
6.5
6.0
5.5
5.0
4.5
4.0
3.5
3.0
2.5
2.0
1.5
1.0
0.5
0.0
-0.5
f1 (ppm)

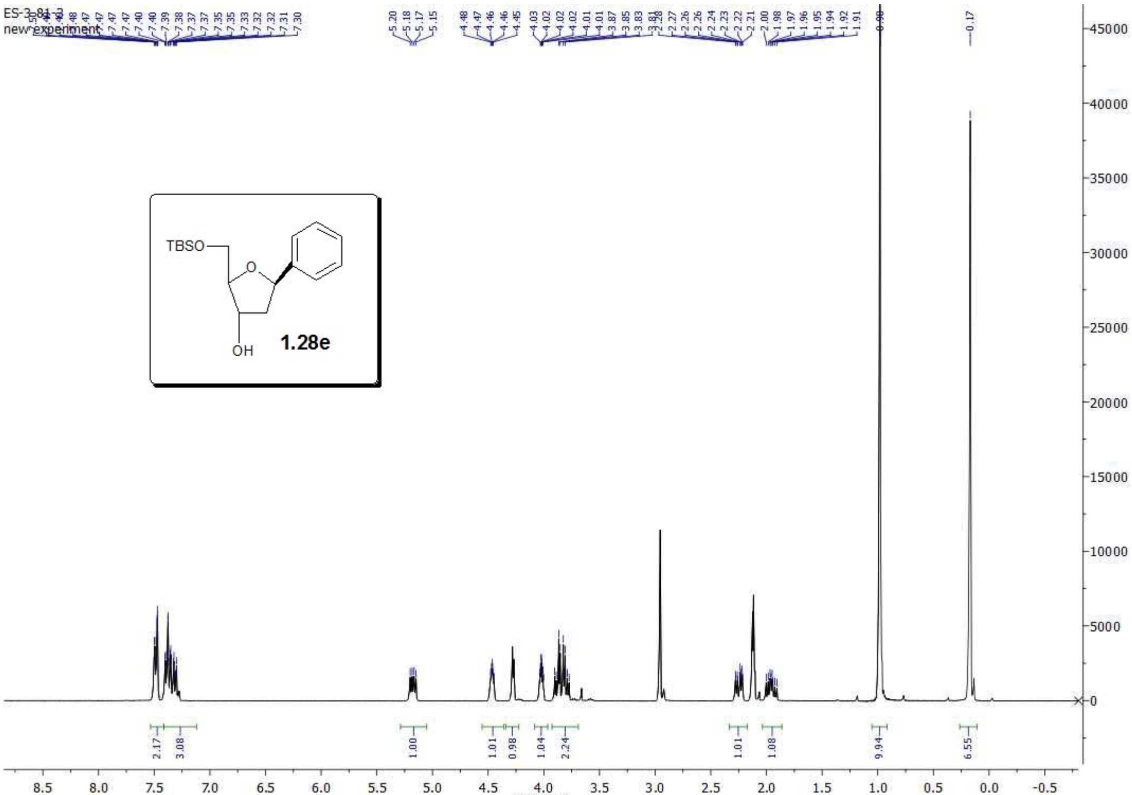
ES-3-81-3
new experiment
7.48 7.47 7.47 7.47 7.40 7.40 7.39 7.38 7.37 7.37 7.35 7.35 7.33 7.32 7.32 7.31 7.30
5.20 5.18 5.17 5.15
4.48 4.47 4.46 4.46 4.45
4.03 4.02 4.02 4.02 4.01 4.01 3.87 3.85 3.83 3.81
2.28 2.27 2.26 2.26 2.24 2.23 2.22 2.21
2.00 1.98 1.97 1.96 1.95 1.94 1.92 1.91
0.98
0.17
TBSO
O
OH
1.28e
2.17 3.08 1.00 1.01 0.98 1.04 2.24 1.01 1.08 9.94 6.55
8.5 8.0 7.5 7.0 6.5 6.0 5.5 5.0 4.5 4.0 3.5 3.0 2.5 2.0 1.5 1.0 0.5 0.0 -0.5
f1 (ppm)
45000 40000 35000 30000 25000 20000 15000 10000 5000 0

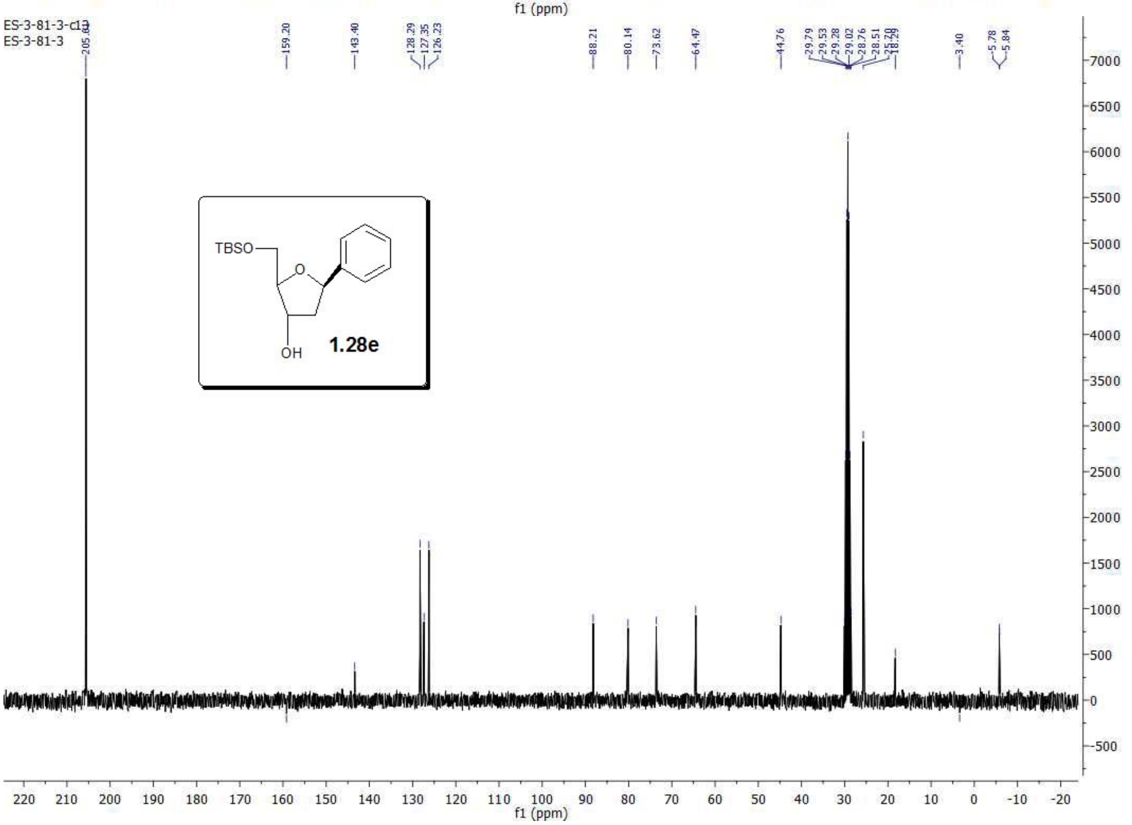
ES-3-81-3-c13
ES-3-81-3
205.60
159.20
143.40
128.29 127.35 126.23
88.21
80.14
73.62
64.47
44.76
29.79 29.53 29.28 29.02 28.76 28.51 25.70 18.29
3.40
-5.78 -5.84
TBSO
O
OH
1.28e
220 210 200 190 180 170 160 150 140 130 120 110 100 90 80 70 60 50 40 30 20 10 0 -10 -20
f1 (ppm)
7000 6500 6000 5500 5000 4500 4000 3500 3000 2500 2000 1500 1000 500 0 -500

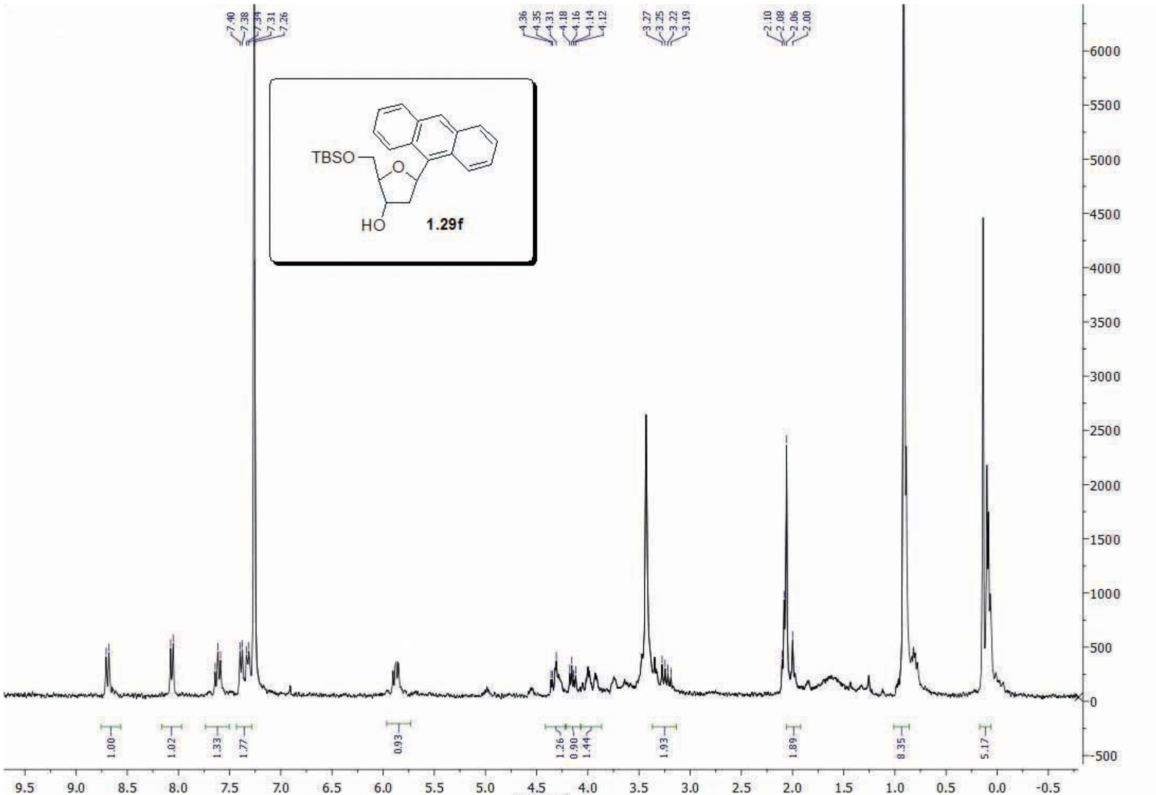
7.40
7.38
7.34
7.31
7.26
4.36
4.35
4.31
4.18
4.16
4.14
4.12
3.27
3.25
3.22
3.19
2.10
2.08
2.06
2.00
TBSO
O
HO
1.29f
1.00
1.02
1.33
1.77
0.93
1.26
0.90
1.44
1.93
1.89
8.35
5.17
f1 (ppm)

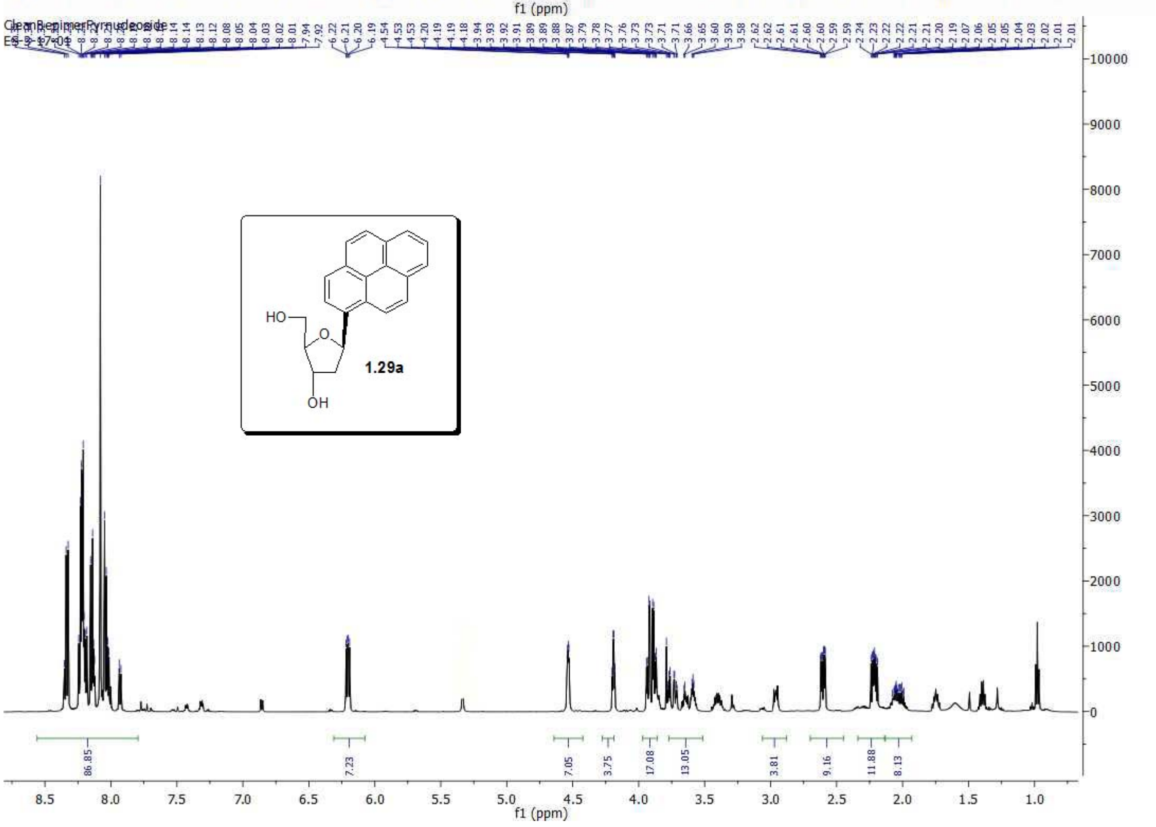
CleanBepimerPyrnudeoside
ES-3-17-01
HO
O
OH
1.29a
86.85
7.23
7.05
3.75
17.08
13.05
3.81
9.16
11.88
8.13
f1 (ppm)

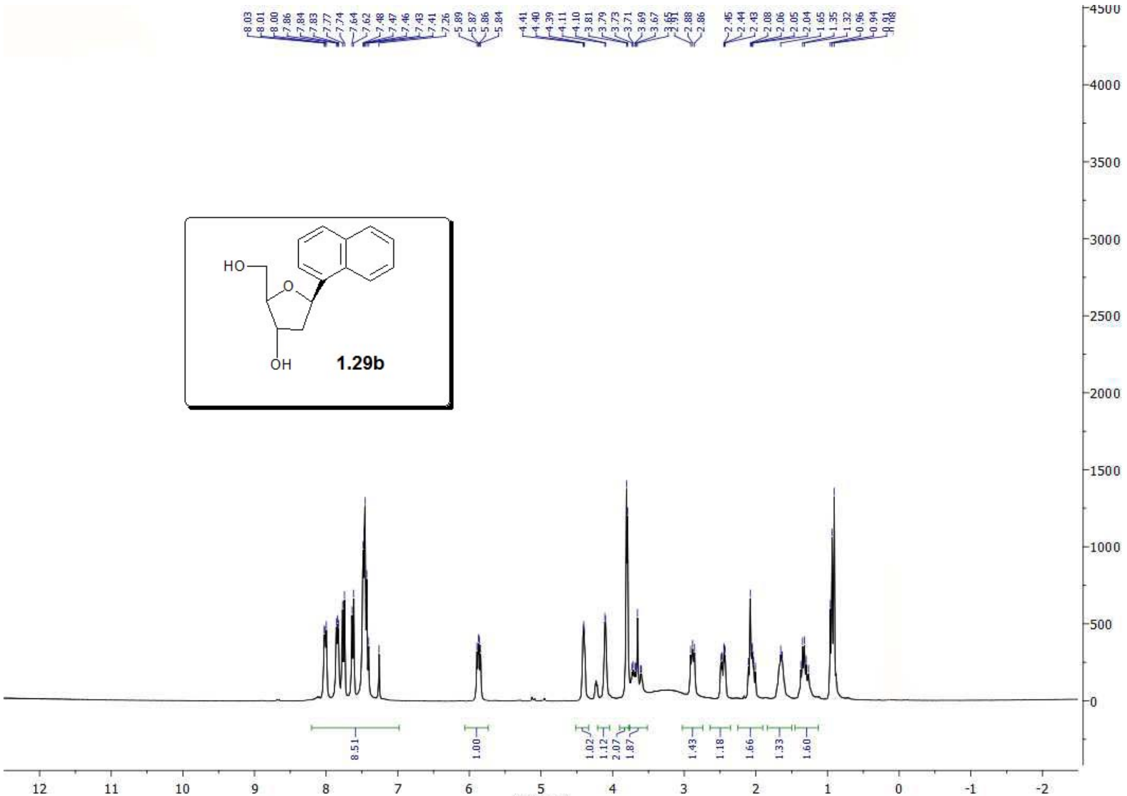
8.03
8.01
8.00
7.86
7.84
7.83
7.77
7.74
7.64
7.62
7.48
7.47
7.46
7.43
7.41
7.26
5.89
5.87
5.86
5.84
4.41
4.40
4.39
4.11
4.10
3.81
3.79
3.73
3.71
3.69
3.67
3.65
2.91
2.88
2.86
2.45
2.44
2.43
2.08
2.06
2.05
2.04
1.65
1.35
1.32
0.96
0.94
0.91
0.88
HO
O
OH
1.29b
8.51
1.00
1.02
1.12
2.07
1.87
1.43
1.18
1.66
1.33
1.60
4500
4000
3500
3000
2500
2000
1500
1000
500
0
12
11
10
9
8
7
6
5
4
3
2
1
0
-1
-2
f1 (ppm)

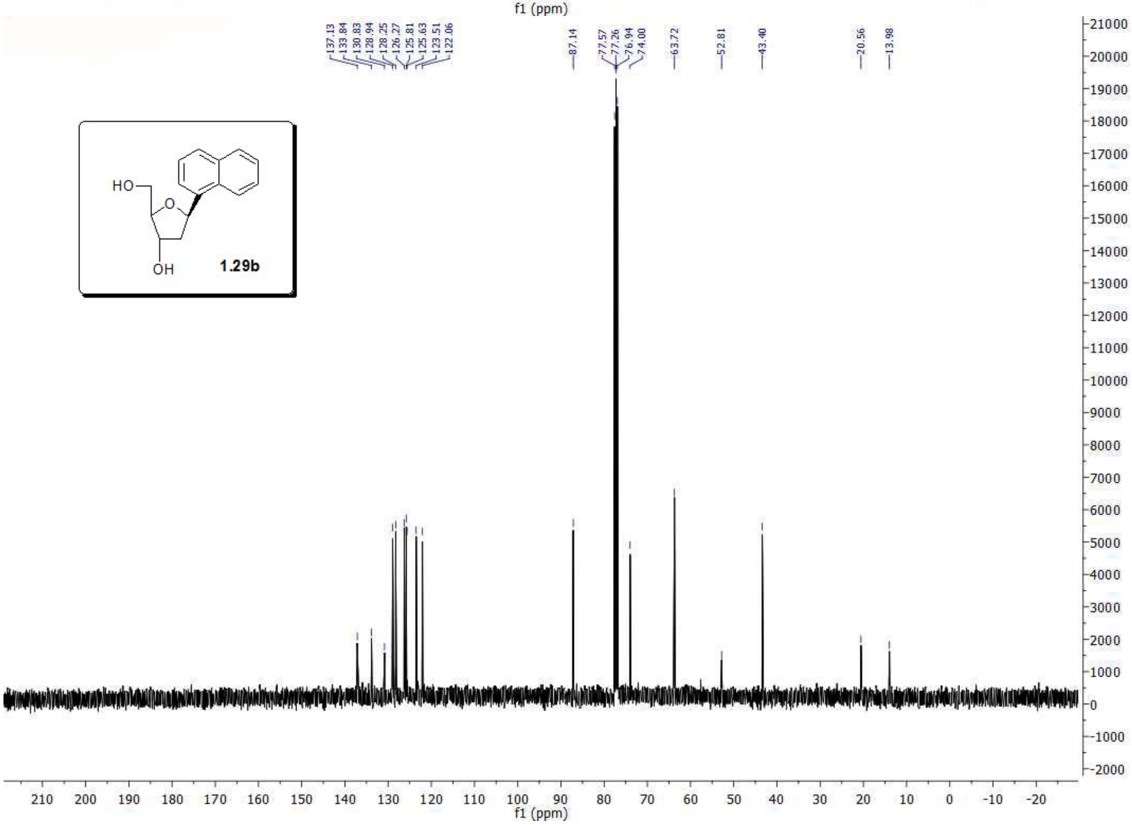
137.13
133.84
130.83
128.94
128.25
126.27
125.81
125.63
123.51
122.06
87.14
77.57
77.26
76.94
74.00
63.72
52.81
43.40
20.56
13.98
HO
O
OH
1.29b
21000
20000
19000
18000
17000
16000
15000
14000
13000
12000
11000
10000
9000
8000
7000
6000
5000
4000
3000
2000
1000
0
-1000
-2000
210
200
190
180
170
160
150
140
130
120
110
100
90
80
70
60
50
40
30
20
10
0
-10
-20
f1 (ppm)

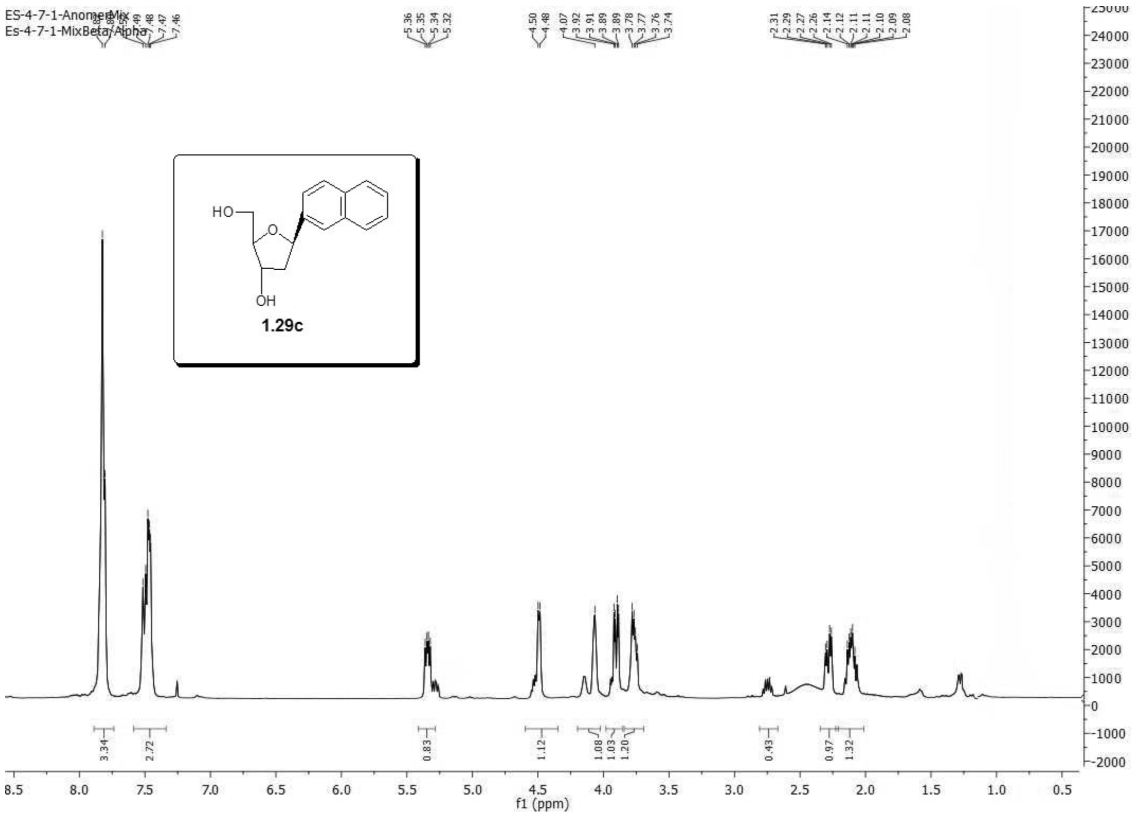
ES-4-7-1-AnomerMix
Es-4-7-1-MixBeta/Alpha
7.49
7.48
7.47
7.46
5.36
5.35
5.34
5.32
4.50
4.48
4.07
3.92
3.91
3.89
3.89
3.78
3.77
3.76
3.74
2.31
2.29
2.27
2.26
2.14
2.12
2.11
2.11
2.10
2.09
2.08
HO
O
OH
1.29c
3.34
2.72
0.83
1.12
1.08
1.03
1.20
0.43
0.97
1.32
f1 (ppm)

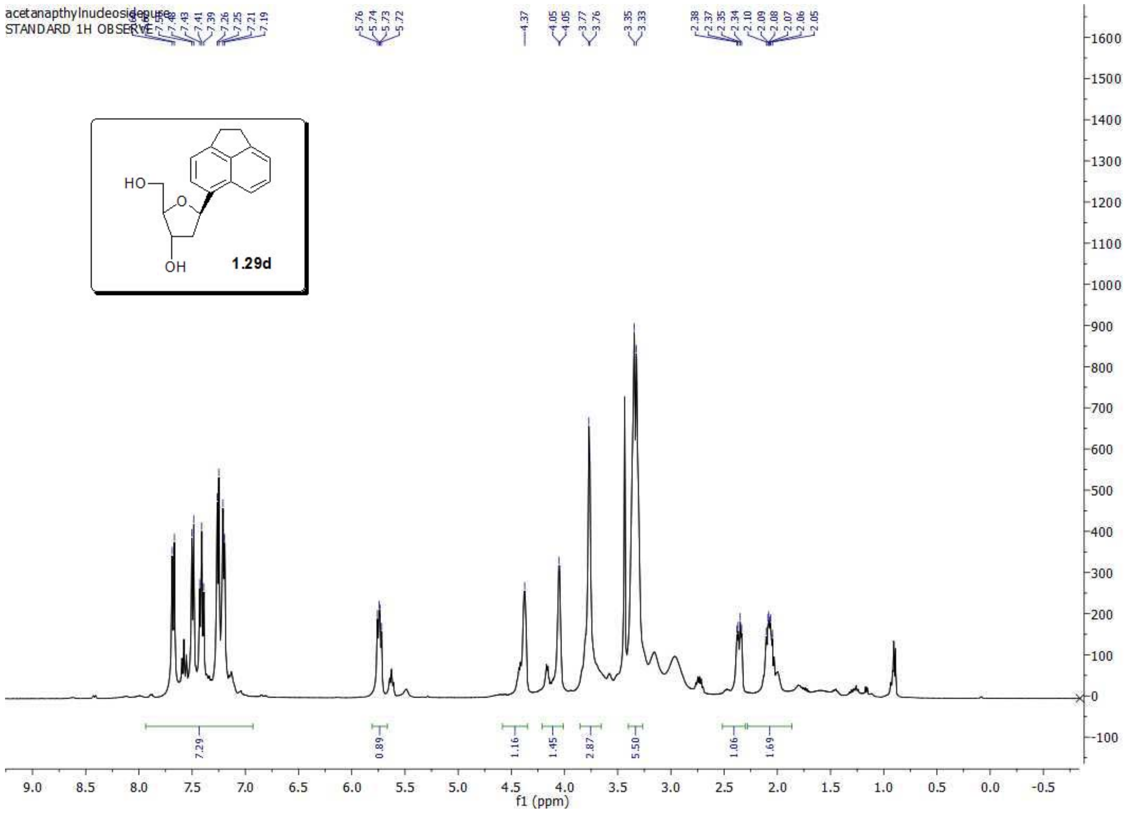
acetanapthylnudeosidepure
STANDARD 1H OBSERVE
7.43
7.41
7.39
7.26
7.25
7.21
7.19
5.76
5.74
5.73
5.72
4.37
4.05
4.05
3.77
3.76
3.35
3.33
2.38
2.37
2.35
2.34
2.10
2.09
2.08
2.07
2.06
2.05
HO
O
OH
1.29d
7.29
0.89
1.16
1.45
2.87
5.50
1.06
1.69
f1 (ppm)

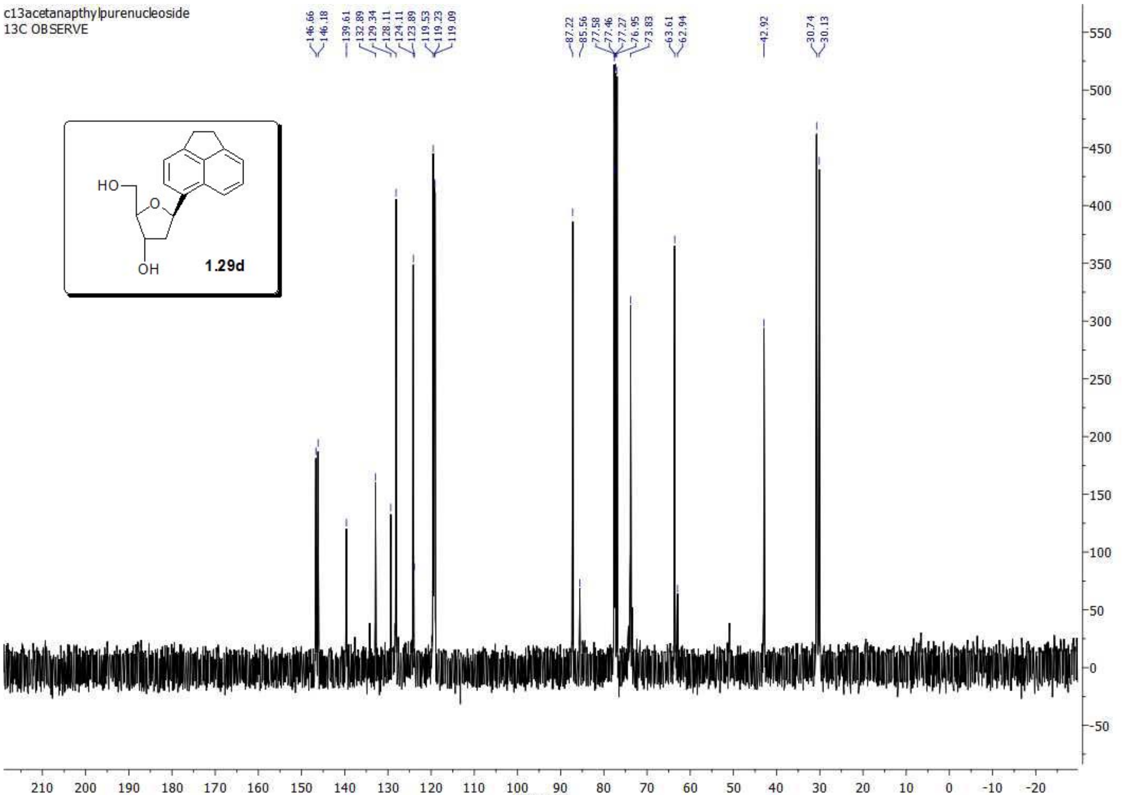
c13acetanapthylpurenucleoside
13C OBSERVE
146.66
146.18
139.61
132.89
129.34
128.11
124.11
123.89
119.53
119.23
119.09
87.22
85.56
77.58
77.46
77.27
76.95
73.83
63.61
62.94
42.92
30.74
30.13
HO
O
OH
1.29d
f1 (ppm)

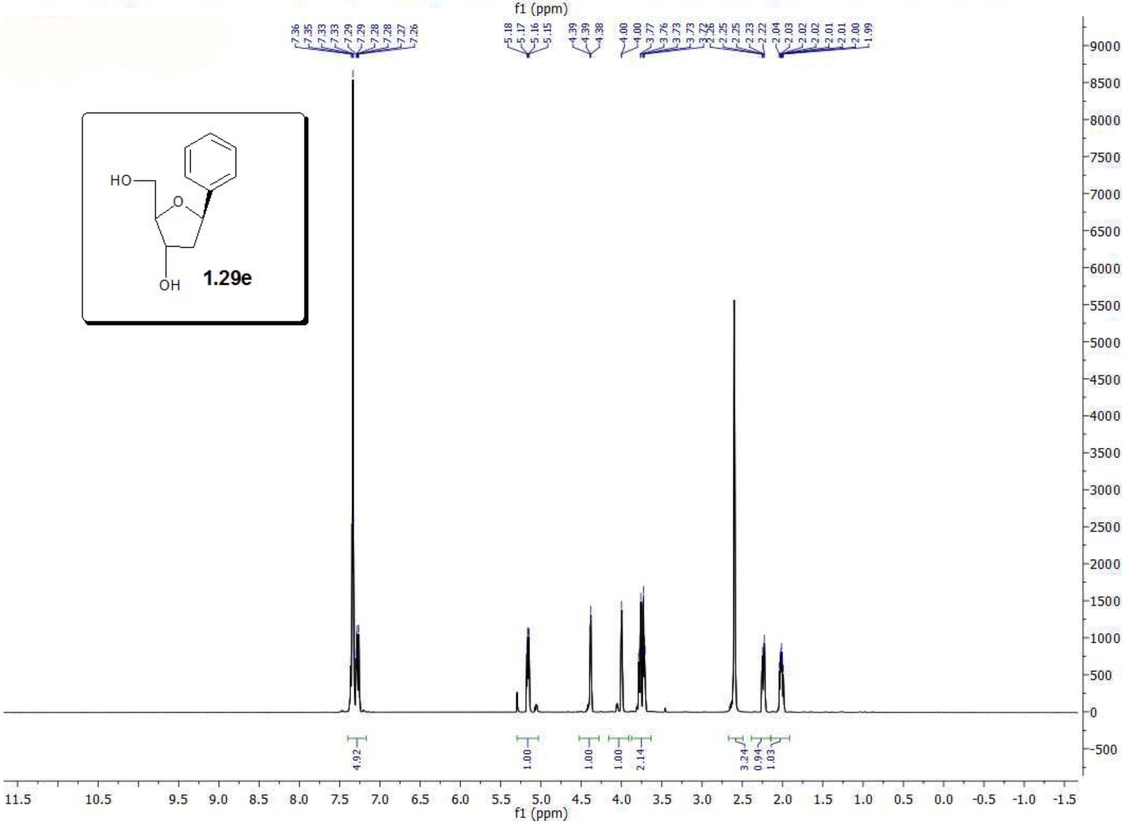
7.36
7.35
7.33
7.33
7.29
7.29
7.28
7.28
7.27
7.26
5.18
5.17
5.16
5.15
4.39
4.39
4.38
4.00
4.00
3.77
3.76
3.73
3.73
2.25
2.25
2.23
2.22
2.04
2.03
2.02
2.02
2.01
2.01
2.00
1.99
HO
O
OH
1.29e
4.92
1.00
1.00
1.00
2.14
3.24
0.94
1.03
f1 (ppm)

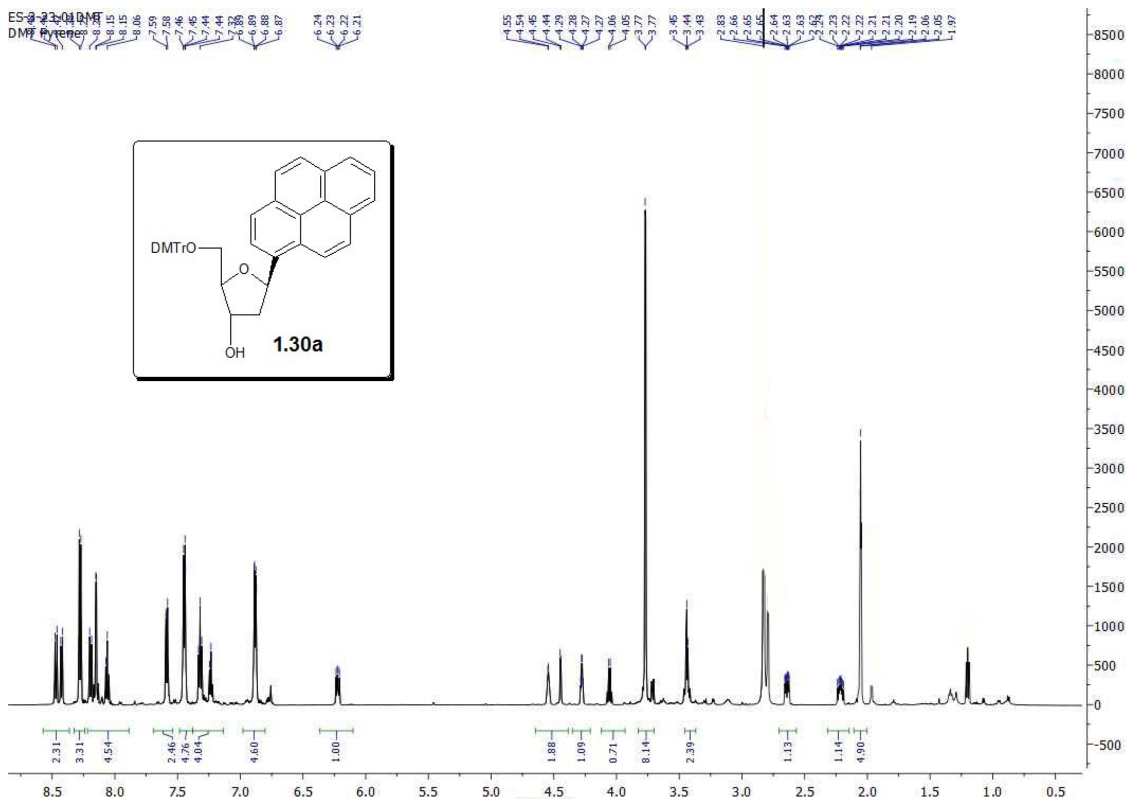
ES-3-23-01DMT
DMT Pyrene
8.15 8.15 8.06 7.59 7.58 7.46 7.45 7.44 7.44 7.32 6.89 6.88 6.87
6.24 6.23 6.22 6.21
4.55 4.54 4.45 4.44 4.29 4.28 4.27 4.27 4.06 4.05 3.77 3.77 3.45 3.44 3.43
2.83 2.66 2.65 2.65 2.64 2.63 2.63 2.62 2.24 2.23 2.22 2.22 2.21 2.21 2.20 2.19 2.06 2.05 1.97
DMTrO
O
OH
1.30a
2.31 3.31 4.54 2.46 4.76 4.04 4.60 1.00 1.88 1.09 0.71 8.14 2.39 1.13 1.14 4.90
8.5 8.0 7.5 7.0 6.5 6.0 5.5 5.0 4.5 4.0 3.5 3.0 2.5 2.0 1.5 1.0 0.5
f1 (ppm)
8500 8000 7500 7000 6500 6000 5500 5000 4500 4000 3500 3000 2500 2000 1500 1000 500 0 -500

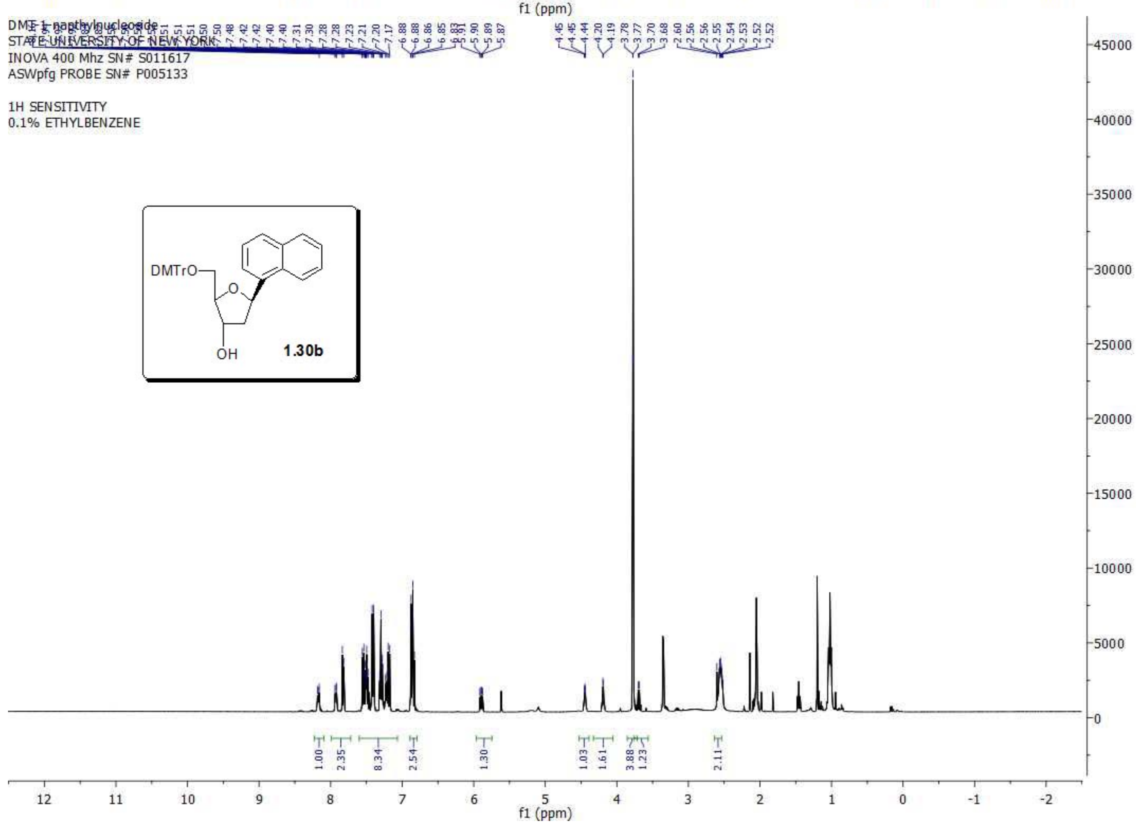
DMT 1-napthylnucleoside
STATE UNIVERSITY OF NEW YORK
INOVA 400 Mhz SN# S011617
ASWpfg PROBE SN# P005133
1H SENSITIVITY
0.1% ETHYLBENZENE
7.51 7.51 7.50 7.48 7.42 7.42 7.40 7.40 7.31 7.30 7.28 7.28 7.23 7.21 7.20 7.17 6.88 6.88 6.86 6.85 6.83 5.91 5.90 5.89 5.87
4.45 4.45 4.44 4.20 4.19 3.78 3.77 3.70 3.68 2.60 2.56 2.56 2.55 2.54 2.53 2.52 2.52 2.52
DMTrO
O
OH
1.30b
1.00 2.35 8.34 2.54 1.30 1.03 1.61 3.88 1.23 2.11
12 11 10 9 8 7 6 5 4 3 2 1 0 -1 -2
f1 (ppm)
45000 40000 35000 30000 25000 20000 15000 10000 5000 0

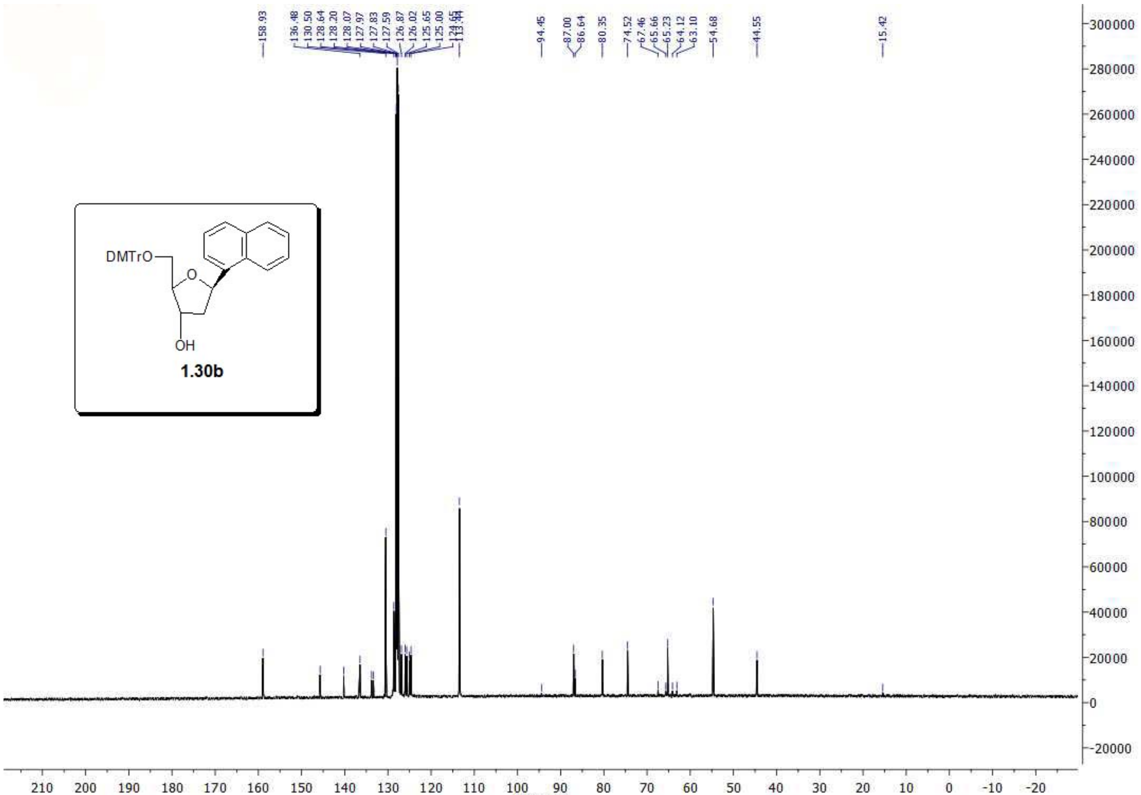
158.93
136.48
130.50
128.64
128.20
128.07
127.97
127.83
127.59
126.87
126.02
125.65
125.00
124.65
113.44
94.45
87.00
86.64
80.35
74.52
67.46
65.66
65.23
64.12
63.10
54.68
44.55
15.42
DMTrO
O
OH
300000
280000
260000
240000
220000
200000
180000
160000
140000
120000
100000
80000
60000
40000
20000
0
-20000
210 200 190 180 170 160 150 140 130 120 110 100 90 80 70 60 50 40 30 20 10 0 -10 -20
f1 (ppm)

1.30b

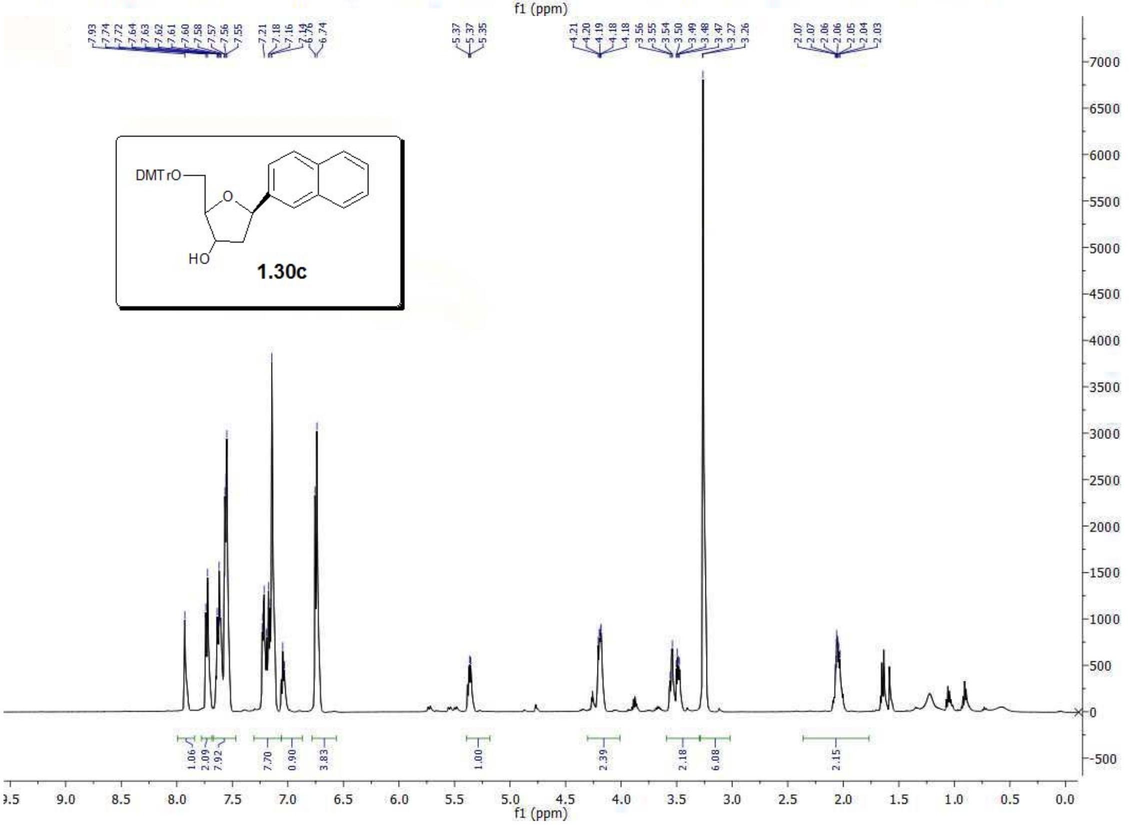
7.93
7.74
7.72
7.64
7.63
7.62
7.61
7.60
7.58
7.57
7.56
7.55
7.21
7.18
7.16
7.14
6.76
6.74
5.37
5.37
5.35
4.21
4.20
4.19
4.18
4.18
3.56
3.55
3.54
3.50
3.49
3.48
3.47
3.27
3.26
2.07
2.07
2.06
2.06
2.05
2.04
2.03
DMTrO
O
HO
7000
6500
6000
5500
5000
4500
4000
3500
3000
2500
2000
1500
1000
500
0
-500
1.06
2.09
7.92
7.70
0.90
3.83
1.00
2.39
2.18
6.08
2.15
9.5 9.0 8.5 8.0 7.5 7.0 6.5 6.0 5.5 5.0 4.5 4.0 3.5 3.0 2.5 2.0 1.5 1.0 0.5 0.0
f1 (ppm)

1.30c

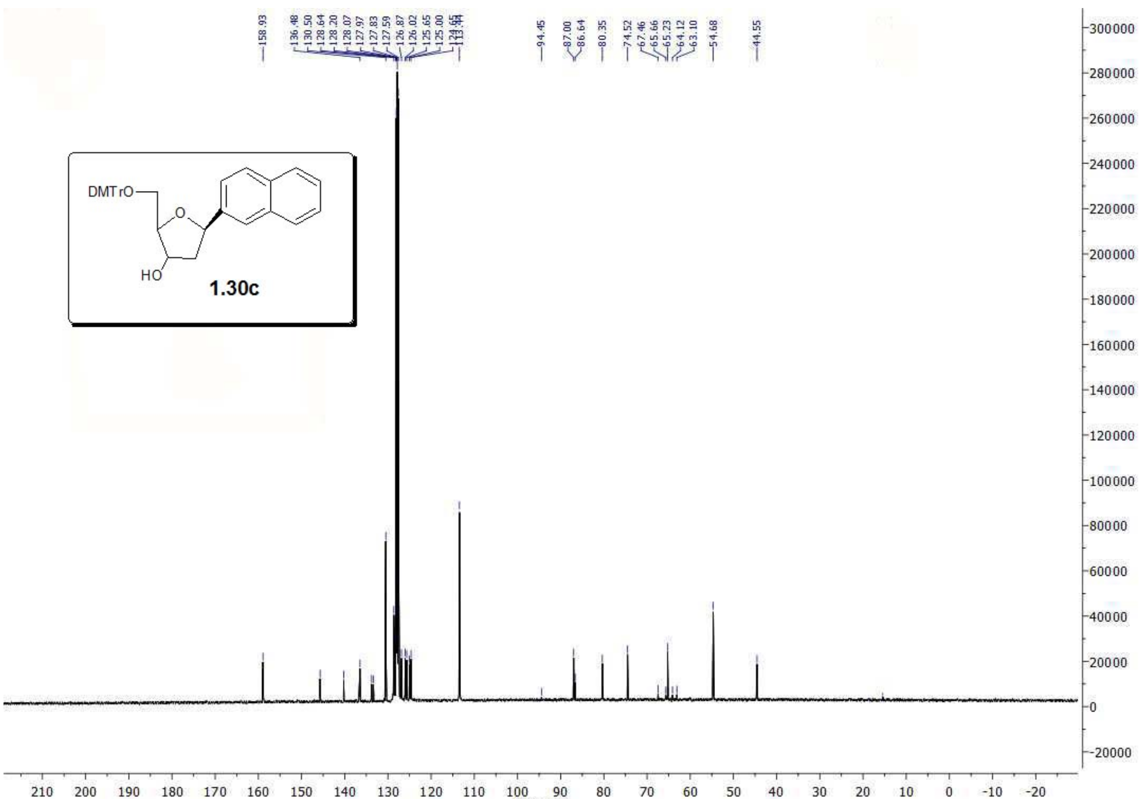
158.93
136.48
130.50
128.64
128.20
128.07
127.97
127.83
127.59
126.87
126.02
125.65
125.00
124.65
113.44
94.45
87.00
86.64
80.35
74.52
67.46
65.66
65.23
64.12
63.10
54.68
44.55
DMTrO
O
HO
1.30c
f1 (ppm)

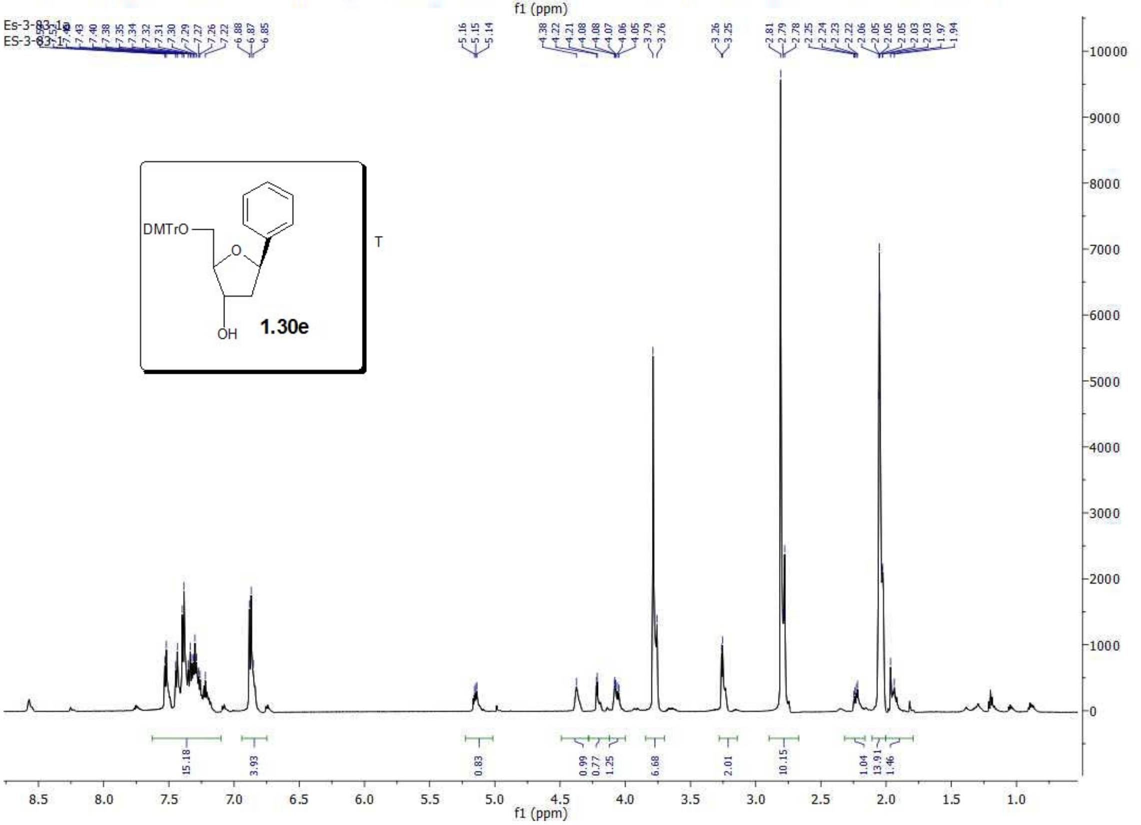
Es-3-83-1e
ES-3-83-1
5.16
5.15
5.14
3.79
3.76
3.26
3.25
2.81
2.79
2.78
DMTrO
O
OH
1.30e
T
15.18
3.93
0.83
0.99
0.77
1.25
6.68
2.01
10.15
1.04
13.91
1.46
f1 (ppm)

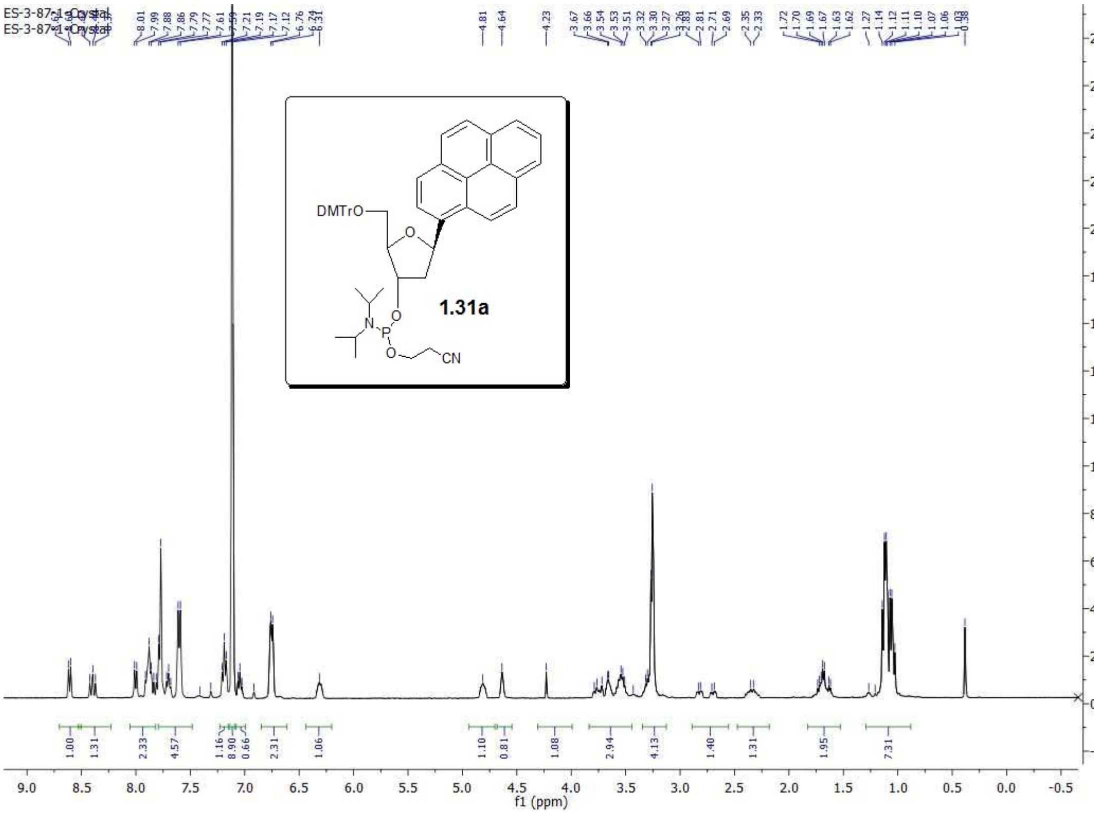
ES-3-87-1-Crystal
DMTrO
O
N
P
CN
1.31a
8.01 7.99 7.88 7.86 7.79 7.77 7.61 7.59 7.21 7.19 7.17 7.12 6.76 6.74 6.31
4.81 4.64 4.23 3.67 3.66 3.54 3.53 3.51 3.32 3.30 3.27 3.26 2.83 2.81 2.71 2.69 2.35 2.33
1.72 1.70 1.69 1.67 1.63 1.62 1.27 1.14 1.12 1.11 1.10 1.07 1.06 0.38
1.00 1.31 2.33 4.57 1.16 8.90 0.66 2.31 1.06 1.10 0.81 1.08 2.94 4.13 1.40 1.31 1.95 7.31
f1 (ppm)

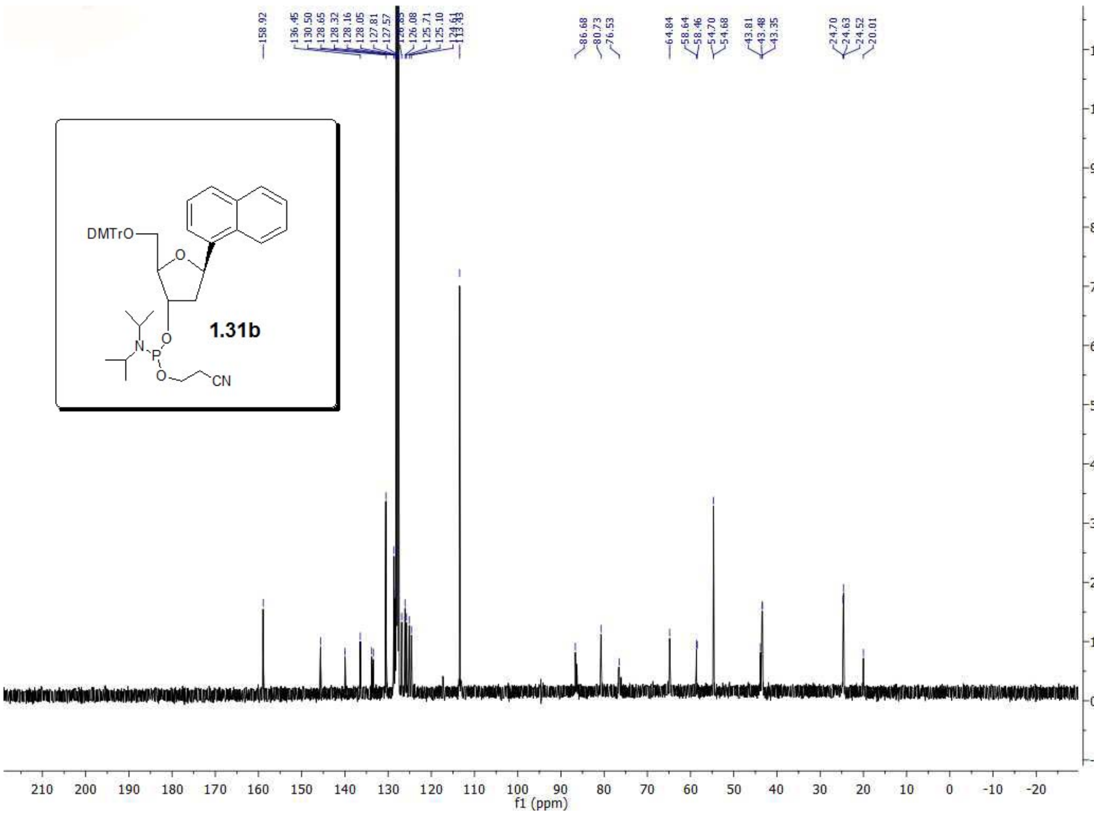
158.92 136.45 130.50 128.65 128.32 128.16 128.05 127.81 127.57 126.08 125.71 125.10 113.33
86.68 80.73 76.53 64.84 58.64 58.46 54.70 54.68 43.81 43.48 43.35 24.70 24.63 24.52 20.01
DMTrO
O
N
P
CN
1.31b
f1 (ppm)

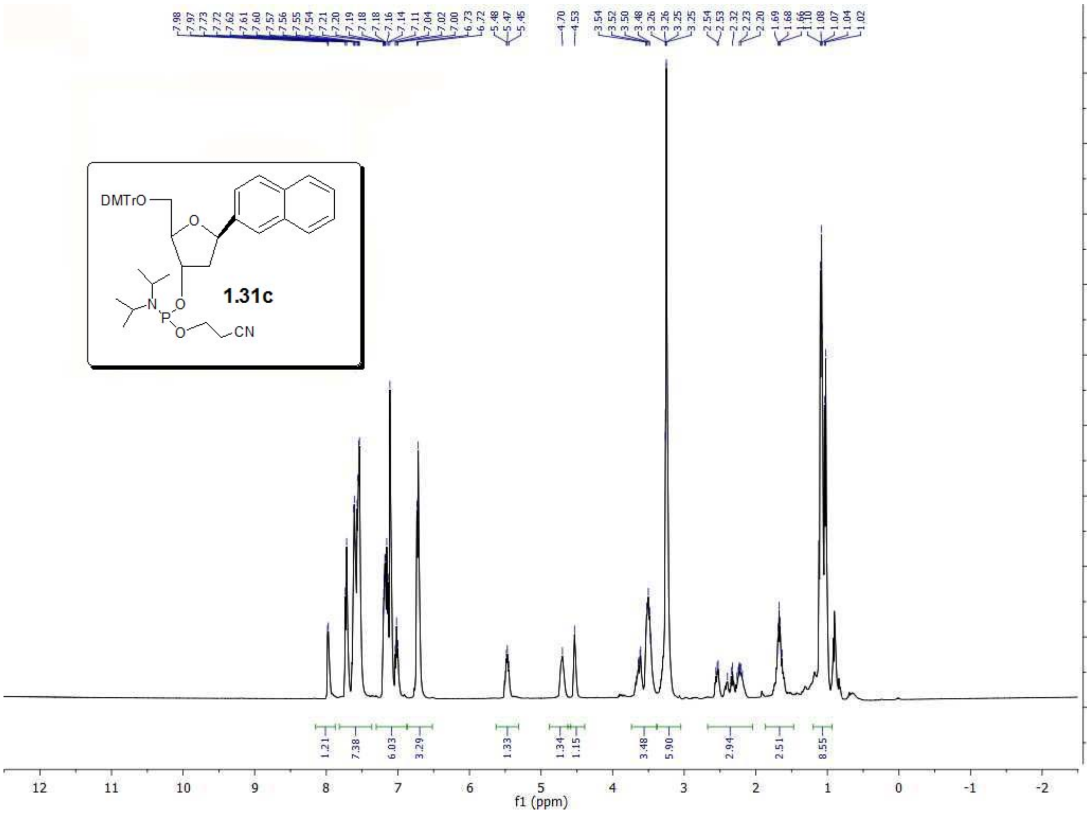

7.98 7.97 7.73 7.72 7.62 7.61 7.60 7.57 7.56 7.55 7.54 7.21 7.20 7.19 7.18 7.18 7.16 7.14 7.11 7.04 7.02 7.00 6.73 6.72 5.48 5.47 5.45 4.70 4.53 3.54 3.52 3.50 3.48 3.26 3.26 3.25 3.25 2.54 2.53 2.32 2.23 2.20 1.69 1.68 1.66 1.10 1.08 1.07 1.04 1.02
DMTrO
O
N
P
O
O
CN
1.31c
9000
8000
7000
6000
5000
4000
3000
2000
1000
0
1.21
7.38
6.03
3.29
1.33
1.34
1.15
3.48
5.90
2.94
2.51
8.55
12 11 10 9 8 7 6 5 4 3 2 1 0 -1 -2
f1 (ppm)

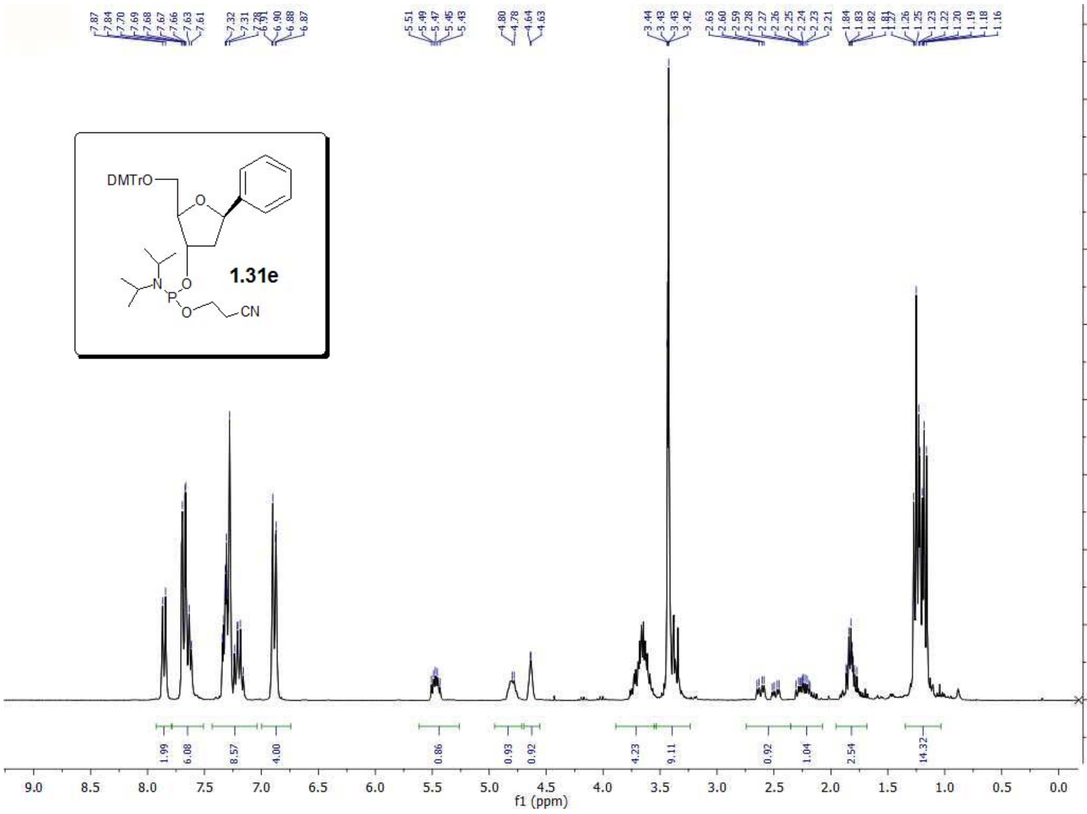

7.87 7.84 7.70 7.69 7.68 7.67 7.66 7.63 7.61 7.32 7.31 7.28 6.91 6.90 6.88 6.87 5.51 5.49 5.47 5.45 5.43 4.80 4.78 4.64 4.63 3.44 3.43 3.43 3.42 2.63 2.60 2.59 2.28 2.27 2.26 2.25 2.24 2.23 2.21 1.84 1.83 1.82 1.81 1.27 1.26 1.25 1.23 1.22 1.20 1.19 1.18 1.16
DMTrO
O
N
P
O
O
CN
1.31e
4500
4000
3500
3000
2500
2000
1500
1000
500
0
1.99
6.08
8.57
4.00
0.86
0.93
0.92
4.23
9.11
0.92
1.04
2.54
14.32
9.0 8.5 8.0 7.5 7.0 6.5 6.0 5.5 5.0 4.5 4.0 3.5 3.0 2.5 2.0 1.5 1.0 0.5 0.0
f1 (ppm)

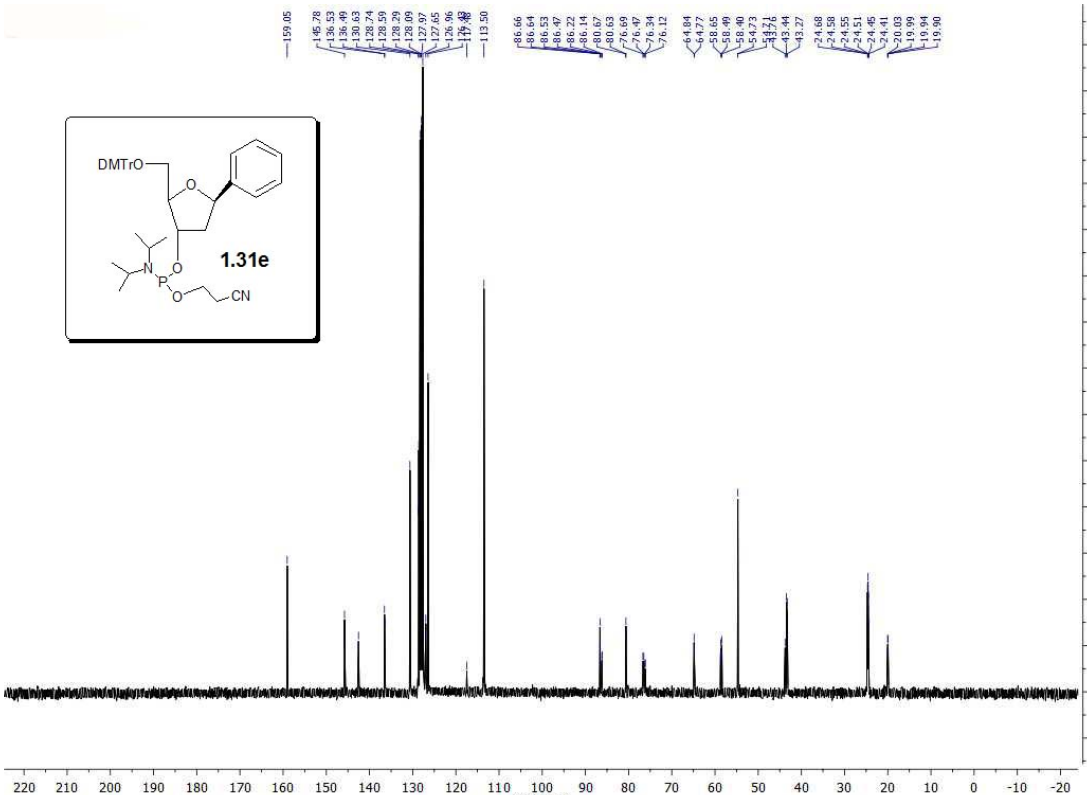
159.05
145.78
136.53
136.49
130.63
128.74
128.59
128.29
128.09
127.97
127.65
126.96
126.43
117.48
113.50
86.66
86.64
86.53
86.47
86.22
86.14
80.67
80.63
76.69
76.47
76.34
76.12
64.84
64.77
58.65
58.49
58.40
54.73
54.71
43.76
43.44
43.27
24.68
24.58
24.55
24.51
24.45
24.41
20.03
19.99
19.94
19.90
DMTrO
O
N
P
O
O
CN
1.31e
7000
6500
6000
5500
5000
4500
4000
3500
3000
2500
2000
1500
1000
500
0
-500
220 210 200 190 180 170 160 150 140 130 120 110 100 90 80 70 60 50 40 30 20 10 0 -10 -20
f1 (ppm)

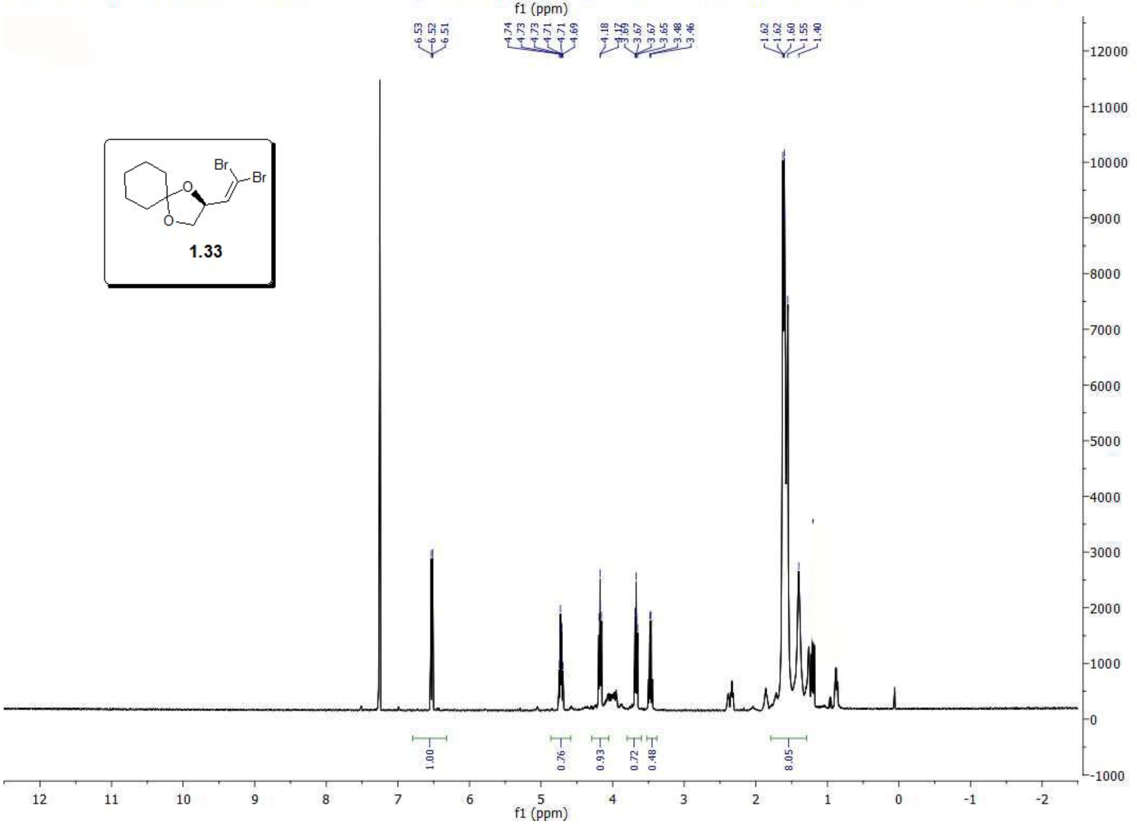
6.53
6.52
6.51
4.74
4.73
4.73
4.71
4.71
4.69
4.18
4.17
3.69
3.67
3.67
3.65
3.48
3.46
1.62
1.62
1.60
1.55
1.40
Br
Br
O
O
1.33
12000
11000
10000
9000
8000
7000
6000
5000
4000
3000
2000
1000
0
-1000
1.00
0.76
0.93
0.72
0.48
8.05
12 11 10 9 8 7 6 5 4 3 2 1 0 -1 -2
f1 (ppm)

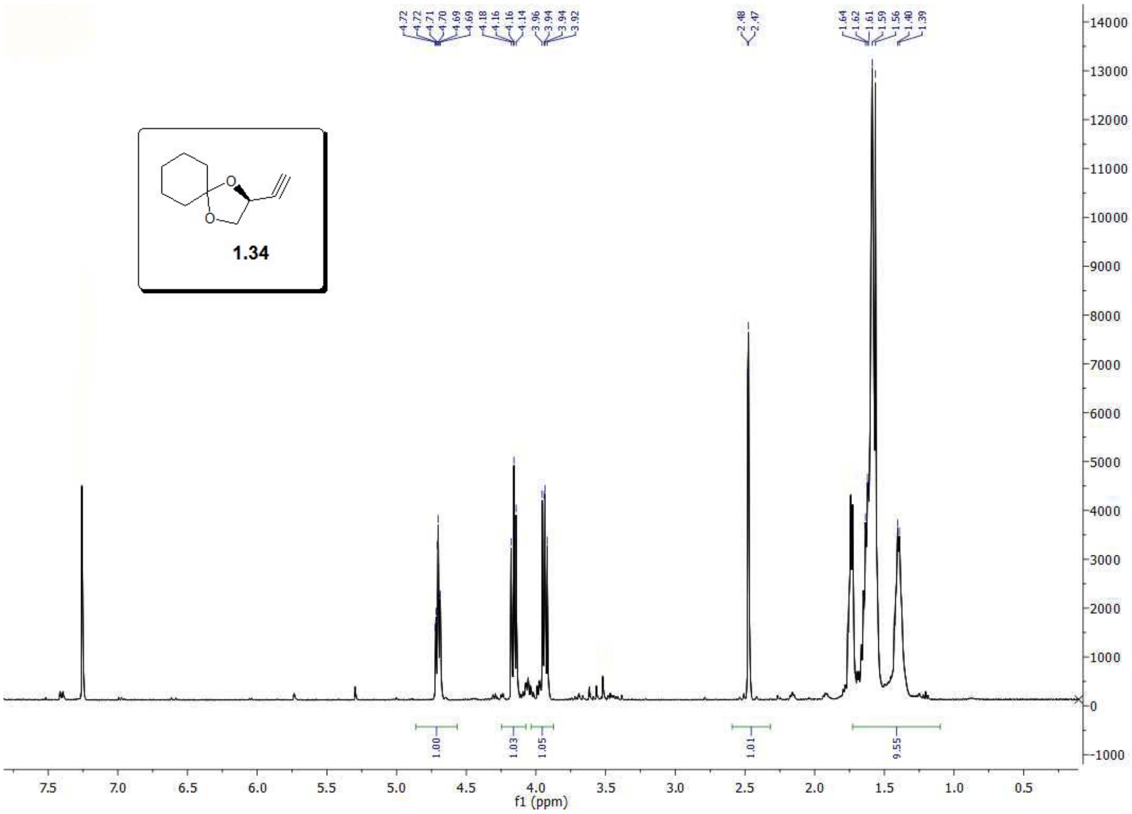

1.34

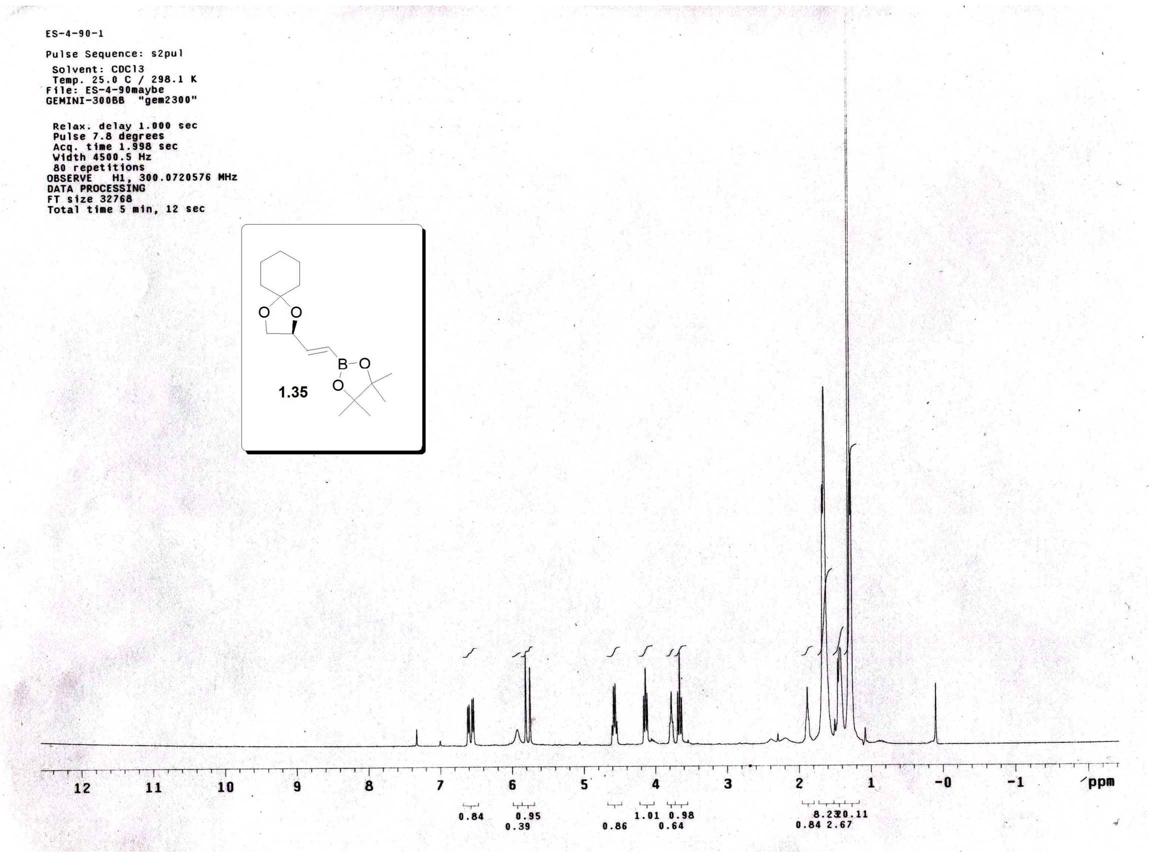

```
ES-4-90-1

Pulse Sequence: s2pul
 Solvent: CDCl3
 Temp. 25.0 C / 298.1 K
File: ES-4-90maybe
GEMINI-300BB  "gem2300"

 Relax. delay 1.000 sec
 Pulse 7.8 degrees
 Acq. time 1.998 sec
 Width 4500.5 Hz
 80 repetitions
OBSERVE   H1, 300.0720576 MHz
DATA PROCESSING
FT size 32768
Total time 5 min, 12 sec
```

1.35

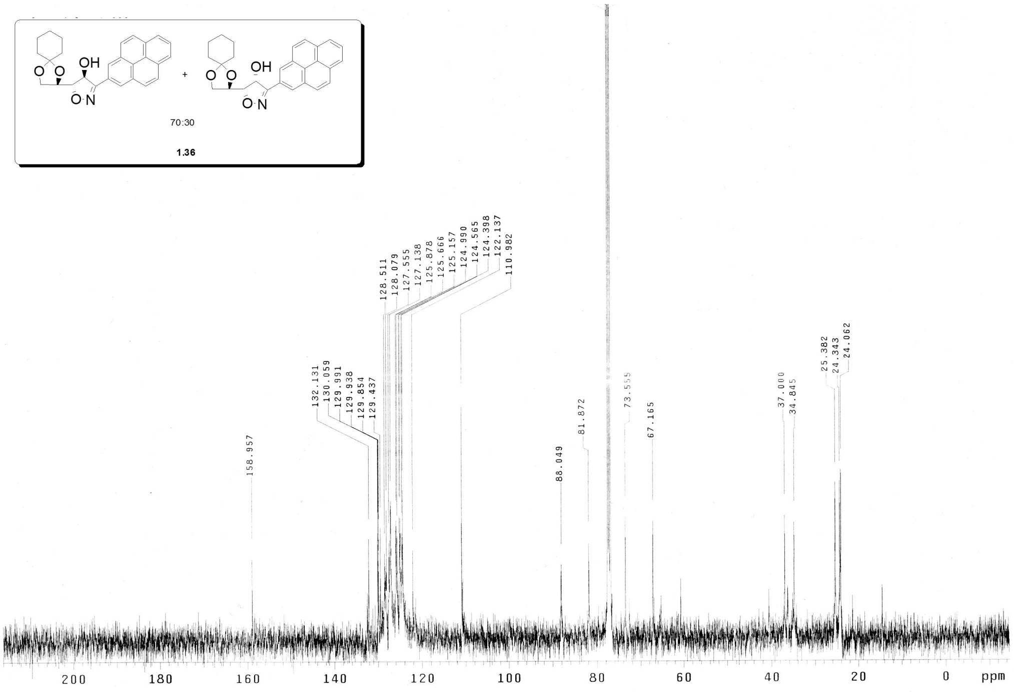
OH
O
O
O N
+
70:30
1.36
158.957
132.131
130.059
129.991
129.938
129.854
129.437
128.511
128.079
127.555
127.138
125.878
125.666
125.157
124.990
124.565
124.398
122.137
110.982
88.049
81.872
73.555
67.165
37.000
34.845
25.382
24.343
24.062
200
180
160
140
120
100
80
60
40
20
0
ppm

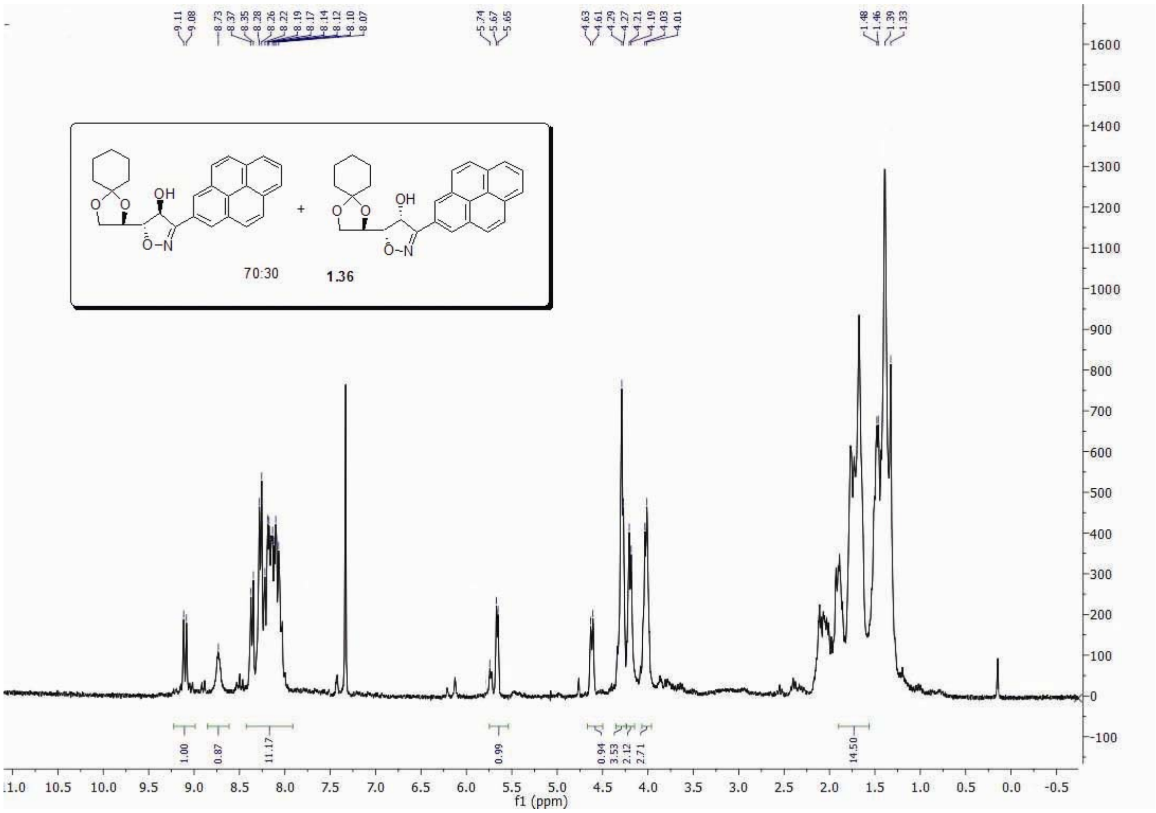
9.11
9.08
8.73
8.37
8.35
8.28
8.26
8.22
8.19
8.17
8.14
8.12
8.10
8.07
5.74
5.67
5.65
4.63
4.61
4.29
4.27
4.21
4.19
4.03
4.01
1.48
1.46
1.39
1.33
OH
O
O
O-N
+
70:30
1.36
1.00
0.87
11.17
0.99
0.94
3.53
2.12
2.71
14.50
1600
1500
1400
1300
1200
1100
1000
900
800
700
600
500
400
300
200
100
0
-100
11.0
10.5
10.0
9.5
9.0
8.5
8.0
7.5
7.0
6.5
6.0
5.5
5.0
4.5
4.0
3.5
3.0
2.5
2.0
1.5
1.0
0.5
0.0
-0.5
f1 (ppm)

Chapter II
Synthesis of Labelled 3,4- Didehydro Retinoic Acid. Introduction of Tritium at C-4 in the Final One-pot Procedure.

2.1 Introduction……………………………………………………………………...93

2.2 Synthetic Approaches…………………………………………………………...96

2.3 Results and Discussion…………………………………………………………100

2.3.1- Preparation of 4-Oxygenated Retinoic Acid Methyl Esters………………100

2.3.2- Preparation of 3,4-ddRA, Purification, and HPLC Characterization...…101

2.3.3- Preparation of 4-T 3,4-ddRA……………………………………………….101

2.3.4 Gene Expression of treated T-labeled ATRA and T-labeled 3,4-ddRA.….102

2.4 Experimental Section…………………………………………………………..105

2.4.1. Hplc-Mass Spectroscopy…………………………………………………….114

2.4.2. Purification of Unlabelled 3,4-ddRA……………………………………….114

2.4.3. Purification of ^{3}H -3,4-ddRA………………………………………………..123

2.5 References………………………………………………………………………127

2.6 Appendix………………………………………………………………………...131

Chapter 2- Synthesis of Labelled 3,4-Didehydro Retinoic Acid. Introduction of Tritium at C-4 in the Final One-pot Procedure.

2.1 Introduction

Vitamin A (retinol, **2.1**) is a micronutrient required for proper embryogenesis and for regulated tissue differentiation in post-natal organisms. Deficiency in this vitamin is associated with xerophthalmia, immune deficiency, night blindness, and growth retardation.[1] With the exception of requirements in vision, most actions of this vitamin are mediated by retinoic acid (RA, **2.2**) which serves as a transcription factor ligand for at least two families of heterodimeric nuclear receptors.[2] The family of transcription factors that is activated is cell- and tissue-type dependent and correlates with binding proteins that deliver RA to the nucleus.[3] Retinoic acid can also inhibit gene transcription through a number of mechanisms that include but are not limited to competition of liganded receptors for coactivators.[4]

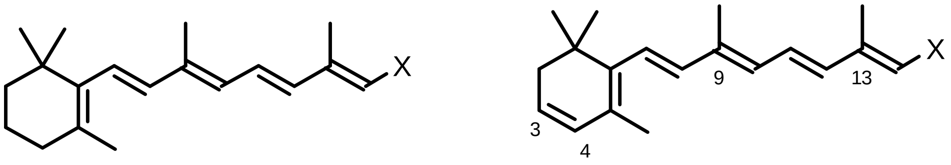

2.1, X = CH_2OH, retinol
2.2, X = CO_2H, retinoic acid (RA)

2.3, X = CH_2OH, 3,4-didehydroretinol
2.4, X = CO_2H,
3,4-didehydroretinoic acid (3,4-ddRA)

Figure 2.1. Structures of Retinol, 3,4-ddRA, RA, and 3,4-didehydroretinol

In human epidermis (skin) and in human epidermal keratinocytes, retinol is converted to 3,4-didehydroretinol (3,4-ddretinol; also called vitamin A2 or 3,4-dehydroretinol, **2.3**) in reactions that are inhibited by ketoconazole and citral.[5] Addition of 3,4-ddretinol to cultured keratinocytes leads to the accumulation of 3,4-ddretinyl esters and 3,4-didehydro retinoic acid (3,4-ddRA, **2.4**).[6] In order to study of the role of 3,4 –ddRA in regulation of keratinocyte differentiation, we needed both tritium-labelled and unlabelled compound. Our desire to synthesize these compounds will help us understand the relative effectiveness of 3,4-ddRA in comparsion to all trans-retinoic acid in gene cell expression.

Ideally, our preparation of unlabelled, 3,4-ddRA would be efficient, convergent, and stereoselective, not requiring chromatographic separation of geometric isomers. However, because of the limitations involved in the handling of radioisotopes, the most important feature of a preparation of labelled 3,4-ddRA is that the label be introduced in the last or nearly last step of the synthetic sequence. Although efficiency and convergence are also desirable, they are secondary to this requirement. Furthermore, although stereoselectivity is beneficial, some loss of the geometric purity of the polyene system during the synthesis could be corrected by a preparative hplc experiment on the final labelled product. With these considerations in mind, we set out to develop a convenient preparation of unlabelled 3,4-ddRA (**2.3**) that could be modified to provide tritium-labelled 3,4-ddRA**.**

There are currently two main industrial synthetic approaches (Scheme 2.1) used to prepare retinoids. It involves construction of a C7-C8 bond or a C11-C12 bond using the Wittig[7] reaction of the appropriate triphenylphosphonium bromide salt or a Horner-Wadsworth-Emmons[8] reaction with a phosphonate. The approaches all make use of β-ionone as a starting material. For these regioselective syntheses, the ethylenic intermediates with the required stereochemistry are needed which require a large number of purification steps and is seen as a disadvantage.There have been many new recent stereoselective alternative examples of retinoids synthesized by tricarbonyliron[9] complexes and palladium catalyzed coupling reactions such as by Stille[10] reaction and Sonogashira[11] coupling.

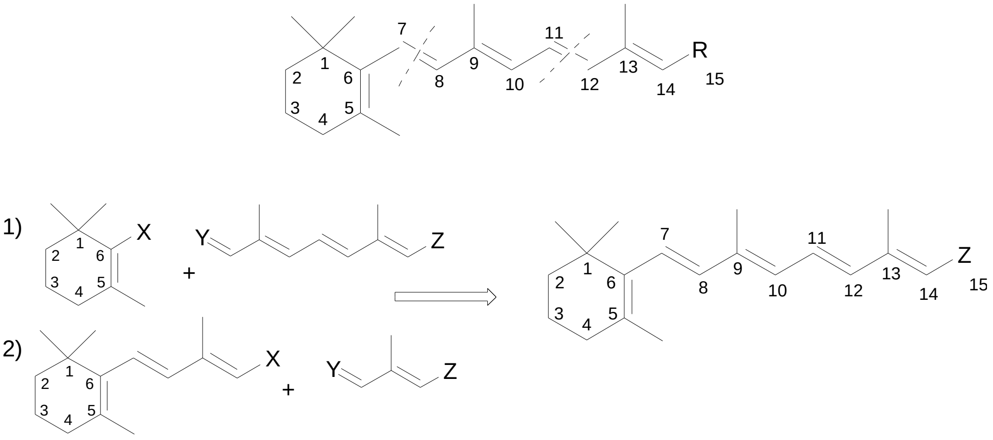
1
2
3
4
5
6
7
8
9
10
11
12
13
14
15
R
1)
2)
X
Y
Z
+

Scheme 2.1. Two Industrial Synthetic Approaches.

One recent new regioselective approach that was directed towards the synthesis of all-trans retinoic acid was reported by Potier (Scheme 2.2)[12]. They synthesized a new C-6 enaminodiester synthon which would condense with the lithium enolate of β-ionone to form a ketoester that when undergone heating eliminates the dimethylamine to introduce

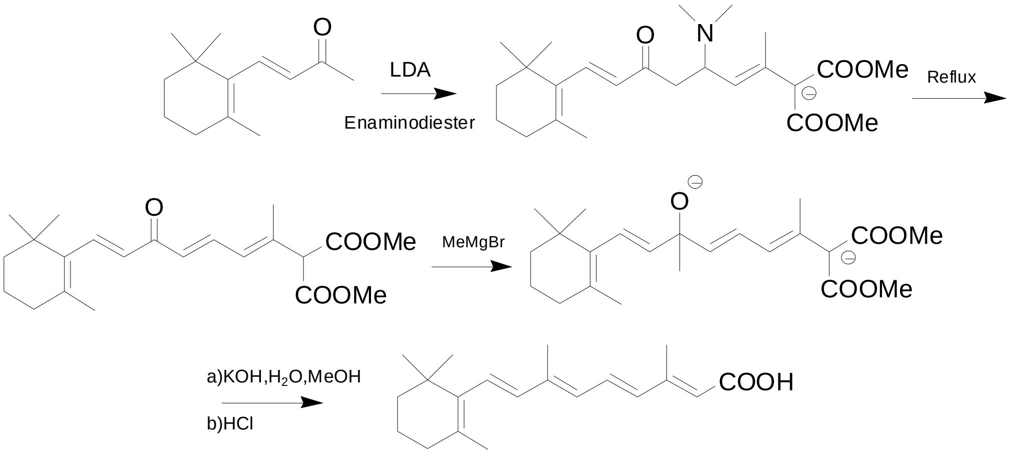
O
LDA
Enaminodiester
N
COOMe
COOMe
Reflux
O
COOMe
COOMe
MeMgBr
O
COOMe
COOMe
a)KOH,H2O,MeOH
b)HCl
COOH

Scheme 2.2. Potier Protocol.

the third double bond in the side chain. The ketone was methylated using a Grignard reagent because of the negative charge stabilization of the two esters. After saponification and decarboxylation, the all-*trans* retinoic acid was obtained regioselectively. This protocol can be performed stepwise or as one pot in good yield. We use this approach to obtain 3,4-didehydroretinoic acid and tritiated 3,4-didehydroretinoic acid.

2.2 Synthetic Approaches

Our first approach was to synthesize a TES protected substituted β-ionone which would undergo the Potier protocol. The final step would involve elimination of silyl group to give a double at the 3,4 position on the ring. The first step (Scheme 2.3) of the synthesis involved bromination of β-ionone followed by nucleophilic addition to give the formic ester and then hydrolysis to give 4-hydroxy-β-ionone in 43% yield over 2 steps. The hydroxylated-β-ionone was protected with chlorotriethylsilane to give compound **2.6** in 78% yield. The Potier protocol was performed in a one pot procedure following aliquots that were taken to monitor the progress of the reaction of each step. Compound

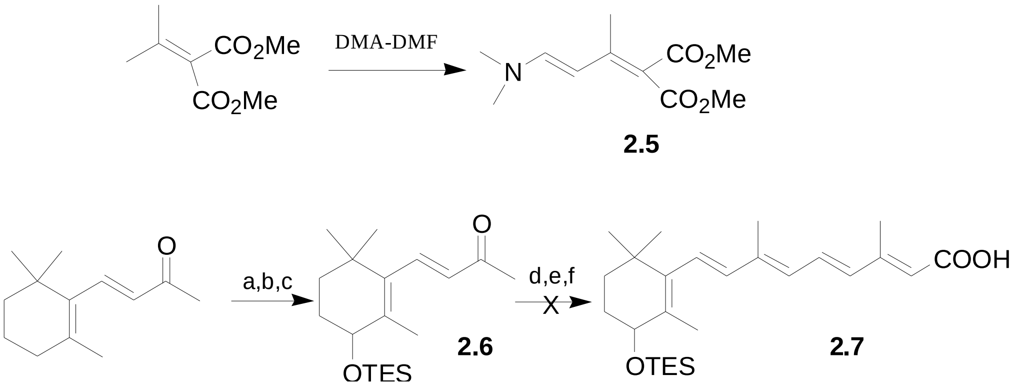

a)NBS, $CHCl_3$ b)$NaCO_2H$, CO_2H c) TESCl, Imidazole d) LDA,DME, **4a** e)MeMgBr,THF f) KOH, EtOH, HCl

Scheme 2.3. First Approach at 3,4 Didehydroretinoic Acid (**2.4**).

2.6 was lithiated and condensed with the C-6 enaminodiester synthon, compound **2.5**. The crude NMR results and IR results showed the proper peaks to what was expected. Following formation of the ketoester, addition of the Grignard reagent methylmagnesium bromide resulted in shifts in olefinic protons as seen in the crude NMR. However, saponification and decarboxylation to the desired compound **2.7** resulted in inconclusive results. The IR showed one desired carbonyl peak at 1710 cm^{-1}. The crude NMR showed heavy overlapping of peaks, isomerization and many byproducts. There was an observed loss of the silyl group in the NMR which did not result in any potential 3, 4-didehydro peaks from the desired compound. Many attempts at purification to elucidate peaks were unsuccessful since the compound was acid sensitive and light sensitive to isomerizations.

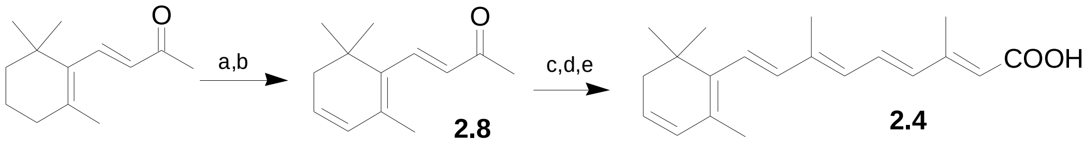

a) NBS, CaO, H$_2$O b) DiethylAniline,Pyridine, 90°C c) LDA,DME, **2.5** e) MeMgBr,THF f) KOH, EtOH, HCl

Scheme 2.4 Second Approach at 3,4 Didehydroretinoic Acid (**2.4**).

Our second approach involved directly introducing the 3,4-double bond into the system before undergoing Potier's protocol. β-ionone was brominated, hydroxylated and eliminated with diethylaniline and pyridine at reflux to give compound **2.8** in 46% yield over 2 steps.

Using Potier's protocol, compound **2.8** underwent the three step process to give compound **2.4** in 3-5% yield as purified by HPLC by our collaborator Dr. Juliana Tafrova in the Department of Oral Pathology and Biology. The 3,4-double bond in the 3-step one pot procedure has disappeared as it was found that the majority of the product recovered from experiment to be all-trans-retinoic acid (ATRA).

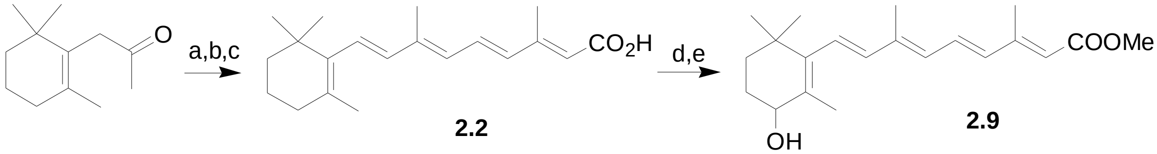

a) LDA,DME, **2.5** b) MeMgBr,THF c) KOH, EtOH, HCl d) $TMSCH_2NH_2$, MeOH e) NBS,H_2O

Scheme 2.5. Third Approach at 3,4 Didehydroretinoic Acid **(2.4).**

Our third and final approach was to modify the ring after having obtained all-trans retinoic acid in hand. Using Potier's method, compound **2.2** was obtained in 41% yield. After obtaining ATRA, trimethylsilyldiazomethane was used to make the methyl ester in nearly quantitative yield. In aqueous acetonitrile, NBS was added to the methyl ester to give compound **2.9** in 72% yield with a mixture of isomers (1:2 ratio) of 13-*cis*-retinoic acid and *all-trans*-retinoic acid. Compound **2.9** was treated with *p*-toluene sulphonic acid in benzene followed by hydrolysis to give the desired compound **2.4** in 60% yield as a

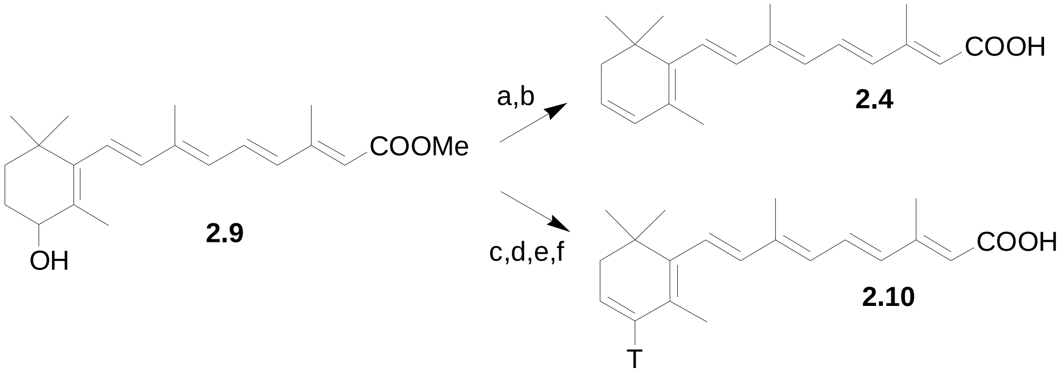

a) pTsOH, benzene b) KOH, EtOH, HCl c) MnO_2, CH_2Cl_2 d) $NaBT_4$ e) pTsOH, benzene f) KOH, EtOH, HCl

Scheme 2.6. Third Approach at 3,4-Didehydroretinoic Acid **(2.4)** and **(2.10).**

mixture of isomers with a ratio of 4.5:1 of ATRA and 13-cis-retinoic acid. After having completed synthesis of compound **2.4**, the tritium labeled 3,4-didehydro retinoic acid would follow. Compound **2.9** was oxidized to ketone **2.5** using MnO_2 in 55% yield giving a 3:1 ration of ATRA and 13-cis-retinoic acid.

For the proposed studies, we planned to place a tritium label on 3,4-ddRA at a position that would not expose it to exchange during its metabolism by human keratinocytes. We considered the sodium borotritide treatment of 4-oxoretinoic acid methyl ester (**2.11**) followed by dehydration of the resulting alcohol (i.e. **2.12 –> 2.13**) and hydrolysis of the ester (**2.13 -> 2.10**) to be a potentially very efficient approach to appropriately labelled 3,4-ddRA (Scheme 2.7). Indeed, this general approach was demonstrated by Tosukhowong and Supasiri whose synthesis of tritium-labelled retinol included the preparation of tritium-labelled ester **2.8** from the 4-oxo ester **2.5**.[13] Thus, we tested the possible sources of 4-oxygenated retinoids for use in Scheme 2.7 or a similar sequence.

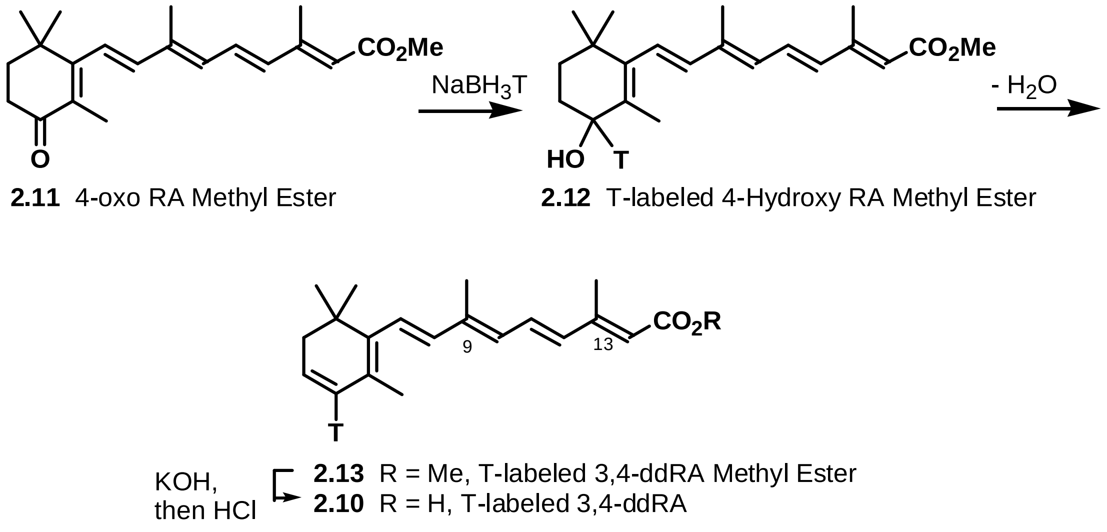

2.11 4-oxo RA Methyl Ester

2.12 T-labeled 4-Hydroxy RA Methyl Ester

2.13 R = Me, T-labeled 3,4-ddRA Methyl Ester

2.10 R = H, T-labeled 3,4-ddRA

Scheme 2.7. Synthesis of T-labeled 3,4-ddRA.

2.3 Results and Discussion

2.3.1- Preparation of 4-Oxygenated Retinoic Acid Methyl Esters

Reported preparations of 4-oxygenated retinoic acid derivatives involve functionalization of RA or another retinoid. At first sight, the reported direct functionalization of retinoic acid methyl ester (**2.14**) to its 4-oxo derivative **2.11** by simply stirring in acidic methanol[14] appeared to be the most attractive of the literature methods. Although mechanistically undefined, this reaction was reported to provide more than 40% of ester **2.11** in one step. In our hands, however, neither *all-trans* RA (ATRA, **2.1**) nor ATRA methyl ester **2.9** afforded detectable 4-oxo derivative under the described conditions (see Scheme 2.8).

On the basis of its brevity, the conversion of RA or RA methyl ester to the 4-oxo compound (**2.5** or **2.11**) by manganese dioxide[15] was also attractive. This direct method has been used in several laboratories, providing all trans 4-oxo RA ester (after chromatography) in modest yields. However, in our hands, the described conditions,[9a] applied to RA ester **2.14** with either commercially obtained MnO_2 or freshly prepared and dried MnO_2,[16] did not result in detectable reaction.

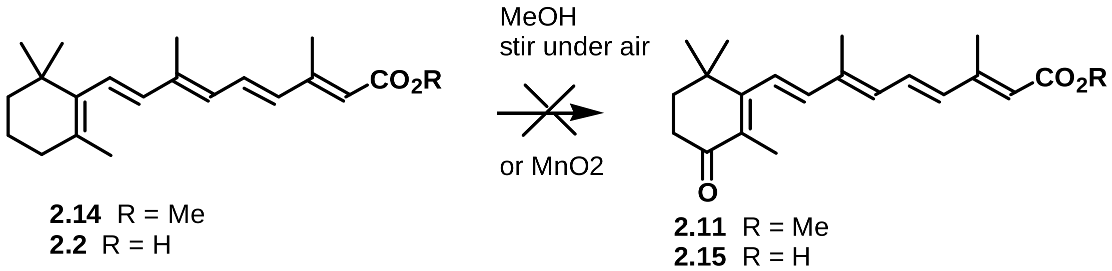

Scheme 2.8. 4-oxo RA ester under acidic methanol conditions.

The two-step synthesis of 4-oxo RA methyl ester (**2.11**) adapted from Hashimoto[17] proved more successful (see Scheme 2.9). Thus, NBS treatment of ATRA methyl ester (**2.14**) in wet acetonitrile, gave 4-hydroxy RA methyl ester **2.9** as a mixture of isomers (2:1 ratio of all trans 4-hydroxy RA methyl ester and the corresponding 13-cis compound) in 72% yield. Oxidation with MnO_2 then afforded the 4-oxo ester **2.11** as a 3:1 mixture of the all trans and 13-cis isomers.

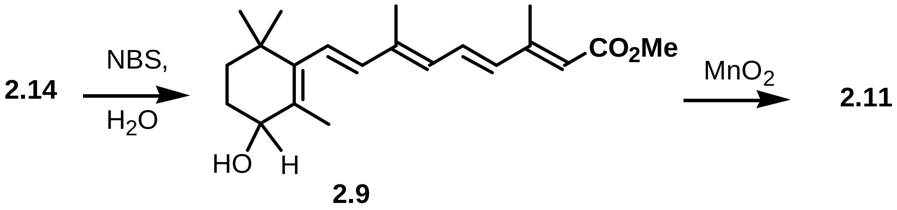

Scheme 2.9. Formation of 4-oxo ester under MnO_2.

2.3.2- Preparation of 3,4-ddRA, Purification, and HPLC Characterization

We next established that the conversion of alcohol **2.11** to 3,4-ddRA was efficient. Thus, we carried out the dehydration and hydrolysis (Scheme 2.10), obtaining the target **2.13** in 60% yield over two steps. The ^{1}H NMR spectrum was consistent with a 4.5:1 mixture of all-trans 3,4-ddRA and 13-cis ddRA.

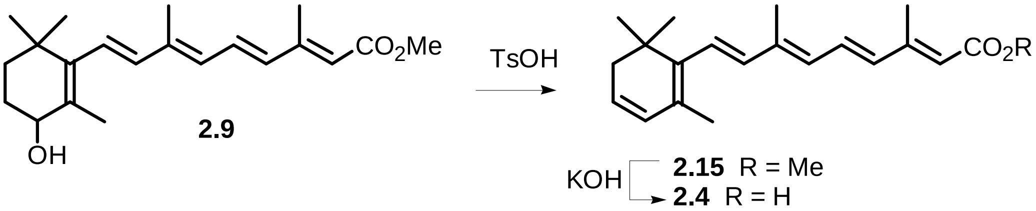

Scheme 2.10. Generation of 3,4 Didehydroretioc Acid.

Finally we demonstrated that very pure all trans 3,4-ddRA could be isolated from the mixture of isomers by semi-preparative HPLC. The 3,4-ddRA was subjected to sequential runs on a NovaPak C18 column and then on a Sunfire C18 column (Figures 2.2-2.4). Repetitive runs allowed the collection of approximately 0.5 mg of material which showed a single peak on analytical HPLC (NovaPak HR C18 column, Figure 2.4C) and a ^{1}H NMR spectrum consistent with that of all trans 3,4-ddRA.

2.3.3- Preparation of 4-T 3,4-ddRA

Satisfied that the steps in Schemes 2.9 and 2.10 were well-behaved in our hands and that all trans 3,4-ddRA could be obtained, we considered extending this chemistry to the implementation of Scheme 2.7. Because we needed to develop a protocol that could be adapted to the preparation of labelled compound, we modified the procedure for the conversion of ketone **2.11** to 3,4-ddRA so as to minimize manipulation of materials. Thus the following three reactions were carried out in a single flask: sodium borohydride reduction of ketone **2.11**, dehydration of alcohol **2.9**, and basic hydrolysis of ester **2.15** followed by acidification. Lyophilization provided a crude reaction residue from which organic material was extracted according to Barua.[13] The radiolabeled material was subjected to sequential runs on a NovaPak C18 column and then on a Sunfire C18 column (Figures 2.2-2.4).

Having established that clean, all trans 3,4-ddRA could be obtained from ketone **2.11** by a one-pot procedure that might be used for the introduction of radioactivity, we applied this method to the preparation of tritium-labelled compound (see Experimental Section for details). Thus ketone **2.11** was treated with sodium borotritide and then with excess sodium borohydride. Then dehydration, hydrolysis, lyophilization, extraction, and purification by semi-preparative HPLC on the NovaPak C18 and Sunfire C18 columns provided material that was considered appropriate for use in cells.

2.3.4 Gene Expression of cultured human keratinocytes treated with ^{3}H ATRA and ^{3}H-3,4-ddRA

The experiments comparing the uptake and metabolism of ^{3}H ATRA and ^{3}H-3,4-ddRA **2.10** were performed by Dr. Juliana Tafrova, Department of Oral Biology and Pathology at Stony Brook University. Keratinocytes cells, in nature, can uptake and convert retinol to 3,4-ddretinol, and both retinoids can serve as a substrate for the synthesis of their active metabolites ATRA and 3,4-ddRA, respectively. They exert their function as transcriptional regulators by serving as ligands for the nuclear retinoid acid receptors, such as RARs and RXRs. Ligand –receptor complexes are formed upon binding of the ligand to these receptors. These complexes can bind to the retinoic acid response elements (RAREs) in the promoter region of the target genes which then recruit other proteins over the promoter. This triggers up/down regulation of the transcription from the target gene.

In order to distinguish the abilities of ATRA and 3,4-ddRA to alter gene expression retinoid depleted normal human keratinocytes (strain NHEK-F) were fed both to ^{3}H ATRA or ^{3}H-3,4-ddRA for 4h. Cultured keratinocytes concentrate these retinoids to different extents and in order to achieve physiologic levels intracellularly (~10 nM), ^{3}H ATRA or ^{3}H-3,4-ddRA were added at 0.25 nM and 1.0 nM, respectively. Also because retinoids are typically 3 – 4 folds more abundant than 3, 4-ddretinoids, comparisons using 1.0 nM ^{3}H ATRA was necessary. Relative change in the gene expression in retinoid-treated versus non-treated control cultures were examined for 84 genes. Twelve of these genes showed different degrees of expression. Eleven of the twelve genes (Figure 2.2) showed less than two fold differences when treated with ^{3}H-ATRA or ^{3}H-3,4ddRA compared to the control.

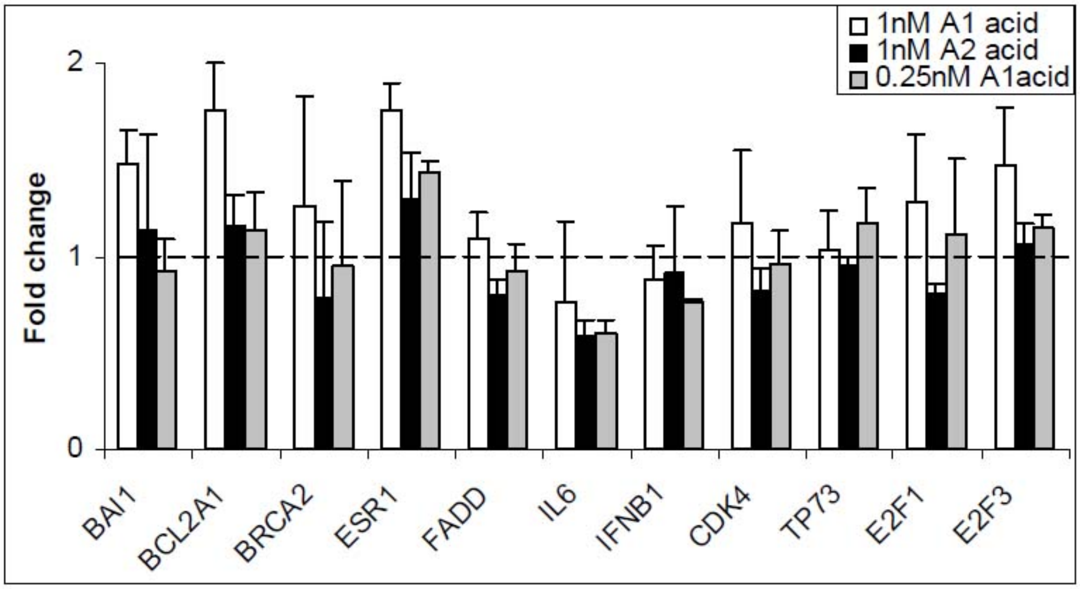

Figure 2.2. Gene expression in NHEK-F. Real time RT-PCR conformation of changes in gene expression due to treatment with Vitamin A1 (ATRA) or A2 acids (3,4-ddRA). Shown in the bar graphs are genes with less than two fold differences.

The expression of one gene shown in Figure 2.3, FASLG, was increased ~ 9 fold in cultures incubated with 0.25 nM or 1.0 nM ATRA. Fas ligand (FasL) and the Fas receptor (FasR) are transmembrane proteins that play an important role in the regulation of the immune system .When soluble Fas ligand is generated, it binds to the FasR, the receptor trimerizes, leading to a series of proteolytic events that end in cell death for the target cell. In comparing the results obtained with ATRA, treatment with 3,4-ddRA (fig. 2.3) did not significantly enhance FASLG expression (~ 1.8 fold). Thus, while both retinoid acids positively or negatively regulated some of the tested genes, their function is considered non-identical. The transcriptional activity of retinoids in general is dependent upon their chemistry and conformation. Hence, this data shows that binding affinity to and conformational changes in the nuclear receptors with which the retinoids interact can lead to differences in the proteins recruited to promoters and as a result in differences in gene transcription. In summary, the data supports that 3,4-ddRA has a unique biological function. Future work could expand gene expression profiling by comparing genes encoding nuclear receptors and coregulators.

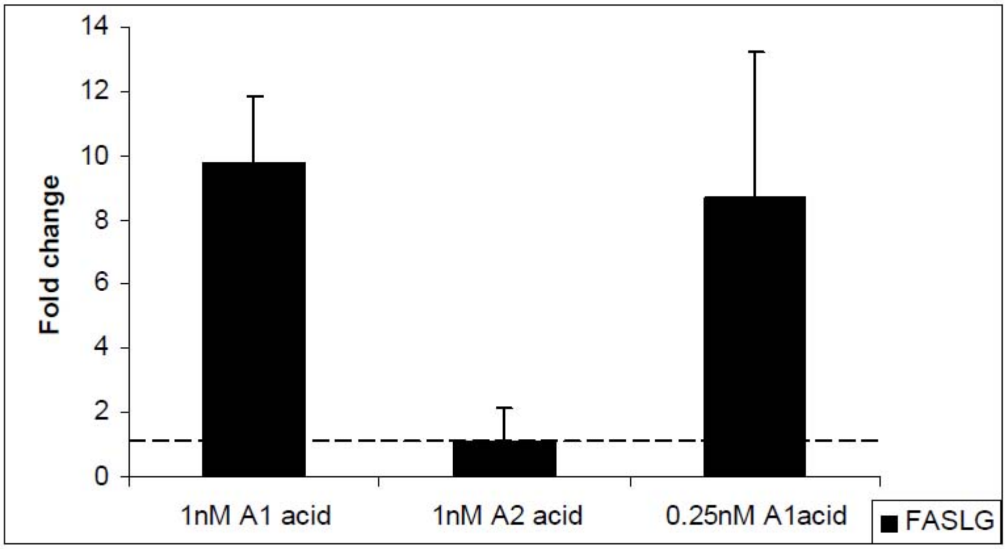

Figure 2.3. Gene expression in NHEK-F. Real time RT-PCR conformation of changes in gene expression due to treatment with ATRA or 3,4-ddRA. Shown in the bar graphs is FASLG gene.

2.4 Experimental Section

General Methods

Unless noted otherwise, all oxygen and moisture-sensitive reactions were executed in oven-dried glassware sealed under a positive pressure of dry argon. Moisture-sensitive solutions and anhydrous solvents were transferred via standard syringe and cannula techniques. Unless stated otherwise, all commercial reagents, were used as received. All solvents were dried under argon atmosphere: THF and diethyl ether were distilled over Na-benzophenone; CH_2Cl_2 was distilled from CaH_2. Extracts from work-up procedures were dried over Na_2SO_4 unless otherwise noted. Flash chromatography was performed with silica gel (32-63 mM); analytical TLC was performed with 0.25 mm EM silica gel 60 F254 plates that were visualized by irradiation (254 nm) or by staining with 10% PMA. IR spectra were recorded on a Galaxy Series FTIR 3000 infrared and Perkin-Elmer 1600 Series FT-IR spectrophotometers. NMR spectra were obtained with Gemini-300 MHz (Varian), Inova-400 MHz (Varian), Inova-500 MHz (Varian), and Inova-600 MHz (Varian) instruments. Chemical shifts for proton NMR are reported in parts per million (ppm) relative to the singlet at 7.26ppm for chloroforim-*d*. Chemical shifts for carbon NMR are reported in ppm with the center line of the triplet for chloroform-d set at 78.00 ppm. The following abbreviations are used in the experimental section for the description of 1H-NMR spectra: singlet (s), doublet (d), triplet (t), quartet (q), multiplet (m), and doublet of doublets (dd). Coupling constants, *J*, are reported in Hertz (Hz).

ATRA was obtained from Sigma Aldrich (Catalog R2625). Alternatively RA was prepared as described by Potier;[18] all-trans RA was separated from 13-cis compound on silica gel with hexane/ethyl acetate mixtures (3:1 to 1:1) as eluent. ATRA methyl ester (7) was prepared from ATRA according to Tosukhowong[7]. All trans 3,4-ddRA and tritium labelled all trans 3,4-ddRA were purified on a Waters 2695 HPLC System with a Waters 2996 photodiode array detector for the NovaPak C18 column and a Waters 600E system controller with a Waters 994 programmable photodiode array detector for the Sunfire C18 column. LC/MS analysis of 3,4-ddATRA was carried out on an Agilent HP 1100 Series with a Metasil C18 column. UV spectra of 3,4-RA and all trans 3,4ddRA were confirmed on a Beckman DU-65 Spectrophotometer (Fig. 3B). The NovaPack C18 prep column has 4 mm particle size and is 5 x 100 mm (Waters Corporation, Milford, MA, cat #: WAT080100). The SunFire C18 column has 5 mm particle size and is 4.6 x 250 mm (Waters, cat #: 186002560). The NovaPack HR C18 has 6 m m particle size and is 3.9x300mm (Waters, cat #: WAT038500). All reactions were performed under Gold/Yellow UV Lights (F40T12). Sodium borotritide was purchased from Perkin Elmer. (25.4 mCi, .96 mg, 150mCi/mmol).

2.5 C-6 Enaminodiester Synthon, 2-(3-Dimethylamino-1-methyl-allylidene)-malonic acid dimethyl ester[12]

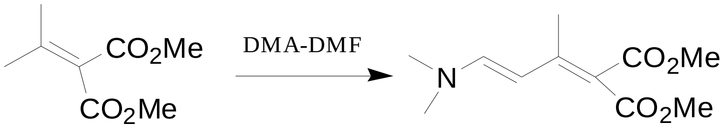

A mixture of Diethyl isopropylidiene malonate (5.00 mL, 24.35 mmole) and dimethylforamide dimethyl acetal (3.48 g, 29.22 mmole) was heated at 95 ^{o}C for 18 hours with a Dean-Stark apparatus. The methanol was drained and then heated at reflux for 2 hours. The solution was concentrated under reduced pressure to give a yellow solid.

The solid was recrystallized from 1:1 ether/pentane to give the desired product (5.11 g, 92%). The NMR spectrum is comparable to what is reported in the literature[12].

^{1}H 300MHz NMR (CDCl3) δ 6.93 (1H, d), 6.11 (1H,d), 4.23(4H, qt), 2.93 (6H,s), 2.14 (3H,s), 1.29 (6H,s), IR (thin film) 2974,1725, 1692,1465, 1390,1250,1030 cm^{-1}, R_f =.25

Generation of 4-Hydroxyl-β-ionone[19]

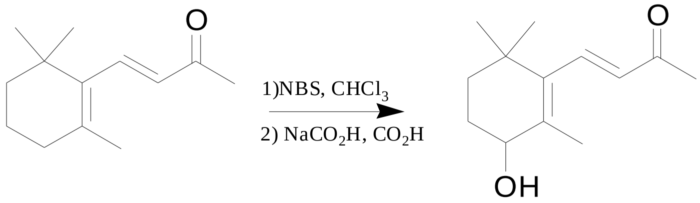

To a boiling solution of CCl_4 (25 mL) with β-Ionone (1.16 g, 6.04 mmole) at 85 °C was added NBS (1.30g, 7.25 mmole) and allowed to reflux for one hour. The solution turned from clear to yellow. After 1 h, the solution was cooled to 30 °C, hexane was added (20 mL) and the filtrate was filtered (white succinimide solid). The reaction mixture was concentrated under reduced pressure at 30 °C on the rotovap. Once concentrated, formic acid (10 mL), sodium formate (560 mg), and dioxane(10 mL) were added.. The reaction was then stirred for 2 hours and then extracted with ether (3 x 20 mL) and washed successively with sodium bicarbonate, water and brine. The crude material was purified by flash chromatography using 3:1 hexanes/ethyl acetate as the eluent. The product obtained is a colorless oil (540 mg, 46%). The NMR spectrum is comparable to what is reported in the literature.

^{1}H 300MHz NMR (CDCl3) δ 7.11 (1H, d), 6.01 (1H,d), 3.96(1H, t), 3.69(1H,bs) 2.18(3H,s), 1.79 (1H,m),1.70(3H,s), 1.59 (2H,m), 1.31 (1H,m), .94 (3H,s), .92(3H,s) R_f =.36

TES-Protected β-ionone 2.6[20]

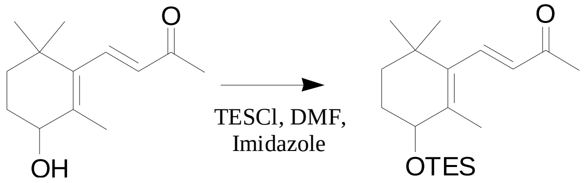

4-Hydroxy-β-Ionone (440 mg, 2.11 mmole) was dissolved in 5 mL of DMF under Argon. Imidazole (350 mg, 5.00 mmole) was added followed by chlorotriethylsilane (380 mg, 2.50 mmole) at room temperature and stirred overnight. The reaction was quenched with water, extracted with ether (3 x 25 mL), washed with $NaHCO_3$, water and brine. The crude material was purified by chromatography using hexanes as an elutant giving a colorless oil (511 mg, 78%).

^{1}H 300MHz NMR (CDCl3) δ 7.20 (1H, d), 6.09 (1H, d), 4.06(1H, t), 2.35(3H, s), 1.88 (1H, m), 1.80 (3H, s), 1.71 (2H, m), 1.42 (1H, m), .1.09 (3H, s), .99 (12H, m) .62(6H, m). IR 2955, 2913,1685, 1682, 1383, 1255 cm^{-1}

Attempts at formation of Compound 2.7

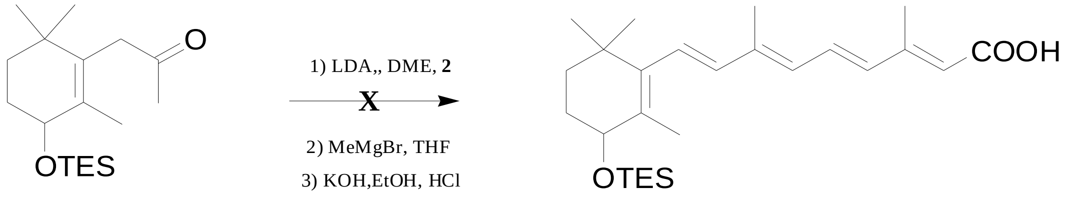

Step 1)

A solution of BuLi (1.6 M in hexanes, 13.2 mL, 21 mmol) was added at -25 °C to iPr_2NH (3.1 mL, 22 mmol) in DME (20 mL), and β-ionone (3.85 g, 20 mmol) in DME (20 mL) was then slowly added at -30/-40 °C. After the mixture had been kept at -30 °C for 20 min, 1a (4.77 g, 1.05 equiv.) in DME (50 mL) was quickly added. The refrigerated bath was then removed and the mixture was allowed to warm to room temperature. After 10 min, the crude mixture was heated at reflux for 2 h (until the evolution of Me_2NH had ceased). The solution was quenched at 0 °C with HCl in water (1 M) and extracted with diethyl ether. The crude product was directly used in the next step. An aliquot was taken to obtain a crude NMR to monitor the progress of the reaction.

1H 600MHz NMR ($CDCl_3$) δ 7.53 (1H, dd), 7.31 (1H, d), 6.48 (1H,d), 6.37(1H,d) 6.21(1H,d), 5.98 (1H,d), 4.06(1H, t), 2.35(3H, s), 2.07(3H,s), 1.82 (2H, m), 1.80 (3H, s), 1.71 (2H, m), 1.42 (1H, m), .1.03 (3H, s), .99 (12H, m) .62(6H, m).

IR 2954, 2938, 2914,1729,1675, 1634, 1239, 1148 cm^{-1}

Step 2)

A solution of MeMgBr (3 M in THF, 7.5 mL, 2.8 equiv.) was added at -10 °C to 4a (2.98 g, 8 mmol) in THF (30 mL). The chilled bath was removed and, 30 min later, the crude mixture was quenched with a satd. solution of NH4Cl and extracted with diethyl ether. The crude product was directly used in the next step.

Step 3)

A solution of retro-retinoate 6a (10.38 g, 25 mmol) in ethanol (250 mL) was saponified with an aqueous ethanolic solution of KOH (8.4 g, 6 equiv.) in water (150 mL) at 40 °C for 45 min. The solvents were distilled under reduced pressure and the crude mixture was acidified with cold HCl (2 m). After extraction with ethyl acetate and conventional workup, the oily product was purified by column chromatography (SiO_2; CH_2Cl_2/MeOH, 98:2). Several fractions were collected to find undesired product in all fractions.

Synthesis of 3,4-didehydro-Beta-Ionone 2.8[19]

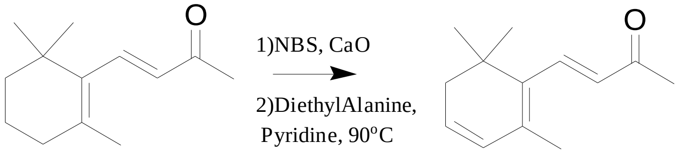

To a boiling solution of CCl_4 (20 mL) with β-Ionone (1.93 g, 10.01 mmole) at 85 ^{o}C was added NBS (2.31g, 13.00 mmole, 1.3 eq.), sodium bicarbonate(2.63 g, 24.50 mmole) and calcium oxide (843 mg, 15.11 mmole, 1.5 eq.) and refluxed for 30 min. After 30 minutes, the reaction was lowered to 40 ^{o}C and diethylaniline (9.60mL, 9.00mmole) and pyridine (.95mL) were added and stirred at 90 ^{o}C for 2 hours. Solution was cooled and precipitate filtered. The reaction was extracted with dichloromethane (3 x 20 mL) and the combined extracts washed with 2% sulfuric acid, dried, and concentrated. The product was purified by column chromatography to give a slight yellow oil (872 mg, 46%) using a 6:1 ratio of hexane/ethyl acetate as the eluent. The NMR spectrum is comparable to what is reported in the literature[21].

^{1}H 300MHz NMR (CDCl3) δ 7.23 (1H, d), 6.15 (1H,d), 5.80(2H, s), 2.23 (3H,s), 2.04 (2H,s), 1.83(3H,s), 1.00 (6H,s) IR 2936, 1669,1361,1256,1150 cm^{-1}

Rf=.49

Synthesis of 2.2 (*all-trans* retinoic acid) from 2.8

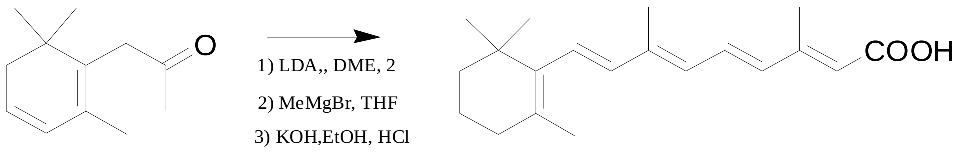

n-Butyllithium (1.6 M in hexanes, 1.1 mL, 1.66mmole) was added at -25 °C to redistilled diisopropylamine (.24 mL, 1.1 equiv.) in DME (2 mL). Dehydro-β-Ionone (290 mg, 1.52 mmol) in DME (2 mL) was then slowly added at -30 °C. The mixture was stirred at this temperature for 30 min, and the enamino ester (407 mg, 1.60 mmol) in DME (5 mL) was then added. The refrigerating bath was removed and, after 20 min, the solution was refluxed for 1 hour. The temperature was cooled to -10 to -5 °C, and methylmagnesium bromide (3 M in THF, 1.25 mL, 3.8 mmole) was added. The temperature was allowed to rise to room temperature and after 1 hour lower back to 0 °C, in which ethanol (2 mL) was added and then KOH (511 mg, 6 eq.) in water (6 mL) were added at 0 °C. After 30 min, the solution was heated at 50 °C for 3 hours. The solvents were distilled under reduced pressure and the crude mixture was acidified with cold HCl (2 M). The oily product was extracted and purified by HPLC. (1-3% yield). The majority of the product is all-trans retinoic acid (ATRA) confirmed by HPLC retention times by our collaborators.

Synthesis of 2.2 (*all-trans* retinoic acid) from beta-ionone[12]

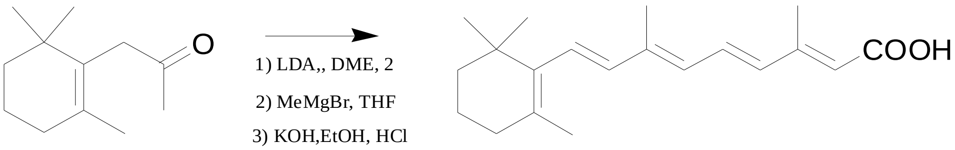

n-Butyllithium (1.6 M in hexanes, 1.75 mL, 2.83mmole) was added at -25 °C to redistilled diisopropylamine (.40 mL, 2.86 mmole) in THF (2.5 mL). β-Ionone (500 mg, 2.60 mmol) in THF (2.5 mL) was then slowly added at -40 °C. The mixture was stirred at this temperature for 30 min, and the enamino ester (696 mg, 2.73 mmole) in THF (6 mL) was then added. The refrigerating bath was removed and, after 20 min, the solution was refluxed for 1 hour. The temperature was cooled to -10 to -5 °C, and methylmagnesium bromide (3 M in THF, 2.20 mL, 6.60 mmole) was added. The temperature was allowed to rise to room temperature and after 1 hour ethanol (15 mL) was added and then KOH (827 mg, 6 equiv.) in water (7.5 mL) were added at 0 °C. After 30 min, the solution was heated at 50 °C for 3 hours. The solvents were distilled under reduced pressure and the crude mixture was acidified with cold HCl (2 M). The product was extracted and purified by column chromatography (285mg, 41%).The NMR spectrum is comparable to the known literature.

^{1}H 300MHz NMR ($CDCl_3$) δ 7.04 (1H, dd), 6.31 (2H, d), 6.16 (1H, s) 6.10(1H,d), 2.35 (3H,s), 2.04(1H,m) 2.00(3H,s), 1.71 (3H,s), 1.61 (2H,m), 1.48(2H,m), 1.02 (6H,s)
R_f =.31

Synthesis of RA Methyl Ester (2.12)[22]

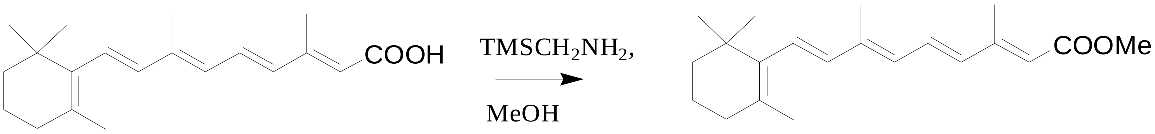

To a stirred solution of retinoic acid (330 mg, 1.1 mmole) in methanol/benzene (2 mL / 7 mL) was added a solution of $TMSCHNH_2$ (250 mg, 2.2 mmole) in 2.0M Ethyl ether at room temperature. The mixture stirred for 1 hour and was concentrated under reduced pressure. The crude material was purified by column chromatography in hexanes as elutant (343mg, 99%). The NMR spectrum is comparable to what is reported in the known literature.

^{1}H 300MHz NMR (CDCl3) δ 7.04 (1H, dd), 6.31 (2H, d), 6.16 (1H, s) 6.10(1H,d), 3.71(3H,s), 2.35 (3H,s), 2.04(1H,m) 2.00(3H,s), 1.71 (3H,s), 1.61 (2H,m), 1.48(2H,m), 1.02 (6H,s).

R_f =.31

4-Hydroxy RA Methyl Ester (2.9) from RA Methyl Ester (2.14) [11]**.** The procedure of Hashimoto[11] was adapted to the methyl ester series. To a solution of RA methyl ester (**2.14)** (343 mg, 1.1 mmol) in acetonitrile/water (30 mL / 0.20 mL) was added NBS (178 mg, 1.1 mmol) at -10 °C under yellow light. After 5 min, N,N-diethylaniline (0.20 mL) was added. The reaction mixture was stirred an additional 15 min and then poured into 5% aq sodium thiosulfate solution. The resulting mixture was extracted with ether three times. The organic solution was washed with 1M aq. HCl, water, and brine and then dried and concentrated. The residue was subjected to column chromatography with 3:1 hexanes/ethyl acetate as eluent giving 261 mg (72%) of a viscous oil. (R_f = 0.36 in 3:1 Hex: EtOAc). The ^{1}H NMR spectrum of this material showed two sets of absorptions; integration of key peaks was consistent with that expected of a 2:1 mixture of the all-E and 13-Z isomers.

All-E-isomer[11] ^{1}H 300 MHz NMR ($CDCl_3$) δ 7.05 (1H, m), 6.33 (2H, d, J = 16.0 Hz), 6.25 (1H, s), 6.19 (1H, m), 5.84 (1H, s), 4.06 (1H, s), 3.76 (3H, s), 2.40 (3H, s), 2.05 (3H, s), 1.88 (3H, s), 1.67 (2H, m), 1.44 (2H, m), 1.07 (6H, s).

Peaks corresponding to the 13-Z-isomer[11]*:* δ 6.33 (2H, d, J = 14.8 Hz), 5.70 (1H, s), 2.12 (3H, s).

4-Oxo Retinoic Acid Methyl Ester (2.11) from 4-Hydroxy Retinoic Acid Methyl Ester (2.9). A solution of 4-hydroxy methyl ester **2.9** (29 mg, 0.088 mmol) was stirred with MnO_2 (110 mg, 1.22 mmol) in dichloromethane (5 mL) at room temperature under yellow light. After 4 hours, the mixture was filtered through Celite and concentrated. The residue was purified by column chromatography with 6:1 Hexanes/Ethyl acetate as the eluent. The NMR spectrum of the material isolated from the column (16 mg, 55%) was consistent with that expected of a 3:1 mixture of all trans/13-cis isomers.[8]

All-E-isomer ^{1}H 400 MHz NMR ($CDCl_3$) δ 7.04 (1H, m), 6.44 (1H, m), 6.39 (2H, s), 6.30 (1H, d, J = 11.2 Hz), 5.88 (1H, s), 3.77 (3H, s), 2.59 (2H, t, J = 5.8 Hz), 2.42 (3H, s), 2.09 (3H, s), 1.92 (3H, s), 1.24 (6H, s).

Peaks corresponding to the 13-Z-isomer[11]*:* δ 7.92 (d, J = 15.2 Hz), 5.70 (s), and 2.16 (s).

3,4-Didehydro RA Methyl Ester (2.15) from 4-Hydroxy RA Methyl Ester (2.9) [11]. A solution of 4-hydroxy methyl ester **2.9** (70 mg, 0.213 mmol) was stirred in dry benzene at 55 °C. p-Toluenesulfonic acid (10 mg, 0.056 mmol) was added and the reaction mixture was stirred for 10 min at this temperature. Ice cold 1% $NaHCO_3$ (5 mL) was poured into the mixture which was then extracted with hexanes (3 x 10 mL). The extracts were combined and the resulting solution was dried and concentrated. The residue was subjected to chromatography on silica with 3:1 hexanes/ethyl acetate as eluent to give the desired methyl ester (30mg, 43%, R_f = 0.51 in 3:1 hex: EtOAc containing a trace (drops per 100 mL of solvent) of acetone).

The NMR spectrum of this product shows two sets of signals that correspond to the all trans and the 13-cis 3,4-ddRA in a ratio of 9:1. *All-E-isomer*: ^{1}H 300 MHz NMR ($CDCl_3$): δ 7.08 (1H, m), 6.35 (2H, s), 6.25 (1H, d, J = 12.9 Hz), 6.19 (1H, d, J = 13.4 Hz), 5.91 (1H, d, J = 11.6 Hz), 5.81 (1H, d, J = 11.5 Hz), 5.70 (1H, s), 3.76 (3H, s), 2.43 (3H, s), 1.95 (3H, s), 1.67 (2H, m), 1.44 (2H, m), 1.07 (6H, s). *Peaks corresponding to the 13-Z-isomer:* : δ 7.86 (d, J = 15.6 Hz), 5.68 (s), and 2.12 (s).

3,4-Didehydro RA (2.4) from 3,4-Didehydro RA Methyl Ester (2.15)[13]. Methyl ester **2.15** (15 mg, 0.048 mmol) in methanol (5 mL) was stirred with an aq methanolic KOH (12 eq, .0.576 mmol) in water (2 mL) at 80 °C for 3 h. The solution was acidified with HCl and then lyophilized, affording 9 mg of a white solid. This material was extracted with $CDCl_3$ and the resulting solution was subjected to ^{1}H NMR analysis. The integration of key peaks was consistent with that expected of a mixture of all-trans and 13-cis 3,4-ddRA in a ratio of 4.5:1. *All-E-isomer:* ^{1}H 400 MHz NMR ($CDCl_3$) δ 7.04 (1H, m), 6.30 (2H, s), 6.20 (1H, d, J = 13.2 Hz), 5.85 (1H, d, J = 9.5 Hz), 5.79 (1H, s),

5.74 (1H, m), 2.36 (3H, s), 2.09 (2H, m), 2.01 (3H, s), 1.87 (3H, s), 1.04 (6H, s). *Peaks corresponding to the 13-Z-isomer:* : δ 7.80 (d, J = 15.3 Hz), 5.66 (s), and 2.33 (s).
^{13}C 400 MHz NMR ($CDCl_3$) δ 172.5, 155.2, 140.2, 138.4, 136.7, 135.3, 131.9, 130.1, 127.9, 125.5, 118.0, 40.2, 34.3, 27.1, 21.5, 14.4.

The NMR sample was recombined with the salts from the lyophilizatin and the solvent was removed under a stream of argon. The resulting material was extracted (see below) to provide samples for hplc-ms and for preparative hplc.

2.4.1. HPLC-Mass Spectroscopy.

A portion of the recombined lyophilization residue was extracted with methanol to provide a sample for hplc-ms analysis. Analysis was performed on a Varian Metasil, C18 column (3µm, 120Å, 4.6 x150 mm) at T=30°C with an ammonium acetate, acetonitrile solvent gradient (20mM NH_4CH_3COO, pH=6.5; Solvent B – CH_3CN; t = 0' , %B =65; t = 3' , %B =65; t = 23' , %B =95) and a flow rate of 1.0 ml / min. Impurities eluted with the solvent front with R_t's = 1.6' and 2.2.' A peak representing 3,4-ddRA eluted with R_t = 8.57' and m/z = 297.1. Under similar conditions, RA eluted as a single peak with R_t = 11.95' and m/z = 299.1 and a mixture of 3,4-ddRA and RA eluted as two peaks with R_t = 8.57' and 11.95'.

2.4.2. Purification of Unlabelled 3,4-ddRA

For further analysis and purification, another portion of the recombined lyophilization residue was extracted by the procedure of Bligh and Dyer.[23] The resulting solution was concentrated under a stream of argon. The residue was dissolved in 50 µL of ethanol. Then 2 mL of methanol was added and the 0.8 mL of doubly distilled water. The mixture was subjected to vortex (desktop shaker) for 1 min. Then 1 mL of chloroform was added and the vortexing was repeated (1 min); a second chloroform addition (1 mL) and vortexing (1 min) procedure was carried out. Finally 1 mL of doubly distilled water was added and the mixture was subjected to vortex (1 min) and then to centrifuging (15 min, 3000 rpm at 4 ^{o}C). The organic phase was transferred to a new test tube and the solvent was evaporated under a stream of argon. The residue from this evaporation was subjected to purification by reverse phase HPLC on a semi-preparative NovaPak C18 column. A 15 minute linear gradient from 10 nM ammonium acetate in methanol:water (68:32) to methanol:dichloromethane (4:1) followed by a 15 min hold at a flow rate of 4 mL/min was used for the separation. As shown in Figure 2.2, materials corresponding to each of five peaks were collected. Peaks 1, 2, and 3 had spectra matching that of 3,4-ddRA.

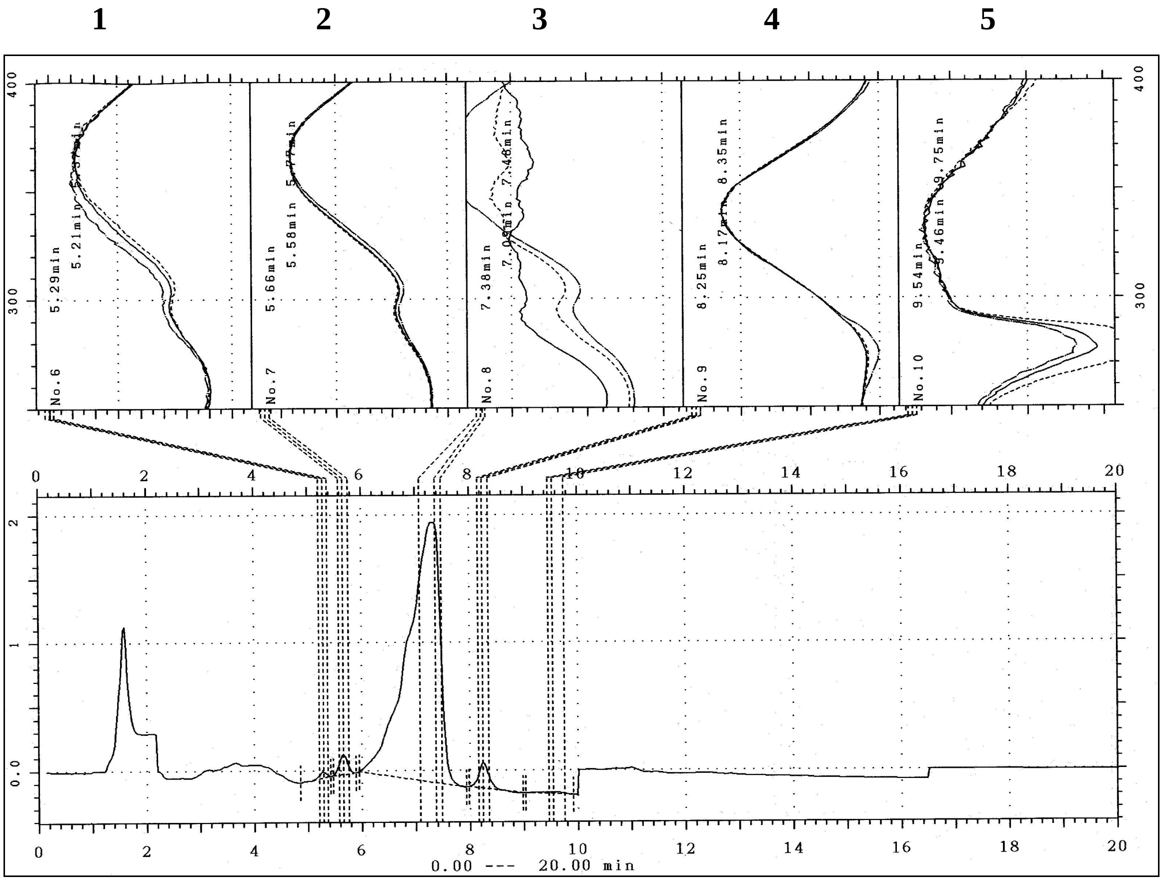

Fig 2.4. Reverse- phase gradient Preparative HPLC Trace. Partial Purification of all trans 3,4-ddRA resolution of ddRA. HPLC trace performed by our collaborator Dr. Juliana Tafrova.

The solution of material represented by peak 3 was concentrated under a stream of argon and subjected to a second reverse phase HPLC purification on a

SunFire C18 column with the same mobile gradient system, but with a flow rate of 1 mL/min. Three peaks, all of which contained material with spectra matching 3,4-ddRA, were eluted (Figure 2.5)

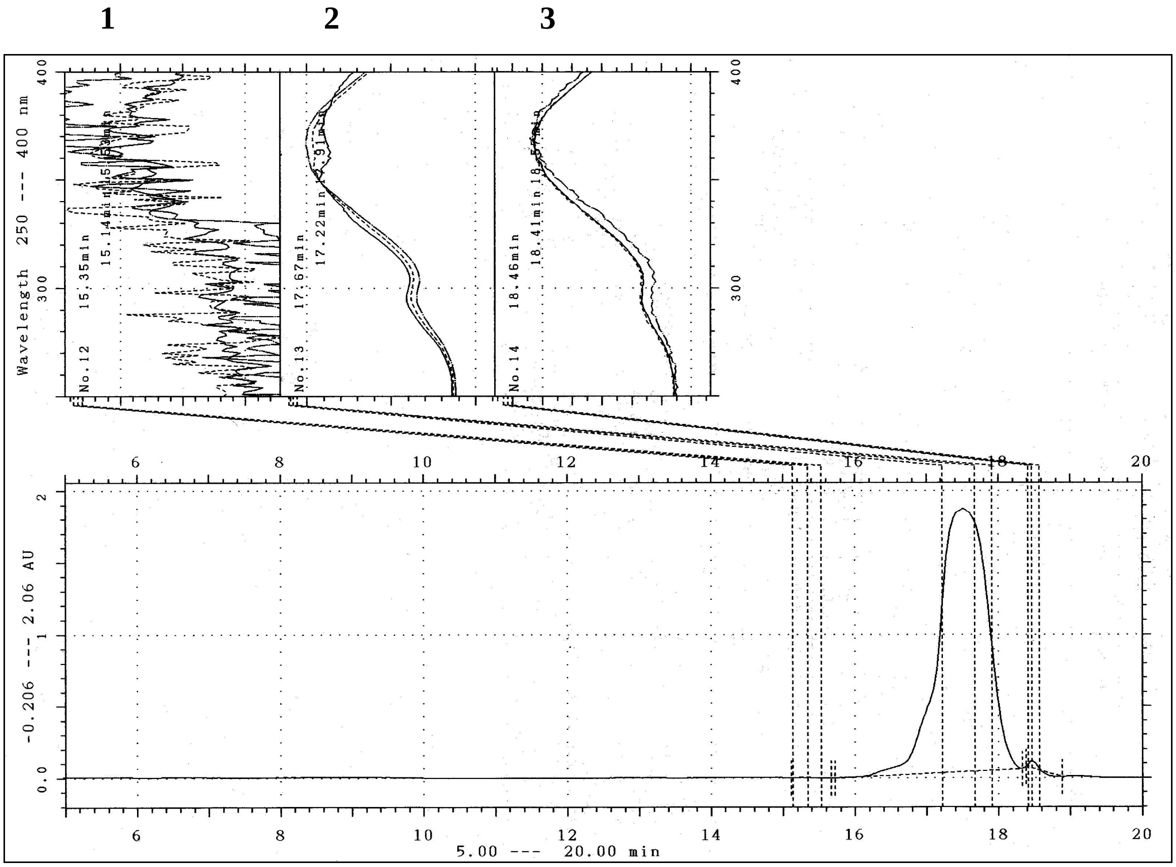

Fig 2.5: Reverse-phase gradient HPLC analysis of partially purified ddRA (2.4) (peak 3) from the previous separation on NovaPackC18 column. HPLC trace performed by our collaborator Dr. Juliana Tafrova.

Peak 3 (Figure 2.4) was collected and further purified by reverse phase HPLC on a Sunfire C18 column. The major peak with retention time between 17.22 – 17.91 minutes corresponds to ddRA (**2.4**).

NMR from HPLC material of 3,4dd-ATRA

^{1}H 600MHz NMR ($CDCl_3$) δ 7.04 (1H, t, J=13.7Hz), 6.33 (1H, m), 6.30 (1H, s), 6.20 (1H, d, J = 11.2 Hz), 5.86 (1H, m), 5.75 (1H,m), 2.54 (2H,s) , 2.10 (3H, s), 2.02 (3H, s), 1.87 (3H, s), 1.04 (6H, s).

Material represented by the major peak was collected and concentrated under a stream of argon. Multiple runs afforded a total of 0.56 mg of a white solid. An NMR spectrum (600 MHz) of this material was consistent with that of all trans 3,4-ddRA (see above); no trace of 13-cis 3,4-ddRA could be detected. In order to determine the retention times of all trans ddRA and all trans RA, an aliquot of the material collected from the SunFire column was subjected to reverse phase HPLC on an analytical NovaPak HR C18 column with absorbance detection at 326 nm. The only peak detected had the retention time (11 min.) and spectra (Figure 2.6A) of 3,4-ddRA. The absorption spectrum of this material was also measured with a separate uv spectrophotometer (Figure 2.6 B).

A. Retinoic acid

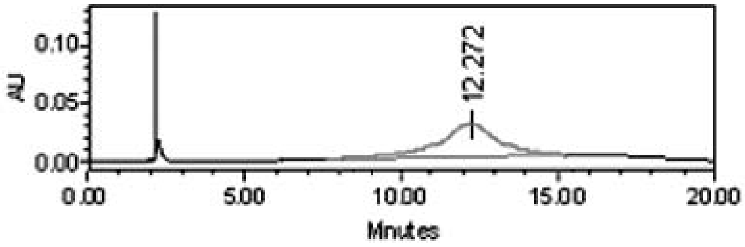

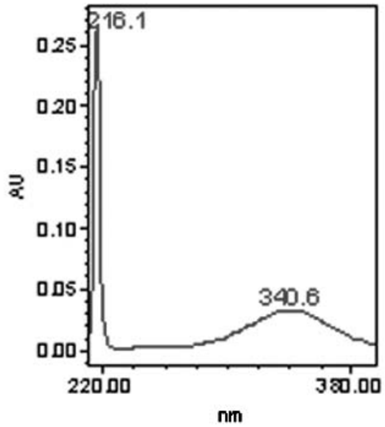

B. 3,4-Didehydroretinoic acid

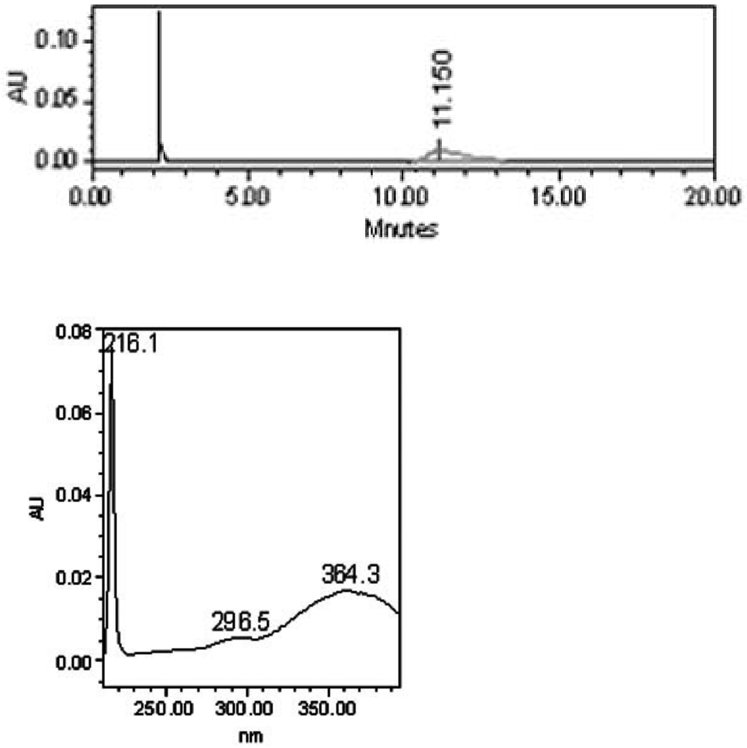

Figure 2.6: Retinoic acid (A) and 3,4-didehydroretinoic acid (B) were characterized by retention times on reverse phase HPLC on a Nova-Pak HR C18 column (upper panel) and by UV spectroscopy (lower panel).

One Pot-Preparation of 3,4-Didehydro RA (2.4) from 4-Oxoretinoic Acid Methyl Ester (2.11). A solution of methyl 4-oxoretinoate (34 mg, 0.10 mmol) in anh methanol (2 mL) in a round bottom flask was treated with sodium borohydride (0.06 mmol, 2.4 mg) at rt. The reaction mixture was allowed to stir for 30 min. Sodium borohydride (10 mg, .26 mmole) was added and the reaction was allowed to proceed for another 30 min or until reaction completed as monitored by TLC. The reaction mixture was concentrated and dried under vacuum (pump). The crude residue was dissolved in anhydrous benzene (5 mL). The flask was capped and placed in a water bath. The temperature of the water bath was raised and maintained at 55 ^{o}C. Then p-toluene sulfonic acid (3 mg) was added and the reaction mixture was stirred for 5 minutes. The reaction mixture was cooled down to room temperature and then concentrated and dried under vacuum (pump). The residue was then redissolved in methanol (7 mL). This crude reaction mixture was treated with an aqueous KOH (1.2 mmol, 12 eq) in water (2 mL). The flask (capped) was placed in a water bath and the temperature of the solution was raised and maintained at 80 ^{o}C . The reaction was monitored by TLC until completion. Afterwards, the reaction mixture was cooled to rt and acidified with 1M aq. HCl. The crude reaction mixture was concentrated and dried by vacuum. The material had undergone the Bligh and Dyer procedure. 3,4-Dehydroretinoic acid material is purified by HPLC purification with a Nova-Pak C18 semi-preparative reverse phase column.

Characterization of the material is determined by the UV wavelength observed from a standard gradient used by our collaborator Dr. Juliana Tafrova in the Department of Oral Biology and Pathology to distinguish between RA and 3,4ddRA. A 15 minute linear gradient from 10 nM ammonium acetate in methanol:water (68:32) to methanol:dichloromethane (4:1) followed by a 15 min hold at a flow rate of 4 mL/min was used for the separation. This gradient had shown that our 3,4ddRA material was believed to be retinoic acid with both having similar retentions times. A small amount of material was separated with the proper UV wavelength using this approach. This procedure was to mimic tritiated material; the crude material had other streaking material under the retention time peaks that was expected. A different gradient had to be used for separation and identification of our material. Our new gradient to be used was in acetonitrile:methanol: deionized water: glacial acetic acid (800:10:10:1). The HPLC traces are shown in Figure 2.7.

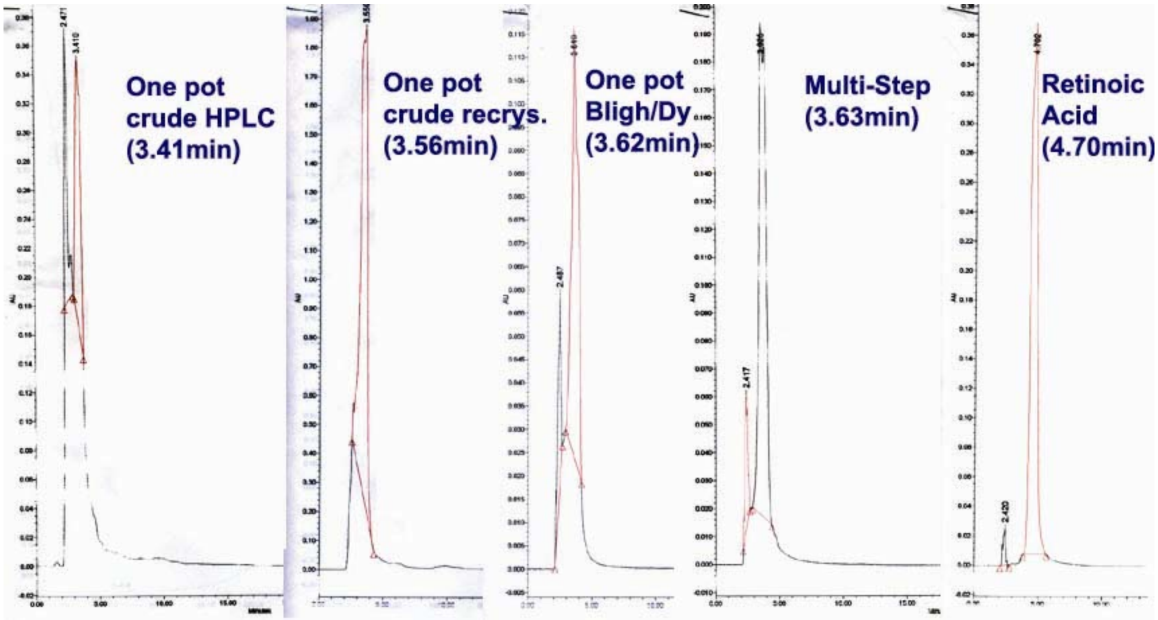

Figure 2.7. HPLC traces of One pot crude, crystallized, Bligh/Dyer, Multi-step Clean and pure RA on the new solvent gradient with retention times. HPLC trace performed by our collaborator Dr. Juliana Tafrova.

The new HPLC gradient had run the clean multistep 3,4-ddRA, RA, and the one pot crude and one pot crude after crystallization with Blight/ Dyer protocol performed. The one pot crude (3.41 min) clearly had a different retention time than that of retinoic acid (4.702 min) and similar to that of our multi-step clean (3.62 min) material. However, the UV wavelength was not consistent with what that was is expected with 3,4 ddRA to that that of retinoic acid. It can be seen in the trace that an unknown impurity is streaking under the desired product. The gradient was increased to the following parameter ratio: (580 mL acetonitrile, 180 mL methanol, 4.6 mL glacial acetic acid, 230 mL deionized water). The following traces have shown in Figure 2.8, 2.9, and 2.10 the clear separation.

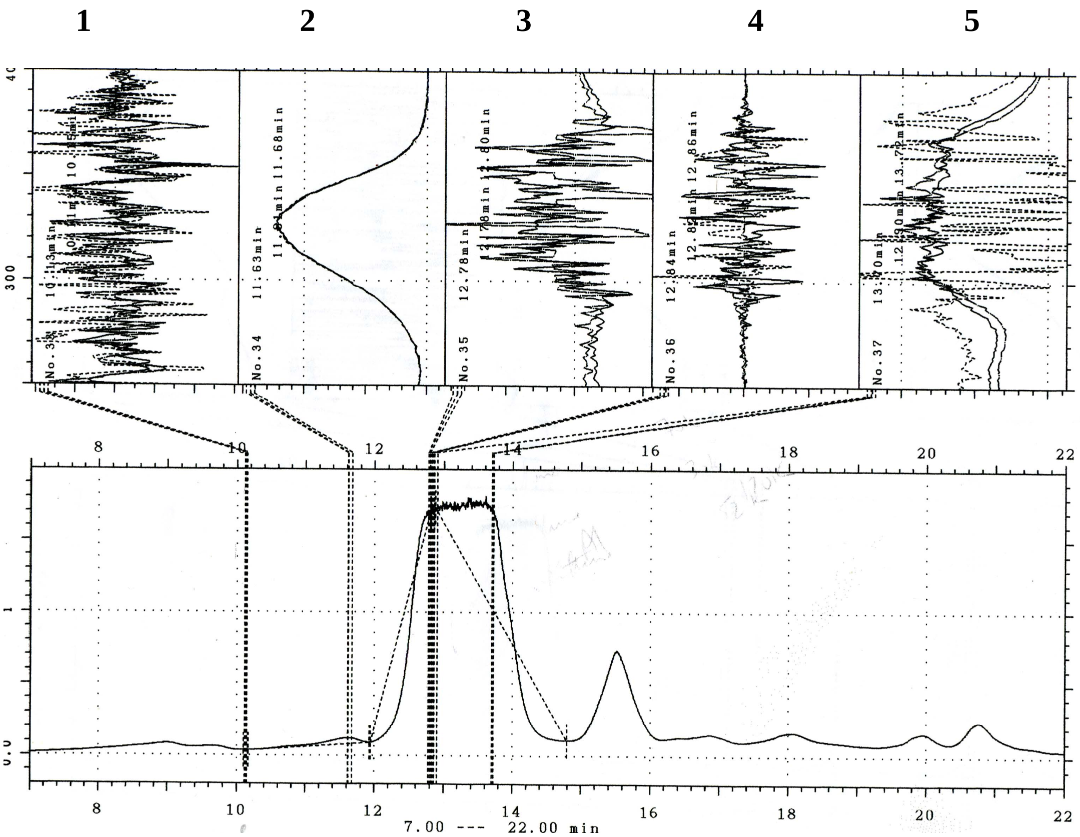

Fig 2.8. Reverse- phase gradient Preparative HPLC Trace. Partial Purification of all trans 3,4-ddRA resolution of ddRA. HPLC trace performed by our collaborator Dr. Juliana Tafrova.

Figure 2.8 shows the impurity resolved and separated from our pure 3,4-didehydroretionic acid. The retention time was found to be 12-14 minutes. This material was collected on a small scale from the HPLC. A mass spectrum is being taken to identify its weight. It is believe that that is material is a retinoid salt.

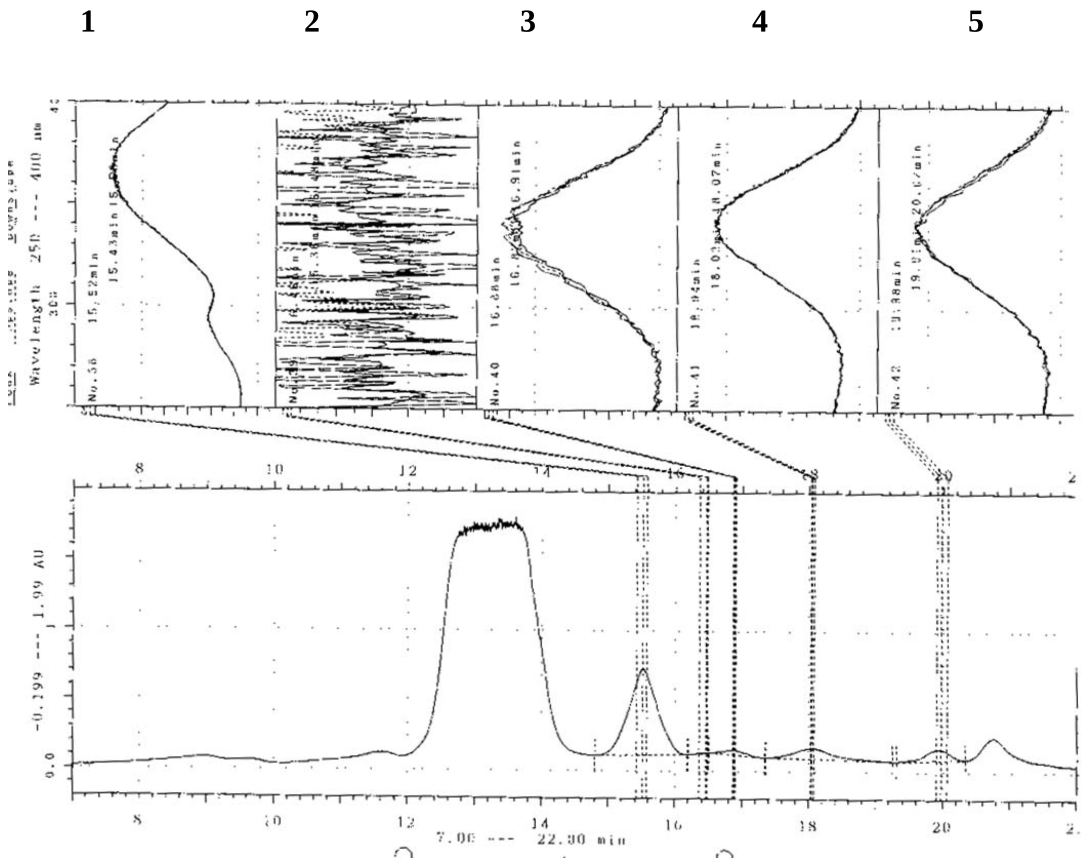

Fig 2.9. Reverse- phase gradient Preparative HPLC Trace. Partial Purification of all trans 3,4-ddRA resolution of ddRA. HPLC trace performed by our collaborator Dr. Juliana Tafrova.

Figure 2.9 shows the separated desired 3,4-didehydroretinoic acid with a retention time of 15.50 minutes with the desired UV wavelength that is characteristic of this material. Finally, a comparison of this desired material (9.228 min) was done to pure RA (21.41 min) and found to have clearly two different retention times as shown in Figure 2.10.

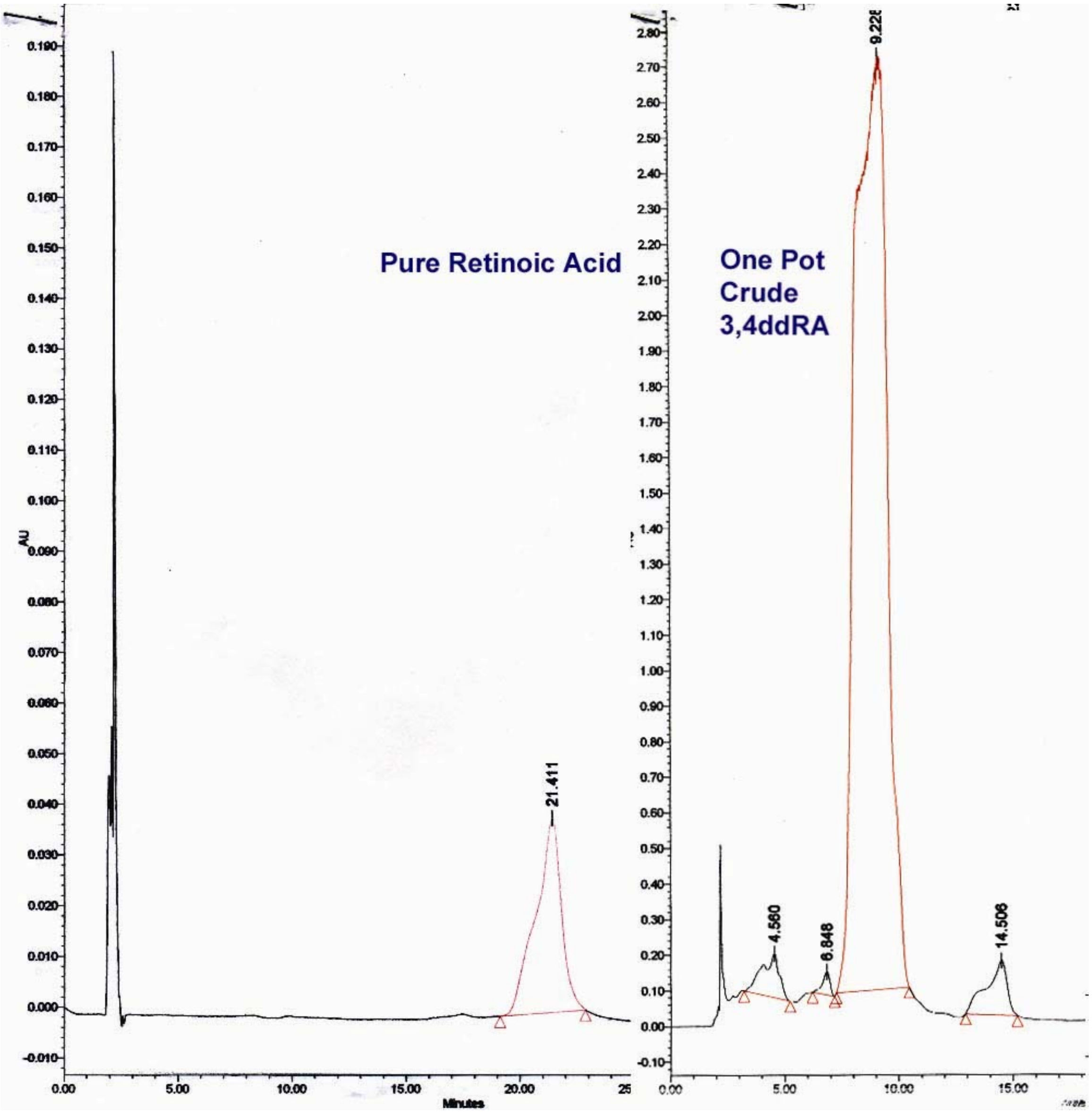

Figure 2.10. Reverse- phase gradient Preparative HPLC Trace. Purification and retention times of all trans 3,4-ddRA resolution and ATRA. HPLC trace performed by our collaborator Dr. Juliana Tafrova.

2.4.3. Purification of ^{3}H -3,4-ddRA

4-Tritio-3,4-ddRA (2.10) The following procedure was performed in a hood that is devoted to the preparation and handling of radioactive materials. Radioactivity was confined to a single flask from the initial reduction through dehydration and hydrolysis steps. A methanol solution (2 mL) of methyl 4-oxoretinoate (silica plate, $R_f = 0.72$ in 3:1 Hex/EA, 3.30 mg, 0.010 mmol) in a round bottom flask was treated with sodium borotritide (0.006 mmol, 0.24 mg, 6.4 mCi) at rt. The flask was capped with a glass stopper and the reaction mixture was allowed to stir for 30 min. Sodium borohydride (50 mg, 1.32 mmol) was added, the stopper was replaced, and the reaction was allowed to proceed for another 10 min. The solution was concentrated by exposure to a stream of argon for several hours and then dried under vacuum (pump). To the residue (R_f = 0.31 in 3:1 Hex/EA) in the original flask was added dry benzene (2 mL). The flask was capped and placed in a water bath. The temperature of the water bath was raised and maintained at 50 ^oC. Then p-toluenesulfonic acid (2 mg) was added. After stirring for 5 min, the reaction mixture showed a TLC spot (silica plate, Hex/EA 3:1) with an R_f = 0.90. After cooling to rt, the solution was concentrated by exposure to a stream of argon for several hours and then the residue was dried under vacuum (pump). It was then redissolved in methanol (3 mL). Still in the original flask, this solution was treated with an aqueous methonalic KOH solution (0.07 mmol, 12 eq) in water (2mL). The flask (capped) was placed in a water bath and the temperature of the solution was raised and maintained at 80 ^oC. The reaction was monitored by TLC (silica plate, R_f = 0.15, Hex/EA 3:1) until completion. Afterwards, the reaction mixture was cooled to rt, acidified with HCl until the solution had pH = 2. The mixture was stirred with ethyl ether and the ether layer was transferred to another flask by pipet. This ether layer was dried by exposure to a stream of argon and the residue extracted by the Bligh and Dyer procedure. The resulting solution was evaporated and purified by HPLC (NovaPak semipreparative and Sunfire columns as above) to tritiated 3,4-ddRA with specific activity 30 dpm/pmol (calculated maximum specific activity 91 dpm/picomol) or 3.85 x 10^5 cpm. Figure 2.11 and Table 2.1 shows the HPLC Traces from the tritiated purifcation using the initial linear solvent gradient. (10 nM ammonium acetate in methanol:water (68:32) to methanol:dichloromethane (4:1))

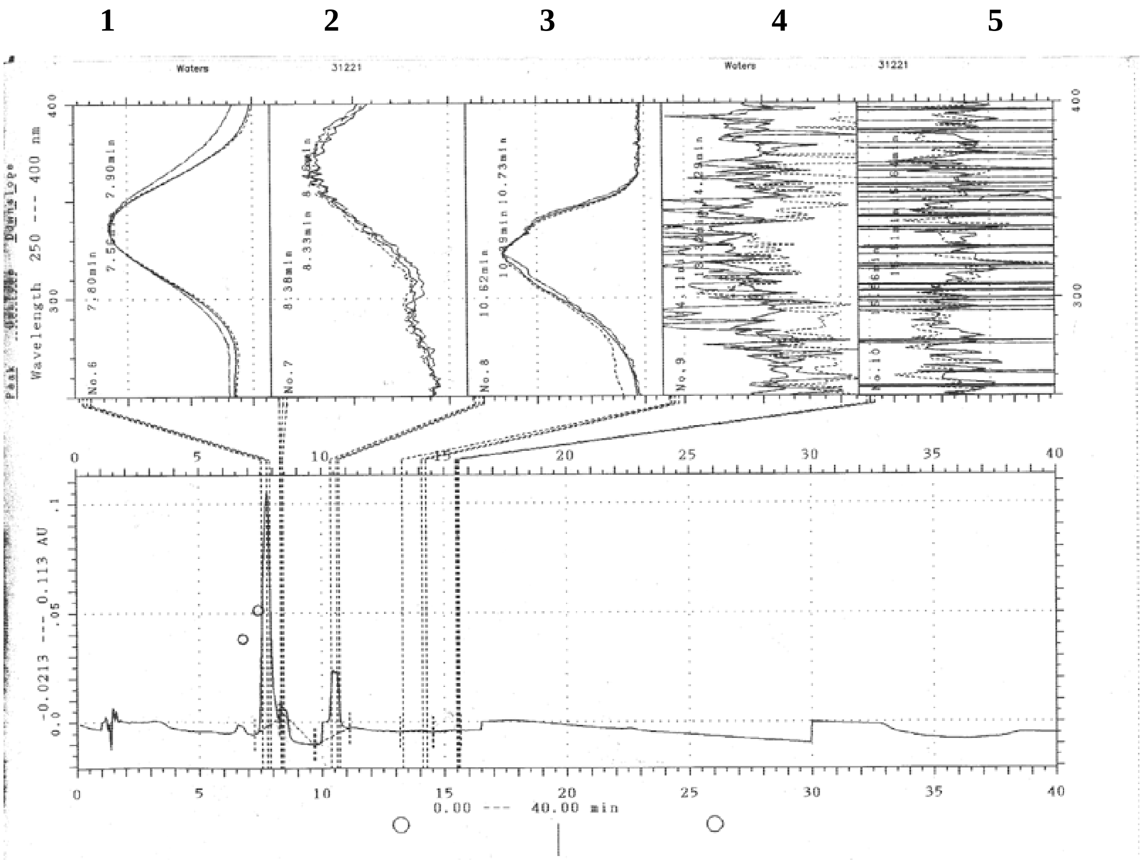

Figure 2.11. Reverse- phase gradient Preparative HPLC Trace. Purification of tritiated 3,4-ddRA using Novapak column system. HPLC trace performed by our collaborator Dr. Juliana Tafrova.

As mentioned, purification was done on the previous solvent gradient using the NovaPak column. Fraction #2 was collected for it had a characteristic UV wavelength to what is expected for retinoids. Fraction #1 also showed strong radioactivity with specific activity 432 dpm/pmol (calculated maximum specific activity 1310 dpm/picomol) or 5.5 x 10^6 cpm. At this time it is believed to be our desired product as well, but this material needs to be purified by the new HPLC gradient. Salt impurities are preventing pure separation with the old gradient system and change in retention times. The peak with retention time 8.38 min. was harvested and was rerun a second time on the NovaPack C18 column. Figure 2.12 shows the trace of this material. This material was harvested and fed to the cells.

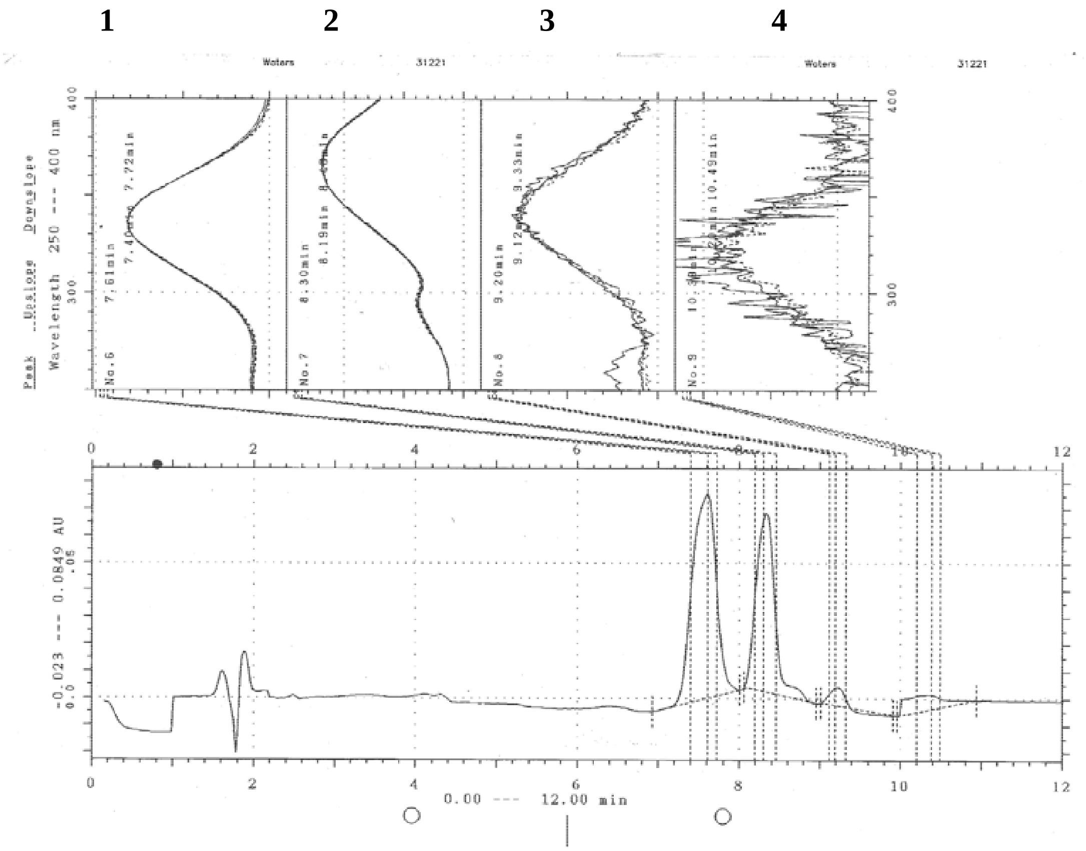

Figure 2.12. Reverse- phase gradient Preparative HPLC Trace. Purification of tritiated 3,4-ddRA using Novapak column system the second time. HPLC trace performed by our collaborator Dr. Juliana Tafrova.

Retention time of the synthesized 3,4-ddRA:

	Cold Clean Multi-step synthesis	^{3}H 3,4-ddRA One-pot synthesis	
		The major peak Fraction#1	^{3}H 3,4-ddRA Fraction#2
Nova-Pak C18	7.38 min.	7.8 min.	8.38 min.
SunFire	17.67 min.	18.65 min.	19.68 min.
Nova-Pak HR C18	11.15 min.	9.943 min.	11.424 min.

Table 2.1 Retention times for ^{3}H 3,4-ddRA and cold 3,4-ddRA. Red indicates crude preparation of the material.

2.5 References

---

[1] (a) DeMaeyer, E. M. The WHO programme of prevention and control of vitamin A deficiency, xerophthalmia and nutritional blindness. *Nutr. Health*. **1986**, *4*, 105-12.

(b) Underwood, B. A. Hypovitaminosis A: International Programmatic Issues. *J Nutr*. **1994** *124* (8 Suppl):1467S-1472S.

(c) Underwood, B. A., Arthur, P. The Contribution of Vitamin A to Public Health. *FASEB J.* **1996**, *10*, 1040-8.

[2] Mangelsdorf, D. J.; Thummel, C.; Beato, M.; Herrlich, P.; Schutz, G.; Umesono, K.; Blumberg, B.; Kastner, P.; Mark, M.; Chambon, P.; Evans, R. M.; Nonsteroid nuclear receptors: what are genetic studies telling us about their role in real life? *Cell*, **1995**, *83*, 835-839.

[3] (a) Shaw, N.; Elholm, M.; Noy, N. Retinoic Acid Is a High Affinity Selective Ligand for the Peroxisome Proliferator-activated Receptor β/δ. *J. Biol. Chem*., **2003**, *278*, 41589-41592.

(b) Schug, T. T.; Berry, D. C.; Shaw, N. S.; Travis, S. N.; Noy, N. Opposing effects of retinoic acid on cell growth result from alternate activation of two different nuclear receptors. *Cell*, **2007**, *129*,:723-33.

(c) Tan, N. S.; Shaw, N. S.; Vinckenbosch, N.; Liu, P.; Yasmin, R.; Desvergne, B.; Wahli, W.; Noy, N.Selective cooperation between fatty acid binding proteins and peroxisome proliferator-activated receptors in regulating transcription. *Mol. Cell Biol.* **2002**, *22*, 5114-27.

(d) Budhu, A. S.; Noy, N. Direct channeling of retinoic acid between cellular retinoic acid-binding protein II and retinoic acid receptor sensitizes mammary carcinoma cells to retinoic acid-induced growth arrest. *Mol. Cell Biol*. **2002**, *22*, 2632-41.

[4] Kamei, Y., Xu, L., Heinzel, T., Torchia, J., Kurokawa, R., Gloss, B., Lin, S-C., Heyman, R. A., Rose, D. W., Glass, C. K., Rosenfeld, MG. A CBP integrator complex mediates transcriptional activation and AP-1 inhibition by nuclear receptors. *Cell*, **1996**, *85*, 403-414.

[5] (a) Törmä, H.; Vahlquist, A. Retinol uptake and metabolism to 3,4-didehydroretinol in human keratinocytes at various stages of differentiation. *Skin Pharmacol*. **1991**, *4*, 154-7.

(b) Andersson, E.; Björklind, C.; Törmä, H.; Vahlquist, A. The metabolism of vitamin A to 3,4-didehydroretinol can be demonstrated in human keratinocytes,

---

melanoma cells and HeLa cells, and is correlated to cellular retinoid-binding protein expression. *Biochim Biophys Acta*, **1994**, *1224*, 349-54.

(c) Rollman, O.; Wood E. J.; Olsson M. J.; Cunliffe W. J. Biosynthesis of 3,4-didehydroretinol from retinol by human skin keratinocytes in culture.*Biochem. J.* **1993**, *293* (Pt 3), 675-82.

(d) Törmä, H.; Vahlquist, A. Vitamin A in skin and serum--studies of acne vulgaris, atopic dermatitis, ichthyosis vulgaris and lichen planus. *J. Invest. Dermatol*. **1985**, 85, 498-500.

(e) Törmä, H.; Vahlquist, A. Biosynthesis of 3,4-didehydroretinol and fatty acyl esters of retinol and 3,4-didehydroretinol by organ-cultured human skin. *Methods Enzymol*. **1990**, *190*, 210-6.

(f) Siegenthaler, G. Retinoic acid formation from retinol and retinal metabolism in epidermal cells. *Methods Enzymol*. **1990**, *189*, 530-6.

(g) Randolph R. K.; Simon M. Characterization of Retinol Metabolism in Cultured Human Epidermal Keratinocytes *J. Biol. Chem*. **1993**, *268*, 9198-9205.

[6] Randolph R. K.; Simon M. All-trans-Retinoic Acid Regulates Retinol and 3,4-Didehydroretinol Metabolism in Cultured Human Epidermal Keratinocytes. *J. Invest. Dermatol.* **1996**, *106*, *168-175.*

[7] *Organic Preparation and Procedures International* ,**1987**, *19*(2-3), 187-195.; Pommer, H. The Witting Reaction in industrial practice. *Angew. Chem*.,**1960**, *22*, 811-819.

[8] Schwieter et al. Synthesis and Characteristics of stereoisomers: *Helvectica Chimica Acta*, **1962**,*45*, 541-548.; Planta et al. *Helvectica Chimica Acta*, **1962**,*45*, 548-561.

[9] Wada, A.; Hiraishi, S.; Takamura, N.; Date, T.; Aoe, K.; Ito, M. A Novel Method for a Stereoselective Synthesis of Trisubstituted Olefin Using Tricarbonyliron Complex: A Highly Stereoselective Synthesis of (all-E)- and (9Z)-Retinoic Acids. *J. Org. Chem.* **1997**, *62*, 4343-4348.; A. Wada, *Vitamin.* **2000**, *74*, 101-121.

[10] J. K. Stille, The Palladium-Catalyzed Cross-Cou- pling Reactions of Organotin Reagents with Organic Electrophiles.*Angew. Chem. Int. Ed. Engl.* **1986**, *25*, 508-524.

---

[11] K. Sonogashira, Y. Tohda, N. Hagihara, A convenient synthesis of acetylenes: catalytic substitutions of acetylenic hydrogen with bromoalkenes, iodoarenes and bromopyridines *Tetrahedron Lett.* **1975**, 4467-4470.

[12] Cartier, D.; Valla, A,; Guillou, R.; Labia, R.; Potier, P. New, Regioselective, One-Pot Synthesis of (all-E) Retinoic Acid and Analogues from Enaminiodiester Synthons. *Eur. J. Org. Chem.*, **2003**, 2250-2253. Cartier, D.; Valla, A,; Guillou, R.; Labia, R.; Potier, P. A new one-pot synthesis of *all E*-retinoic acid via a new enaminodiester synthon. *Tetrahedron Letters*, **2003**, *44*, 5789–5790.

[13] The sodium borotritide reduction of the methyl ester of 4-oxo retinoic acid followed by dehydration has been described: see Tosukhowong, P.; Supasiri, T. *J. Label. Comp. Radiopharm.*, **1985**, *22*, 925-930.

[14] Tanaka, H.; Kagechika, H.; Shudo, K. Specific Oxidation of Retinoic Acid to 4-oxo-Retinoic Acid in Diluted Acid Solutions. *Chem. Pharm. Bull.* **1995**, *43*, 356-358.

[15] (a) For the synthesis of all trans 4-oxo retinol acetate from all trans retinol acetate and the synthesis of all trans 4-oxo RA methyl ester from ATRA methyl ester by direct MnO_2 oxidation, see: Samokyszyn, V. M.; Gall, W. E.; Zawada, G.; Freyaldenhoven, M. A.; Chen, G.; Mackenzie, P. I.; Tephyl, T. R.; Radominska-Pandya, A. *J. Biol. Chem.* **2000**, *275*, 6908-6914.
(b) This procedure has been used successfully by others. See Patel, J. B.; Huynh, C. K.; Handratta, V. D.; Gediya, L. K.; Brodie, A. M. H.; Goloubeva, O. G.; Clement, O. O.; Nanne, I. P.; Soprano, D. R.; Njar, V. C. O. *J. Med. Chem.* **2004**, *47*, 6716-6729.

[16] (a) Staab, H. A.; Manschreck, A. *Chem. Ber*., **1961**, *95*, 284. (b) Attenburrow, J.; Cameron, F. B.; Chapman, R. M.; Evans, R. M.; Hems, B. A.; Jansen, A. B. A.; Walker, T. A Synthesis of Vitamin A from CycloHexanone. *J. Chem. Soc.* **1952**, *194*, 1094-1111.

[17] Hashimoto, N.; Fujimoto, Y. One Step and Convenient Preparations of 4-Hydroxylretinal and 4-Oxoretinal.. *Synthetic Commun.*, **1999**, *29*, 3793-3797.

[18] Cartier, D.; Valla, A,; Guillou, R.; Labia, R.; Potier, P. New, Regioselective, One-Pot Synthesis of (all-E) Retinoic Acid and Analogues from Enaminiodiester Synthons. *Eur. J. Org. Chem.*, **2003**, 2250-2253.

[19] Rosenberger. M.; McDougal, P.; Bahr, J. Canthaxanthin. A new total synthesis. *J. Org.Chem*. **1982**, 47, 2130-2134.

[20] Borhan, B; Souto, M.L.; Um, J.M.; Nakanishi, K.; Efficient Synthesis of 11 cis-retinoids. *Chemistry-A European Journal*, **1999**, *5*, 1172-1175.

---

[21] Koji, N.; Rando, R.; Nesnas, R. Synthesis of biotinylated retinoids for cross-linking and isolation of retinol binding proteins. *Tetrahedron*, **2002**, *58*, 6577-6584**.**

[22] Presser, A; Hufner, A; Trimethylsilyldiazomethane – A Mild and Efficient Reagent for the Methylation of Carboxylic Acids and Alcohols in Natural Products *Monatshefte fur Chemie* , **2004**, 135, 1015–1022

[23] Bligh, E.G., and Dyer, W.J A rapid method of total lipid extraction and purification. *Can. J.Biochem.Physiol* . **1959**, *37*, 911-917.

2.6 Appendix for Chapter II

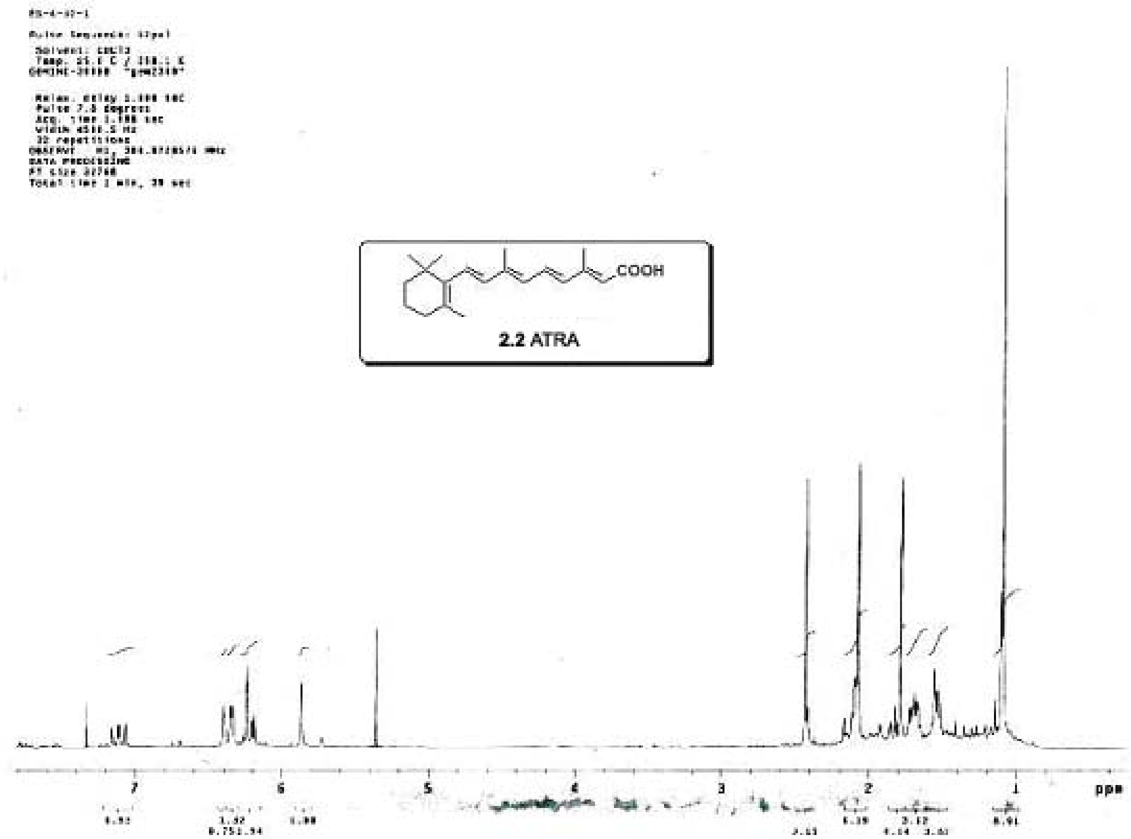

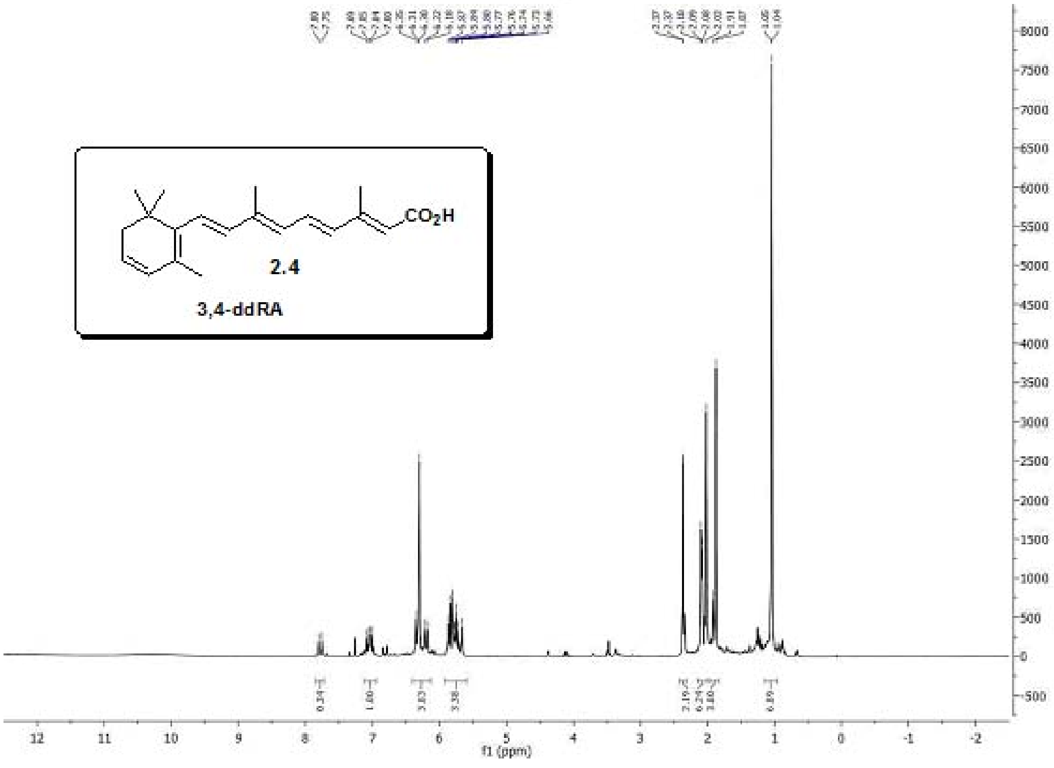

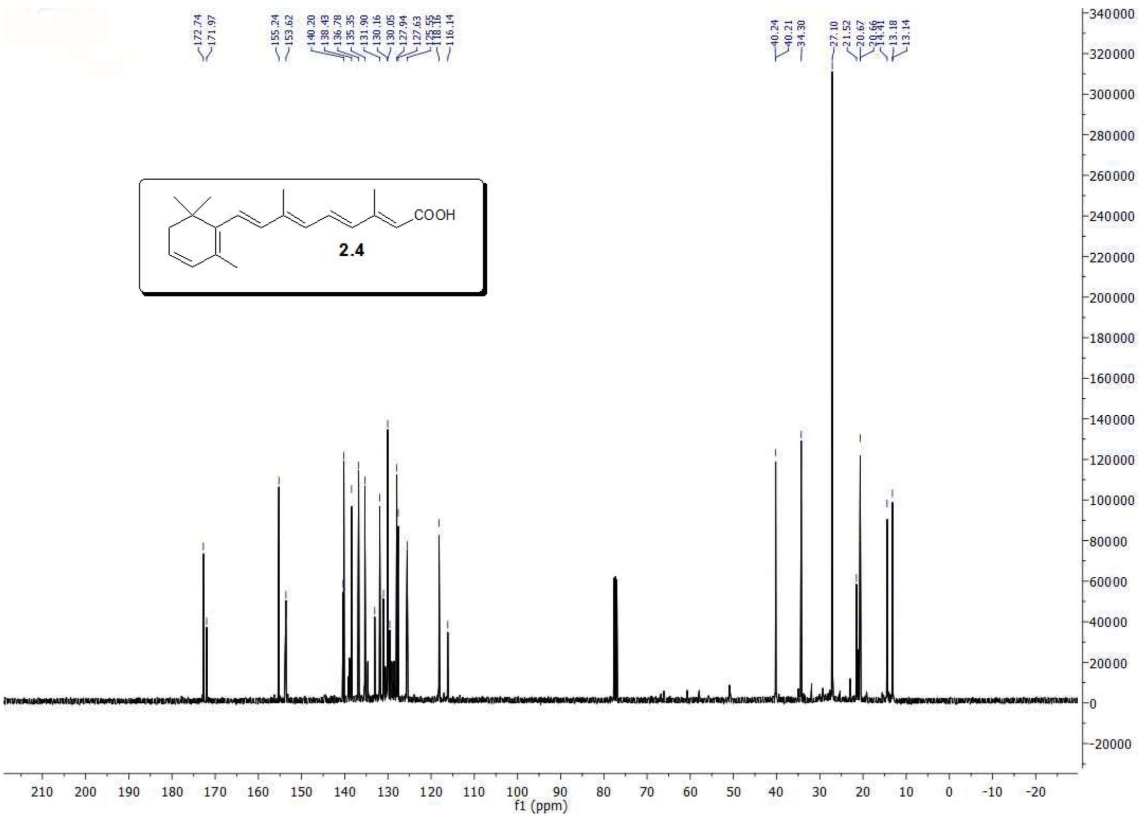
172.74
171.97
155.24
153.62
140.20
138.43
136.78
135.35
131.90
130.16
130.05
127.94
127.63
125.55
118.16
116.14
40.24
40.21
34.30
27.10
21.52
20.67
20.66
14.41
13.18
13.14
COOH
2.4
340000
320000
300000
280000
260000
240000
220000
200000
180000
160000
140000
120000
100000
80000
60000
40000
20000
0
-20000
210 200 190 180 170 160 150 140 130 120 110 100 90 80 70 60 50 40 30 20 10 0 -10 -20
f1 (ppm)

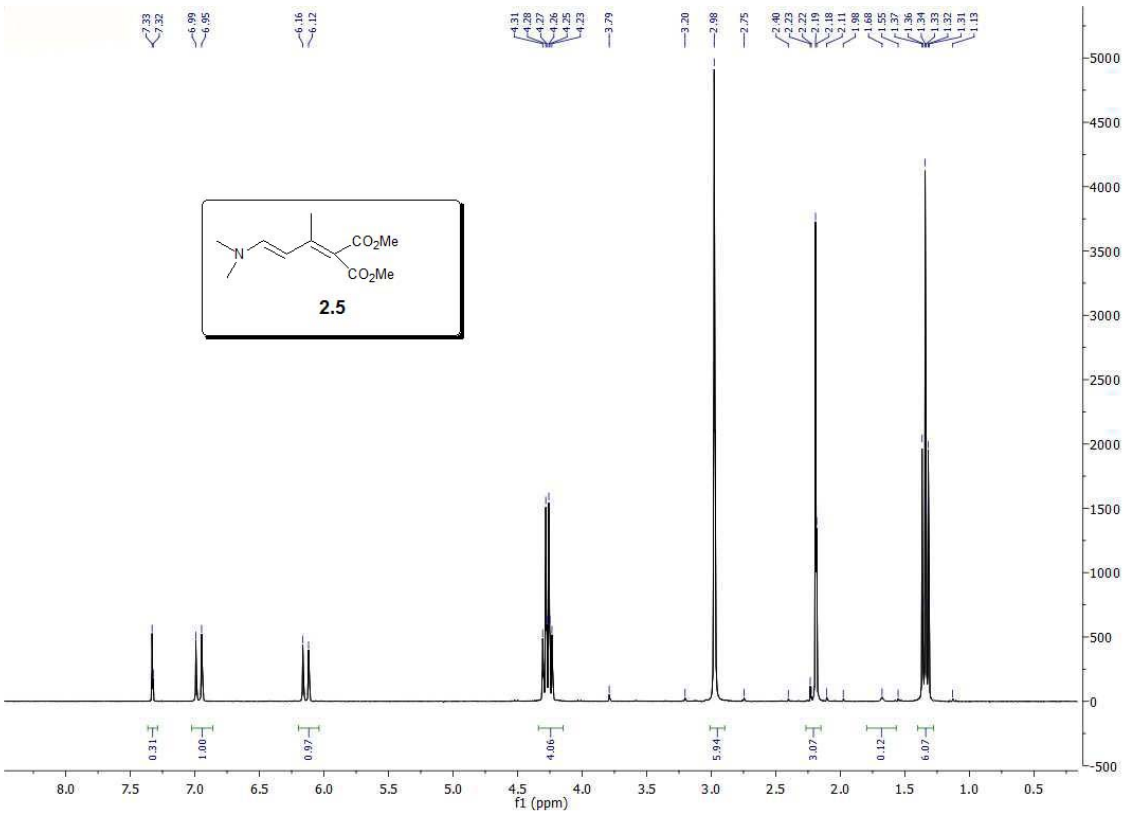
7.33
7.32
6.99
6.95
6.16
6.12
4.31
4.28
4.27
4.26
4.25
4.23
3.79
3.20
2.98
2.75
2.40
2.23
2.22
2.19
2.18
2.11
1.98
1.68
1.55
1.37
1.36
1.34
1.33
1.32
1.31
1.13
N
CO2Me
CO2Me
2.5
5000
4500
4000
3500
3000
2500
2000
1500
1000
500
0
-500
0.31
1.00
0.97
4.06
5.94
3.07
0.12
6.07
8.0 7.5 7.0 6.5 6.0 5.5 5.0 4.5 4.0 3.5 3.0 2.5 2.0 1.5 1.0 0.5
f1 (ppm)

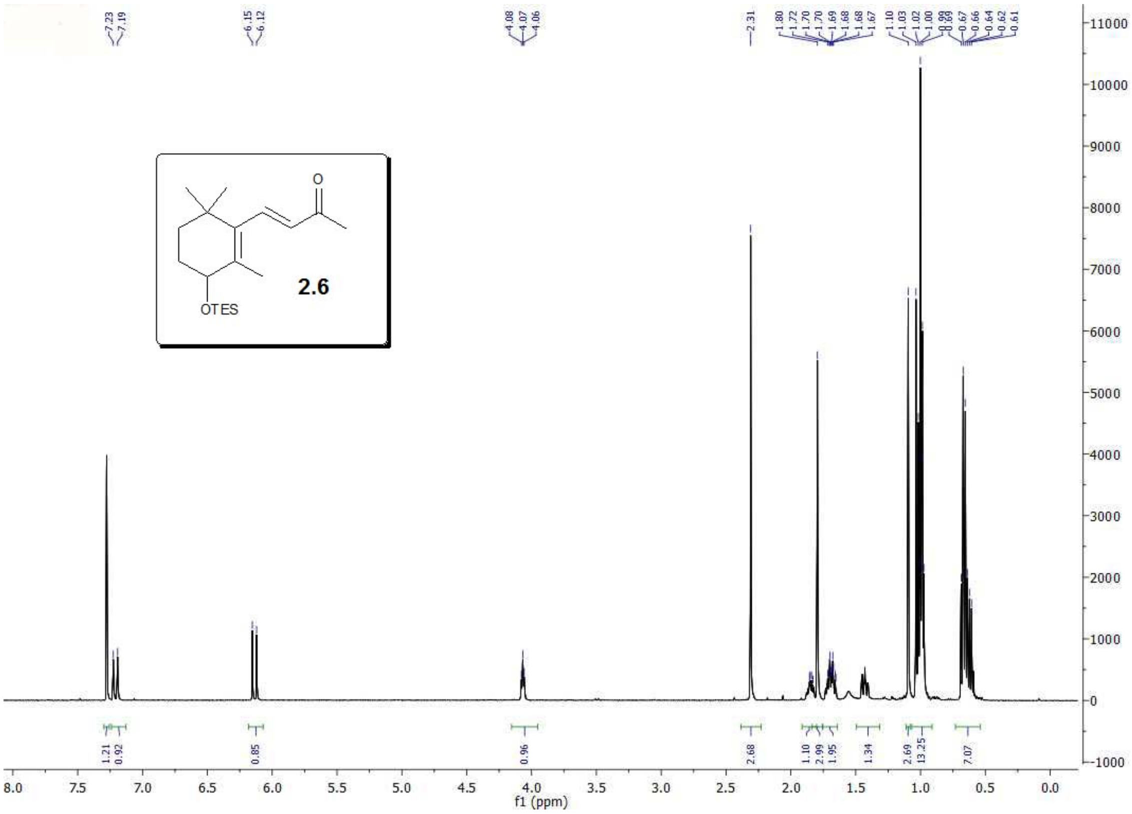
7.23
7.19
6.15
6.12
4.08
4.07
4.06
2.31
1.80
1.72
1.70
1.70
1.69
1.68
1.68
1.67
1.10
1.03
1.02
1.00
0.99
0.98
0.67
0.66
0.64
0.62
0.61
O
OTES
2.6
1.21
0.92
0.85
0.96
2.68
1.10
2.99
1.95
1.34
2.69
13.25
7.07
11000
10000
9000
8000
7000
6000
5000
4000
3000
2000
1000
0
-1000
8.0
7.5
7.0
6.5
6.0
5.5
5.0
4.5
4.0
3.5
3.0
2.5
2.0
1.5
1.0
0.5
0.0
f1 (ppm)

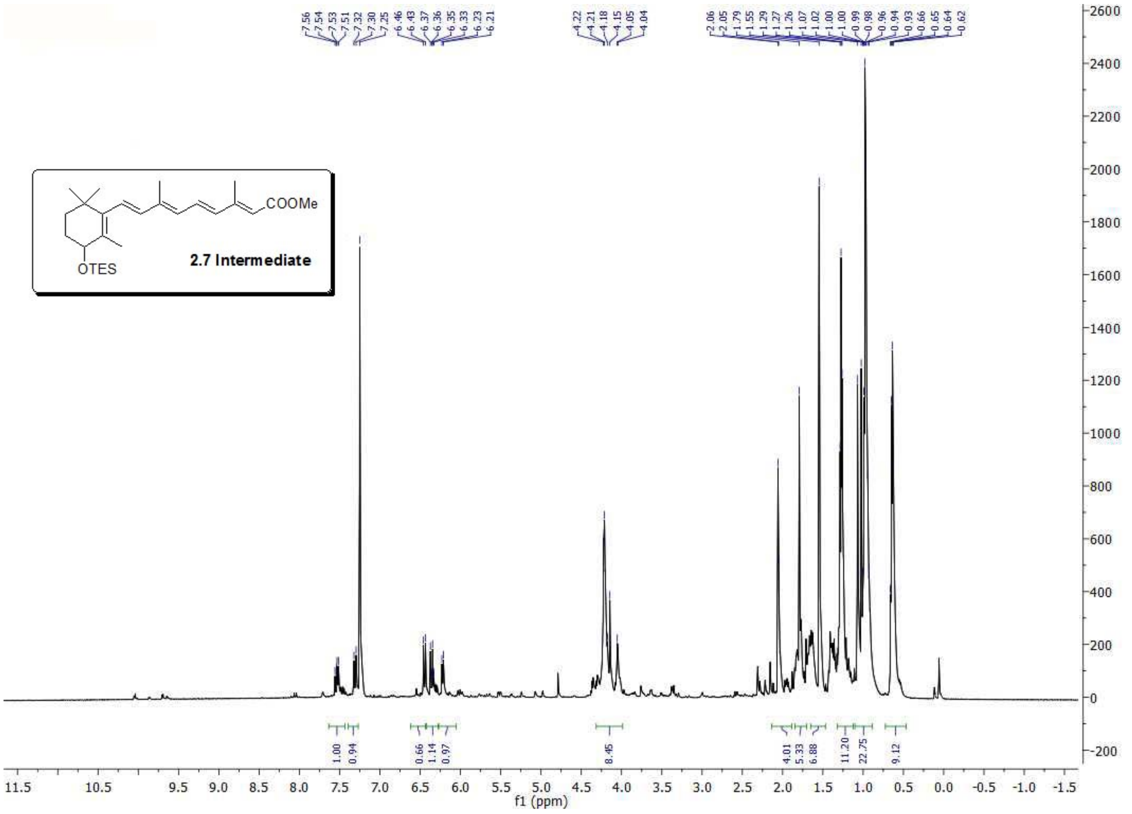
7.56
7.54
7.53
7.51
7.32
7.30
7.25
6.46
6.43
6.37
6.36
6.35
6.33
6.23
6.21
4.22
4.21
4.18
4.15
4.05
4.04
2.06
2.05
1.79
1.55
1.29
1.27
1.26
1.07
1.02
1.00
0.99
0.98
0.96
0.94
0.93
0.66
0.65
0.64
0.62
COOMe
OTES
2.7 Intermediate
1.00
0.94
0.66
1.14
0.97
8.45
4.01
5.33
6.88
11.20
22.75
9.12
2600
2400
2200
2000
1800
1600
1400
1200
1000
800
600
400
200
0
-200
11.5
10.5
9.5
9.0
8.5
8.0
7.5
7.0
6.5
6.0
5.5
5.0
4.5
4.0
3.5
3.0
2.5
2.0
1.5
1.0
0.5
0.0
-0.5
-1.0
-1.5
f1 (ppm)

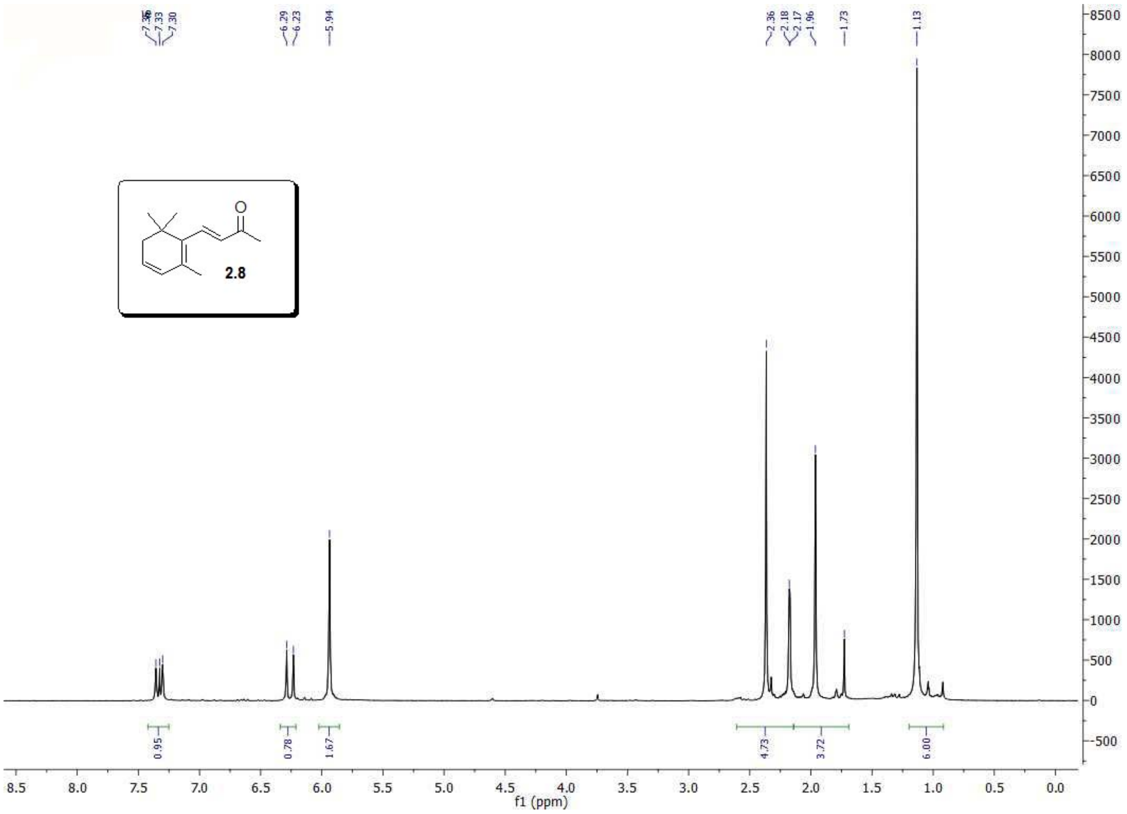
2.8
7.36
7.33
7.30
6.29
6.23
5.94
2.36
2.18
2.17
1.96
1.73
1.13
0.95
0.78
1.67
4.73
3.72
6.00
8.5
8.0
7.5
7.0
6.5
6.0
5.5
5.0
4.5
4.0
3.5
3.0
2.5
2.0
1.5
1.0
0.5
0.0
f1 (ppm)
8500
8000
7500
7000
6500
6000
5500
5000
4500
4000
3500
3000
2500
2000
1500
1000
500
0
-500

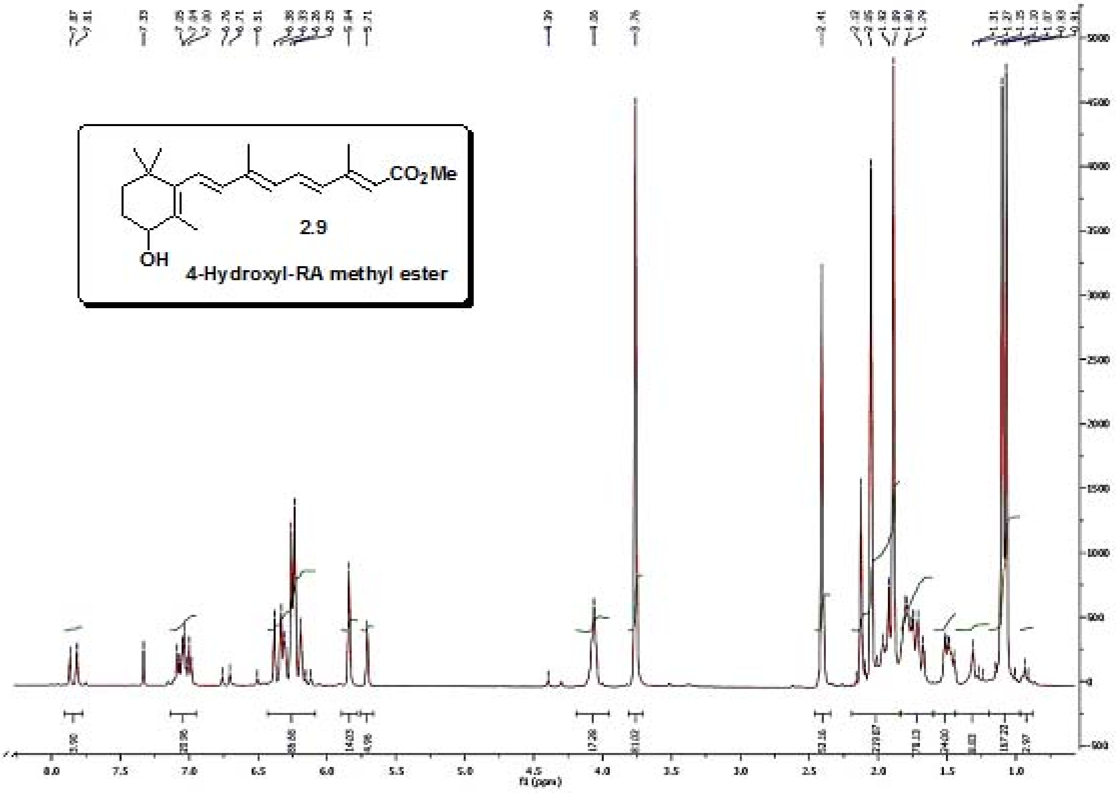
CO2Me
OH
2.9
4-Hydroxyl-RA methyl ester
7.87
7.81
7.33
7.05
7.04
7.00
6.76
6.71
6.51
6.38
6.33
6.28
6.23
5.84
5.71
4.39
4.06
3.76
2.41
2.12
2.05
1.92
1.89
1.80
1.79
1.31
1.27
1.25
1.20
1.07
0.93
0.91
3.00
20.96
88.88
14.03
4.98
17.28
81.02
53.16
229.67
78.13
24.00
8.83
167.22
2.97
8.0
7.5
7.0
6.5
6.0
5.5
5.0
4.5
4.0
3.5
3.0
2.5
2.0
1.5
1.0
f1 (ppm)
5000
4500
4000
3500
3000
2500
2000
1500
1000
500
0
-500

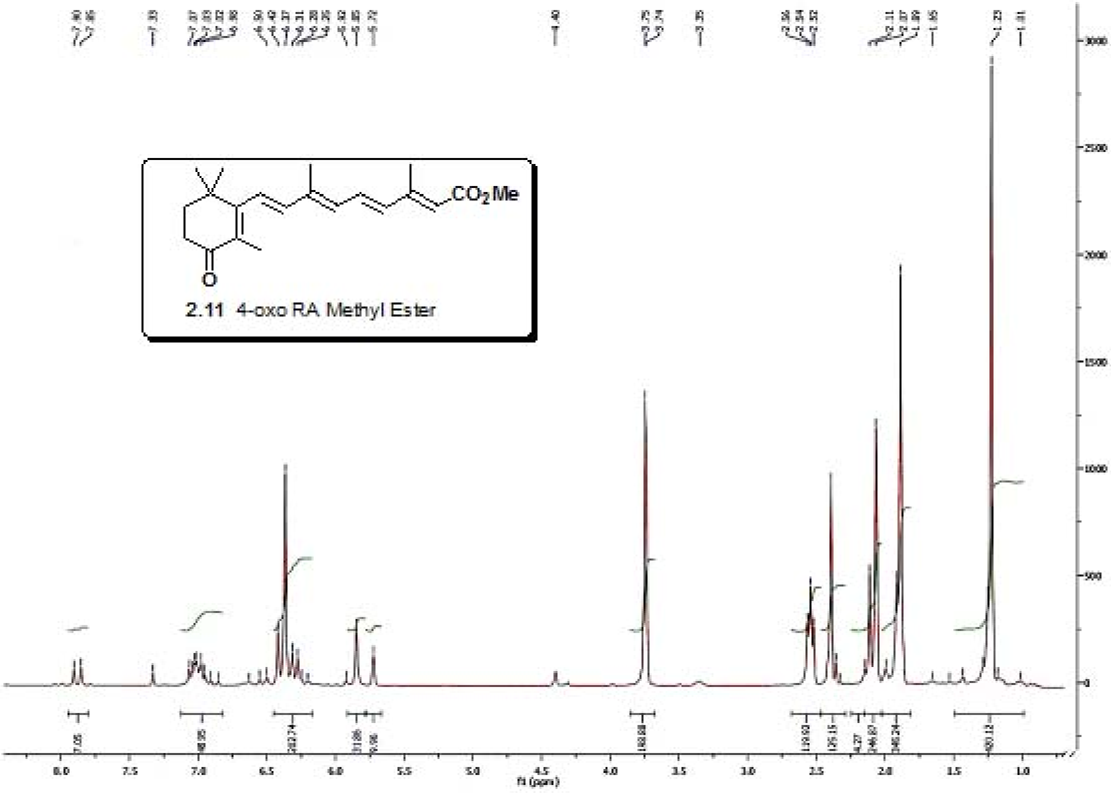
7.90
7.86
7.33
7.07
7.03
7.02
6.98
6.50
6.42
6.37
6.31
6.28
6.26
5.92
5.85
5.72
4.40
3.75
3.74
3.35
2.56
2.54
2.52
2.11
2.07
1.89
1.65
1.23
1.01
CO2Me
O
2.11 4-oxo RA Methyl Ester
7.05
48.95
282.74
31.86
6.06
188.88
179.93
125.15
4.27
246.87
246.24
420.12
8.0
7.5
7.0
6.5
6.0
5.5
5.0
4.5
4.0
3.5
3.0
2.5
2.0
1.5
1.0
f1 (ppm)
3000
2500
2000
1500
1000
500
0

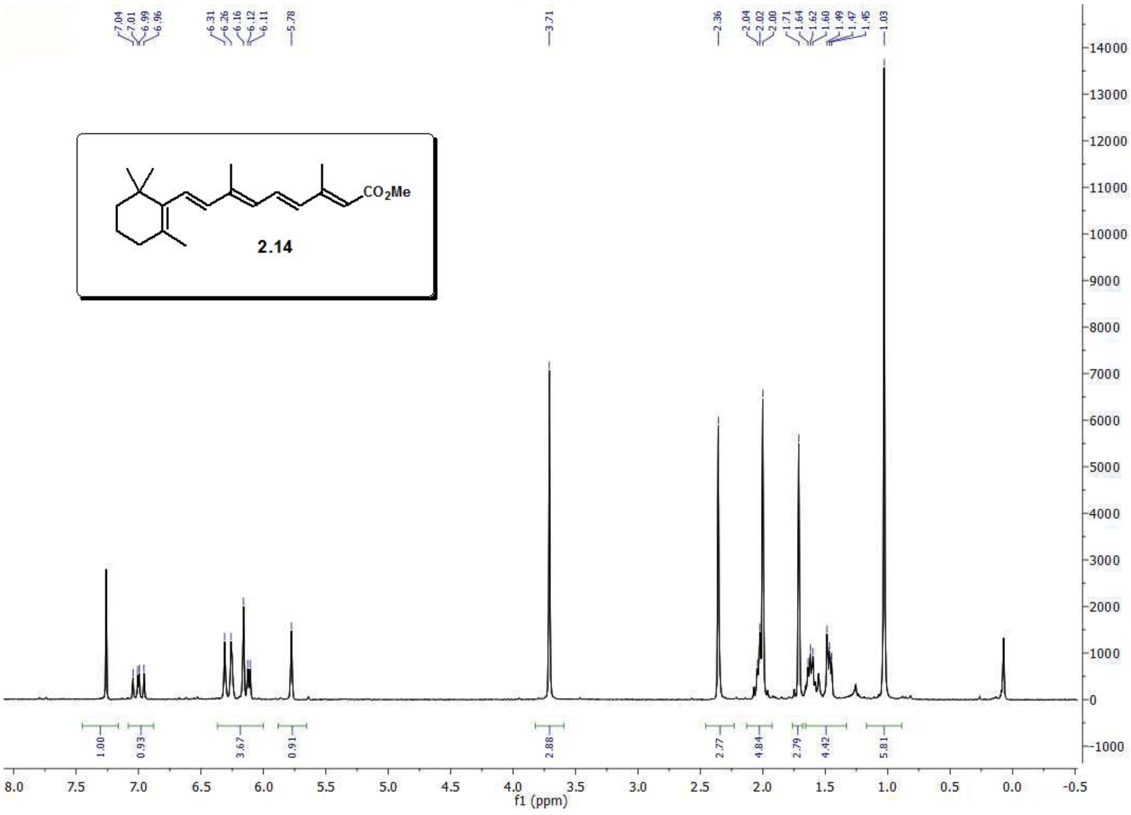
7.04
7.01
6.99
6.96
6.31
6.26
6.16
6.12
6.11
5.78
3.71
2.36
2.04
2.02
2.00
1.71
1.64
1.62
1.60
1.49
1.47
1.45
1.03
CO2Me
2.14
1.00
0.93
3.67
0.91
2.88
2.77
4.84
2.79
4.42
5.81
8.0
7.5
7.0
6.5
6.0
5.5
5.0
4.5
4.0
3.5
3.0
2.5
2.0
1.5
1.0
0.5
0.0
-0.5
f1 (ppm)
14000
13000
12000
11000
10000
9000
8000
7000
6000
5000
4000
3000
2000
1000
0
-1000

Chapter III

Binding Site of the Bisabsoqual Natural Products in Human Squalene Synthase

3.1 Introduction…………………………………………………………………….137

3.2 Background…………………………………………………………..……138

3.2.1 Identification of the active site of squalene synthases………..…………….139

3.2.2 Pfizer crystal structure…………………………………………...….….141

3.3 Structural Results and Discussion of Bisabosqual A-D and CP-320-473...……144

3.3.1 Validation Data CP-320473………………………………………..………145

3.3.2 Bisabosqual A Data………………………………………….………..146

3.3.3 Bisabosqual B Data………………………………………….………..148

3.3.4 Bisabosqual C Data…………………………………………………..…150

3.3.5 Bisabosqual D Data…………………………………………..….…....152

3.4 Correlation of Binding Energies with IC$_{50}$ values for Squalene Synthases……154

3.4.1 Binding Energy Correlations for MM-GBSW and MM-PBSA with IC$_{50}$ Data…………………………………………………………………………….155

3.5 Analogs designed to be improved Squalene Synthase Inhibitors………...…….156

3.5.1 Compound 3.6 Data……………………………………………….....….157

3.5.2 Compound 3.7 Data…………………………………………...…...…158

3.5.3 Compounds 3.8-3.15 Data…………………………………………..…..158

3.5.4 Proposed Binding of Presqualene by overlaying to Bisabosqual A……..……162

3.6 Conclusion…………………………………………………………………163

3.7 Experimental Section…………………………………………………...164

3.8 References………………………………………………………………….194

Chapter 3 – Binding Site of the Bisabsoqual Natural Products in Human Squalene Synthase

3.1 Introduction

Although the statin drugs enjoy remarkable success in combating the hypercholesteremia caused by genetic factors and that associated with diet, age, obesity, and lack of exercise, they are not always without their drawbacks. In some patients, these HMGCoA reductase inhibitors do not reduce low-density lipoprotein (LDL) cholesterol to desired levels and, in others, these drugs are myotoxic.[1,2,3] Consequently, there is significant interest in inhibitors of enzymes that catalyze steps later in the cholesterol biosynthesis pathway.

Squalene synthase inhibitors,[4] somewhat neglected for a period of time, are being actively pursued again. One of these compounds recently advanced to Phase III clinical trials. Studies suggest that, as a class, these compounds are not myotoxic and that, in fact, they could offer some advantage if given in combination with a statin.[5,6,7]

Bisbosquals A, B, C and D (**1-4**)[8] inhibit squalene synthases from *Saccharomyces cerevisiae* and *Candida albicans* and also from HepG2 and rat liver cells at the micromolar levels. The structures of the bisabosquals are small, compact, and rigid with few rotatable bonds. They provide well-defined scaffolds for libraries of compounds that will fulfill the criteria of Veber[9] and Lipinski[10] for solubility and permeability. Therefore they are attractive lead compounds for drug development. (Figure 3.1)

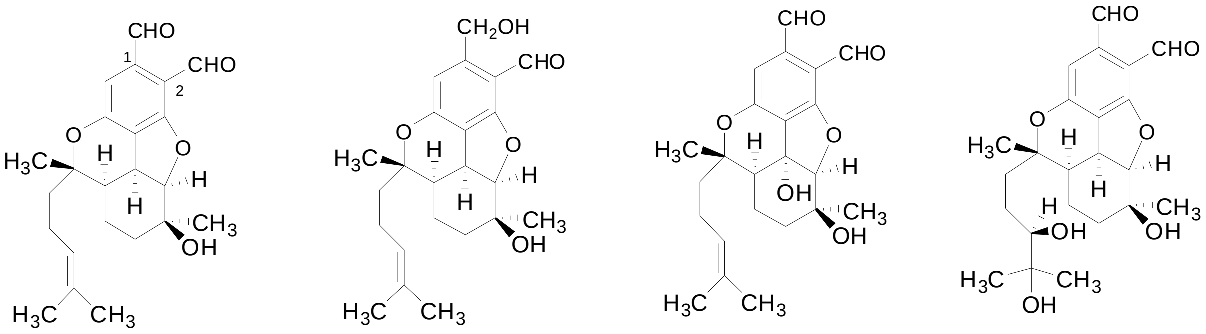

3.1 Bisbosqual A **3.2** Bisbosqual B **3.3** Bisbosqual C **3.4** Bisbosqual D

Figure 3.1. The Bisabosqual Natural Products

In order to understand the protein-ligand interactions that lead to inhibition of human squalene synthase by the four bisabosquals, we performed docking studies. Here we describe the binding modes of these natural products in the second half reaction site of squalene synthase.

3.2 Background

Squalene synthase converts two molecules of farnesyl pyrophosphate to squalene in two well-defined steps. First it effects the unsymmetrical dimerization of farnesyl pyrophosphate (FPP) to presqualene pyrophosphate (PSQPP, a cyclopropylcarbinyl pyrophosphate); this conversion is known as the first half reaction. Then, it catalyzes the generation of a cyclopropyl carbinyl / cyclobutyl / homoallyl cation that undergoes NADPH reduction to squalene in the second half reaction.[11] The second step is believed to occur at a separate second and non-identical catalytic site within the same active site pocket. Figure 1 shows the mechanistic pathway for both conversions.

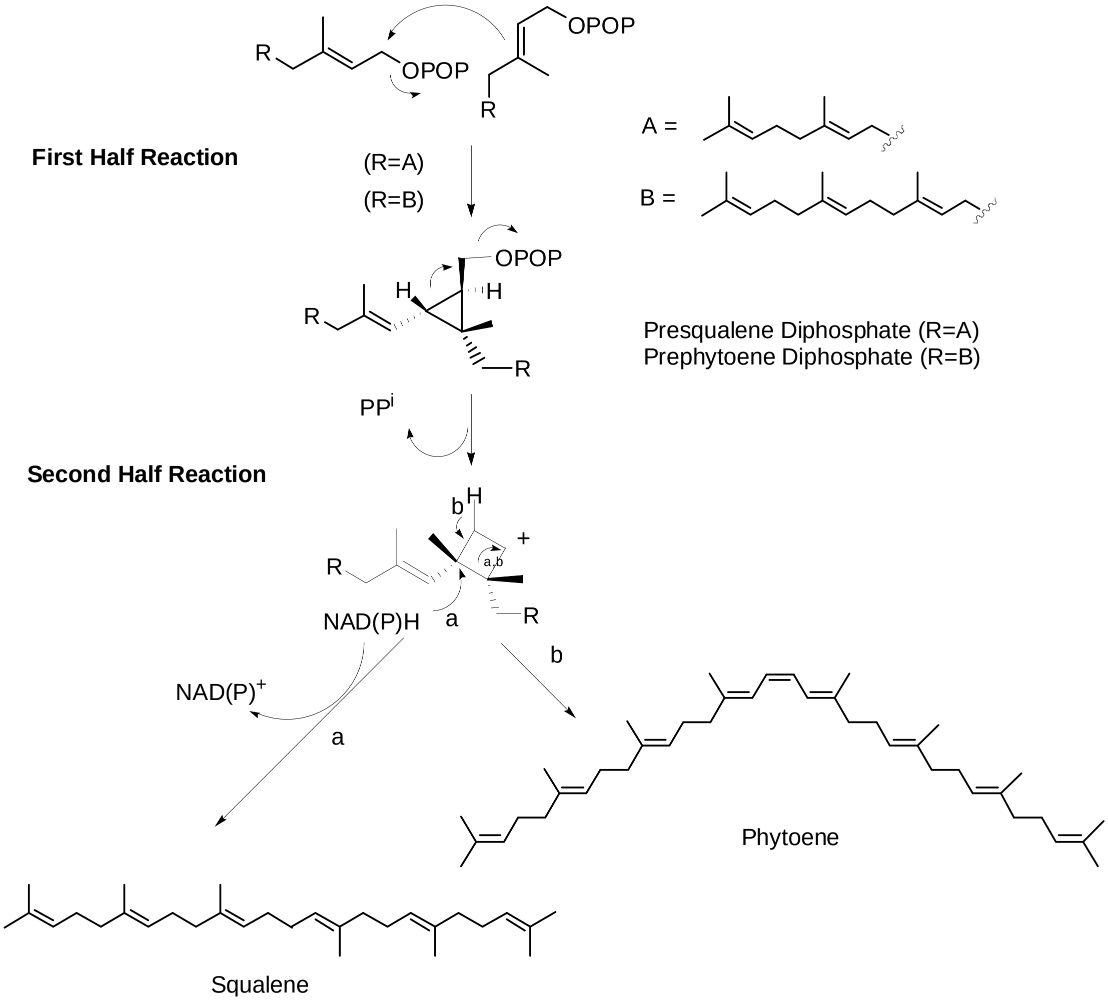
R
OPOP
OPOP
R
First Half Reaction
(R=A)
(R=B)
A =
B =
OPOP
H
H
R
R
Presqualene Diphosphate (R=A)
Prephytoene Diphosphate (R=B)
PP^i
Second Half Reaction
b
H
+
R
a,b
R
NAD(P)H
a
b
NAD(P)$^+$
a
Phytoene
Squalene

Figure 3.2. Biosynthetic conversion of two FPP molecules to squalene and two GGPP molecules to phytoene. Scheme from Enzyme Nomenclature, 1992, Academic Press, San Diego, California, ISBN 0-12-227164-5: http://www.chem.qmul.ac.uk/iubmb/enzyme/reaction/terp/sqnp.html

3.2.1 Identification of the active site of squalene synthases[12,9,10]

Previous works have shown that human,[13] rat,[14] and yeast[15] squalene synthases have all been cloned, expressed, and sequenced by several groups.[16,17] Three regions of high sequence identity were found and believed to be part of the catalytic active site pocket. Using the rat protein, Schechter et al. subjected these three regions to point mutation.[18] The results indicated that aspartates in the ^{219}DYLED^{223} and ^{80}DTLED^{84} sequences play key roles in catalysis.

Enzyme inactivation studies have implicated arginines as important residues in reactions catalyzed by squalene synthases. The sequences of the squalene synthases and the phytoene synthases are aligned in Figure 3.3.[19] In the sequence alignment, the conserved residues that are believed to line the active site of the first half reaction in both enzymes are colored green, red, and cyan and those believed to line the active site of the second half reaction of the squalene synthases are magenta, yellow and blue. The former sequences are highly conserved in both squalene synthases and phytoene synthases. The squalene synthases are related to the plant phytoene synthases.[20] Both couple linear isoprenoid pyrophosphates in a head-to-head fashion (Figure 3.2). The phytoene synthases couple two molecules of geranyl geranyl pyrophosphate (GGPP),[21] to give phytoene, a 40-carbon terpene. The latter are conserved in the squalene synthases and not in the phytoene synthases. The rearrangement in the second half reaction of squalene synthase differs from that in phytoene synthesis in that the coupling reaction is not a reduction and does not involve NADPH (compare conversions in Figures 3.2).

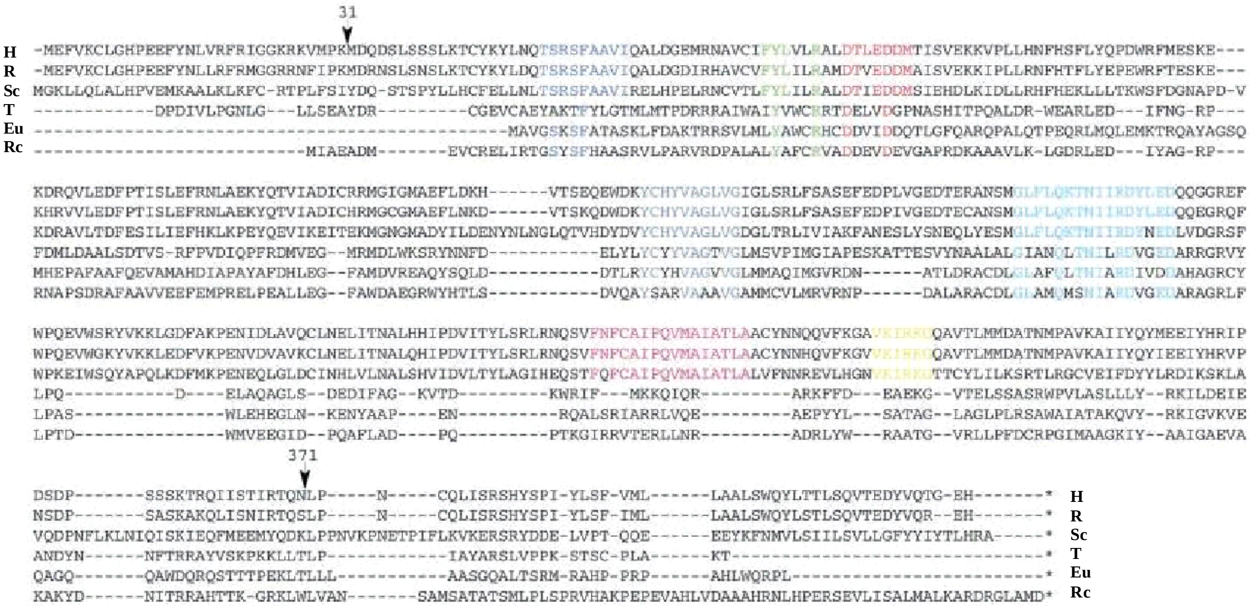

Figure 3.3- Sequences of Squalene Synthases. The first three sequences represent the human (H), rat (R), and *Saccharomyces cerevisiae (Sc)*, squalene synthases.[6, 22 ,10,11] The next three are phytoene synthases from tomato (T), *Erwinia uredovora (Eu)*, and *Rhodobacter capsulate (Rc)*.

3.2.2 Pfizer crystal structure[23]

More recently, the crystal structures of human squalene synthase complexed by each of four synthetic inhibitors[24] were reported by the Pandit / Danley / Harwood group at Pfizer. On the basis of these structures, those of related FPP-utilizing enzymes, and site-directed mutagenesis experiments, Pandit et al. proposed that the active site for the first half reaction is located in a region surrounded by the conserved aspartate- and arginine-containing sequences (Asp80-Asp84 and Asp219-223) and Tyr 171. Furthermore, they proposed that the location of drug-binding, in a hydrophobic cavity under a loop or "flap" is the site of the second half-reaction. The residues that line the interior of this hydrophobic pocket and those in the "flap" are conserved in all squalene synthases.

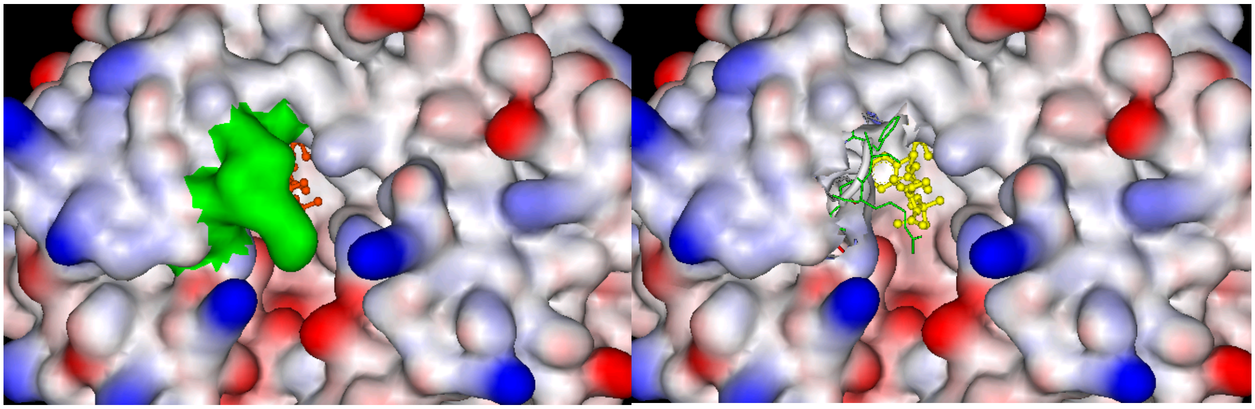

Figure 3.4, constructed from the pdbfile 1EZF of Pandit et al., shows the binding site region with the "flap" (residues Tyr 50, Arg 52, Ser 51, Ser53 and Phe54, colored in green) in place. Figure 1b offers the same view with the flap removed; it shows the underlying cavity and the position of the drug, CP-402473. The hydrophilic and hydrophobic regions of the surface are shaded red and blue respectively.

The sites of the two half reactions are found to lie in a channel. (Figure 3.4) This structural feature suggests that the enzyme shuttles the intermediate PSQPP directly from the first to the second half reaction site. This model is consistent with the observation that PSQPP is not released from the enzyme. One end of the channel is exposed to solvent, whereas the other end leads to a completely enclosed pocket surrounded by conserved hydrophobic residues. The regions identified as the active sites of the two half-reactions are located in the central channel.[25] In order to illustrate the channel of the binding pocket with CP-320473, we show three different perspectives (Figure 3.5) of the active site region. Residues 80-84 and 219-223, involved in the first half reaction, are colored in purple. Residues involved in second half reaction, including residues 50-54, Phe 288, Cys 289, and Pro 292. CP-320473 inhibits the enzyme by binding in the site of the second half reaction.

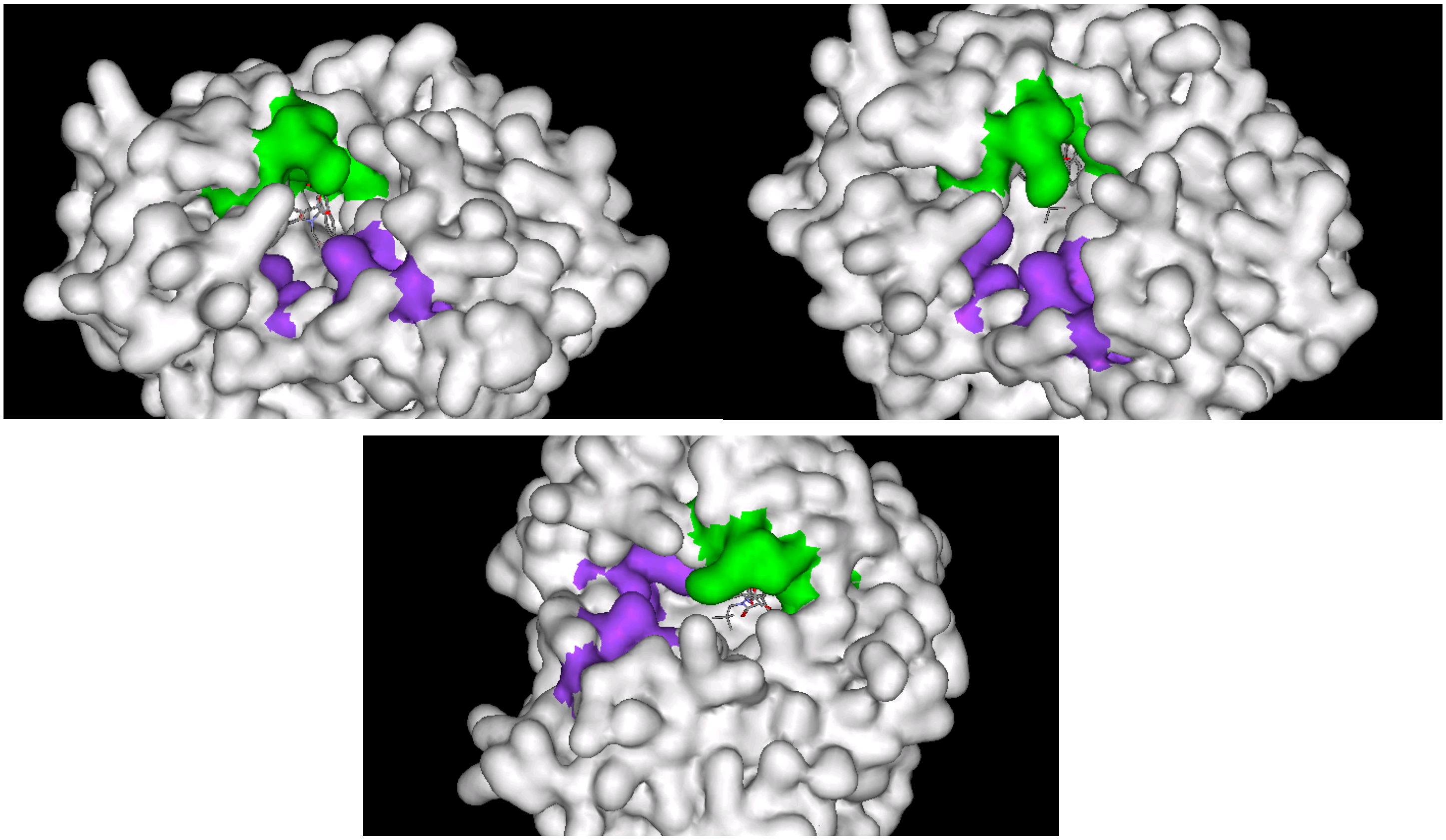

Figure 3.5. CP-420472 bound by Squalene Synthase. Three different views of the 1st half and 2nd half reaction site regions colored in purple and green respectively.

Figure 3.6 shows the interior of the binding channel (colored yellow) and its dimensions. The residues involved in the first half reaction (80-84 and 219-223, residues colored purple) cover a vertical distance of 9 Angstroms. Those in the second half reaction (51-54 colored in green) having a distance between the two sets of residues (80-84 and 219-223) is 8 Angstroms. The distance from the second half reaction site (under the flap) to the end of the channel is 16 Angstroms.

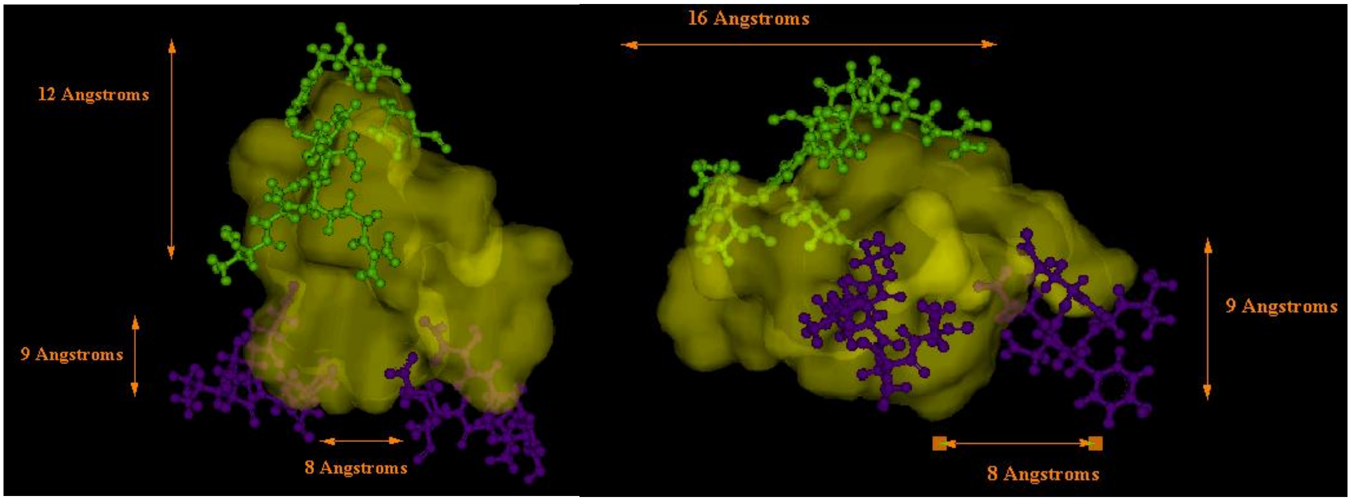

Figure 3.6. Active site channel from two different perspectives.

After understanding the binding site pocket of the human squalene synthase from several different perspectives, we pursued the docking of the four bisabosqual natural products that lead to inhibition of the protein. These studies are intended to lay the groundwork for the rational design of novel analogs that would be tested for improved inhibitory activity and give insight into a proposed mapping of the mechanism movement in the pocket.

3.3 Structural Results and Discussion of Bisabosqual A-D and CP-320-473

Before docking the bisabosquals into the binding site of human squalene synthase, we validated the computation protocol for this protein. This is done by taking a free ligand and docking it into its protein binding site, then comparing it with the experimentally observed protein binding site. Usually, the experimental data comes from X-ray structures found in the PDB. A prediction is generally found acceptable if the RMSD value between the docked ligand and the experimentally determined ligand is under 2.0 Å.[26]

The modeling result for docking CP-320473 into the binding site of human squalene synthase was virtually identical to the crystal structure 1EZF. These results demonstrate the high accuracy of the Discovery Studio protocol with the protein receptor as shown in Figure 3.8. RMSD (all atom) = 1.27 Å, RMSD (heavy atom) =1.23 Å.

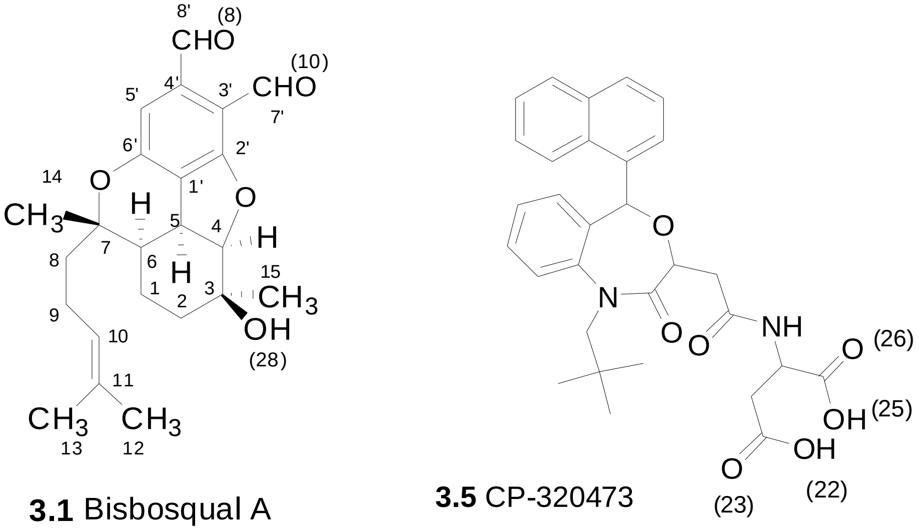

3.1 Bisbosqual A

3.5 CP-320473

Figure 3.7. Numbering systems for bisabosquals and for CP-320473

3.3.1 Validation Data CP-320473

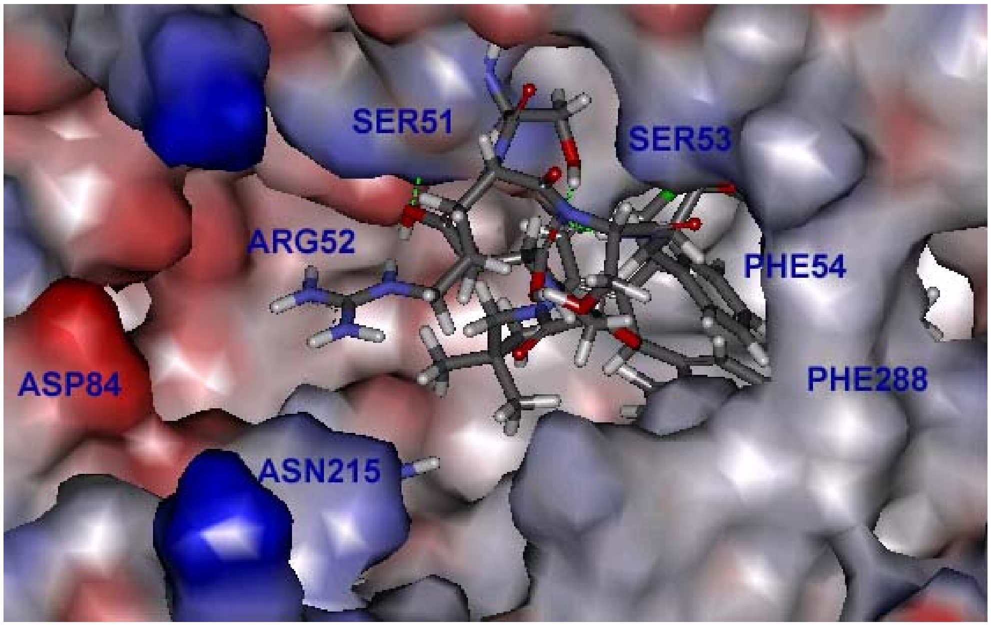
SER51
SER53
ARG52
PHE54
ASP84
PHE288
ASN215

Figure 3.8. Images of the docked ligand CP-320473 in the active site with neighboring residues. The protein surface area is rendered to show the electrostatic potential. The top image shows the flap as stick residues (51-54) whereas the bottom image shows the flap removed from the surface area.

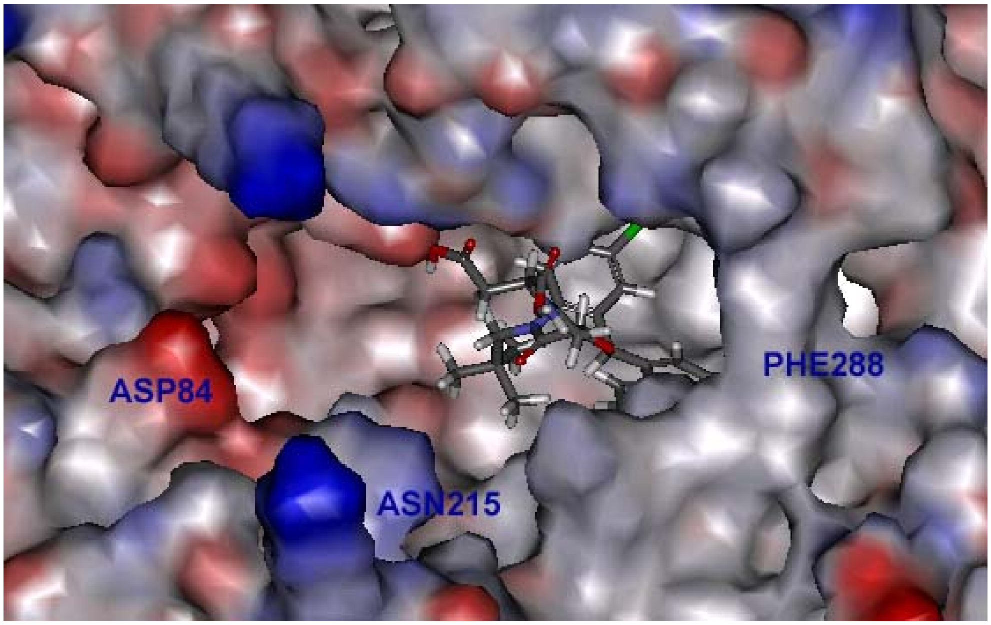
ASP84
PHE288
ASN215

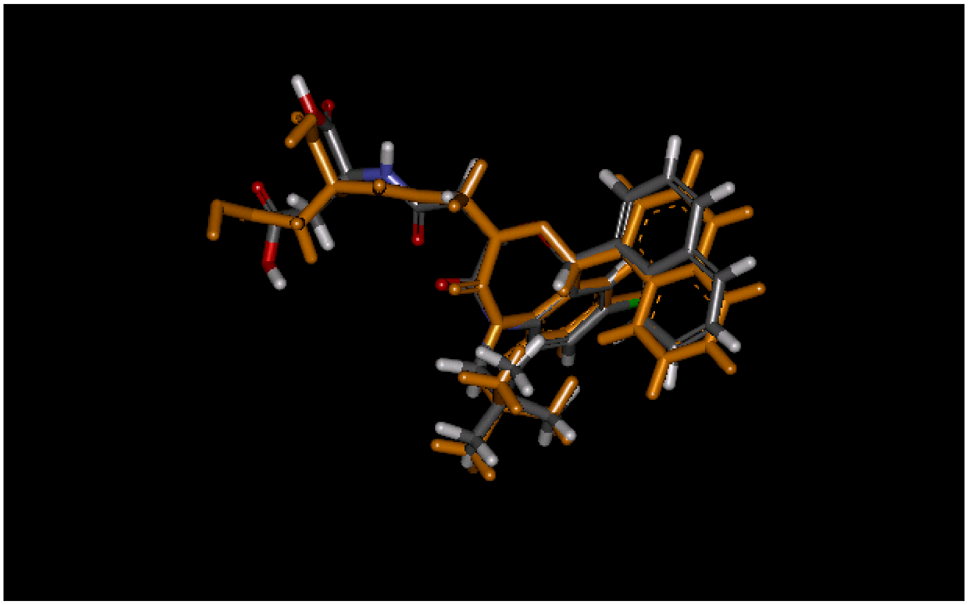

Figure 3.9. Superimposed on the image of CP-320473 is the structure of the docked ligand (orange). The position of the docked ligand is virtually identical to that of the ligand in the x-ray crystal structure from 1EZF. RMSD (all atom) = 1.27 Å, RMSD (heavy atom) =1.23 Å.

These results demonstrated the high accuracy of the CDOCKER protocol with the protein receptor. Docking of all bisabosqual compounds proceeded after this validation.

3.3.2 Bisabosqual A Data

Docking of bisabosqual A with the validated protocol (described in Experimental Section) placed it in the region recognized to be the binding site for the second half reaction of SQS, i.e. under the flap formed by residues Arg-52, Ser-53, and Phe-54; see Figure 3.10. In Figure 3.11, the flap has been removed so that one can see interactions of bisabosqual A with the floor and walls of the binding cavity. Figure 3.12 shows bisabosqual A surrounded by amino acid residues with which it has interactions.

In the docked structure, both the C7’ and C8’ aldehydes are heavily hydrogen bonded by the conserved residues (51-54) in the flap. The tertiary alcohol has strong hydrogen bonding with Asn 215. Unlike CP-320743, which has pi-stacking with Phe 54 and Tyr 73, bisabosqual A sits too far from these residues to display interactions with them.

Bisabosqual A sits closer to the arginine rich region assigned to the first half reaction than does CP-320743.

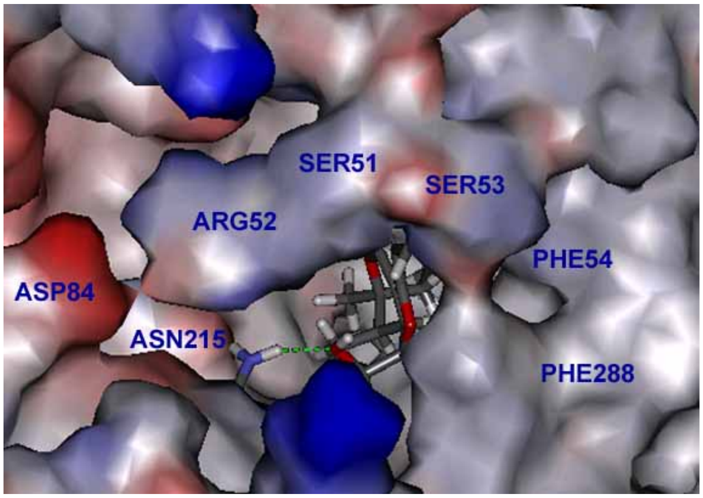
SER51
SER53
ARG52
PHE54
ASP84
ASN215
PHE288

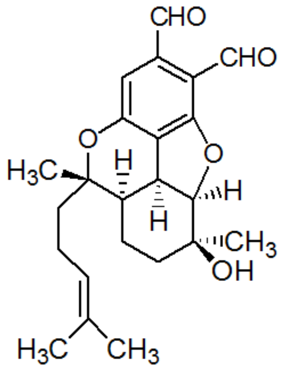
CHO
CHO
O
O
H
H
H
H_3C
CH_3
OH
H_3C
CH_3

3.1 Bisbosqual A

Figure 3.10. Bisabosqual A docked in human SQS. The dotted green lines represent hydrogen bonds. The image on the left shows the protein surface, rendered to display the electrostatic potential, with positions of conserved residues Ser-51, Arg-52, Ser-53, Phe-54, Asp-84, Asn215, and Phe288. In the right image, the original structure is shown.

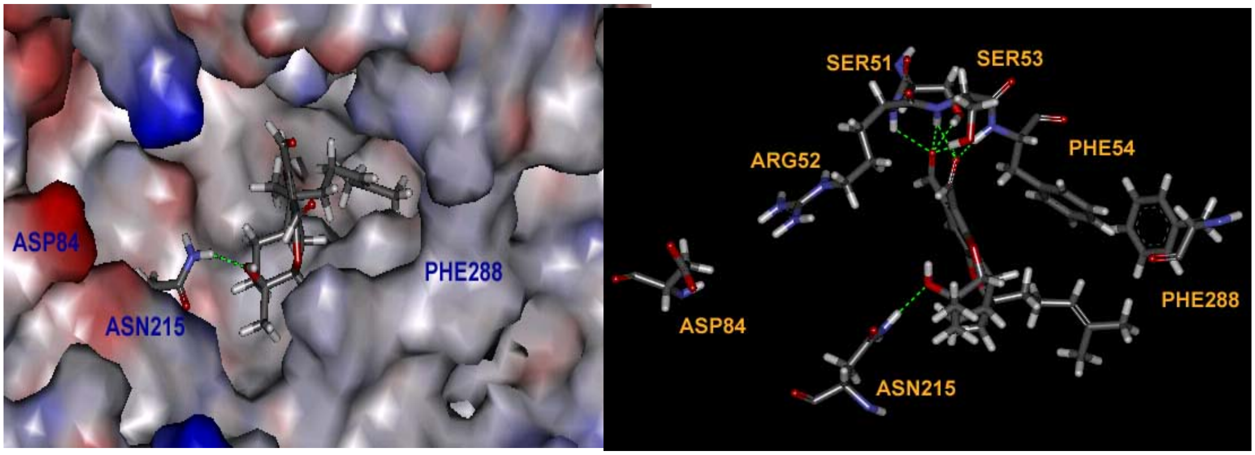
ASP84
ASN215
PHE288
SER51
SER53
ARG52
PHE54
PHE288
ASP84
ASN215

Figure 3.11. Bisabosqual A docked in human SQS. The image on the left shows the protein surface without the flap. The image on the right shows bisabosqual with the nearest neighbor residues.

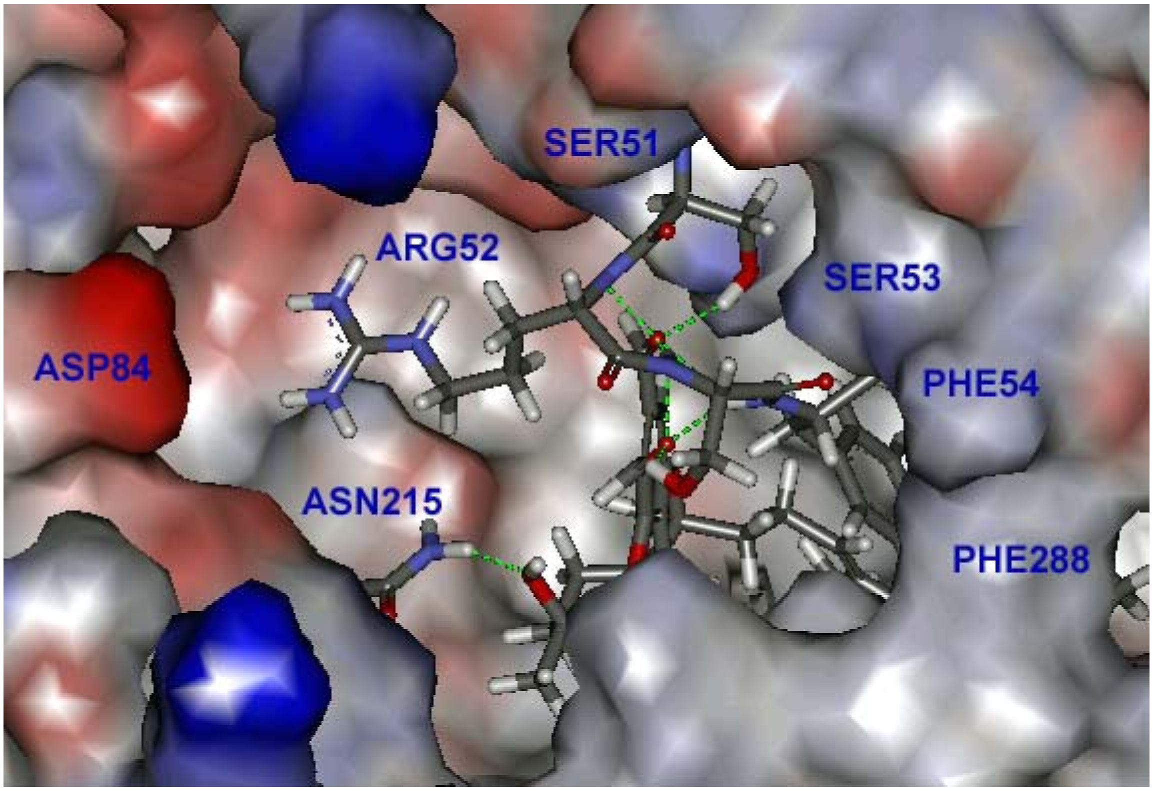

Figure 3.12. Bisabosqual A in the binding pocket site with the conserved residues shown as stick figures with the rest of the protein rendered as an electrostatic potential surface.

3.3.3 Bisabosqual B Data

The docked complex of bisabosqual B and squalene synthase is shown in Figure 3.13. The benzylic alcohol is encased in hydrogen bonding with Ser-51, Ser-53 and Phe-54. The C-7’ aldehyde has hydrogen bonding with Ser-53. Bisabosqual B sits farther from first half reaction site than does bisabosqual A and does not have a binding interaction with Arg 52.

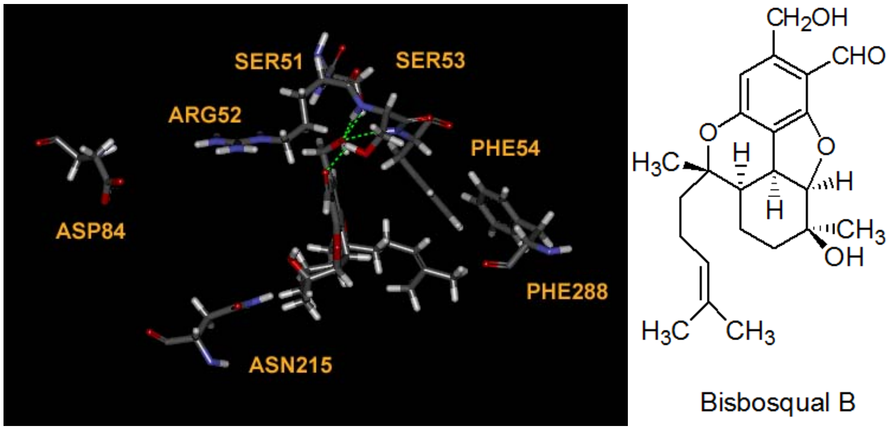
SER51
SER53
ARG52
PHE54
ASP84
PHE288
ASN215
CH2OH
CHO
O
H3C
H
O
H
H
CH3
OH
H3C
CH3
Bisbosqual B

Figure 3.13 Bisabosqual B with its neighboring residues in the active site.

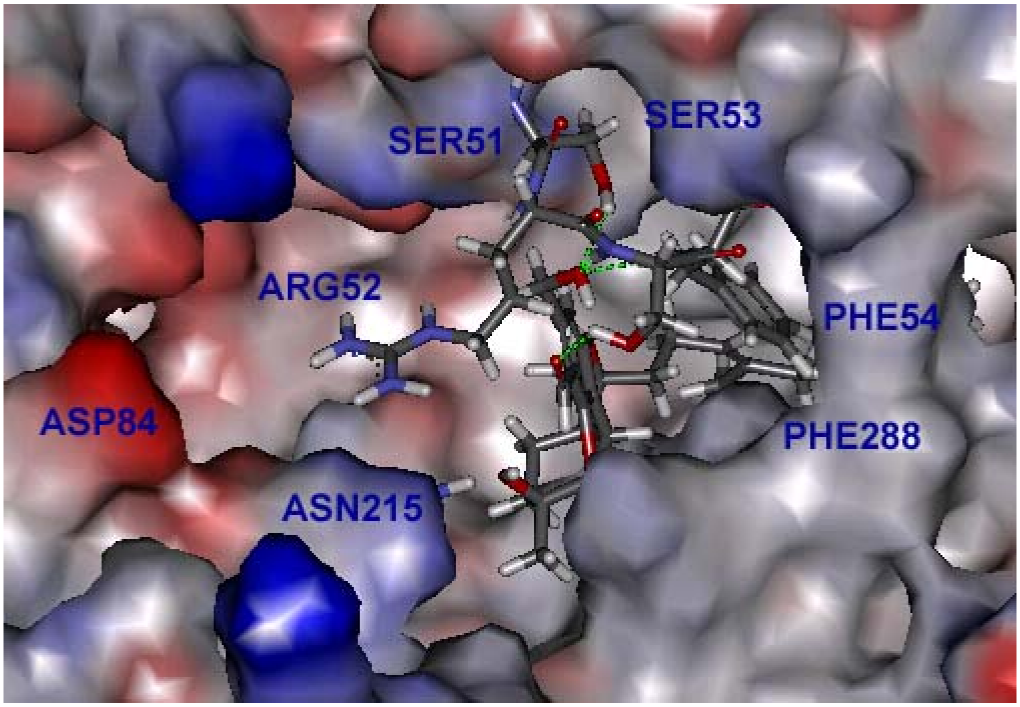
SER51
SER53
ARG52
PHE54
ASP84
PHE288
ASN215

Figure 3.14. Image of docked Bisabosqual B shown in the active site with neighboring residues. The protein surface area is rendered showing the electrostatic potential. The key hydrogen bonding interactions are labeled in dotted green lines. In the image, the conserved "flap" is displayed as stick residues.

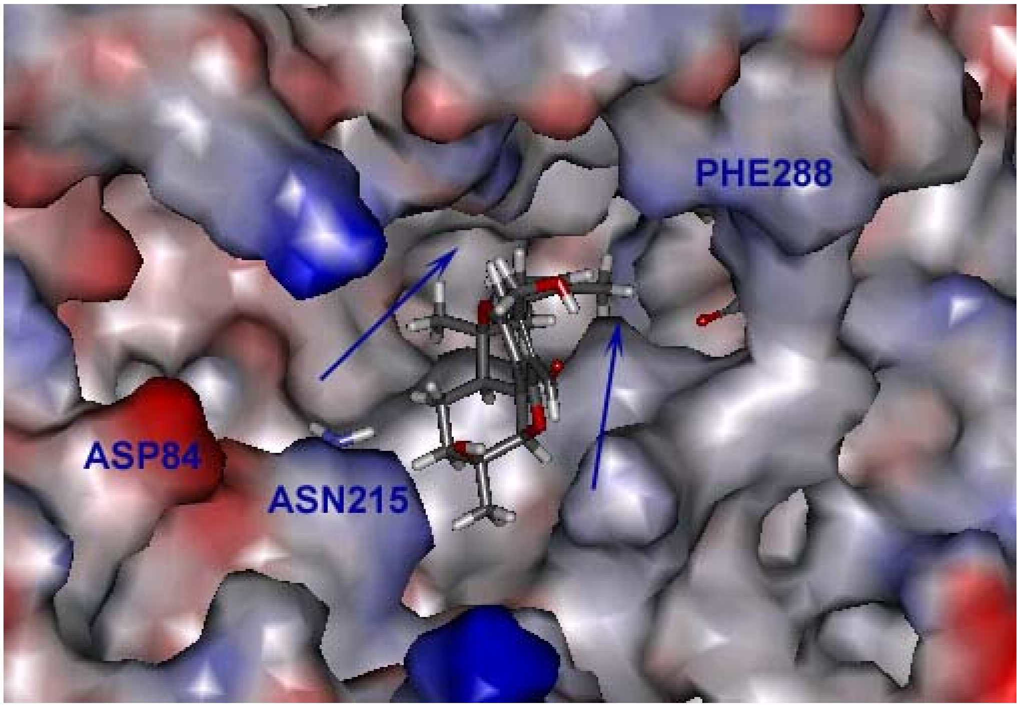
PHE288
ASP84
ASN215

Figure 3.15. Image of docked Bisabosqual B shown in the active site with neighboring residues. The protein surface area is rendered showing the electrostatic potential. The “flap” has been removed; the arrows point to the closed hydrophobic terminus of the channel.

3.3.4 Bisabosqual C Data

The docked structure of bisabosqual C is shown in Figure 3.16 and 3.17. Like bisabosqual A, bisabosqual C shows heavy hydrogen bonding of both C8’ and C7’ aldehyde groups with residues 51-54 and of the C3 tertiary hydroxyl group with Asn 215.

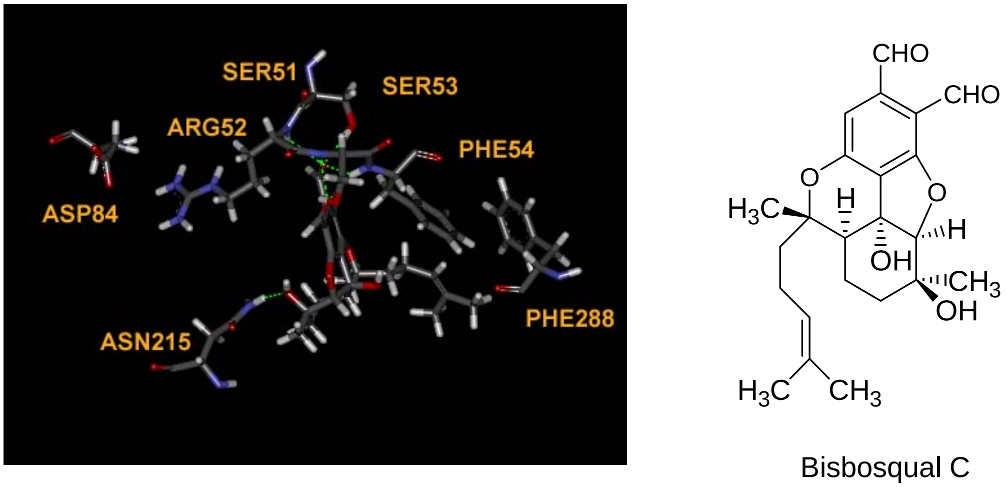
SER51
SER53
ARG52
PHE54
ASP84
PHE288
ASN215
CHO
CHO
O
O
H
H
OH
H3C
CH3
OH
H3C
CH3

Bisbosqual C

Figure 3.16. Bisabosqual C with its neighboring residues in the active site.

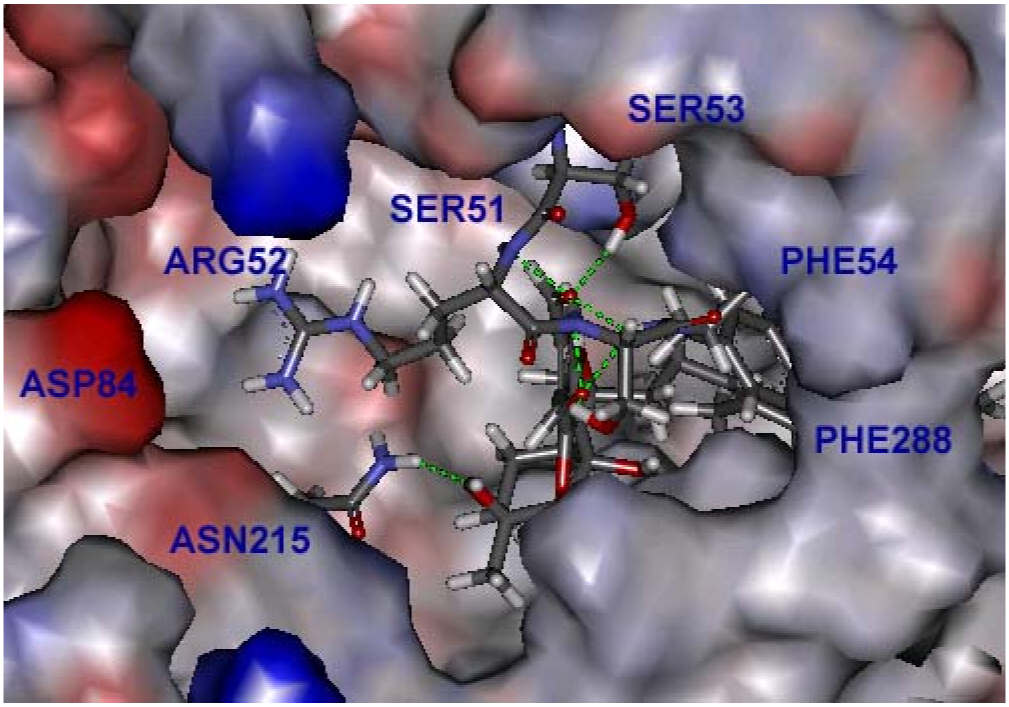
SER53
SER51
ARG52
PHE54
ASP84
PHE288
ASN215

Figure 3.17. Image of docked Bisabosqual C shown in the binding site with neighboring residues. The protein surface area is rendered showing the electrostatic potential. The key hydrogen bonding interactions are labeled in dotted green lines. The conserved active site “flap” is displayed as stick residues. The arrow points to the closed hydrophobic terminus of the channel.

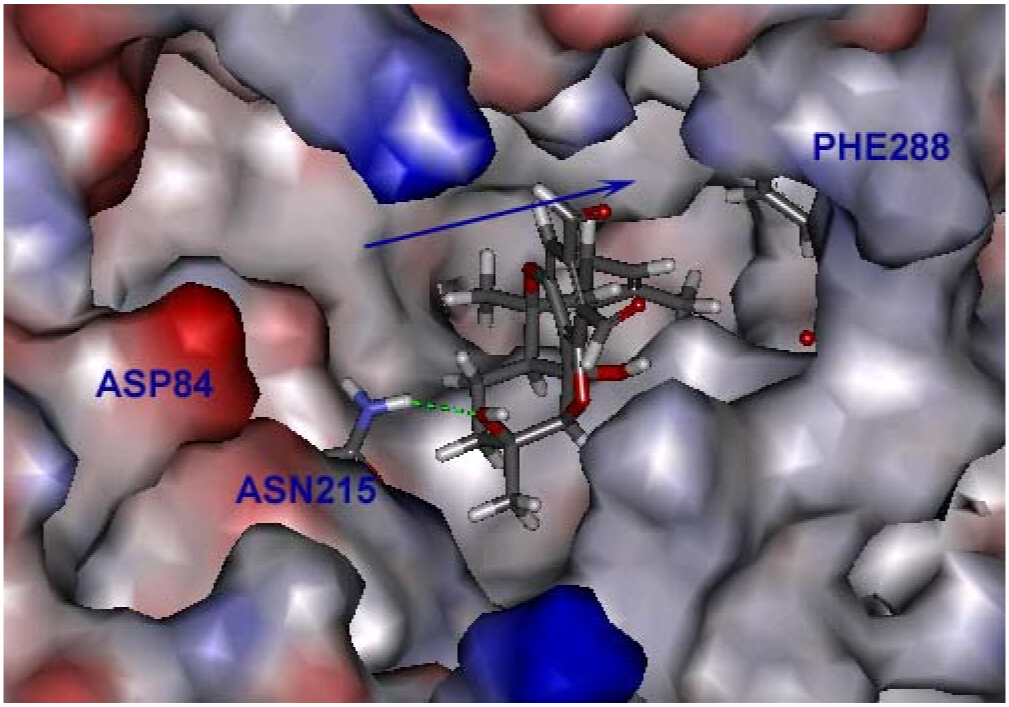
PHE288
ASP84
ASN215

3.3.5 Bisabosqual D Data

The docking studies with bisabosqual D show that the only hydrogen bonding apparent is between the C8’and C7’ aldehydes with the conserved residues (51-54) in the flap. The side chain of bisabosqual D, unlike that of the other bisabosquals, has no pi stacking with Phe 288 and Tyr 73 in the hydrophobic channel.

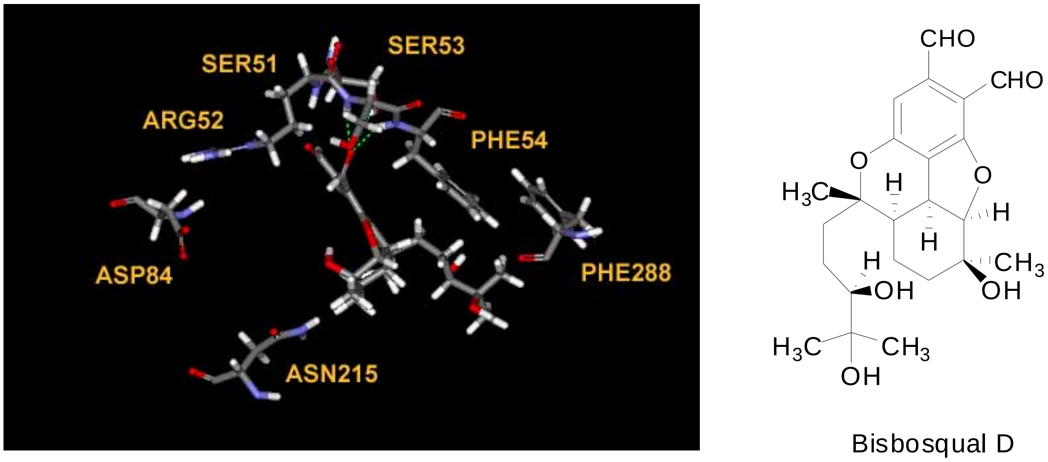
SER51
SER53
ARG52
PHE54
ASP84
PHE288
ASN215
CHO
CHO
O
O
H_3C
H
H
H
H
CH_3
OH
OH
H_3C
CH_3
OH

Bisbosqual D

Figure 3.18. Bisabosqual D with its neighboring residues in the active site.

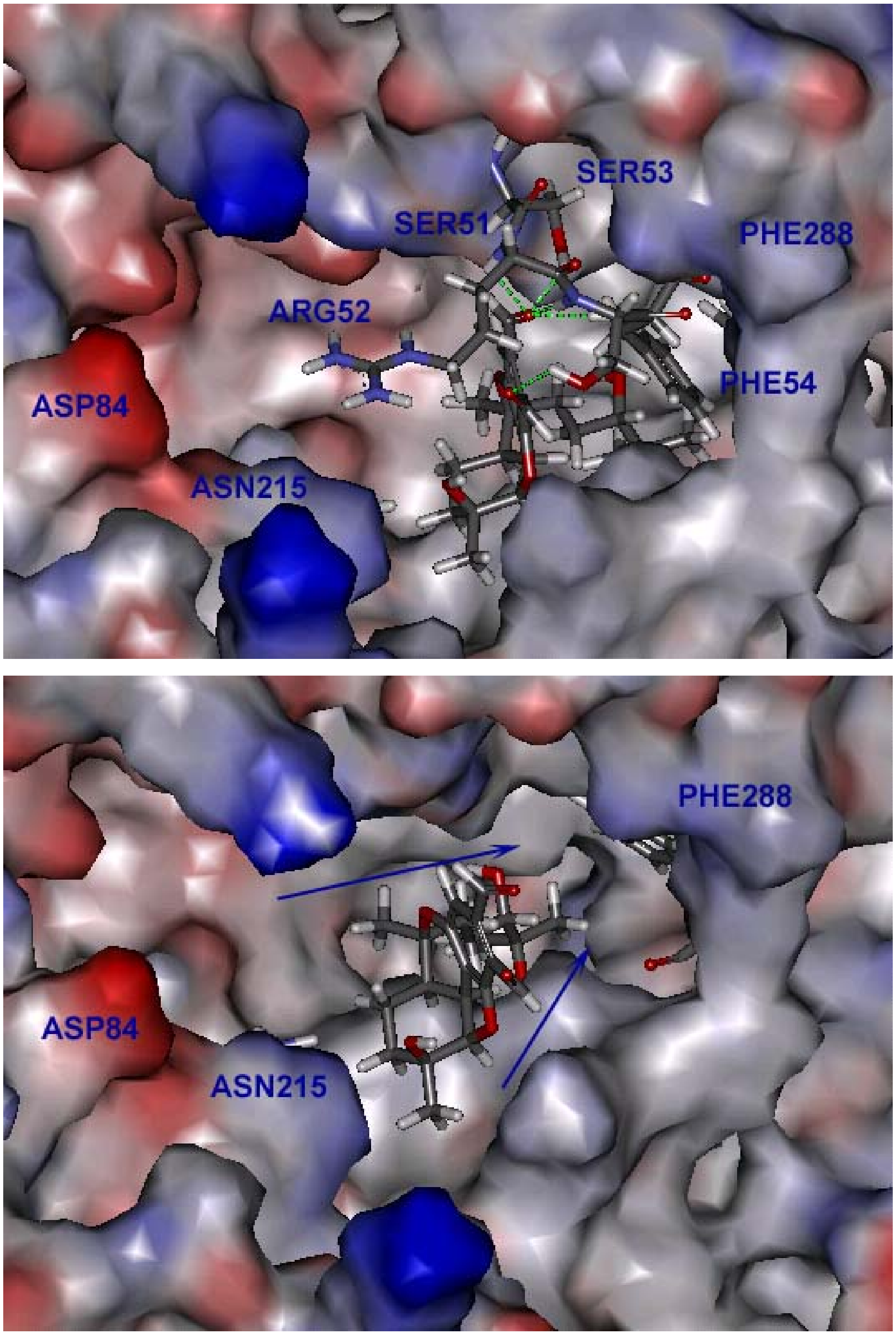
SER53
SER51
PHE288
ARG52
PHE54
ASP84
ASN215
PHE288
ASP84
ASN215

Figure 3.19. Image of docked Bisabosqual D shown in the active site with neighboring residues. The protein surface area is rendered showing the electrostatic potential. The key hydrogen bonding interactions are labeled in dotted green lines. The conserved active site "flap" is displayed as stick residues. In the bottom image, the "flap" has been removed; the arrows point to the closed hydrophobic terminus of the channel.

The four bisabosquals showed good binding affinity to the second half reaction site. Energy analysis reveals that affinity is driven primarily by favorable hydrogen bonding interactions.

3.4 Correlation of Binding Energies with IC_{50} values for Squalene Synthases

Accurate scoring of docked ligand poses remains a general problem in the field of structure-based design. Rigorous methods, such as free energy perturbation, for calculating the binding affinity of a ligand to a receptor are too computationally expensive for practical use. We used physics-based methods to estimate the binding energies.

The MM-GBSW (Molecular Mechanics Generalized Born with a Simple Switching Function) energy analysis[27] was used to estimate binding free energies for the four bisabosquals with human squalene synthase. The table below shows the experimental IC_{50} data made available by Mingawa.

Table 3.1. Inhibitory activities of bisabosquals A, B, C and D against squalene synthases

Compound	IC_{50} (ug/ml)			
	SC	CA	HepG2	Rat liver
Bisabosqual A	0.43	0.25	0.95	2.5
Bisabosqual B	31.5	50	12	>100
Bisabosqual C	1.0	1.0	0.9	5.8
Bisabosqual D	18.5	12	5.1	37

CA = ***Candida albicans*** is a diploid fungus (a form of yeast),
SC = ***Saccharomyces cerevisiae*** is a species of budding yeast.
Hep G2 = (Hepatocellular carcinoma, human) Hep G2 is a perpetual cell line which was derived from liver tissue.

In order to compare the results of the molecular modeling study with measured enzyme inhibitory activities, we constructed a linear free energy correlation for the four bisabosqual natural products. The best models were selected on the basis of CDOCKER[28] energies and Ludi scoring functions.[29] Table 3.2 shows our results.

Table 3.2. IC_{50} values for Bisabosqual A-D in the Hep G2 assay[9], the three scoring functions, and calculated binding energies[30].

Bisabosqual	A	B	C	D	CP-320473
pIC_{50}	5.6066	4.5074	5.647	4.9221	7.2518
CDOCKER_Energy	11.407	17.855	16.245	2.027	-60.548
CDocker_Interaction Energy	-62.151	-48.072	-62.103	-54.633	-74.687
Ludi Score Estimate 3	833	573	876	730	686
MM-PBSA Binding Energy (kcal/mol)	-39.791	-13.583	-31.685	-14.629	-52.109
MM-GBSW Binding Energy (kcal/mol)	-47.092	-26.495	-47.843	-27.151	-60.620

3.4.1 Binding Energy Correlations for MM-GBSW and MM-PBSA with IC_{50} Data

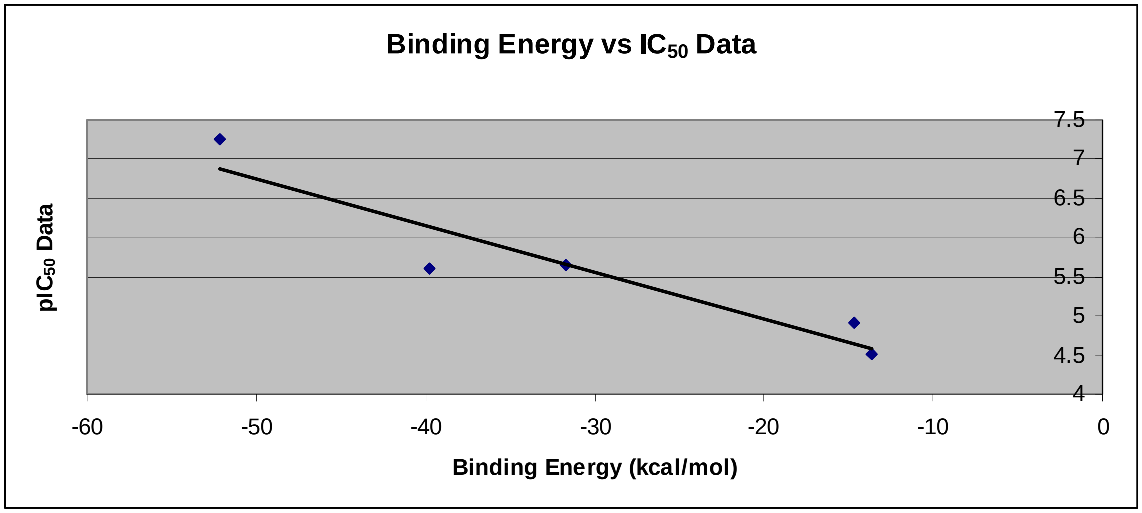

Figure 3.20. Correlation between MM-PBSA calculated binding energy and experimental IC_{50} data for Squalene Synthase. $pIC_{50}=-\log_{10}([IC_{50}\,M])$.Correlation coefficient squared = .88

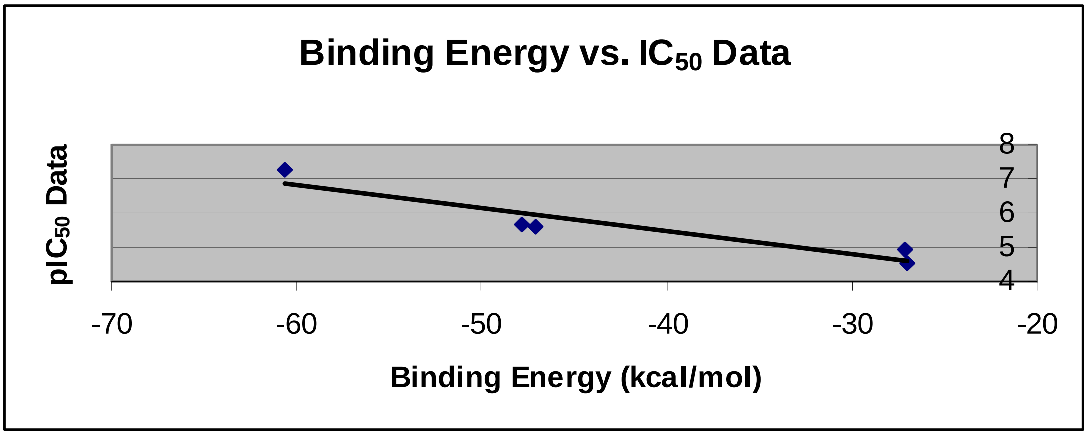

Figure 3.21. Correlation between MM-GBSW calculated binding energy and experimental IC_{50} data for Squalene Synthase. $pIC_{50}=-\log_{10}([IC_{50}\,M])$.Correlation coefficient squared = .88.

The energy analysis results from MM-GBSW showed a good linear correalation between the experimental IC_{50} data and the binding energies calculated. The MM-PBSA[31] approach has become a popular method for calculating binding affinities as well. We calculated our docked structures using both approaches and find that correlations are similar and decent in comparison to the MM-GBSW approach. Our molecular modeling suggests the mode of inhibition of human squalene synthase by the bisabosqual. The different poses of the four natural products helped to describe the relative importance of interactions with key amino acid residues and the flexibility of the interior of the channel. This information was helpful in the design of bisabosqual analogs and other human squalene synthase inhibitors.

3.5 Analogs designed to be improved Squalene Synthase Inhibitors

After studying the binding site of human squalene synthase with bisabosqual, an investigation to rationally design bisabosqual analogs was performed. The isoprene unit was modified with several functional groups in order to obtain better binding affinity. Our initial approach started with elongating the isoprene unit in order to investigate if we can shift the bisabosquals from the second half reaction to the first half. We wanted to see how long and deep the hydrophobic channel cavity was and if we can get to the end of it or block it in some way. Hence we started our modeling of compounds **3.6** and **3.7**. The following compounds have been modeled in the active site pocket.

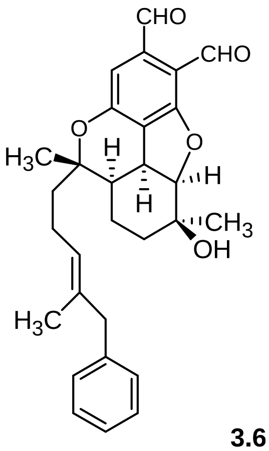

3.6

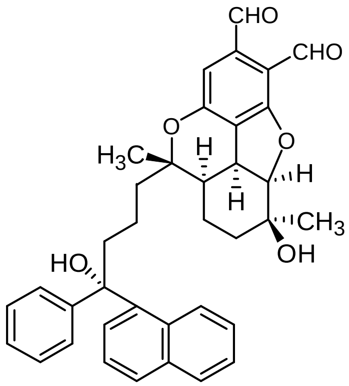

3.7

Figure 3.22. Structures of Bisabosqual Analogs 3.6 and 3.7

3.5.1 Compound 3.6 Data

The docking studies with compound **3.6** show that the only hydrogen bonding apparent is between the C8’and C7’ aldehydes with the conserved residues (51-54) in the flap. The chain elongation of the isoprene with a phenyl group resulted in the chain moving downward away from the hydrophobic channel as shown in Figure 3.23. We expected the hydrophobic channel inward to be filled. No visible pi stacking interactions are occurring with Phe54, Tyr 73, or Phe 288.

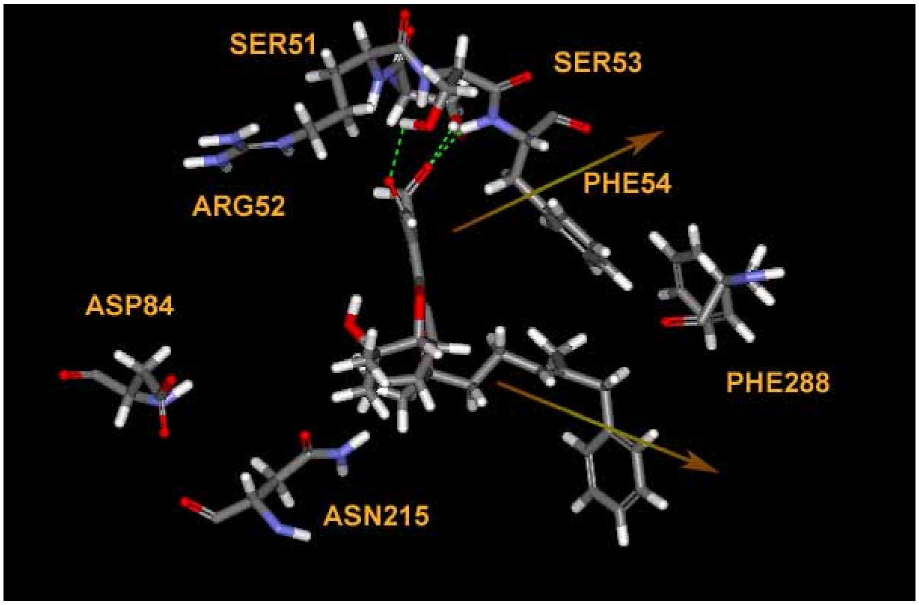

Figure 3.23. Compound 3.6 with its neighboring residues in the active site.

3.5.2 Compound 3.7 Data

In efforts to block the hydrophobic channel and shift bisabosqual toward the first half reaction site, compound **3.7** was designed and docked into the protein. The phenyl/naphthyl chain was expected to wrap around Phe288 to exhibit a “butterfly” or Y shape.

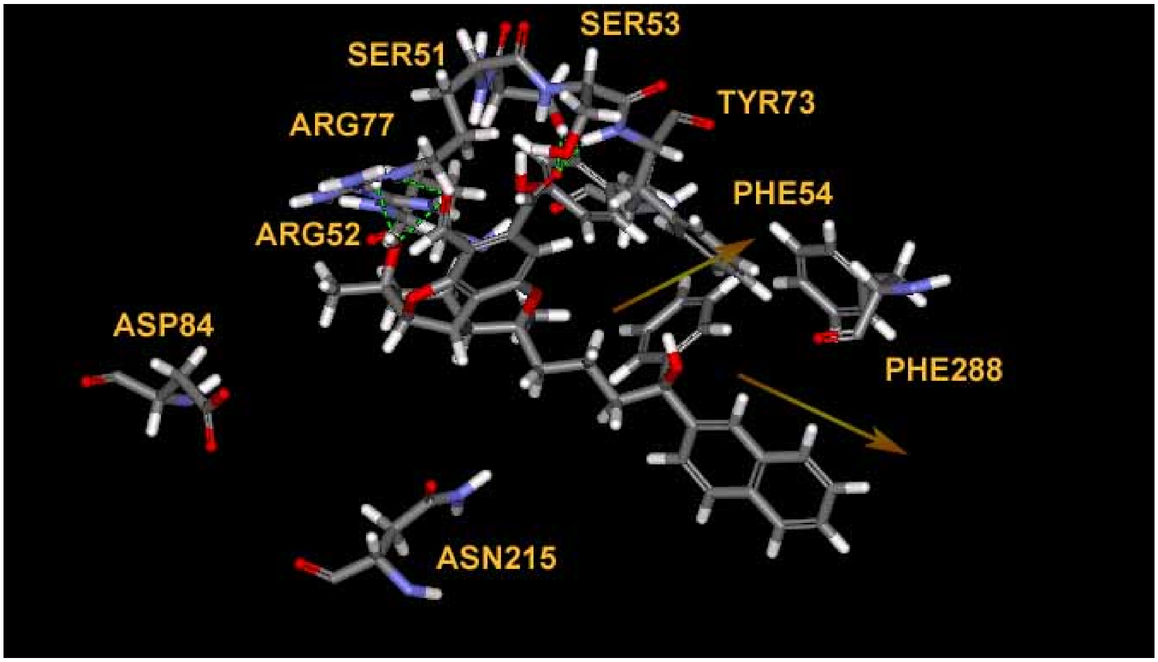

Figure 3.24. Compound 3.7 with its neighboring residues in the active site.

This aromatic system and chain elongation caused a shift towards the first half reaction instead of filling the channel still. New hydrogen bonding interactions are being observed with Arg77. It is believed that the aromatic groups are too bulky to enter the inward hydrophobic channel and alkyl chains would fit better.

3.5.3 Compounds 3.8-3.15 Data

After docking compounds **3.6** and **3.7**, we designed various compounds (**3.8 – 3.15**) of different less bulky groups hoping to mimic what we believe would be happening in the squalene synthase case. Ludi fragment scoring libraries were used to generate potential side chain advantages in the binding pocket of the protein. The following compounds designed and docked are shown below.

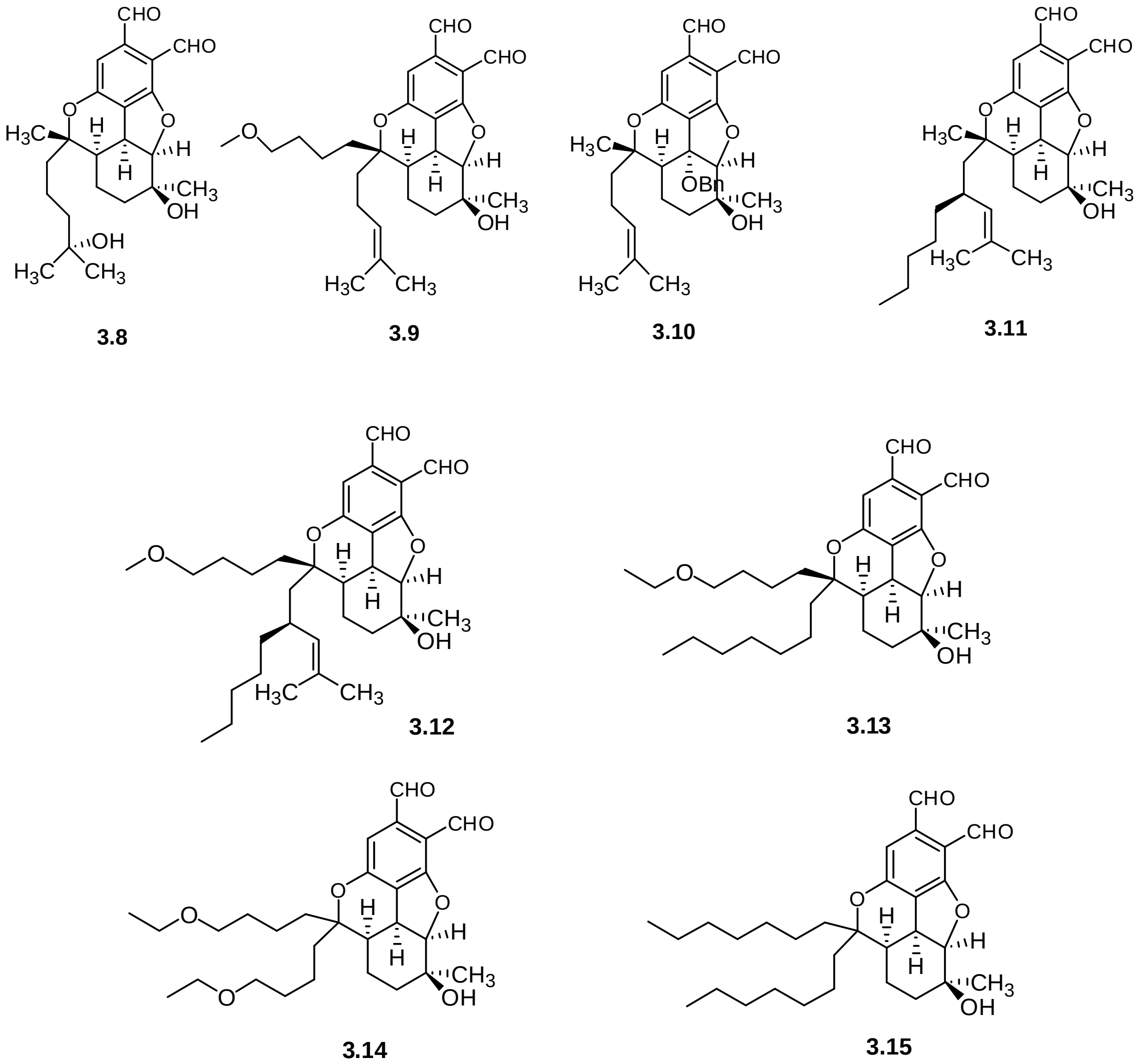

3.8 3.9 3.10 3.11

3.12 3.13

3.14 3.15

Figure 3.25. Rationally designed bisabosqual analogs 3.8-3.15.

The best docked structure for each compound is reported, visualized and superimposed on top of each other to show where the side chain ends up in the pocket.(Figure 3.26) After all the results were compiled, the binding energies were calculated to compare against bisabsquals A-D inhibitory activities. The known data was extrapolated for all the new compounds designed and is shown in Table 3.3.

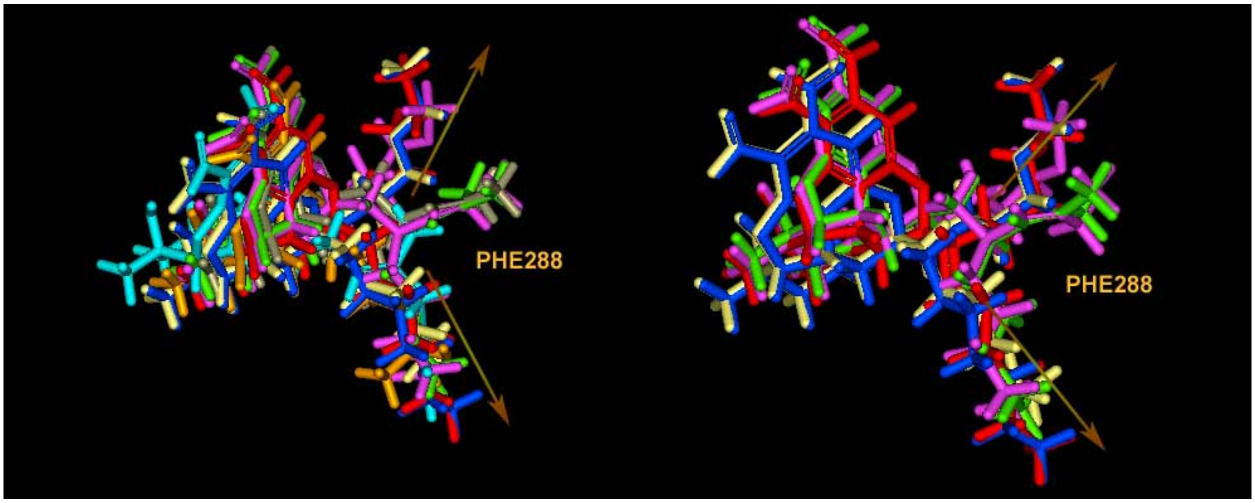

Figure 3.26. Compounds **3.8-3.15** superimposed with each compound color coded as follows. Compound **3.6** = cyan, **3.7** = purple, **3.8** =orange, **3.9** = gray, **3.11**= green, **3.12** =pink, **3.13** = blue , **3.14** = yellow, **3.15** = red. The image on the left shows compounds 3.8-3.15 while the image on the right shows compounds 3.11-3.15.

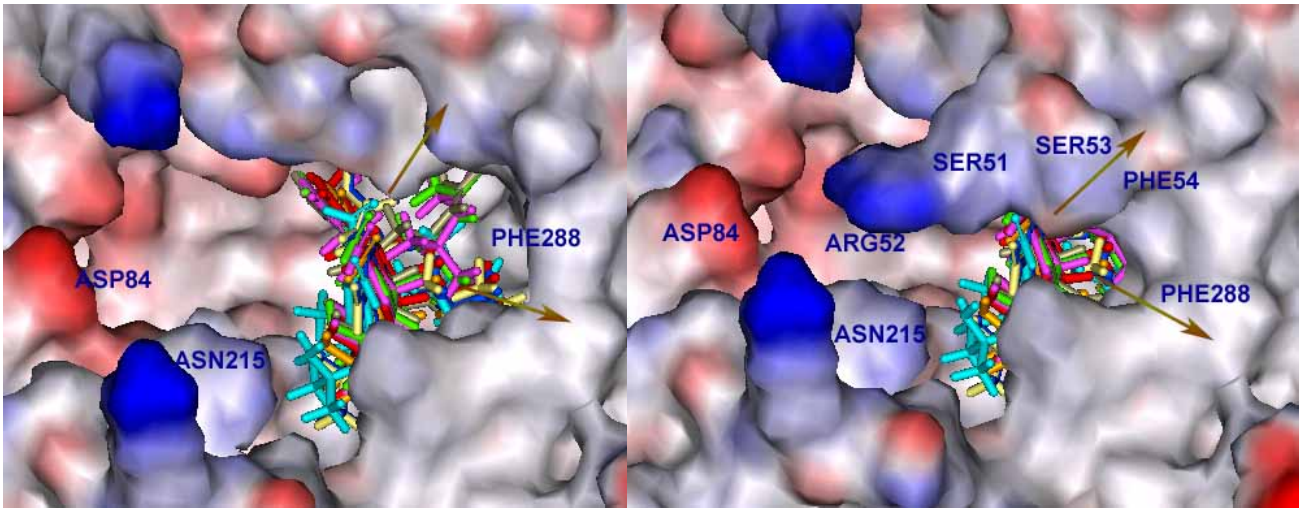

Figure 3.27. Compounds **3.8-3.15** superimposed with surface area generated without the flap (left image) and with the flap. (right image) Each compound color coded as follows. Compound **3.6** = cyan, **3.7** = purple, **3.8** =orange, **3.9** = gray, **3.11**= green, **3.12** =pink, **3.13** = blue , **3.14** = yellow, **3.15** = red.

Figure 3.27 shows the rendered electrostatic potential surface area of human squalene synthase for each compound. All the side chains are extending in the Y shaped hydrophobic pocket that is located adjacent under the second half reaction "flap." Initially, looking at compounds **3.8-3.13** in the pocket, we observe that certain side chains either sit inward or outward in the pocket. They give good suggestions on the volume of the depth of the hydrophobic pocket. However, compounds **3.8-3.13** are mostly unrealistic to synthesize and the isoprene unit in the natural bisabosquals A, B, and C are synthetically challenging already as well. For easier synthetic design, compounds **3.14** and **3.15** were rationally designed to eliminate the introduction of the chiral side chain.

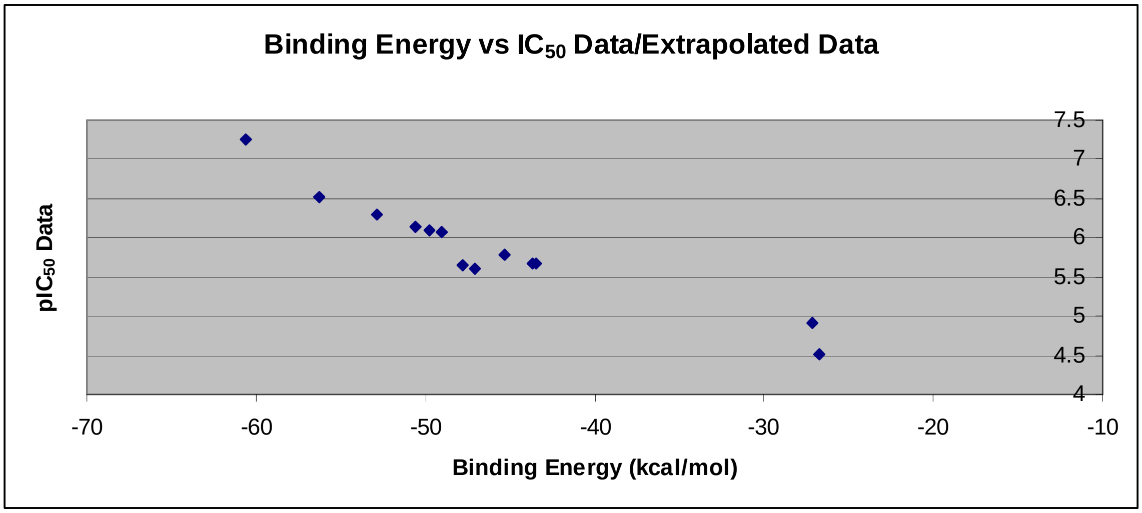

Figure 3.28. Correlation between MM-GBSW calculated binding energy and experimental IC$_{50}$ data for Squalene Synthase with the extrapolated data for compounds **3.6-3.15**. pIC$_{50}$=-log$_{10}$([IC$_{50}$ M]).

Compound	pIC$_{50}$	CDOCKER Energy	CDocker Interaction Energy	Ludi Score 1	Ludi Score 2	Ludi Score 3	Binding Energy (PBSA) (kcal/mol)	Binding Energy (GBSW) (kcal/mol)
3.1	5.6066	11.407	-62.151	892	731	833	-39.791	-47.092
3.2	4.5074	17.855	-48.072	634	524	573	-13.583	-26.694
3.3	5.647	16.245	-62.103	926	716	876	-31.685	-47.843
3.4	4.9221	2.027	-54.633	615	516	730	-14.629	-27.151
3.5	7.2518	-60.548	-74.6871	693	590	686	-52.109	-60.620
3.6	(5.670)	-16.995	-59.804	752	612	635	-21.694	-43.467
3.7	(5.681)	2.349	-64.192	655	578	759	-31.880	-43.624
3.8	(5.791)	-5.035	-54.694	655	531	752	-33.094	-45.275
3.9	(6.063)	14.763	-62.190	695	596	762	-31.067	-49.039
3.10	-------	--------------	------------	-------	-------	-------	-------------	-------------
3.11	(6.149)	12.086	-62.888	776	657	859	-36.227	-50.613
3.12	(6.525)	3.927	-72.804	787	659	855	-38.350	-56.231
3.13	(6.297)	-19.513	-67.825	724	617	709	-39.691	-52.818
3.14	(6.091)	-19.821	-66.970	722	600	741	-53.940	-49.749
3.15	(6.349)	-17.815	-67.616	754	610	753	-40.069	-53.599

Table 3.3. Compounds **3.6-3.15** were designed, not synthesized or tested. The data was extrapolated from the known tested inhibitory activity. Compound **3.10** failed to be docked in the active site.

The binding energies were calculated and reported in the linear correlation plot shown by Figure 3.28 and Table 3.3 for the compounds **3.6 -3.15**. We extrapolated the data points from the correlation for insight into their potential activity. The binding energies of MM-GBSW and MM-PBSA quantified the effects of different side chain analogs. This linear relationship correlated with the data of the four natural bisabosqual compounds. Aside from compound **3.10**, which failed to dock in the pocket, the binding affinity in general for the designed structures were better than bisabosqual A-D. Although compounds **3.14** and **3.15** were not found to have to have the best binding energy in the table, synthetically they are excellent candidates to pursue.

3.5.4 Overlay of Bisabosqual A to Presqualene

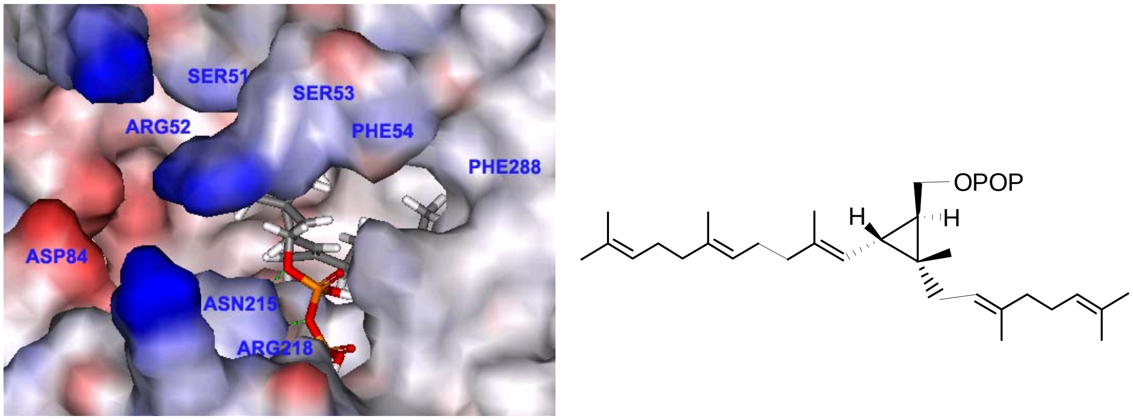
SER51
SER53
ARG52
PHE54
PHE288
ASP84
ASN215
ARG218
OPOP
H
H

Figure 3.29. Presqualene overlayed with surface area rendered with the flap (left image) and structure of presqualene. (right image)

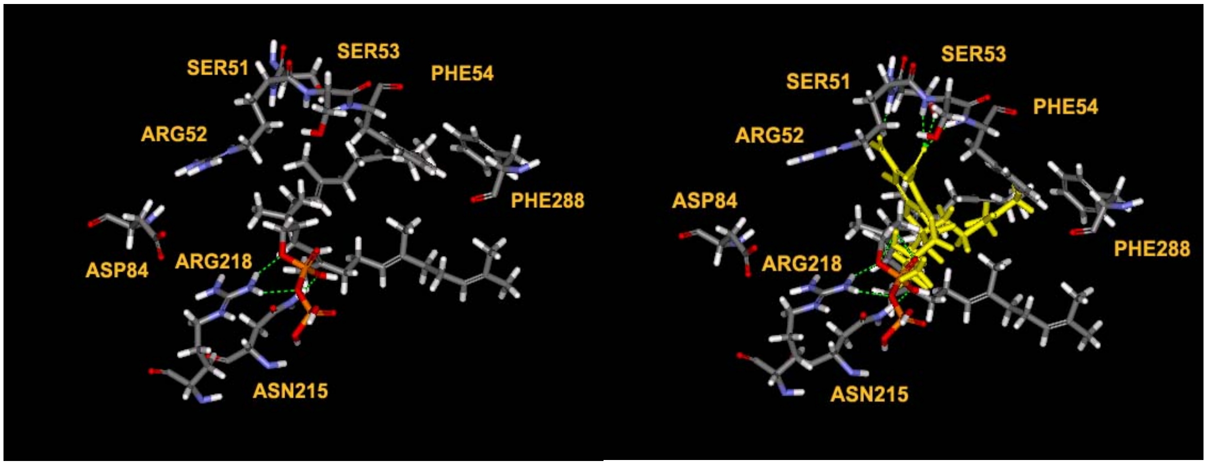
SER51
SER53
PHE54
ARG52
PHE288
ASP84
ARG218
ASN215
SER51
SER53
PHE54
ARG52
ASP84
PHE288
ARG218
ASN215

Figure 3.30. Presqualene overlayed with bisabosqual A (shown in yellow) with its neighboring residues in the active site.

Presqualene diphosphate, the intermediate between the first and second half reaction, was overlayed with bisabosqual A for final insight into the mode of inhibition in the binding site pocket. We propose that potentially the diphosphate binds to the arginine and asparagines in the second half reaction with cyclopropyl group under the flap with the shorter chain directed towards the inner hydrophobic pocket. Mechanisms for the conversion of presqualene to squalene have been suggested to undergo rearrangements based on cyclopropylcarbinyl cations. Shielding of water or solvent by the flap would prevent these highly reactive carbocations from being prematurely quenched.

The longer chain extends far into the hydrophobic pocket of the second half reaction site. (Figure 3.29) The overlay of bisabosqual A to presqualene diphosphate shows that the aldehydes bind in a different region to what was expected to the diphosphate of presqualene. The isoprene unit is similar in length and distance to hydrophobic pocket as is shown in Figure 3.30. This overlay could explain the potential inhibitory activity of squalene synthase with bisabosqual.

3.6 Conclusion

The results obtained in this study suggest the mode of inhibition of human squalene synthase by the bisabosqual. The different poses of the four natural products help to describe the relative importance of interactions with key amino acid residues and the flexibility of the interior of the channel. This information is helpful in the design of bisabosqual analogs and other human squalene synthase inhibitors. Our studies gave structural insights about the plausible binding modes for bisabosqual derivatives with the human squalene synthase.

3.7 Experimental Section

3.7.0 Materials and Methods – General Steps of the Docking Procedure

All docking was carried out in Discovery Studio 2.5.5 by Accelrys. The procedure[32] consisted of the following steps.

3.7.1 Preparation of the Ligand Structures -Preliminary Parameters

3.7.1.i Build Fragment tool

The 3D structures of the bisabosquals were built with the Build Fragment tool. For each, the geometry was optimized and checked for proper chirality. The sketching tool can be used manually to create the ligand or can be generated from adding or fusing fragments from a library. All ligands were minimized to an RMS gradient of .001.

3.7.2 Preparation of the Receptor -Prelimary Parameters

3.7.2.i Protein Report and Utilities tool

The crystal structure of human squalene synthase complexed with Pfizer's compound CP-320473 (pdb code 1EZF)[23] was retrieved from the Protein Data Bank. The protein file was prepared using the Clean Protein subtool. It corrected for incomplete residues, removes alternate conformations by retaining one set, capped termini, and added hydrogens to all of the amino acid residues. The inhibitor CP-320473 drug was removed from the structure file. All water molecules were removed. The CHARMm Forcefield was applied and the energy of the protein was minimized. Bond orders and formal charges were manually inspected.

3.7.3 Examination of Potential Binding Sites for the Bisabosquals

3.7.3.i Define and Edit Binding Site tool

The Binding Site tool can be used to search for potential binding regions of the bisabosquals. It defines region sites in a protein cavity where binding interactions can occur. For validation purposes, several sites were discovered and we identified the large interior channel as the only reasonable binding site for the bisabosquals. Since the binding site is already known from the x-crystal structure 1EZF, we defined specific coordinates from that structure. A sphere with a default radius of 15 Angstroms centered at the position of the CP-30473 molecule in the crystal structure 1EZF was generated. The ‘bulk’ of the receptor, defined as protein atoms outside the binding site sphere, was held rigid during the docking process while the protein and ligand atoms within the sphere were allowed to move.

3.7.4 De Novo Structure Generation

3.7.4.i Receptor-Ligand Interactions CDOCKER Protocol

The CDOCKER [33] protocol was used for de novo structure generation of the bisabosquals. The protocol docks ligands into an active site using CHARMm. CHARMm uses a molecular dynamics (MD) scheme to dock ligands into a receptor binding site. Random ligand conformations are generated using high-temperature MD. The conformations are then translated into the binding site. Candidate poses are then created using random rigid-body rotations followed by simulated annealing. A final minimization is then used to refine the ligand poses. The Dock Ligands (CDOCKER) docking protocol was used in Discovery Studio with the following parameters:

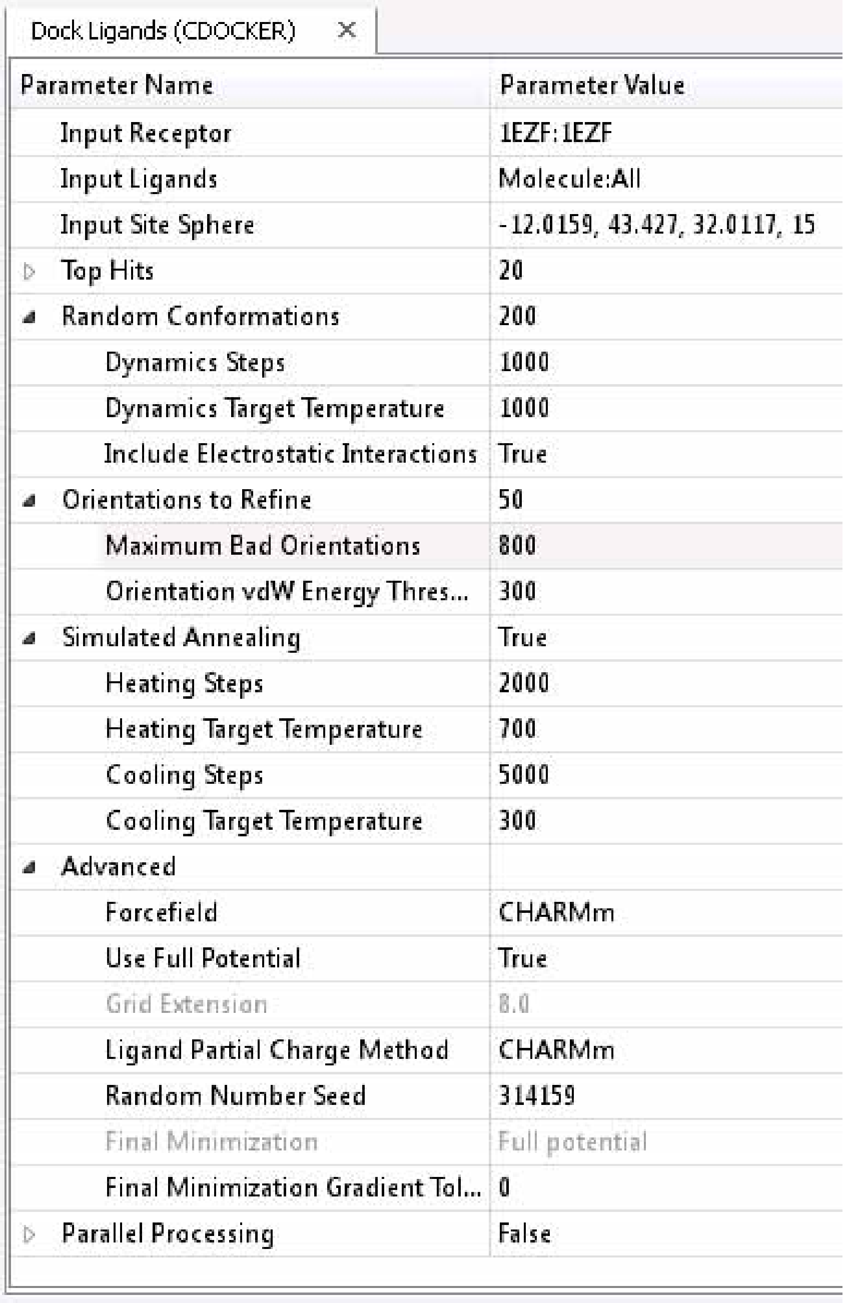

Dock Ligands (CDOCKER)

Parameter Name	Parameter Value
Input Receptor	1EZF:1EZF
Input Ligands	Molecule:All
Input Site Sphere	-12.0159, 43.427, 32.0117, 15
▷ Top Hits	20
◢ Random Conformations	200
Dynamics Steps	1000
Dynamics Target Temperature	1000
Include Electrostatic Interactions	True
◢ Orientations to Refine	50
Maximum Bad Orientations	800
Orientation vdW Energy Thres...	300
◢ Simulated Annealing	True
Heating Steps	2000
Heating Target Temperature	700
Cooling Steps	5000
Cooling Target Temperature	300
◢ Advanced	
Forcefield	CHARMm
Use Full Potential	True
Grid Extension	8.0
Ligand Partial Charge Method	CHARMm
Random Number Seed	314159
Final Minimization	Full potential
Final Minimization Gradient Tol...	0
▷ Parallel Processing	False

Figure 3.31. CDOCKER Parameter Values

The input ligand parameter value varied depending which bisaboqual compound was used in the run. The input site sphere always remained the same as a set value defined from the CP-320743. This value was the 3D (X, Y, Z, and radius) coordinates in space.

3.7.5 Scoring Ligands

3.7.5.i Score Ligand Poses protocol

This protocol was used to score ligands using a series of scoring functions (Ludi estimate 1, 2, and 3). The parameters are shown below.

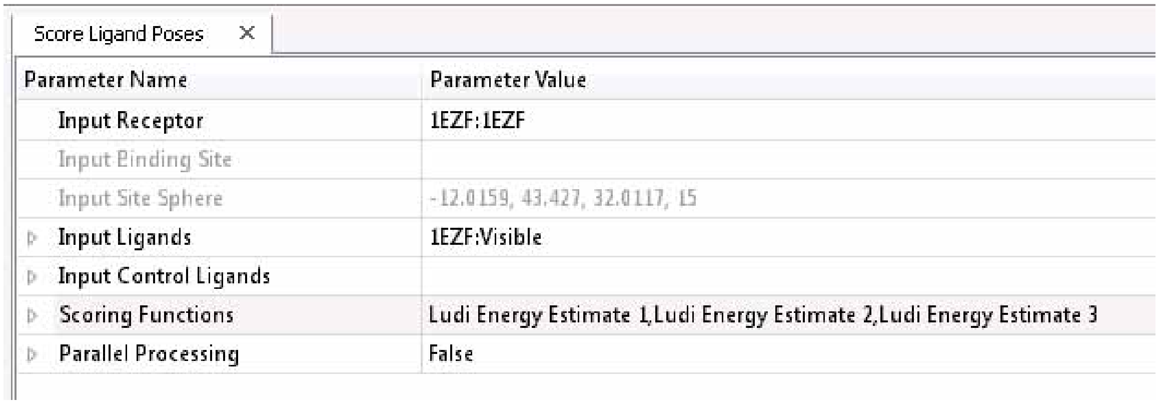

Parameter Name	Parameter Value
Input Receptor	1EZF:1EZF
Input Binding Site	
Input Site Sphere	-12.0159, 43.427, 32.0117, 15
Input Ligands	1EZF:Visible
Input Control Ligands	
Scoring Functions	Ludi Energy Estimate 1,Ludi Energy Estimate 2,Ludi Energy Estimate 3
Parallel Processing	False

Figure 3.32. Score Ligand Poses Parameter Values

The input ligand parameter value varied depending which bisaboqual compound was used in the run. The input site sphere always remained the same as a set value defined from the CP-320743. This value was the 3D (X, Y, Z, and radius) coordinates in space.

3.7.6 Analyzing Scored Ligands

3.7.6.i Analysis Protocol

The selections of the best poses were done on the basis of CDOCKER (Charmm) energies, CDOCKER interaction energies and from Ludi scoring functions (Ludi estimates 1, 2, and 3). These poses were minimized further in the presence of implicit solvent models.

3.7.7 Implicit Solvent Ligand Minimization

3.7.7.i Ligand Minimization Protocol

The protocol minimizes a series of ligand poses using CHARMm (customized to include Implicit Solvent Methods) v 1.1. Minimization is performed in the presence of the receptor (*in situ*) if *Input Receptor* is specified; otherwise they are minimized in a vacuum. For *in situ* minimization, the receptor is held rigid. However any residues with atoms inside *Minimization Sphere of Flexible Atoms*, or specified as *Flexible Residues* are allowed to move.

The Ligand Minimization protocol was used in Discovery Studio with the following parameters:

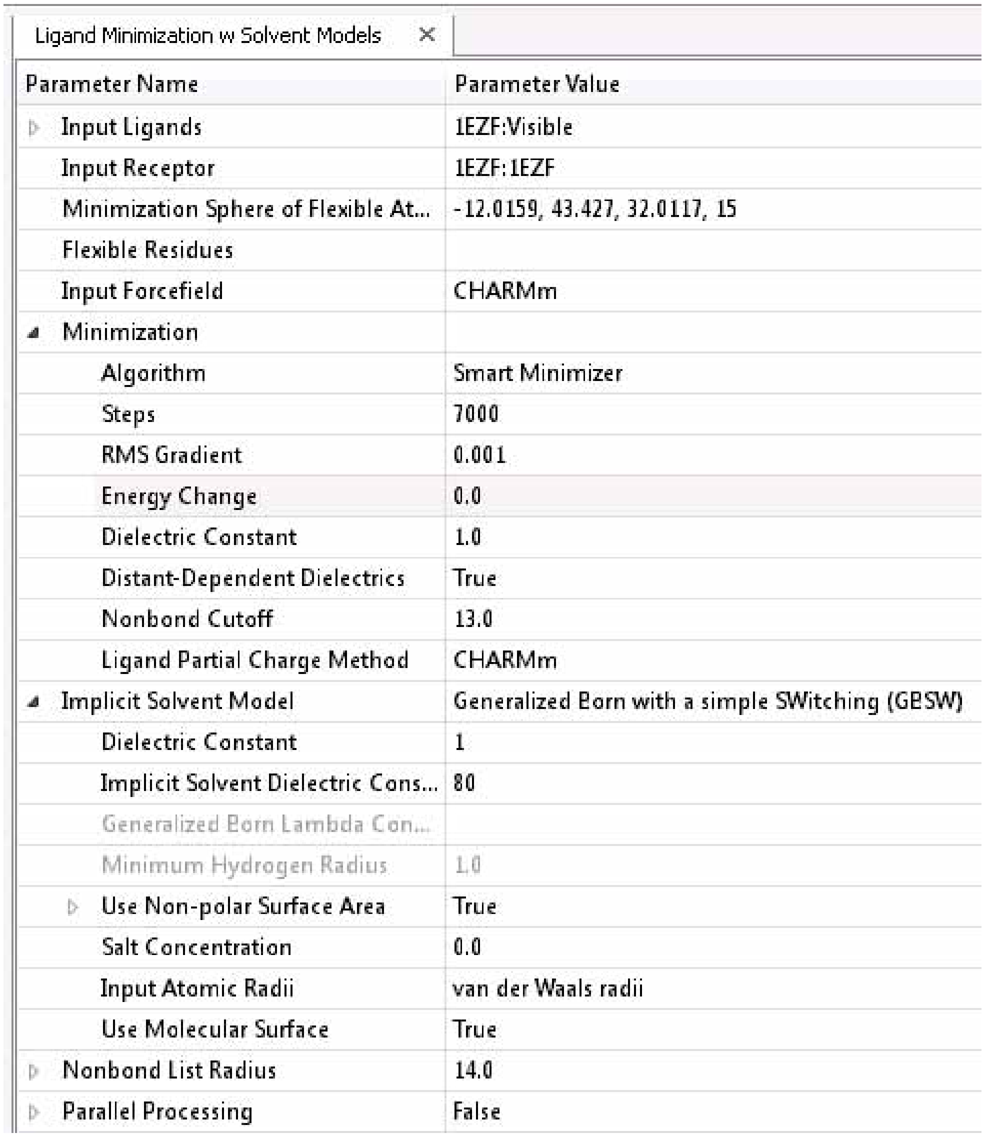

Parameter Name	Parameter Value
▷ Input Ligands	1EZF:Visible
Input Receptor	1EZF:1EZF
Minimization Sphere of Flexible At...	-12.0159, 43.427, 32.0117, 15
Flexible Residues	
Input Forcefield	CHARMm
◢ Minimization	
Algorithm	Smart Minimizer
Steps	7000
RMS Gradient	0.001
Energy Change	0.0
Dielectric Constant	1.0
Distant-Dependent Dielectrics	True
Nonbond Cutoff	13.0
Ligand Partial Charge Method	CHARMm
◢ Implicit Solvent Model	Generalized Born with a simple SWitching (GBSW)
Dielectric Constant	1
Implicit Solvent Dielectric Cons...	80
Generalized Born Lambda Con...	
Minimum Hydrogen Radius	1.0
▷ Use Non-polar Surface Area	True
Salt Concentration	0.0
Input Atomic Radii	van der Waals radii
Use Molecular Surface	True
▷ Nonbond List Radius	14.0
▷ Parallel Processing	False

Figure 3.33. Ligand Minimization with Solvent Models Parameter Values

The input receptor parameter value was the 1EZF protein and the input ligand parameter value varied depending which bisaboqual compound was used in the run.

3.7.8 Binding Energies of Ligands

3.7.8.i Calculate Binding Energy Protocol

The protocol estimates binding free energy using CHARMm implicit solvation models. The binding free energy is estimated between each ligand and the receptor. The free energy of binding for a receptor-ligand complex can be calculated from the free energies of the complex, the receptor, and the ligand. Using CHARMm based energies and implicit solvation methods it is possible to estimate these free energies and thus calculate an estimate for the overall binding free energy.

Optionally, an *in situ* ligand minimization step can be performed prior to the binding energy calculation. This was not performed. In addition, the loss in ligand conformational entropy can be estimated and was performed.

The Calculate Binding Energy protocol was used in Discovery Studio with the following parameters:

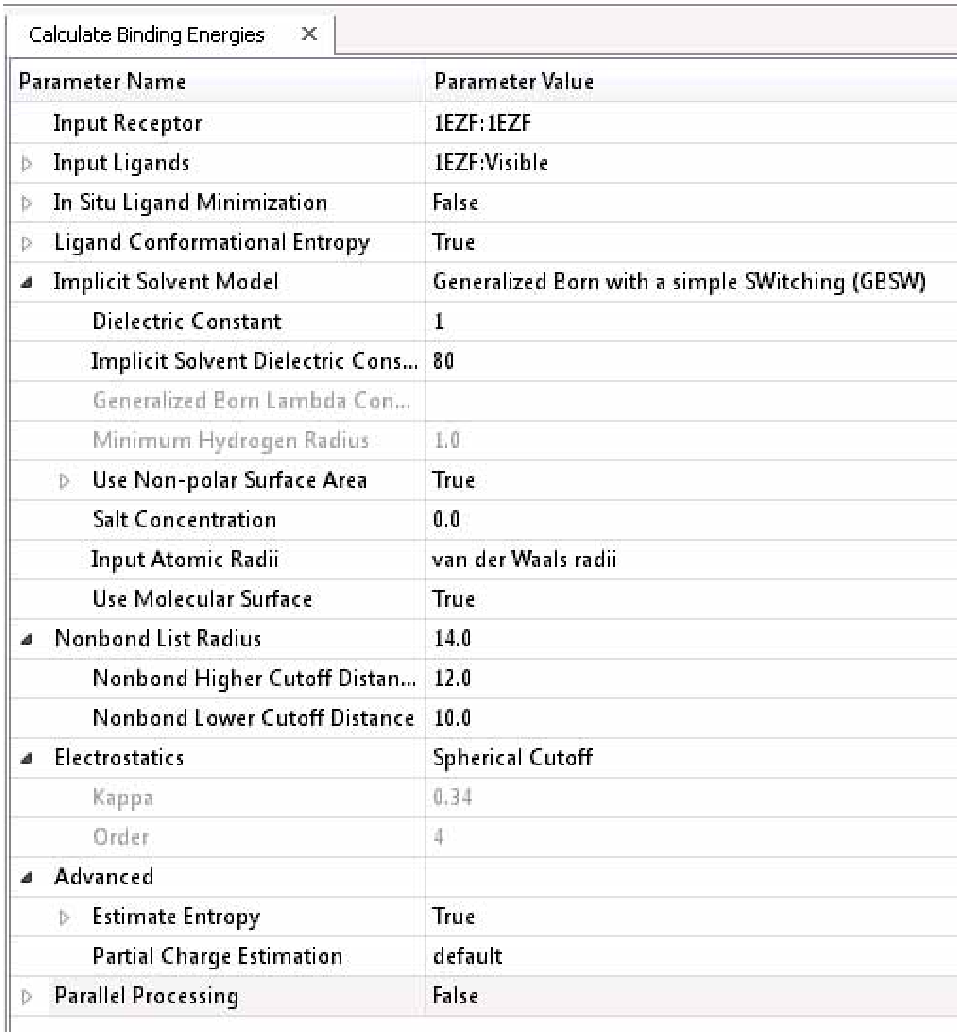

Parameter Name	Parameter Value
Input Receptor	1EZF:1EZF
Input Ligands	1EZF:Visible
In Situ Ligand Minimization	False
Ligand Conformational Entropy	True
Implicit Solvent Model	Generalized Born with a simple SWitching (GBSW)
Dielectric Constant	1
Implicit Solvent Dielectric Cons...	80
Generalized Born Lambda Con...	
Minimum Hydrogen Radius	1.0
Use Non-polar Surface Area	True
Salt Concentration	0.0
Input Atomic Radii	van der Waals radii
Use Molecular Surface	True
Nonbond List Radius	14.0
Nonbond Higher Cutoff Distan...	12.0
Nonbond Lower Cutoff Distance	10.0
Electrostatics	Spherical Cutoff
Kappa	0.34
Order	4
Advanced	
Estimate Entropy	True
Partial Charge Estimation	default
Parallel Processing	False

Figure 3.34. Calculate Binding Energy Parameter Values

The input receptor parameter value was the 1EZF protein and the input ligand parameter value varied depending which bisaboqual compound was used in the run.

3.7.9 Validation of CP-320473

3.7.10 Validation with Implicit Solvent Model MM-GBSW

CDOCKER ENERGY = -60.5489

CDOCKER INTERACTION ENERGY = -74.6871

Ligand Energy (kcal/mol) = -89.05956

Protein Energy (kcal/mol) = -16033.046875

Complex Energy (kcal/mol) = -16183.78229

Binding Energy (kcal/mol) = -61.68171

Total Binding Energy (kcal/mol) = -60.62023

Entropic Energy (kcal/mol) = 23.01080

Ligand Conformational Energy (kcal/mol) = 1.06148

Ligand Conformational Entropy (kcal/mol-K) = 1.06148

Ludi Score Estimate 1 = 693

Ludi Score Estimate 2 = 590

Ludi Score Estimate 3 = 686

3.7.10.i H-bonding Interactions

O-22

Arg77 OH 2.47 Angstroms

O - 23

Arg52 1.80 Angstroms

O - 25

Ser53 OH 2.24 Angstroms

O - 26

Ser51 OH 1.22 Angstroms

Ser53 NH 1.89 Angstroms

Phe54 NH 1.50 Angstroms

3.7.10.ii Pi Stacking Interaction

Phe288 Pi-Pi 5.12 Angstroms

Phe54 Pi-Sigma 2.74 Angstroms

3.7.11 CP-320473 with Implicit Solvent MM-PBSA

Ligand Energy (kcal/mol) = -85.4188

Protein Energy (kcal/mol) = -16298.2001

Complex Energy (kcal/mol) = -16436.7

Binding Energy (kcal/mol) = -53.0810

Total Binding Energy (kcal/mol) = -52.019

Entropic Energy (kcal/mol) = 23.0180

Ligand Conformational Energy (kcal/mol) = 1.06148

Ligand Conformational Entropy (kcal/mol-K) = 1.06148

3.7.12 Bisabosqual A with Implicit Solvent Model MM-GBSW

Total Binding Energy (kcal/mol) = -47.09244

Entropic Energy (kcal/mol) = 21.97830

Ligand Conformational Energy (kcal/mol) = 4.52057

Ligand Conformational Entropy (kcal/mol-K) =1.2721

Ludi Score Estimate 1 = 892

Ludi Score Estimate 2 = 731

Ludi Score Estimate 3 = 833

3.7.12.i H-bonding Interactions

O-8

- Ser51 OH 1.81 Angstroms
- Arg52 NH 2.07 Angstroms
- Ser53 OH 2.02 Angstroms
- Phe54 NH 2.38 Angstroms

O - 10

- Ser53 NH 2.11 Angstroms
- Ser53 OH 1.52 Angstroms
- Phe54 NH 1.68 Angstroms

O - 28

- Asn215 NH 2.17 Angstroms

3.7.12.ii Pi Stacking Interaction

Phe288 (~4.10A)

3.7.13 Bisabosqual A with Implicit Solvent MM-PBSA

Ligand Energy (kcal/mol) = 34.5108

Protein Energy (kcal/mol) = -16392.5

Complex Energy (kcal/mol) = -16402.3

Binding Energy (kcal/mol) = -44.3108

Total Binding Energy (kcal/mol) = -36.8208

Entropic Energy (kcal/mol) = 21.97830

Ligand Conformational Energy (kcal/mol) = 4.52057

Ligand Conformational Entropy (kcal/mol-K) =1.2721

3.7.14 Bisabosqual B with Implicit Solvent Model MM-GBSW

CDOCKER ENERGY = 17.8552

CDOCKER INTERACTION ENERGY = -48.0724

Ligand Energy (kcal/mol) = 32.45848

Protein Energy (kcal/mol) = -13844.612305

Complex Energy (kcal/mol) = -13839.11752

Binding Energy (kcal/mol) = -26.96369

Total Binding Energy (kcal/mol) = -26.495

Entropic Energy (kcal/mol) = 21.98690

Ligand Conformational Energy (kcal/mol) = 0.46869

Ligand Conformational Entropy (kcal/mol-K) = 0.46869

Ludi Score Estimate 1 = 634

Ludi Score Estimate 2 = 524

Ludi Score Estimate 3 = 573

3.7.14.i H-bonding Interactions

O-8

    Ser51 OH 2.00 Angstroms
    Ser53 NH 2.05 Angstroms
    Phe54 NH 1.92 Angstroms

O - 10

Ser53 OH 2.20 Angstroms

O - 28

Asn215 NH 4.31 Angstroms

3.7.15 Bisabosqual B with Implicit Solvent MM-PBSA

Ligand Energy (kcal/mol) = 33.3937
Protein Energy (kcal/mol) = -14209.5
Complex Energy (kcal/mol) = -14190.1
Binding Energy (kcal/mol) = -13.9937
Total Binding Energy (kcal/mol) = -13.58306
Entropic Energy (kcal/mol) = 22.16350
Ligand Conformational Energy (kcal/mol) = 0.41064
Ligand Conformational Entropy (kcal/mol-K) = 0.41064

3.7.16 Bisabosqual C with Implicit Solvent Model MM-GBSW

CDOCKER ENERGY = 16.2453
CDOCKER INTERACTION ENERGY = -62.1032
Ligand Energy (kcal/mol) = 53.11066
Protein Energy (kcal/mol) = -16094.274414
Complex Energy (kcal/mol) = -16093.69714
Binding Energy (kcal/mol) = -52.53339
Total Binding Energy (kcal/mol) = -47.84258
Entropic Energy (kcal/mol) = 22.02480
Ligand Conformational Energy (kcal/mol) = 4.69081
Ligand Conformational Entropy (kcal/mol-K) = 0.97872
Ludi Score Estimate 1 = 926
Ludi Score Estimate 2 = 716
Ludi Score Estimate 3 = 876

3.7.16.i H-bonding Interactions

O-8

Ser51 OH 1.70 Angstroms
Arg52 NH 2.26 Angstroms
Ser53 NH 1.50 Angstroms
Phe54 NH 1.83 Angstroms

O - 10

Ser53 NH 2.33 Angstroms
Ser53 OH 1.08 Angstroms
Phe54 NH 2.00 Angstroms

O - 28

Asn215 NH 2.13 Angstroms

3.7.17 Bisabosqual C with Implicit Solvent Model MM-PBSA

Ligand Energy (kcal/mol) = 52.5954
Protein Energy (kcal/mol) = -16401.599
Complex Energy (kcal/mol) = -16381.
Binding Energy (kcal/mol) = -32.09579
Total Binding Energy (kcal/mol) = -31.68515
Entropic Energy (kcal/mol) = 22.02480
Ligand Conformational Energy (kcal/mol) = 0.41064
Ligand Conformational Entropy (kcal/mol-K) = 0.41064

3.7.18 Bisabosqual D with Implicit Solvent Model MM-GBSW

CDOCKER ENERGY = 2.0207
CDOCKER INTERACTION ENERGY = -54.633
Ligand Energy (kcal/mol) = -9.69705
Protein Energy (kcal/mol) = -16,189.732
Complex Energy (kcal/mol) = -16234.0406

Binding Energy (kcal/mol) = -34.6111

Total Binding Energy (kcal/mol) = -27.151

Entropic Energy (kcal/mol) = 22.10980

Ligand Conformational Energy (kcal/mol) = 7.49669

Ligand Conformational Entropy (kcal/mol-K) = 0.41874

Ludi Score Estimate 1 = 615

Ludi Score Estimate 2 = 516

Ludi Score Estimate 3 = 730

3.7.18.i H-bonding Interactions

O - 10

Ser51 OH 2.40 Angstroms

Ser53 NH 2.38 Angstroms

Phe54 NH 2.01 Angstroms

3.7.18.ii Pi-bonding Interactions

Phe54 pi-pi 5.44 Angstroms

3.7.19 Bisabosqual D with Implicit Solvent MM-PBSA

Ligand Energy (kcal/mol) = -12.4561

Protein Energy (kcal/mol) = -16478.00

Complex Energy (kcal/mol) = -16507.70

Binding Energy (kcal/mol) = -17.2439

Total Binding Energy (kcal/mol) = -14.6294

Entropic Energy (kcal/mol) = 22.10980

Ligand Conformational Energy (kcal/mol) = 2.61453

Ligand Conformational Entropy (kcal/mol-K) = 0.42593

3.7.20 Compound 3.6 Data

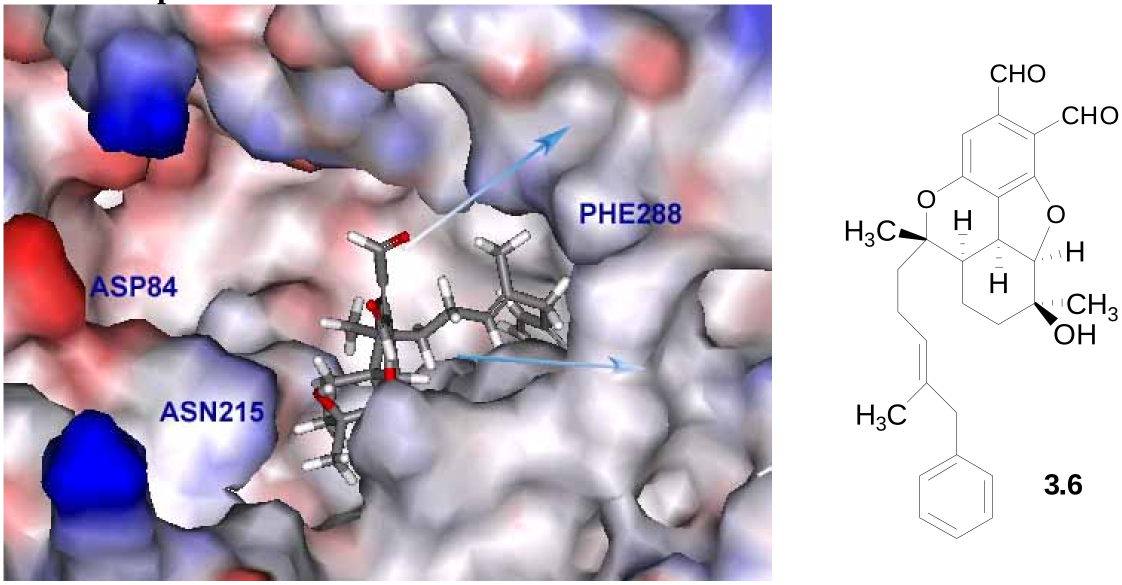

Figure 3.35. Image of docked compound **3.6** shown in the active site with neighboring residues. The protein surface area is rendered showing the electrostatic potential. The image on the left has the “flap” removed; the arrows point to the closed hydrophobic terminus of the channel. The image on the right shows the structure of compound **3.6**.

3.7.21 Compound 3.6 with Implicit Solvent MM-GBSW

CDOCKER ENERGY = 16.9953

CDOCKER INTERACTION ENERGY = -59.8039

Ligand Energy (kcal/mol) = 31.80727

Protein Energy (kcal/mol) = -16200.67382

Complex Energy (kcal/mol) = -16212.33407

Binding Energy (kcal/mol) = -43.46751

Total Binding Energy (kcal/mol) = -43.05687

Entropic Energy (kcal/mol) = 22.56020

Ligand Conformational Energy (kcal/mol) = 0.41064

Ligand Conformational Entropy (kcal/mol-K) = 0.41064

Ludi Score Estimate 1 = 752

Ludi Score Estimate 2 = 612

Ludi Score Estimate 3 = 635

3.7.21.i H-bonding Interactions

O-8

Ser51 OH 1.89 Angstroms

Phe54 NH 2.14 Angstroms

O - 10

Ser53 NH 2.19 Angstroms

3.7.22 Compound 3.6 with Implicit Solvent MM-PBSA

Ligand Energy (kcal/mol) = 33.7047

Protein Energy (kcal/mol) = -16482.5

Complex Energy (kcal/mol) = -16470.9

Binding Energy (kcal/mol) = -22.10470

Total Binding Energy (kcal/mol) = -21.694

Entropic Energy (kcal/mol) = 22.56050

Ligand Conformational Energy (kcal/mol) = 0.41064

Ligand Conformational Entropy (kcal/mol-K) = 0.41064

3.7.23 Compound 3.7 Data

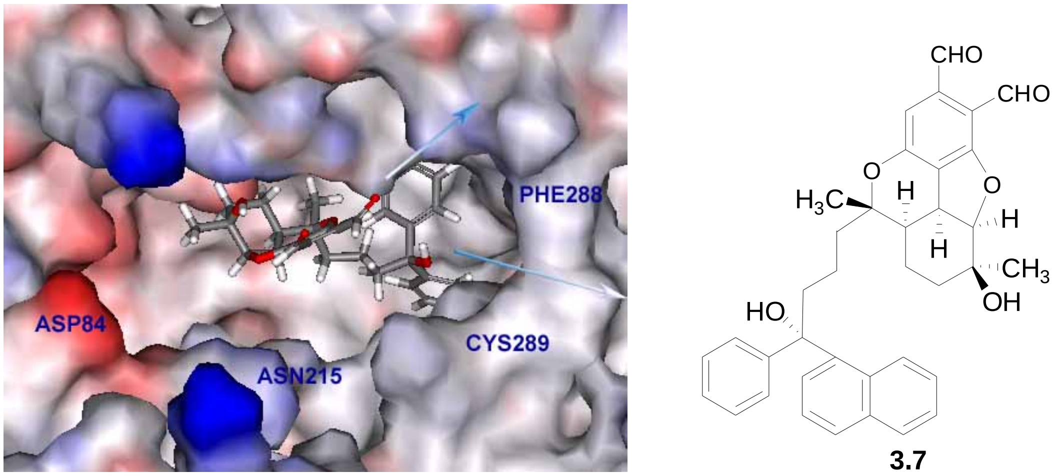

3.7

Figure 3.36. Image of docked compound **3.7** shown in the active site with neighboring residues. The protein surface area is rendered showing the electrostatic potential. The image on the left has the "flap" removed; the arrows point to the closed hydrophobic terminus of the channel. The image on the right shows the structure of compound **3.7**.

3.7.24 Compound 3.7 with Implicit Solvent MM-GBSW

CDOCKER ENERGY = -2.34852

CDOCKER INTERACTION ENERGY = -64.1921

Ligand Energy (kcal/mol) = 4.65169

Protein Energy (kcal/mol) = -161999.438

Complex Energy (kcal/mol) = -16238.82189

Binding Energy (kcal/mol) = -44.03510

Total Binding Energy (kcal/mol) = -43.62446

Entropic Energy (kcal/mol) = 23.14350

Ligand Conformational Energy (kcal/mol) = 0.41064

Ligand Conformational Entropy (kcal/mol-K) = 0.41064

Ludi Score Estimate 1 = 655

Ludi Score Estimate 2 = 578

Ludi Score Estimate 3 = 759

3.7.24.i H-bonding Interactions

O-8

Ser51 OH 1.48 Angstroms

Phe54 NH 1.95 Angstroms

O - 10

Arg52 NH 1.79 Angstroms

O - 28

Arg77 NH 2.06 Angstroms

Arg77 NH 2.36 Angstroms

3.7.25 Compound 3.7 with Implicit Solvent MM-PBSA

Ligand Energy (kcal/mol) = 3.6911

Protein Energy (kcal/mol) = -16483.4004

Complex Energy (kcal/mol) = -16512.000

Binding Energy (kcal/mol) = -32.29071

Total Binding Energy (kcal/mol) = -31.8801

Entropic Energy (kcal/mol) = 23.14350

Ligand Conformational Energy (kcal/mol) = 0.41064

Ligand Conformational Entropy (kcal/mol-K) = 0.41064

3.7.26 Compounds 3.8 Data

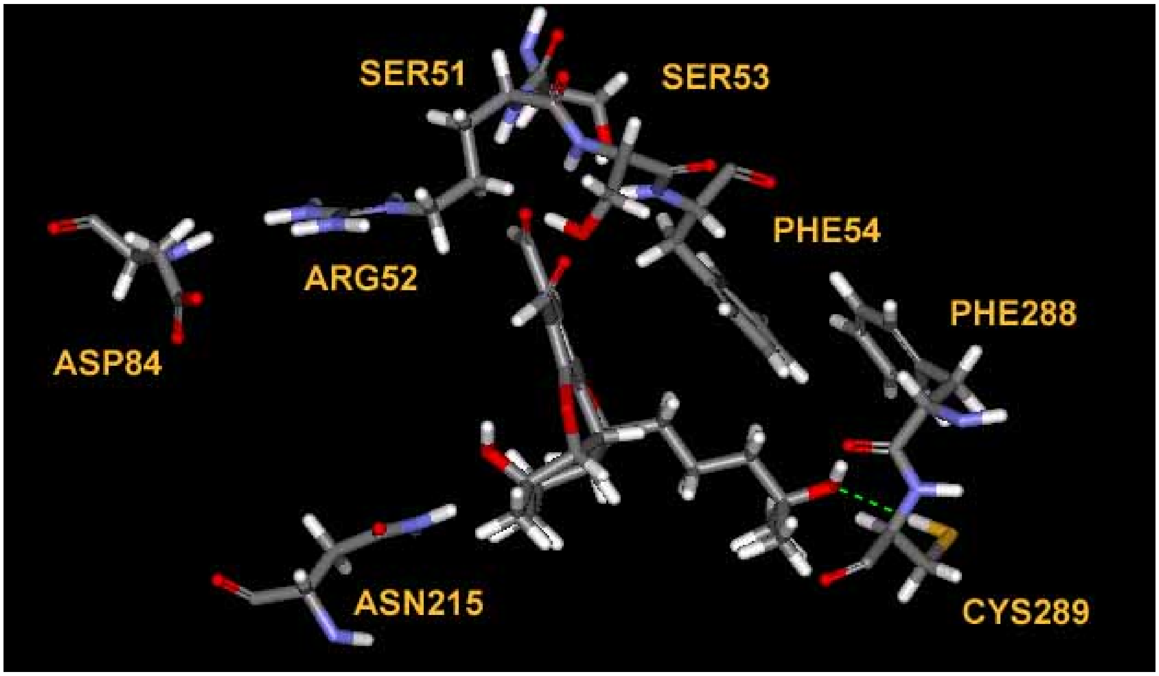
SER51
SER53
PHE54
ARG52
ASP84
PHE288
ASN215
CYS289

Figure 3.37. Compound 3.8 with its neighboring residues in the active site.

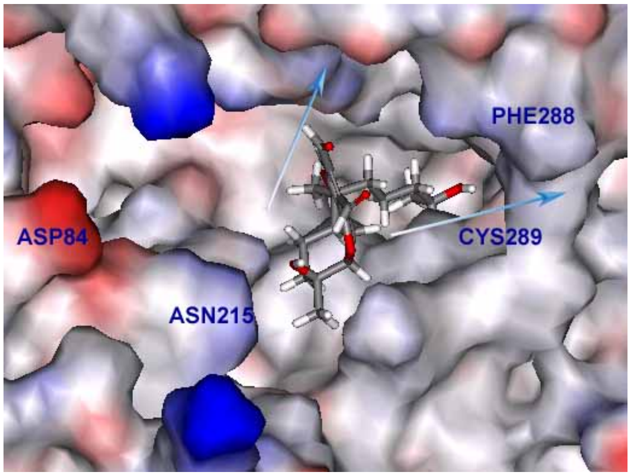
PHE288
ASP84
CYS289
ASN215

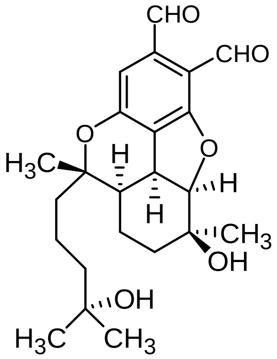
CHO
CHO
O
O
H3C
H
H
H
CH3
OH
OH
H3C
CH3

3.8

Figure 3.38. Image of docked compound **3.8** shown in the active site with neighboring residues. The protein surface area is rendered showing the electrostatic potential. The image on the left has the "flap" removed; the arrows point to the closed hydrophobic terminus of the channel. The image on the right shows the structure of compound **3.8**.

3.7.27 Compound 3.8 with Implicit Solvent MM-GBSW

CDOCKER ENERGY = -5.03446

CDOCKER INTERACTION ENERGY = -54.6942

Ligand Energy (kcal/mol) = -5.06631

Protein Energy (kcal/mol) = -16186.4169

Complex Energy (kcal/mol) = -16237.169

Binding Energy (kcal/mol) = -45.68591

Total Binding Energy (kcal/mol) = -45.27527

Entropic Energy (kcal/mol) = 22.09270

Ligand Conformational Energy (kcal/mol) = 0.41064

Ligand Conformational Entropy (kcal/mol-K) = 0.41064

Ludi Score Estimate 1 = 655

Ludi Score Estimate 2 = 531

Ludi Score Estimate 3 = 752

3.7.27.i H-bonding Interactions

O-55

Cys289 SH 2.42 Angstroms

3.7.27.ii Pi-bonding Interactions

Phe54 pi-pi 5.14 Angstroms

3.7.28 Compound 3.8 with Implicit Solvent MM-PBSA

Ligand Energy (kcal/mol) = -7.69411

Protein Energy (kcal/mol) = -16468.400

Complex Energy (kcal/mol) = -16509.60

Binding Energy (kcal/mol) = -33.50550

Total Binding Energy (kcal/mol) = -33.09487

Entropic Energy (kcal/mol) = 22.09270

Ligand Conformational Energy (kcal/mol) = 0.41064

Ligand Conformational Entropy (kcal/mol-K) = 0.41064

3.7.29 Compounds 3.9 Data

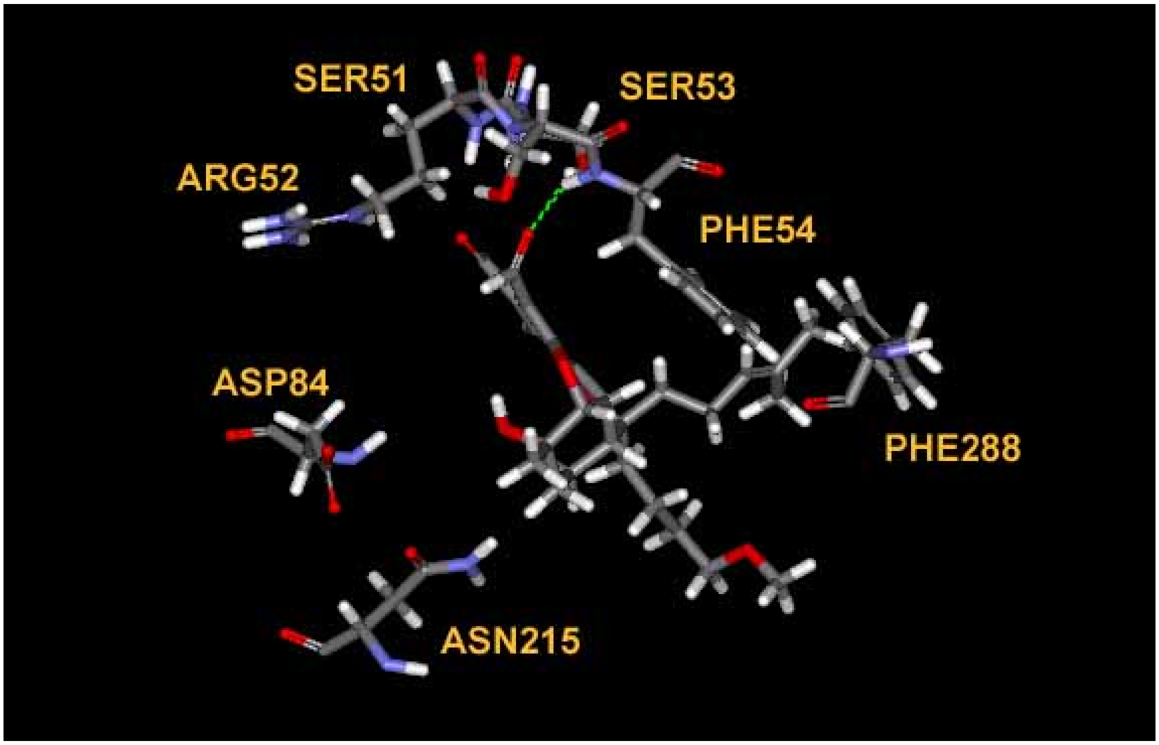
SER51
SER53
ARG52
PHE54
ASP84
PHE288
ASN215

Figure 3.39. Compound 3.9 with its neighboring residues in the active site.

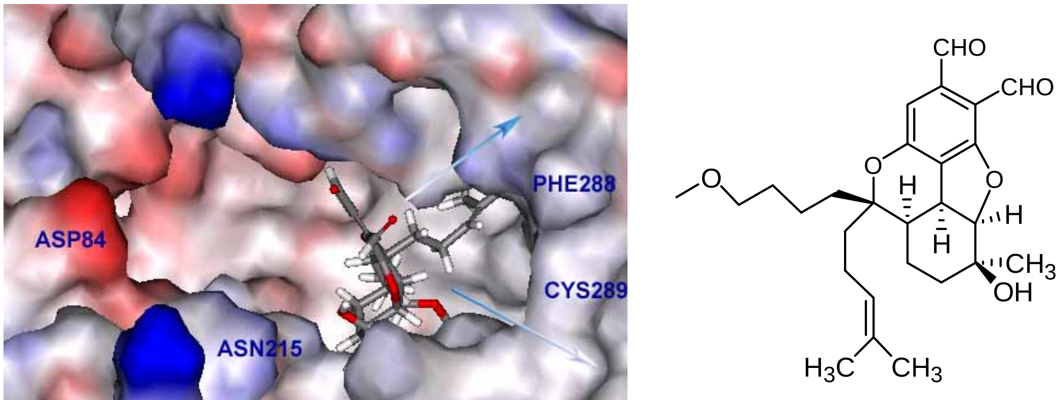
PHE288
ASP84
CYS289
ASN215
CHO
CHO
O
O
O
H
H
H
CH3
OH
H3C
CH3

3.9

Figure 3.40. Image of docked compound **3.9** shown in the active site with neighboring residues. The protein surface area is rendered showing the electrostatic potential. The image on the left has the “flap” removed; the arrows point to the closed hydrophobic terminus of the channel. The image on the right shows the structure of compound **3.9**.

3.7.30 Compound 3.9 with Implicit Solvent MM-GBSW

CDOCKER ENERGY = 14.7628

CDOCKER INTERACTION ENERGY = -62.19

Ligand Energy (kcal/mol) = 33.48973

Protein Energy (kcal/mol) = -16191.851562

Complex Energy (kcal/mol) = -16207.81171

Binding Energy (kcal/mol) = -49.44988

Total Binding Energy (kcal/mol) = -49.03924

Entropic Energy (kcal/mol) = 22.42560

Ligand Conformational Energy (kcal/mol) = 0.41064

Ligand Conformational Entropy (kcal/mol-K) = 0.41064

Ludi Score Estimate 1 = 695

Ludi Score Estimate 2 = 596

Ludi Score Estimate 3 = 762

3.7.30.i H-bonding Interactions

O-10

Ser51 OH 2.31 Angstroms

Phe54 NH 2.18 Angstroms

3.7.30.ii Pi-bonding Interactions

Phe54 pi-pi 5.80 Angstroms

3.7.31 Compound 3.9 with Implicit Solvent MM-PBSA

Ligand Energy (kcal/mol) = 35.9785

Protein Energy (kcal/mol) = -16478.50

Complex Energy (kcal/mol) = -16474.00

Binding Energy (kcal/mol) = -31.47850

Total Binding Energy (kcal/mol) = -31.0678

Entropic Energy (kcal/mol) = 22.4256

Ligand Conformational Energy (kcal/mol) = 0.41064

Ligand Conformational Entropy (kcal/mol-K) = 0.41064

3.7.32 Compounds 3.11 Data

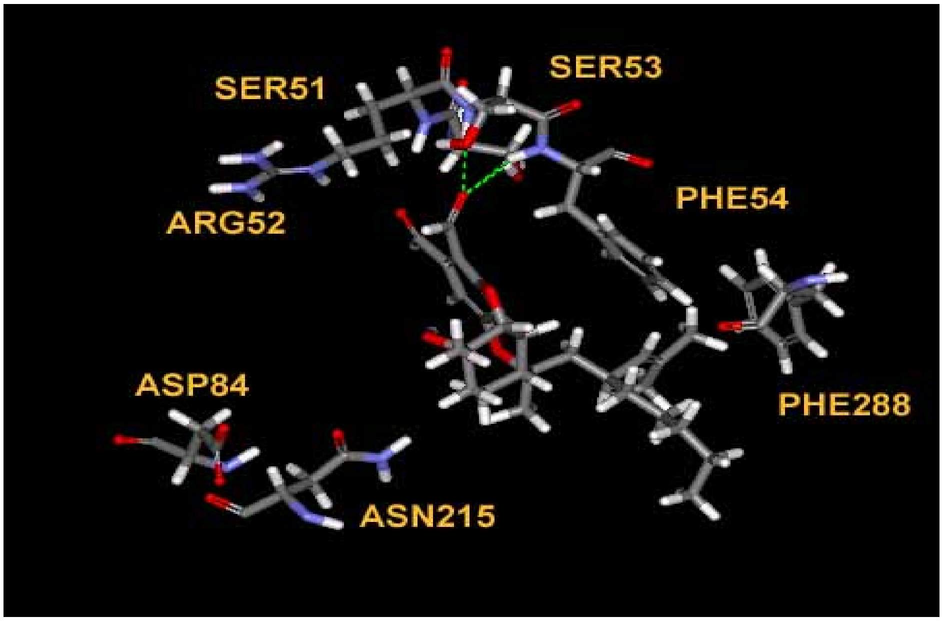
SER51
SER53
ARG52
PHE54
ASP84
PHE288
ASN215

Figure 3.41. Compound 3.11 with its neighboring residues in the active site.

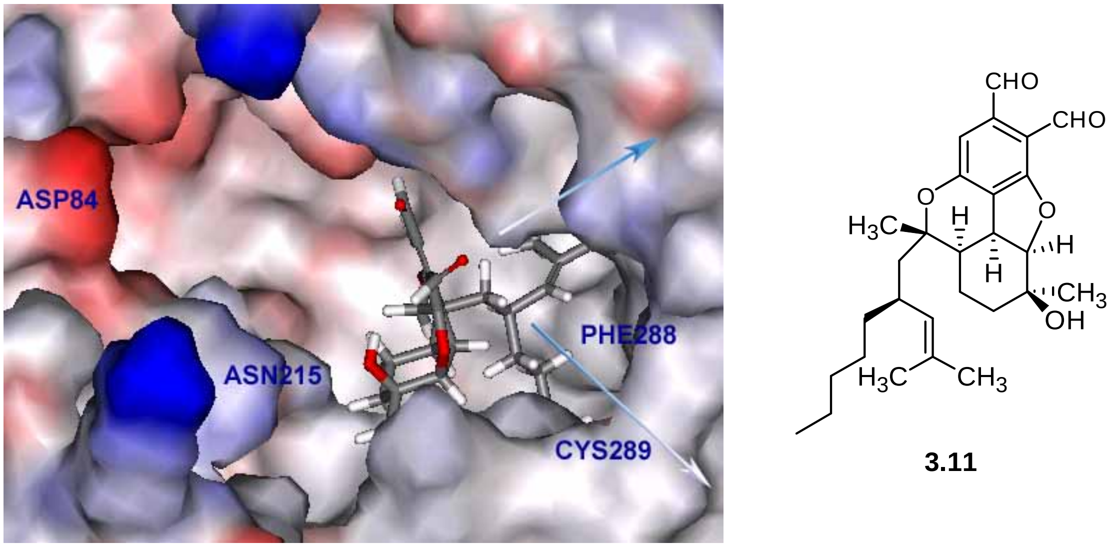
ASP84
ASN215
PHE288
CYS289
CHO
CHO
O
O
H3C
H
H
H
CH3
OH
H3C
CH3
3.11

Figure 3.42. Image of docked compound **3.11** shown in the active site with neighboring residues. The protein surface area is rendered showing the electrostatic potential. The image on the left has the “flap” removed; the arrows point to the closed hydrophobic terminus of the channel. The image on the right shows the structure of compound **3.11**.

3.7.33 Compound 3.11 with Implicit Solvent MM-GBSW

CDOCKER ENERGY = 12.0869

CDOCKER INTERACTION ENERGY = -62.888

Ligand Energy (kcal/mol) = 33.977

Protein Energy (kcal/mol) = -16190.500

Complex Energy (kcal/mol) = -16207.600

Binding Energy (kcal/mol) = -51.0243

Total Binding Energy (kcal/mol) = -50.613

Entropic Energy (kcal/mol) = 22.8157

Ligand Conformational Energy (kcal/mol) = 0.41064

Ligand Conformational Entropy (kcal/mol-K) = 0.41064

Ludi Score Estimate 1 = 776

Ludi Score Estimate 2 = 657

Ludi Score Estimate 3 = 859

3.7.33.i H-bonding Interactions

O-10

Ser51 OH 2.45 Angstroms

Ser53 OH 2.34 Angstroms

Phe54 NH 2.17 Angstroms

3.7.33.ii Pi-bonding Interactions

Phe54 pi-pi 5.60 Angstroms

3.7.44 Compound 3.11 with Implicit Solvent MM-PBSA

Ligand Energy (kcal/mol) = 37.4387

Protein Energy (kcal/mol) = -16475.4003

Complex Energy (kcal/mol) = -16474.60

Binding Energy (kcal/mol) = -36.638

Total Binding Energy (kcal/mol) = -36.227

Entropic Energy (kcal/mol) = 22.4444

Ligand Conformational Energy (kcal/mol) = 0.41064

Ligand Conformational Entropy (kcal/mol-K) = 0.41064

3.7.45 Compounds 3.12 Data

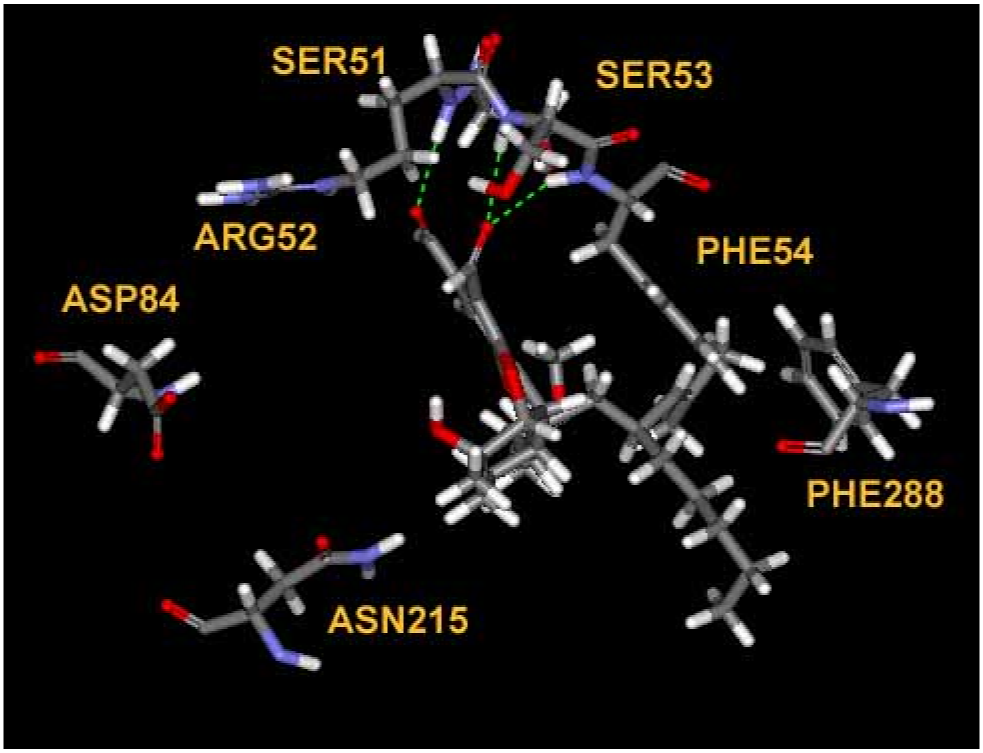
SER51
SER53
ARG52
PHE54
ASP84
PHE288
ASN215

Figure 3.43. Compound 3.12 with its neighboring residues in the active site.

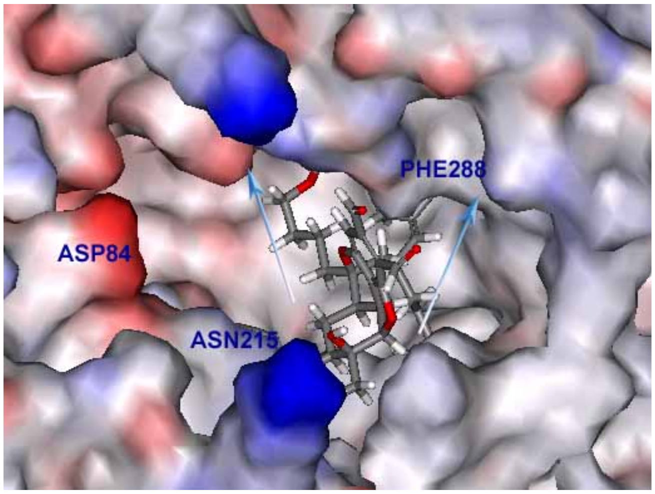
PHE288
ASP84
ASN215

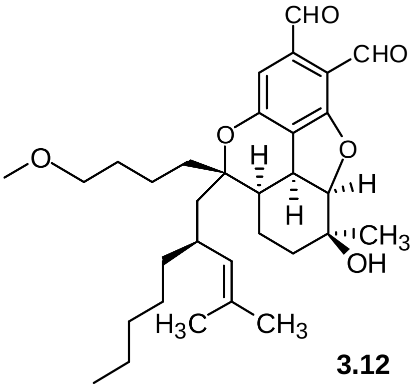
CHO
CHO
O
O
O
H
H
H
CH3
OH
H3C
CH3

3.12

Figure 3.44. Image of docked compound **3.12** shown in the active site with neighboring residues. The protein surface area is rendered showing the electrostatic potential. The image on the left has the “flap” removed; the arrows point to the closed hydrophobic terminus of the channel. The image on the right shows the structure of compound **3.12**.

3.7.46 Compound 3.12 with Implicit Solvent MM-GBSW

CDOCKER ENERGY = 3.92655

CDOCKER INTERACTION ENERGY = -72.804

Ligand Energy (kcal/mol) = 36.2913

Protein Energy (kcal/mol) = -16191.00

Complex Energy (kcal/mol) = -16207.81171

Binding Energy (kcal/mol) = -56.642

Total Binding Energy (kcal/mol) = -56.231

Entropic Energy (kcal/mol) = 22.8157

Ligand Conformational Energy (kcal/mol) = 0.41064

Ligand Conformational Entropy (kcal/mol-K) = 0.41064

Ludi Score Estimate 1 = 787

Ludi Score Estimate 2 = 659

Ludi Score Estimate 3 = 855

3.7.46.i H-bonding Interactions

O-8

Arg52 NH 2.26 Angstroms

O-10

Ser53 OH 2.32 Angstroms

Phe54 NH 2.20 Angstroms

3.7.46.ii Pi-bonding Interactions

Phe54 pi-pi 5.49 Angstroms

3.7.47 Compound 3.12 with Implicit Solvent MM-PBSA

Ligand Energy (kcal/mol) = 39.5618

Protein Energy (kcal/mol) = -16474.50

Complex Energy (kcal/mol) = -16473.70

Binding Energy (kcal/mol) = -38.761

Total Binding Energy (kcal/mol) = -38.350

Entropic Energy (kcal/mol) = 22.8157

Ligand Conformational Energy (kcal/mol) = 0.41064

Ligand Conformational Entropy (kcal/mol-K) = 0.41064

3.7.48 Compounds 3.13 Data

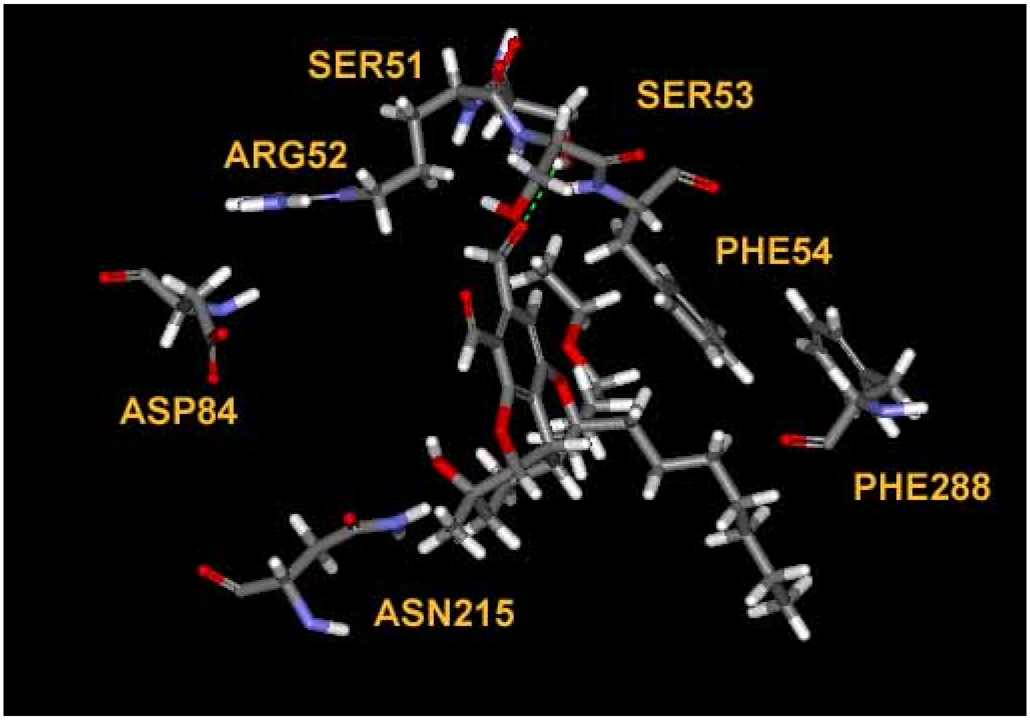
SER51
SER53
ARG52
PHE54
ASP84
PHE288
ASN215

Figure 3.45. Compound 3.13 with its neighboring residues in the active site.

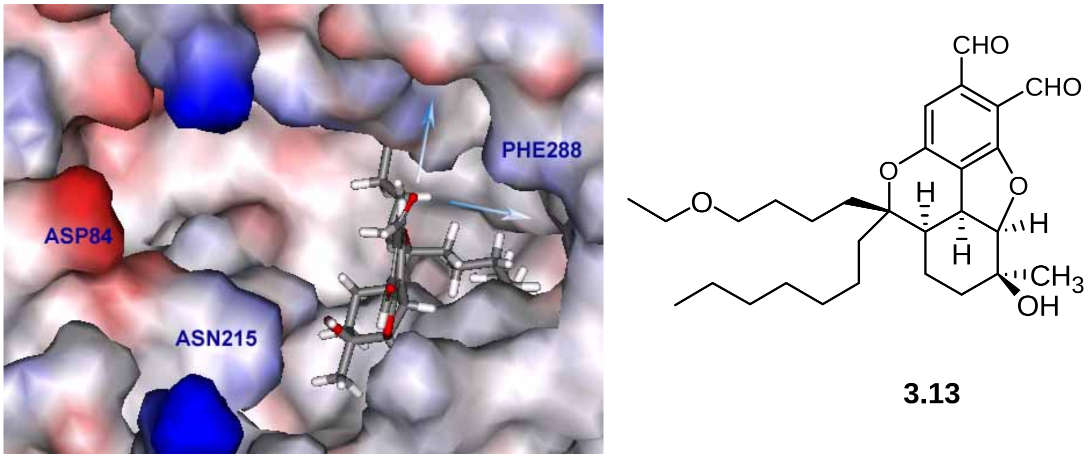
PHE288
ASP84
ASN215
CHO
CHO
O
O
O
H
H
H
CH3
OH

3.13

Figure 3.46. Image of docked compound **3.13** shown in the active site with neighboring residues. The protein surface area is rendered showing the electrostatic potential. The image on the left has the “flap” removed; the arrows point to the closed hydrophobic terminus of the channel. The image on the right shows the structure of compound **3.13**.

3.7.49 Compound 3.13 with Implicit Solvent MM-GBSW

CDOCKER ENERGY = -19.513

CDOCKER INTERACTION ENERGY = -67.8252

Ligand Energy (kcal/mol) = 33.977

Protein Energy (kcal/mol) = -16,204.10

Complex Energy (kcal/mol) = -16253.30

Binding Energy (kcal/mol) = -52.8178

Total Binding Energy (kcal/mol) = -52.8178

Entropic Energy (kcal/mol) = 22.7547

Ligand Conformational Energy (kcal/mol) = 0

Ligand Conformational Entropy (kcal/mol-K) = 0

Ludi Score Estimate 1 = 724

Ludi Score Estimate 2 = 617

Ludi Score Estimate 3 = 709

3.7.49.i H-bonding Interactions

O-8

Ser51 OH 2.11 Angstroms

3.7.50 Compound 3.13 with Implicit Solvent MM-PBSA

Ligand Energy (kcal/mol) = 5.5026

Protein Energy (kcal/mol) = -16476.3007

Complex Energy (kcal/mol) = -16510.9

Binding Energy (kcal/mol) = -40.1018

Total Binding Energy (kcal/mol) = -39.691

Entropic Energy (kcal/mol) = 22.7547

Ligand Conformational Energy (kcal/mol) = 0.41064

Ligand Conformational Entropy (kcal/mol-K) = 0.41064

3.7.51 Compounds 3.14 Data

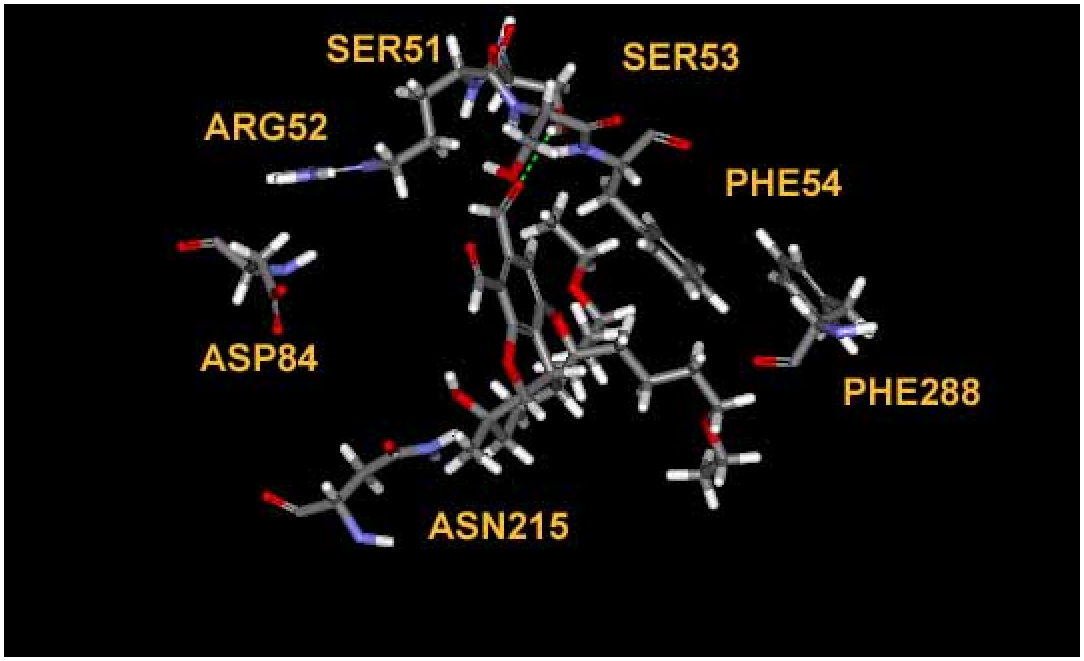
SER51
SER53
ARG52
PHE54
ASP84
PHE288
ASN215

Figure 3.47. Compound 3.14 with its neighboring residues in the active site.

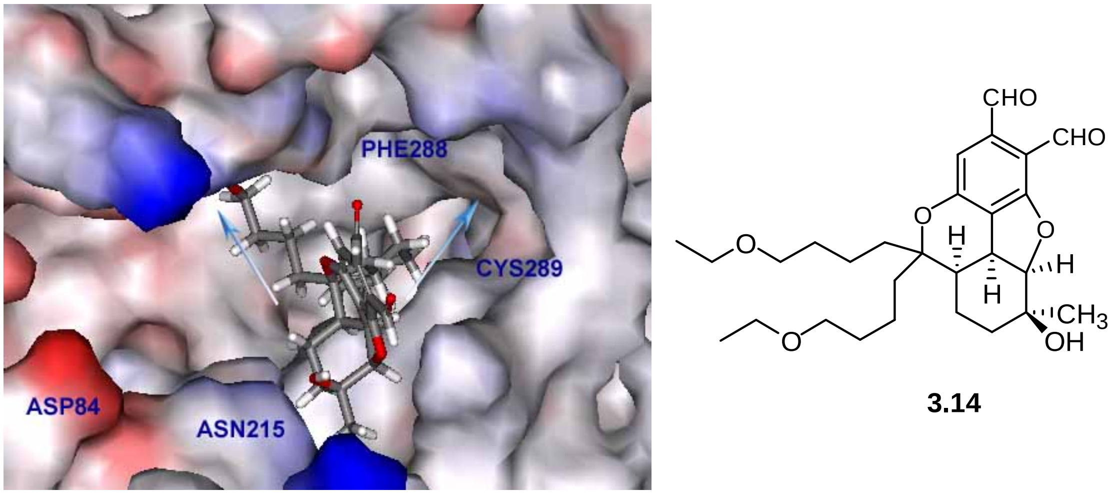
PHE288
CYS289
ASP84
ASN215
CHO
CHO
O
O
H
H
H
O
CH3
OH
O

3.14

Figure 3.48. Image of docked compound **3.14** shown in the active site with neighboring residues. The protein surface area is rendered showing the electrostatic potential. The image on the left has the "flap" removed; the arrows point to the closed hydrophobic terminus of the channel. The image on the right shows the structure of compound **3.14**.

3.7.52 Compound 3.14 with Implicit Solvent MM-GBSW

CDOCKER ENERGY = -19.8218

CDOCKER INTERACTION ENERGY = -66.9701

Ligand Energy (kcal/mol) = -0.27352

Protein Energy (kcal/mol) = -16,204.828

Complex Energy (kcal/mol) = -16,255.262

Binding Energy (kcal/mol) = -50.1601

Total Binding Energy (kcal/mol) = -49.749

Entropic Energy (kcal/mol) = 22.70430

Ligand Conformational Energy (kcal/mol) = 0.41064

Ligand Conformational Entropy (kcal/mol-K) = 0.41064

Ludi Score Estimate 1 = 722

Ludi Score Estimate 2 = 600

Ludi Score Estimate 3 = 741

3.7.52.i H-bonding Interactions

O-8

Ser51 NH 2.14 Angstroms

3.7.53 Compound 3.14 with Implicit Solvent MM-PBSA

Ligand Energy (kcal/mol) = 2.25386

Protein Energy (kcal/mol) = -16,471.3007

Complex Energy (kcal/mol) = -16,523.40

Binding Energy (kcal/mol) = -54.3508

Total Binding Energy (kcal/mol) = -53.940

Entropic Energy (kcal/mol) = 22.7043

Ligand Conformational Energy (kcal/mol) = 0.41064

Ligand Conformational Entropy (kcal/mol-K) = 0.41064

3.7.54 Compounds 3.15 Data

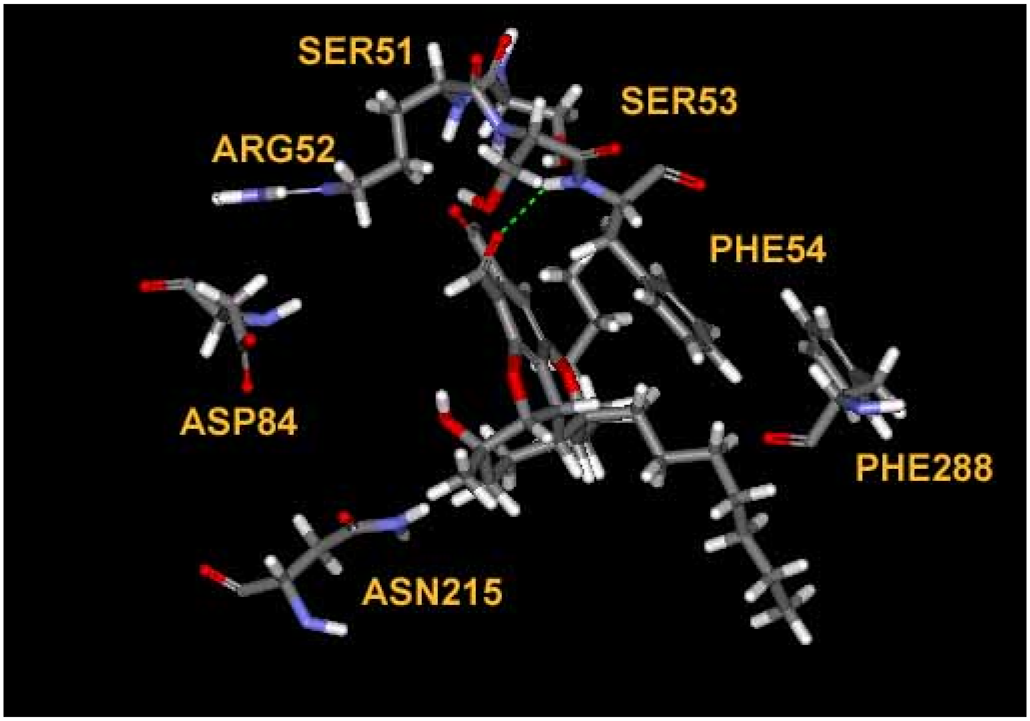
SER51
SER53
ARG52
PHE54
ASP84
PHE288
ASN215

Figure 3.49. Compound 3.15 with its neighboring residues in the active site.

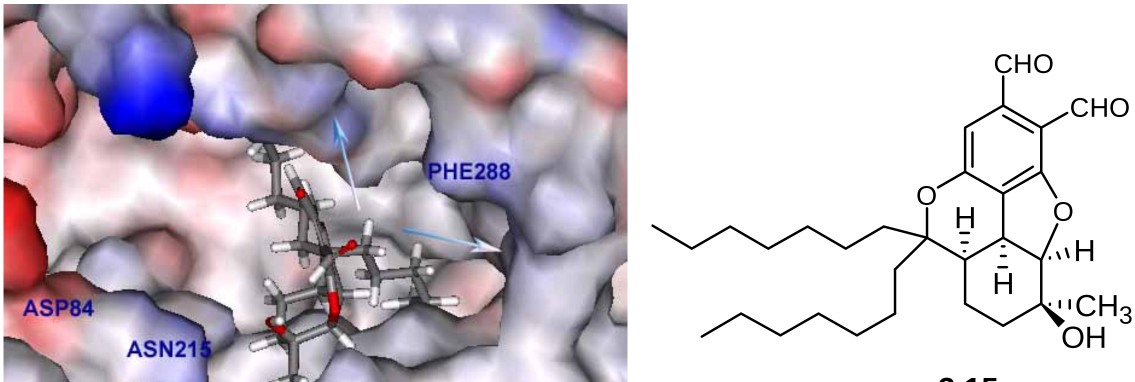
PHE288
ASP84
ASN215
CHO
CHO
O
O
H
H
H
CH3
OH

3.15

Figure 3.50. Image of docked compound **3.15** shown in the active site with neighboring residues. The protein surface area is rendered showing the electrostatic potential. The image on the left has the “flap” removed; the arrows point to the closed hydrophobic terminus of the channel. The image on the right shows the structure of compound **3.15**.

3.7.55 Compound 3.15 with Implicit Solvent MM-GBSW

CDOCKER ENERGY = -17.8152

CDOCKER INTERACTION ENERGY = -67.6167

Ligand Energy (kcal/mol) = 15.8019

Protein Energy (kcal/mol) = -16,191.0

Complex Energy (kcal/mol) = -16,229.60

Binding Energy (kcal/mol) = -54.0102

Total Binding Energy (kcal/mol) = -53.599

Entropic Energy (kcal/mol) = 22.7003

Ligand Conformational Energy (kcal/mol) = 0.41064

Ligand Conformational Entropy (kcal/mol-K) = 0.41064

Ludi Score Estimate 1 = 754

Ludi Score Estimate 2 = 610

Ludi Score Estimate 3 = 753

3.7.55.i H-bonding Interactions

O-10

Phe54 NH 2.24 Angstroms

3.7.55.ii Pi-bonding Interactions

Phe54 Pi-Pi 5.078 Angstroms

3.7.56 Compound 3.15 with Implicit Solvent MM-PBSA

Ligand Energy (kcal/mol) = 17.9806

Protein Energy (kcal/mol) = -16473.3007

Complex Energy (kcal/mol) = -16495.80

Binding Energy (kcal/mol) = -40.4798

Total Binding Energy (kcal/mol) = -40.069

Entropic Energy (kcal/mol) = 22.7003

Ligand Conformational Energy (kcal/mol) = 0.41064

Ligand Conformational Entropy (kcal/mol-K) = 0.41064

3.8 References

---

[1] Vaklavas, C.; Chatzizisis, Y. S.; Ziakas, A.; Zamboulis, C.; Giannoglou, G. D. "Molecular basis of statin-associated myopathy." *Atherosclerosis* (Amsterdam, Netherlands), (**2009**), *202*, 18-28.

[2] (a) Davidson, M. H. "Squalene synthase inhibition: a novel target for the management of dyslipidemia. " *Curr. Atherosclerosis Rep*. **2007**, *9*, 78-80.

(b) Flint, O. P.; Masters, B. A.; Gregg, R. E.; Durham, S. K. "HMG CoA reductase inhibitor-induced myotoxicity: pravastatin and lovastatin inhibit the geranylgeranylation of low-molecular-weight proteins in neonatal rat muscle cell culture." *Toxicology and Applied Pharmacology* **1997**, 145, 99-110.

[3] Charlton-Menys, V. Durrington, P. N. "Squalene Synthase Inhibitors. Clinical Pharmacology and Cholesterol-Lowering Potential," *Drugs*, **2007**, 67, 11-16.

[4] Biller, S.A.; Neuenschwander, K; Ponpipom, M. M.; Poulter, C. Dale. "Squalene synthase inhibitors." *Current Pharmaceutical Design* **1996**, *2*, 1-40.

[5] Flint, Oliver P.; Masters, Barbara A.; Gregg, Richard E.; Durham, Stephen K. "Inhibition of cholesterol synthesis by squalene synthase inhibitors does not induce myotoxicity in vitro." *Toxicology and Applied Pharmacology* **1997**, 145, 91-98.

[6] Nishimoto, T.; Amano, Y.; Tozawa, R.i; Ishikawa, E.; Imura, Y.; Yukimasa, H.; Sugiyama, Y.. "Lipid-lowering properties of TAK-475, a squalene synthase inhibitor, in vivo and in vitro." *British Journal of Pharmacology* **2003**, *139*, 911-918.

[7] Menys, V. C.; Durrington, P. N. "Squalene synthase inhibitors" *Brit. J. Pharm.* **2003**, *139*, 881-882.

[8] (a) Minagawa, K.; Kouzuki, S.; Nomura, K.; Kawamura, Y.; Tani, H.; Terui, Y.; Nakai, H.; Kamigauchi, T.; "Bisabosquals, novel squalene synthase inhibitors. II. Physico-chemical properties and structure elucidation."*Journal of Antibiotics.* **2001**, *54*, 896-903.

(b) Minagawa, K; Kouzuki, S.; Nomura, K.; Yamaguchi, T.; Kawamura, Y.; Matsushima, K.; Tani, H.; Ishii, K.; Tanimoto, T.; Kamigauchi, T.." Bisabosquals, Novel Squalene Synthase Inhibitors. Part 1. Taxonomy, Fermentation, Isolation and Biological Activities." *Journal of Antibiotics.* **2001**, *54*, 890-895

(c) Thompson, J. F.; Danley, D. E.; Mazzalupo, S.; Milos, P. M.; Lira, M.E.; Harwood, H. J., Jr. *Archives of Biochemistry and Biophysics.* **1998**, *350*, 283-290.

[9] Veber, D. F.; Johnson, S. R.; Cheng, H.-Y.; Smith, B. R.; Ward, K. W.; Kopple, K.D. “Molecular Properties That Influence the Oral Bioavailability of Drug Candidates.” *J. Med. Chem.* **2002**, 45, 2615-2623.

[10] (a) Lipinski, C. A.; Lombardo, F; Dominy, B W.; Feeney, P J. “Experimental and computational approaches to estimate solubility and permeability in drug discovery and development settings” *Adv. Drug Delivery Rev.* **1997**, *23*, 3-25. (b) Lipinski, C. A.; “Drug-like properties and the causes of poor solubility and poor permeability” *J. Pharm. Tox. Methods*, **2000**, *44*, 235-249.

[11] Blagg, B. S. J.; Jarstfer, M. B.; Rogers, D. H.; Poulter, C. D. “Recombinant Squalene Synthase. A Mechanism for the Rearrangement of Presqualene Diphosphate to Squalene.” *J. Am. Chem. Soc.* **2002**, *124*, 8846-8853.

[12] Guan, Guimin; Dai, Pei-Hua; Osborne, Timothy F.; Kim, Jae B.; Shechter, I.” Multiple Sequence Elements are involved in the Transcriptional Regulation of the Human Squalene Synthase Gene.” *Journal of Biological Chemistry*. **1997**, *272,* 10295-10302.

[13] Robinson, Gordon W.; Tsay, Yim H.; Kienzle, Bernadette K.; Smith-Monroy, Constance A.; Bishop, Richard W. **“**Conservation between human and fungal squalene synthetases: Similarities in structure, function, and regulation**.”** *Molecular and Cellular Biology*, **1993**, *13*, 2706-17.

[14] Gu, P., Ishii, Y., Spencer, T. A., and Shechter, I. “ Function-Structure Studies and Identification of Three Enzyme Domains Involved in the Catalytic Activity in Rat Hepatic Squalene Synthase.“ *J. Biol. Chem.*1998, *273*, 12515–12525**.**

[15] (a) Robinson, Gordon W.; Tsay, Yim H.; Kienzle, Bernadette K.; Smith-Monroy, Constance A.; Bishop, Richard W. “Conservation between human and fungal squalene synthetases: Similarities in structure, function, and regulation.” *Molecular and Cellular Biology* **1993**, *13*, 2706-17.

(b) Fegueur, M.; Richard, L.; Charles, A. D.; Karst, F. **“**Isolation and primary structure of the ERG9 gene of Saccharomyces cerevisiae encoding squalene synthetase.” *Current Genetics* **1991**, *20*, 365-72.

(c) Jennings, Susan M.; Tsay, Yim H.; Fisch, Tobe M.; Robinson, Gordon W. “Molecular cloning and characterization of the yeast gene for squalene

---

synthetase." *Proceedings of the National Academy of Sciences of the United States of America* **1991**, *88*, 6038-42.

[16] Gu, P., Ishii, Y., Spencer, T. A., and Shechter, I. " Function-Structure Studies and Identification of Three Enzyme Domains Involved in the Catalytic Activity in Rat Hepatic Squalene Synthase." *J. Biol. Chem.***1998**, *273*, 12515–12525.

[17] Robinson,G.W.; Tsay, Y.H.; Kienzle, B.K.; Bishop, R.W. "Conservation between human and fungal squalene synthetases: similarities in structure, function, and regulation." *Mol. Cell. Biology*, **1993**, *13*, 2706-2717.

[18] Guan, Guimin; Dai, Pei-Hua; Osborne, Timothy F.; Kim, Jae B.; Shechter,I." Multiple Sequence Elements are involved in the Transcriptional Regulation of the Human Squalene Synthase Gene." *Journal of Biological Chemistry*. **1997**, *272,* 10295-10302.

[19] Robinson,G.W.; Tsay, Y.H.; Kienzle, B.K.; Bishop, R.W. "Conservation between human and fungal squalene synthetases: similarities in structure, function, and regulation." *Mol. Cell. Biology*, **1993**, *13*, 2706-2717.

[20] Robinson,G.W.; Tsay, Y.H.; Kienzle, B.K.; Bishop, R.W. "Conservation between human and fungal squalene synthetases: similarities in structure, function, and regulation." *Mol. Cell. Biology*, **1993**, *13*, 2706-2717.

[21] Hosfield, D. J.; Zhang, Y.; Dougan, D. R.; Broun, A.; Tari, L. W.; Swanson, R. V.; Finn, J. "Structural Basis for Bisphosphonate-mediated Inhibition of Isoprenoid Biosynthesis." *J. Biol. Chem.* **2004**, *279*, 8526-8529.

[22] Guan, Guimin; Dai, Pei-Hua; Osborne, Timothy F.; Kim, Jae B.; Shechter, I." Multiple Sequence Elements are involved in the Transcriptional Regulation of the Human Squalene Synthase Gene." *Journal of Biological Chemistry*. **1997**, *272,* 10295-10302.

[23] Pandit, J.; Danley, D. E.; Schulte, G. K.; Mazzalupo, S.; Pauly, T. A.; Hayward, C.M.; Hamanaka, E. S.; Thompson, J. F.; Harwood, H. J., Jr. "Crystal structure of human squalene synthase. A key enzyme in cholesterol biosynthesis" *J. Biol. Chem.* **2000**, *275*, 30610-30617

[24] Pandit, J.; Danley, D. E.; Schulte, G. K.; Mazzalupo, S.; Pauly, T. A.; Hayward, C.M.; Hamanaka, E. S.; Thompson, J. F.; Harwood, H. J., Jr. "Crystal structure of human squalene synthase. A key enzyme in cholesterol biosynthesis" *J. Biol. Chem.* **2000**, *275*, 30610-30617.

[25] Pandit, J.; Danley, D. E.; Schulte, G. K.; Mazzalupo, S.; Pauly, T. A.; Hayward,

---

C.M.; Hamanaka, E. S.; Thompson, J. F.; Harwood, H. J., Jr. “Crystal structure of human squalene synthase. A key enzyme in cholesterol biosynthesis” *J. Biol. Chem.* **2000**, *275*, 30610-30617

[26] Verdonk M.L, Cole J.C, Hartshorn M.J, Murray C.W, Taylor R.D. “Improved Protein- Ligand Docking Using GOLD.” *PROTEINS:Structure, Function, and Genetics* **2003**, *52***,** 609-623.

[27] (a) Massova, I.; Kollman, P. A.. Combined molecular mechanical and continuum solvent approach (MM-PBSA/GBSA) to predict ligand binding. *Perspectives in Drug Discovery and Design* **2000**, *18* (Hydrophobicity and Solvation in Drug Design, Pt. II), 113-135. (b) Srinivasan, J., Cheatham, T.E., Cieplak, P., Kollman, P.A. and Case, D.A., Continuum Solvent Studies of the Stability of DNA, RNA, and Phosphoramidate-DNA Helixes. *J. Am. Chem. Soc*., **1998**, *120*, 9401-9409.

[28] (a) Wu, G.; Robertson, D. H.; Brooks, C. L., III; Vieth, M. Detailed analysis of grid-based molecular docking: A case study of CDOCKER-A CHARMm-based MD docking algorithm. *J. Comput. Chem.* **2003**, *24*, 1549–1562 (b) Erickson, J. A.; Jalaie, M.; Robertson, D. H.; Lewis, R. A.; Vieth, M. Lessons in molecular recognition: the effects of ligand and protein flexibility on molecular docking accuracy. *J. Med. Chem.* **2004**, *47*, 45–55.

[29] Böhm, H. J. The computer program Ludi: a new method for the de novo design of enzyme inhibitors. *J. Comput. Aided Mol. Des*. **1992**, *1*, 61-78.

[30] (a) Barreiro G.; Guimaraes C. R. W.; Tubert-Brohman I.; Lyons T. M; Tirado-Rives J.; Jorgensen W. L. Search for non-nucleoside inhibitors of HIV-1 reverse transcriptase using chemical similarity, molecular docking, and MM-GB/SA scoring. *J. Chem. Inf. Model.* **2007,** *47*, 2416-2428, (b) de Jonge, M.R.; Koymans, L. M. H.; Vinkers, M.; Daeyaert, F. F. D; Heeres, J.; Lewi, P.J.; Janssen, P. A. J. Structure Based Activity Prediction of HIV-1 Reverse Transcriptase Inhibitors. *J. Med. Chem.* **2005,** *48*, 2176- 2183, (c) Carta, A.; Pricl,S.; Piras, S.; Fermeglia, M.; La Colla, P.; Loddo, R. Activity and molecular modeling of a new small molecule active against NNRTI-resistant HIV-1 mutants. *Eur. J. Med. Chem.* **2009,** *44*, 5117–5122.

[31] Kuhn,B.; Gerber,P.; Schulz-Gasch, T.; Stahl, M. “Validation and Use of the MM-PBSA Approach for Drug Discovery.” *J. Med. Chem.* **2005**, *48*, 4040-4048.

[32] (a) Wu, G.; Robertson, D. H.; Brooks, C. L., III; Vieth, M. *J. Comput. Chem.* **2003**, *24*, 1549–1562 (b) Erickson, J. A.; Jalaie, M.; Robertson, D. H.; Lewis, R. A.; Vieth, M.*J. Med. Chem.* **2004**, *47*, 45–55.

[33] (a) Wu, G.; Robertson, D. H.; Brooks, C. L., III; Vieth, M. *J. Comput. Chem.* **2003**, *24*, 1549– 1562 (b) Erickson, J. A.; Jalaie, M.; Robertson, D. H.; Lewis, R. A.; Vieth, M.*J. Med. Chem.* **2004**, *47*, 45–55.

List of Full References

References for Chapter 1

[1] Kool, E.T.; Rumney, S.; Paris, P.L.; Ren, R.X.; Chaudhuri, N.C. Napthalene, Phenanthrene, and Pyrene as DNA Base Analogues: Synthesis, Structure, and Fluorescene in DNA, *J.Am.Chem.Soc*., **1996**; 118; 7671-7678.

[2] Woski, S.A.; Challa, H. Solution Phase Synthesis of Potential DNA Binding Molecules Based on the PNA Backbone. *Tetra. Lett*., **1999**; 40; 419-422.

[3] Thomson, S.A.; Josey, J.A.; Cadilla, R.; Gaul, M.D.; Hassman, F.;Luzzio, M.J.; Pipe,A.J.; Reed, K.L.; Ricca, D.J.; Wiethe, R.W.; Noble, S.A. Fmoc Mediated Synthesis of Peptide Nucleic Acids. *Tetrahedron*,**1995**, *51*, 6179-6194.

[4] Kool, E.T.; Matray, T.J. Selective and Stable DNA Base Pairing without Hydrogen Bonds. *J. Am. Chem.Soc.* **1998**,*120*, 6191-6192.

[5] (a) Beuck, C.; Singh, I.; Bhattacharya, W.H.; Parmar, V.S.; Seitz, O.; Weinhold, W. Polycyclic Aromatic DNA-Base Surrogates: High-Affinity Binding to an Adenine-Specific Base-Flipping DNA Methyltransferase. *Angew. Chem. Int. Ed*. **2003**, *42*, 3958-3960.

(b) Singh, I.; Parmar, V.S.; Seitz, O.; Prasad, A.K.; Hecker, W. Local disruption of DNA-base stacking by bulky base surrogates. *Chem.Comm*, **2002**, 500-501.

[6] (a) Wichai,U. Woski, S.A. Disiloxane-Protected 2-Deoxyribonolactone as an Efficient Precursor to 1,2-Dideoxy-1-β-aryl-d-ribofuranoses. *Org. Lett.*,**1999**, *8*, 1173-1175.

(b) Wichai, U., Woski, S. A. An improved route to 1,2-dideoxy-β-1-phenyl-D-ribofuranose. *Bioorg. Med. Chem. Lett*., **1998**, *8*, 3465-3468.

[7] Chen, D.W.; Janda, K. D.; Beuscher, A.E.; Stevens, R.C. Wirsching P. Lerner, R.A. Preparation of Stilbene-Tethered Nonnatural Nucleosides for Use with Blue-Fluorescent Antibodies, *J. Org.Chem*, **2001**; 1725-1732.

[8] Kool, E. T.; Chaudhuri, N.C. An Efficient Method for the Synthesis of Aromatic C-nucleosides. *Tet.Lett.,* **1995;** 36; 1795-1798

[9] (a) Zhang, H.C.; Daves, G. D. Jr. Syntheses of Two Pyridine C-Nucleosides as "Deletion-Modified" Analogs of dT and dC. *J. Org. Chem.* **1992**, *57*,4690-4696.

(b) Farr, R.. N; Kwok,D.-I.;Cheng, J.C.-Y.;Daves, G.D.,Jr. Synthetic C-glycosides related to the gilvocarcin, ravidomycin, and chrysomycin antibiotics. *J. Org. Chem.* **1992**, *57*, 2093-2100.

(c) Farr,R.. N; Kwok,D.-I.; Daves, G.D.,Jr. C-Glycoside synthesis by palladium-catalyzed iodoaglycon-glycal coupling.*Organometallics.* **1990**,*97*,3151-3156.

(d) Farr,R.. N; Daves, G.D., Efficient Synthesis of 2′-Deoxy-β-D-furanosyl C-Glycosides. Palladium-Mediated Glycal-Aglycone Coupling and Stereocontrolled β- and α-Face Reductions of 3-Keto-furanosyl Moieties_Jr. *J. Carbohydrate Chem.* **1990**, *9*,653-660.

(e) Daves, G.D.,Jr._Syntheses of 2'-deoxypseudouridine, 2'-deoxyformycin B, and 2',3'-dideoxyformycin B by palladium-mediated glycal-aglycon coupling_*Acc. Chem. Res.* **1990**, *23*, 201-206. For recent applications of the Daves approach to aryl C-glycosides, see (a) Hsieh, H. –P.; McLaughlin, L.W. *J. Org. Chem.* **1995**,*60*,5356-5459 and (b) Wang, Z.-W.;Wiebe,L.I.; Balzarini, J.; De Clercq, E.; Knaus,E. E. *J. Org. Chem.* **2000**,*65*, 9214-9219.

[10] (a) Kozikowski, A. P.; Ghosh, A.K. Diastereoselection in intermolecular nitrile oxide cycloaddition (NOC) reactions: confirmation of the "anti-periplanar effect" through a simple synthesis of 2-deoxy-D-ribose. *J. Am. Chem.Soc.* **1982**, *104*, 5788. and Diastereofacial Selection in Nitrile Oxide Cycloaddition Reactions. *J. Org. Chem.* **1984**,*49* ,2762-2772.

(b) Kozikowski, A. P. Asymmetric induction in nitrone cycloadditions: a total synthesis of acivicin by double asymmetric induction. Acc. *Chem.Res.* **1984**, *17*, 410-416.

(c) see also Gravestock, M.B.; Patron, R. M.; Todd, C. J. Stereoselective Cycloaddition of Nitrile Oxides to a Dispiroketal- Protected But-3-ene-1,2-diol.*Tetrahedron Assymetry,* **1995**,*6*, 2723-2730.

(d) Jager, V.; Schohe, R., Synthesis of amino sugars via isoxazolines DL- and D-lividosamine (2-amino-2, 3-dideoxy-*ribo*-hexose) derivatives from 4-vinyl-1,3-dioxolanes and nitroacetaldehyde acetals. *Tetrahedron*, **1984**, 2199.

[11] Bergeimer, S.R; Stanchina, D.M. Acylnitrene Route to Vicinal Amino Alcohols. Application to the Synthesis of (−)-Bestatin and Analogues*J. Org. Chem.* **1999**, *64*, 2852- 2859.

[12] (a) Chen, D.W.; Janda, K.; Preparation of Stilbene-Tethered Nonnatural Nucleosides for Use with Blue-Fluorescent Antibodies, *J. Org.Chem*, **2001**; 1725-1732.

b) Kool, E.T.; Rumney, S.; Paris, P.L.; Ren, R.X.; Chaudhuri, N.C. Napthalene, Phenanthrene, and Pyrene as DNA Base Analogues: Synthesis, Structure, and Fluorescene in DNA, *J.Am.Chem.Soc*., **1996**; 118; 7671-7678.

[13] Litvinovskaya, R.P.; Drach, S.V., Khripach, V.A. Synthesis of polyhydroxylated steroid side chains through 22-isoxazol-5'-ylsteroid.s *Rus, J. Org, Chem*. **1998**, *34*, 647-654.

[14] Shi, H.; Liu, H.; Bloch, R.; Mandville, G.. A Novel Efficient and Stereoselective Synthesis of cis- or trans-2,5-Disubstituted Tetrahydrofurans.*Tetrahedron*, **2001**, *57*, 9335-9341.

[15] Jiang, B.; Ma, P. An Improved Synthesis of 3,4-*O*-Isopropylidene Butyne. *Synth.Communication*,**1995**, 25,3641.

[16] (a) Bestmann, H.J.; Roth, G.J.; Muller, S.; An Improved One-pot Procedure for the Synthesis of Alkynes from Aldehydes. *Synlett*, **1996**, 521

(b) Brown, D.G.; Velthuisen, E.J.; Commerford, R.G.; Hoye, T.R. A Convenient Synthesis of Dimethyl (Diazomethyl) phosphonate. *J .Org.Chem*., **1996**, 61, 2540-2541.

(c) Baum, J.S.; Shook, D.A. Diazo transfer reactions with p-acetamidobenzenesulfonylazide. *Synth. Commun*., **1987**,17, 1709-1716.

(d) Kitamura, M.; Tokunaga, M.; Noyori,R. Asymmetric Hydrogenation of .beta.-Keto Phosphonates: A Practical Way to Fosfomycin *J.Am.Chem.Soc*. **1995**, 117, 2931-2932.

[17] Zhang, A.; Kan, Y.; Zhao, G-L.; Jiang, B.1,3-Dipolar Cycloaddition of Chirally Modified Vinylboronic Ester with Nitrile Oxides. *Tetrahedron*, **2000**, *56*, 965-970.

[18] Kobayashki, M.; Kotoku, N.; Sumii, Y.; Hayashi, T. Synthesis of CD-ring structure of cortistatin A, an anti-angiogenicsteroidal alkaloid from marine sponge. *Tet. Lett.* **2008**, *49*, 7078–7081.

References for Chapter 2

1 (a) DeMaeyer, E. M. The WHO programme of prevention and control of vitamin A deficiency, xerophthalmia and nutritional blindness. *Nutr. Health*. **1986**, *4*, 105-12.

(b) Underwood, B. A. Hypovitaminosis A: International Programmatic Issues. *J Nutr*. **1994** *124* (8 Suppl):1467S-1472S.

(c) Underwood, B. A., Arthur, P. The Contribution of Vitamin A to Public Health**.** *FASEB J.* **1996**, *10*, 1040-8.

2 Mangelsdorf, D. J.; Thummel, C.; Beato, M.; Herrlich, P.; Schutz, G.; Umesono, K.; Blumberg, B.; Kastner, P.; Mark, M.; Chambon, P.; Evans, R. M.; Nonsteroid nuclear receptors: what are genetic studies telling us about their role in real life? *Cell*, **1995**, *83*, 835-839.

3 (a) Shaw, N.; Elholm, M.; Noy, N. Retinoic Acid Is a High Affinity Selective Ligand for the Peroxisome Proliferator-activated Receptor β/δ. *J. Biol. Chem.*, **2003**, *278*, 41589-41592.

(b) Schug, T. T.; Berry, D. C.; Shaw, N. S.; Travis, S. N.; Noy, N. Opposing effects of retinoic acid on cell growth result from alternate activation of two different nuclear receptors. *Cell*, **2007**, *129*,:723-33.

(c) Tan, N. S.; Shaw, N. S.; Vinckenbosch, N.; Liu, P.; Yasmin, R.; Desvergne, B.; Wahli, W.; Noy, N.Selective cooperation between fatty acid binding proteins and peroxisome proliferator-activated receptors in regulating transcription. *Mol. Cell Biol.* **2002**, *22*, 5114-27.

(d) Budhu, A. S.; Noy, N. Direct channeling of retinoic acid between cellular retinoic acid-binding protein II and retinoic acid receptor sensitizes mammary carcinoma cells to retinoic acid-induced growth arrest. *Mol. Cell Biol*. **2002**, *22*, 2632-41.

4 Kamei, Y., Xu, L., Heinzel, T., Torchia, J., Kurokawa, R., Gloss, B., Lin, S-C., Heyman, R. A., Rose, D. W., Glass, C. K., Rosenfeld, MG. A CBP integrator complex mediates transcriptional activation and AP-1 inhibition by nuclear receptors. *Cell*, **1996**, *85*, 403-414.

5 (a) Törmä, H.; Vahlquist, A. Retinol uptake and metabolism to 3,4-didehydroretinol in human keratinocytes at various stages of differentiation. *Skin Pharmacol*. **1991**, *4*, 154-7.

(b) Andersson, E.; Björklind, C.; Törmä, H.; Vahlquist, A. The metabolism of vitamin A to 3,4-didehydroretinol can be demonstrated in human keratinocytes, melanoma cells and HeLa cells, and is correlated to cellular retinoid-binding protein expression. *Biochim Biophys Acta*, **1994**, *1224*, 349-54.

(c) Rollman, O.; Wood E. J.; Olsson M. J.; Cunliffe W. J. Biosynthesis of 3,4-didehydroretinol from retinol by human skin keratinocytes in culture.*Biochem. J.* **1993**, *293* (Pt 3), 675-82.

(d) Törmä, H.; Vahlquist, A. Vitamin A in skin and serum--studies of acne vulgaris, atopic dermatitis, ichthyosis vulgaris and lichen planus. *J. Invest. Dermatol*. **1985**, 85, 498-500.

(e) Törmä, H.; Vahlquist, A. Biosynthesis of 3,4-didehydroretinol and fatty acyl esters of retinol and 3,4-didehydroretinol by organ-cultured human skin. *Methods Enzymol*. **1990**, *190*, 210-6.

(f) Siegenthaler, G. Retinoic acid formation from retinol and retinal metabolism in epidermal cells. *Methods Enzymol*. **1990**, *189*, 530-6.

(g) Randolph R. K.; Simon M. Characterization of Retinol Metabolism in Cultured Human Epidermal Keratinocytes *J. Biol. Chem*. **1993**, *268*, 9198-9205.

[6] Randolph R. K.; Simon M. All-trans-Retinoic Acid Regulates Retinol and 3,4-Didehydroretinol Metabolism in Cultured Human Epidermal Keratinocytes. *J. Invest. Dermatol.* **1996**, *106*, *168-175.*

[7] *Organic Preparation and Procedures International* ,**1987**, *19*(2-3), 187-195.; Pommer, H. The Witting Reaction in industrial practice. *Angew. Chem.*,**1960**, *22*, 811-819.

[8] Schwieter et al. Synthesis and Characteristics of stereoisomers: *Helvectica Chimica Acta*, **1962**,*45*, 541-548.; Planta et al. *Helvectica Chimica Acta*, **1962**,*45*, 548-561.

[9] Wada, A.; Hiraishi, S.; Takamura, N.; Date, T.; Aoe, K.; Ito, M. A Novel Method for a Stereoselective Synthesis of Trisubstituted Olefin Using Tricarbonyliron Complex: A Highly Stereoselective Synthesis of (all-E)- and (9Z)-Retinoic Acids. *J. Org. Chem.* **1997**, *62*, 4343-4348.; A. Wada, *Vitamin.* **2000**, *74*, 101-121.

[10] J. K. Stille, The Palladium-Catalyzed Cross-Cou- pling Reactions of Organotin Reagents with Organic Electrophiles.*Angew. Chem. Int. Ed. Engl.* **1986**, *25*, 508-524.

[11] K. Sonogashira, Y. Tohda, N. Hagihara, A convenient synthesis of acetylenes: catalytic substitutions of acetylenic hydrogen with bromoalkenes, iodoarenes and bromopyridines *Tetrahedron Lett.* **1975**, 4467-4470.

[12] Cartier, D.; Valla, A,; Guillou, R.; Labia, R.; Potier, P. New, Regioselective, One-Pot Synthesis of (all-E) Retinoic Acid and Analogues from Enaminiodiester Synthons. *Eur. J. Org. Chem.*, **2003**, 2250-2253. Cartier, D.; Valla, A,; Guillou, R.; Labia, R.; Potier, P. A new one-pot synthesis of *all E*-retinoic acid via a new enaminodiester synthon. *Tetrahedron Letters*, **2003**, *44*, 5789–5790.

[13] The sodium borotritide reduction of the methyl ester of 4-oxo retinoic acid followed by dehydration has been described: see Tosukhowong, P.; Supasiri, T. *J. Label. Comp. Radiopharm.*, **1985**, *22*, 925-930.

[14] Tanaka, H.; Kagechika, H.; Shudo, K. Specific Oxidation of Retinoic Acid to 4-oxo-Retinoic Acid in Diluted Acid Solutions. *Chem. Pharm. Bull.* **1995**, *43*, 356-358.

[15] (a) For the synthesis of all trans 4-oxo retinol acetate from all trans retinol acetate and the synthesis of all trans 4-oxo RA methyl ester from ATRA methyl ester by direct MnO_2 oxidation, see: Samokyszyn, V. M.; Gall, W. E.; Zawada, G.; Freyaldenhoven, M. A.; Chen, G.; Mackenzie, P. I.; Tephyl, T. R.; Radominska-Pandya, A. *J. Biol. Chem.* **2000**, *275*, 6908-6914.

(b) This procedure has been used successfully by others. See Patel, J. B.; Huynh, C. K.; Handratta, V. D.; Gediya, L. K.; Brodie, A. M. H.; Goloubeva, O. G.; Clement, O. O.; Nanne, I. P.; Soprano, D. R.; Njar, V. C. O. *J. Med. Chem.* **2004**, *47*, 6716-6729.

[16] (a) Staab, H. A.; Manschreck, A. *Chem. Ber*., **1961**, *95*, 284. (b) Attenburrow, J.; Cameron, F. B.; Chapman, R. M.; Evans, R. M.; Hems, B. A.; Jansen, A. B. A.; Walker, T. A Synthesis of Vitamin A from CycloHexanone. *J. Chem. Soc.* **1952**, *194*, 1094-1111.

[17] Hashimoto, N.; Fujimoto, Y. One Step and Convenient Preparations of 4-Hydroxylretinal and 4-Oxoretinal.. *Synthetic Commun.*, **1999**, *29*, 3793-3797.

[18] Cartier, D.; Valla, A,; Guillou, R.; Labia, R.; Potier, P. New, Regioselective, One-Pot Synthesis of (all-E) Retinoic Acid and Analogues from Enaminiodiester Synthons. *Eur. J. Org. Chem.*, **2003**, 2250-2253.

[19] Rosenberger. M.; McDougal, P.; Bahr, J. Canthaxanthin. A new total synthesis. *J. Org.Chem*. **1982**, 47, 2130-2134.

[20] Borhan, B; Souto, M.L.; Um, J.M.; Nakanishi, K.; Efficient Synthesis of 11 cis-retinoids. *Chemistry-A European Journal*, **1999**, *5*, 1172-1175.

[21] Koji, N.; Rando, R.; Nesnas, R. Synthesis of biotinylated retinoids for cross-linking and isolation of retinol binding proteins. *Tetrahedron*, **2002**, *58*, 6577-

6584.

[22] Presser, A; Hufner, A; Trimethylsilyldiazomethane – A Mild and Efficient Reagent for the Methylation of Carboxylic Acids and Alcohols in Natural Products *Monatshefte fur Chemie* , **2004**, 135, 1015–1022

[23] Bligh, E.G., and Dyer, W.J A rapid method of total lipid extraction and purification. *Can. J.Biochem.Physiol* . **1959**, *37*, 911-917.

References for Chapter 3

[1] Vaklavas, C.; Chatzizisis, Y. S.; Ziakas, A.; Zamboulis, C.; Giannoglou, G. D. "Molecular basis of statin-associated myopathy." *Atherosclerosis* (Amsterdam, Netherlands), **2009**, *202*, 18-28.

[2] (a) Davidson, M. H. "Squalene synthase inhibition: a novel target for the management of dyslipidemia. " *Curr. Atherosclerosis Rep*. **2007**, *9*, 78-80.

(b) Flint, O. P.; Masters, B. A.; Gregg, R. E.; Durham, S. K. "HMG CoA reductase inhibitor-induced myotoxicity: pravastatin and lovastatin inhibit the geranylgeranylation of low-molecular-weight proteins in neonatal rat muscle cell culture." *Toxicology and Applied Pharmacology* **1997**, 145, 99-110.

[3] Charlton-Menys, V. Durrington, P. N. "Squalene Synthase Inhibitors. Clinical Pharmacology and Cholesterol-Lowering Potential," *Drugs*, **2007**, 67, 11-16.

[4] Biller, S.A.; Neuenschwander, K; Ponpipom, M. M.; Poulter, C. Dale. "Squalene synthase inhibitors." *Current Pharmaceutical Design* **1996**, *2*, 1-40.

[5] Flint, Oliver P.; Masters, Barbara A.; Gregg, Richard E.; Durham, Stephen K. "Inhibition of cholesterol synthesis by squalene synthase inhibitors does not induce myotoxicity in vitro." *Toxicology and Applied Pharmacology* **1997**, 145, 91-98.

[6] Nishimoto, T.; Amano, Y.; Tozawa, R.i; Ishikawa, E.; Imura, Y.; Yukimasa, H.; Sugiyama, Y.. "Lipid-lowering properties of TAK-475, a squalene synthase inhibitor, in vivo and in vitro." *British Journal of Pharmacology* **2003**, *139*, 911-918.

[7] Menys, V. C.; Durrington, P. N. "Squalene synthase inhibitors" *Brit. J. Pharm.* **2003**, *139*, 881-882.

[8] (a) Minagawa, K.; Kouzuki, S.; Nomura, K.; Kawamura, Y.; Tani, H.; Terui, Y.; Nakai, H.; Kamigauchi, T.; "Bisabosquals, novel squalene synthase inhibitors. II. Physico-chemical properties and structure elucidation."*Journal of Antibiotics.* **2001**, *54*, 896-903.

(b) Minagawa, K; Kouzuki, S.; Nomura, K.; Yamaguchi, T.; Kawamura, Y.; Matsushima, K.; Tani, H.; Ishii, K.; Tanimoto, T.; Kamigauchi, T..” Bisabosquals, Novel Squalene Synthase Inhibitors. Part 1. Taxonomy, Fermentation, Isolation and Biological Activities.” *Journal of Antibiotics.* **2001**, *54,* 890-895

(c) Thompson, J. F.; Danley, D. E.; Mazzalupo, S.; Milos, P. M.; Lira, M.E.; Harwood, H. J., Jr. *Archives of Biochemistry and Biophysics.* **1998**, *350*, 283-290.

[9] Veber, D. F.; Johnson, S. R.; Cheng, H.-Y.; Smith, B. R.; Ward, K. W.; Kopple, K.D. “Molecular Properties That Influence the Oral Bioavailability of Drug Candidates.” *J. Med. Chem.* **2002**, 45, 2615-2623.

[10] (a) Lipinski, C. A.; Lombardo, F; Dominy, B W.; Feeney, P J. “Experimental and computational approaches to estimate solubility and permeability in drug discovery and development settings” *Adv. Drug Delivery Rev.* **1997**, *23*, 3-25.
(b) Lipinski, C. A.; “Drug-like properties and the causes of poor solubility and poor permeability” *J. Pharm. Tox. Methods*, **2000**, *44*, 235-249.

[11] Blagg, B. S. J.; Jarstfer, M. B.; Rogers, D. H.; Poulter, C. D. “Recombinant Squalene Synthase. A Mechanism for the Rearrangement of Presqualene Diphosphate to Squalene.” *J. Am. Chem. Soc.* **2002**, *124*, 8846-8853.

[12] Guan, Guimin; Dai, Pei-Hua; Osborne, Timothy F.; Kim, Jae B.; Shechter, I.” Multiple Sequence Elements are involved in the Transcriptional Regulation of the Human Squalene Synthase Gene.” *Journal of Biological Chemistry*. **1997**, *272,* 10295-10302.

[13] Robinson, Gordon W.; Tsay, Yim H.; Kienzle, Bernadette K.; Smith-Monroy, Constance A.; Bishop, Richard W. **“**Conservation between human and fungal squalene synthetases: Similarities in structure, function, and regulation**.”** *Molecular and Cellular Biology*, **1993**, *13*, 2706-17.

[14] Gu, P., Ishii, Y., Spencer, T. A., and Shechter, I. “ Function-Structure Studies and Identification of Three Enzyme Domains Involved in the Catalytic Activity in Rat Hepatic Squalene Synthase.“ *J. Biol. Chem.***1998**, *273*, 12515–12525**.**

[15] (a) Robinson, Gordon W.; Tsay, Yim H.; Kienzle, Bernadette K.; Smith-Monroy, Constance A.; Bishop, Richard W. “Conservation between human and fungal squalene synthetases: Similarities in structure, function, and regulation.” *Molecular and Cellular Biology* **1993**, *13,* 2706-17.

(b) Fegueur, M.; Richard, L.; Charles, A. D.; Karst, F. **“**Isolation and primary structure of the ERG9 gene of Saccharomyces cerevisiae encoding squalene synthetase.” *Current Genetics* **1991**, *20,* 365-72.

(c) Jennings, Susan M.; Tsay, Yim H.; Fisch, Tobe M.; Robinson, Gordon W. "Molecular cloning and characterization of the yeast gene for squalene synthetase." *Proceedings of the National Academy of Sciences of the United States of America* **1991**, *88*, 6038-42.

16 Gu, P., Ishii, Y., Spencer, T. A., and Shechter, I. " Function-Structure Studies and Identification of Three Enzyme Domains Involved in the Catalytic Activity in Rat Hepatic Squalene Synthase." *J. Biol. Chem*.**1998**, *273*, 12515–12525.

17 Robinson,G.W.; Tsay, Y.H.; Kienzle, B.K.; Bishop, R.W. "Conservation between human and fungal squalene synthetases: similarities in structure, function, and regulation." *Mol. Cell. Biology*, **1993**, *13*, 2706-2717.

18 Guan, Guimin; Dai, Pei-Hua; Osborne, Timothy F.; Kim, Jae B.; Shechter,I." Multiple Sequence Elements are involved in the Transcriptional Regulation of the Human Squalene Synthase Gene." *Journal of Biological Chemistry*. **1997**, *272,* 10295-10302.

19 Robinson,G.W.; Tsay, Y.H.; Kienzle, B.K.; Bishop, R.W. "Conservation between human and fungal squalene synthetases: similarities in structure, function, and regulation." *Mol. Cell. Biology*, **1993**, *13*, 2706-2717.

20 Robinson,G.W.; Tsay, Y.H.; Kienzle, B.K.; Bishop, R.W. "Conservation between human and fungal squalene synthetases: similarities in structure, function, and regulation." *Mol. Cell. Biology*, **1993**, *13*, 2706-2717.

21 Hosfield, D. J.; Zhang, Y.; Dougan, D. R.; Broun, A.; Tari, L. W.; Swanson, R. V.; Finn, J. "Structural Basis for Bisphosphonate-mediated Inhibition of Isoprenoid Biosynthesis." *J. Biol. Chem.* **2004**, *279*, 8526-8529.

22 Guan, Guimin; Dai, Pei-Hua; Osborne, Timothy F.; Kim, Jae B.; Shechter, I." Multiple Sequence Elements are involved in the Transcriptional Regulation of the Human Squalene Synthase Gene." *Journal of Biological Chemistry*. **1997**, *272,* 10295-10302.

23 Pandit, J.; Danley, D. E.; Schulte, G. K.; Mazzalupo, S.; Pauly, T. A.; Hayward, C.M.; Hamanaka, E. S.; Thompson, J. F.; Harwood, H. J., Jr. "Crystal structure of human squalene synthase. A key enzyme in cholesterol biosynthesis" *J. Biol. Chem.* **2000**, *275*, 30610-30617

24 Pandit, J.; Danley, D. E.; Schulte, G. K.; Mazzalupo, S.; Pauly, T. A.; Hayward, C.M.; Hamanaka, E. S.; Thompson, J. F.; Harwood, H. J., Jr. "Crystal structure of human squalene synthase. A key enzyme in cholesterol biosynthesis" *J. Biol. Chem.* **2000**, *275*, 30610-30617.

25 Pandit, J.; Danley, D. E.; Schulte, G. K.; Mazzalupo, S.; Pauly, T. A.; Hayward,

C.M.; Hamanaka, E. S.; Thompson, J. F.; Harwood, H. J., Jr. "Crystal structure of human squalene synthase. A key enzyme in cholesterol biosynthesis" *J. Biol. Chem.* **2000**, *275,* 30610-30617

[26] Verdonk M.L, Cole J.C, Hartshorn M.J, Murray C.W, Taylor R.D. "Improved Protein- Ligand Docking Using GOLD." *PROTEINS:Structure, Function, and Genetics* **2003**, *52*, 609-623.

[27] (a) Massova, I.; Kollman, P. A.. Combined molecular mechanical and continuum solvent approach (MM-PBSA/GBSA) to predict ligand binding. *Perspectives in Drug Discovery and Design* **2000**, *18* (Hydrophobicity and Solvation in Drug Design, Pt. II), 113-135. (b) Srinivasan, J., Cheatham, T.E., Cieplak, P., Kollman, P.A. and Case, D.A., Continuum Solvent Studies of the Stability of DNA, RNA, and Phosphoramidate-DNA Helixes. *J. Am. Chem. Soc.*, **1998**, *120*, 9401-9409.

[28] (a) Wu, G.; Robertson, D. H.; Brooks, C. L., III; Vieth, M. Detailed analysis of grid-based molecular docking: A case study of CDOCKER-A CHARMm-based MD docking algorithm. *J. Comput. Chem.* **2003**, *24*, 1549–1562 (b) Erickson, J. A.; Jalaie, M.; Robertson, D. H.; Lewis, R. A.; Vieth, M. Lessons in molecular recognition: the effects of ligand and protein flexibility on molecular docking accuracy. *J. Med. Chem.* **2004**, *47*, 45–55.

[29] Böhm, H. J. The computer program Ludi: a new method for the de novo design of enzyme inhibitors. *J. Comput. Aided Mol. Des*. **1992**, *1*, 61-78.

[30] (a) Barreiro G.; Guimaraes C. R. W.; Tubert-Brohman I.; Lyons T. M; Tirado-Rives J.; Jorgensen W. L. Search for non-nucleoside inhibitors of HIV-1 reverse transcriptase using chemical similarity, molecular docking, and MM-GB/SA scoring. *J. Chem. Inf. Model.* **2007,** *47*, 2416-2428, (b) de Jonge, M.R.; Koymans, L. M. H.; Vinkers, M.; Daeyaert, F. F. D; Heeres, J.; Lewi, P.J.; Janssen, P. A. J. Structure Based Activity Prediction of HIV-1 Reverse Transcriptase Inhibitors. *J. Med. Chem.* **2005,** *48*, 2176- 2183, (c) Carta, A.; Pricl,S.; Piras, S.; Fermeglia, M.; La Colla, P.; Loddo, R. Activity and molecular modeling of a new small molecule active against NNRTI-resistant HIV-1 mutants. *Eur. J. Med. Chem.* **2009,** *44*, 5117–5122.

[31] Kuhn,B.; Gerber,P.; Schulz-Gasch, T.; Stahl, M. "Validation and Use of the MM-PBSA Approach for Drug Discovery." *J. Med. Chem.* **2005**, *48*, 4040-4048.

[32] (a) Wu, G.; Robertson, D. H.; Brooks, C. L., III; Vieth, M. *J. Comput. Chem.* **2003**, *24*, 1549–1562 (b) Erickson, J. A.; Jalaie, M.; Robertson, D. H.; Lewis, R. A.; Vieth, M.*J. Med. Chem.* **2004**, *47*, 45–55.

[33] (a) Wu, G.; Robertson, D. H.; Brooks, C. L., III; Vieth, M. *J. Comput. Chem.* **2003**, *24*, 1549– 1562 (b) Erickson, J. A.; Jalaie, M.; Robertson, D. H.; Lewis, R. A.; Vieth, M.*J. Med. Chem.* **2004**, *47*, 45–55.